

Remote Sensing Tools for the
Objective Quantification of Tree
Structural Condition
from Individual Trees to Landscape
Scale Assessment



Jon Murray

This thesis is submitted for the degree of

Doctor of Philosophy

October 2018

Lancaster Environment Centre

Faculty of Science and Technology

For Sue, Beth, Erin, Henry and Ozzy.

“The importance of the forest canopy to forestry and forest research has been reflected in the ingenuity of foresters in devising methods and instruments to measure it.”

(Jennings, Brown et al. 1999)

Declaration

This thesis has not been submitted in support of an application for another degree at this or any other university. It is the result of my own work and includes nothing that is the outcome of work done in collaboration except where specifically indicated. Many of the ideas in this thesis were the product of discussion with my supervisory team; Prof. Alan Blackburn, Dr. Duncan Whyatt and Dr. Chris Edwards.

Excerpts of this thesis have been published to the following academic publications:

Murray, J., G.A. Blackburn, J.D. Whyatt and C. Edwards (2018). "Using Fractal Analysis of Crown Images to Measure the Structural Condition of Trees." *Forestry: An International Journal of Forest Research* **91**(4): 480-491.

Murray, J., Gullick, D., Blackburn, G. A., Whyatt, J. D., & Edwards, C. (2019). ARBOR: A new framework for assessing the accuracy of individual tree crown delineation from remotely-sensed data. *Remote Sensing of Environment*, 231, 111256.

Jon Murray

MSc, PGCE, BSc (Hons)

Lancaster University, UK

Abstract

Tree management is the practice of protecting and caring for trees for sustainable, defined objectives. However, there are often conflicts between maintaining trees and the obligation to protect targets, such as people or infrastructure, from the risks associated with the failure of trees and major limbs. Where there are targets worthy of protection, tree structural condition is typically monitored relative to the prescribed management objectives. Traditionally, field methods for capturing data on tree structural condition are manual with a tree surveyor taking very limited direct measurements, and only from parts of the tree that are within reach from the ground. Consequently, large sections of the tree remain unmeasured due to the logistical complications of accessing the aerial structure. Therefore, the surveyor estimates tree part sizes, approximates counts of relevant tree features and uses personal interpretation to infer the significance of the observations. These techniques are temporally and logistically demanding, and largely subjective.

This thesis develops solutions to the limitations of traditional methods through the development of remote sensing (RS) tools for assessing tree structural condition, in order to inform tree management interventions. For individual trees, a proximal photogrammetry technique is developed for objectively quantifying tree structural condition by measuring the self-affinity of tree crowns in fractal dimensions. This can identify the individual tree crown complexity along a structural condition continuum, which is more effective than the traditional categorical approach for monitoring tree condition. Moving out in scale, a framework is developed which optimises the match-pairing agreement between ground reference tree data and RS-derived individual tree crown (ITC) delineations in order to quantify the accuracy of different ITC

delineation algorithms. The framework is then used to identify an optimal ITC delineation algorithm which is applied to aerial laser scanning data to map individual trees and extract a point cloud for each tree. Metrics are then derived from the point cloud to classify a tree according to its structural condition, a process which is then applied to the tree population across an entire landscape. This provides information with which to spatially optimise tree survey and management resources, improve the decision making process and move towards proactive tree management.

The research presented in this thesis develops RS tools for assessing tree structural condition, at a range of investigative scales. These objective, data-rich tools will enable resource-limited tree managers to direct remedial interventions in an optimised and precise way.

Acknowledgements

There are always many people to thank for their individual help during the course of a project like this, too many to name everyone individually, but I extend genuine gratitude to all those who have helped me on this journey. Especially to all the office dwellers of B31a, and in particular to Miss B for, you know, absolutely everything! Hopefully, these brief words will go some small way in conveying my appreciation to everyone who has helped over the years.

To my supervisors Alan, Duncan and Chris, I am of course, so very grateful for all the help and insight you have provided over the years. In particular during difficult times where your support and guidance was most needed, and was freely given. Thank you all.

To Vassil, my thanks for the many hours of help with the fieldwork, always with a genuine interest and willingness to shoulder whatever task (and equipment!) you could.

A special thanks to Mr. Oswald Copperpot for the many hours spent surveying in the woods and never complaining or wanting to go home early, no matter how grotty the days were! Sadly, you passed before seeing me get to the end of this but I know I couldn't have got here without your company and friendship along the way.

To my three amazing children, Beth, Erin and Henry. I am so indebted to all of you for putting up with my endless hours on the computer, and for cheering me up when things went wrong. I know as a result I missed a lot of your growing up and

irreplaceable family time. I can't make any of that lost time back, but I promise you that things will be better now this PhD is finally finished!

Finally, to Sue. Although it has turned out not to have been the journey that we originally hoped for, I offer you my thanks for all your support which ultimately helped me to reach the end, and to finish this '*little job*'.

Jon Murray

October 2018

Contents

1 INTRODUCTION.....	1
1.1 Thesis Aim and Objectives	3
1.2 Thesis Structure	3
2 LITERATURE REVIEW.....	6
2.1 The Problem of Subjectivity	6
2.1.1 <i>Subjectivity and Tree Management</i>	9
2.2 The Development of Tree Surveying.....	13
2.2.1 <i>Plot Establishment for Site Surveys</i>	15
2.3 Decision Support Systems for Tree Management	16
2.4 Tree Structure.....	18
2.4.1 <i>Dynamic Change in Tree Structure</i>	18
2.4.2 <i>Phenotypic Tree Structure</i>	19
2.5 The General Principles of Remote Sensing in the Environment	21
2.5.1 <i>Remote Sensing and Trees</i>	22
2.5.2 <i>LiDAR</i>	23
2.6 Photogrammetry.....	30
2.6.1 <i>Proximal Hemispheric Imagery</i>	31
2.6.2 <i>Landscape Scale Photogrammetric Investigations</i>	32
2.7 Unique Programming Requirements of RS Data.....	33
2.7.1 <i>Canopy Height Model Data Pits</i>	34
2.7.2 <i>Data Threshold Manipulation</i>	36
2.7.3 <i>Weighting as a Data Filter</i>	37
2.8 Aerial Laser Scanning.....	38
2.8.1 <i>ALS Tree Investigation</i>	39
2.8.2 <i>Individual Tree Crown Delineation</i>	40
2.9 From the Past to the Future.....	43
2.9.1 <i>Predicted Remote Sensing Trends</i>	45
2.10 Summary	47
3 FIELD SITES, METHODS & LIDAR DATA SPECIFICATION	50
3.1 Field Sites.....	51
3.1.1 <i>Eaves Wood, Lancashire, UK</i>	51
3.1.2 <i>Potter Hill Fields and Park Fields, Silverdale, Lancashire, UK</i>	53
3.2 Tree Survey Methodology	53
3.3 Photogrammetry Field Methodology	55
3.4 ALS Survey Plot Location and Establishment.....	56
3.4.1 <i>Real Time Kinematic GPS and Total Station Surveying</i>	57
3.4.2 <i>Survey Plot Establishment</i>	60
3.5 Site and Data Summary	62
3.6 LiDAR Data Specification.....	63
4 USING FRACTAL ANALYSIS OF CROWN IMAGES TO MEASURE THE STRUCTURAL CONDITION OF TREES.....	66
4.1 Preamble	66
4.2 Introduction.....	68
4.3 Methodology.....	72
4.3.1 <i>Field Methodology Development</i>	74
4.3.2 <i>Camera Set-up</i>	76
4.3.3 <i>Image Acquisition and Spatial Sampling Strategy</i>	76
4.3.4 <i>Image Preparation</i>	79
4.3.5 <i>Defining the Image Analysis Area</i>	80

4.3.6 Predictor Variable Creation	81
4.3.7 Calculating Statistical Probabilities	85
4.3.8 Outlining Classification Thresholds	86
4.4 Results	87
4.5 Discussion	91
4.6 Conclusion	96
4.7 Funding	96
4.8 Supplementary Information	97
4.9 Acknowledgements	97
4.10 Conflict of interest statement	97
5 ARBOR: A NEW FRAMEWORK FOR ASSESSING THE ACCURACY OF INDIVIDUAL TREE CROWN DELINEATION FROM REMOTELY- SENSED DATA	98
5.1 Preamble	98
5.2 Introduction	101
5.3 Aim and Objectives	104
5.4 Methodology	105
5.4.1 Quantifying the Similarity of a Tree as Represented in RS-derived and Ground Reference Datasets	105
5.4.2 Gaussian Overlapping and the Jaccard Similarity Coefficient	106
5.5 Optimal Algorithm for Matching Populations of Trees Represented in both RS- derived and Ground Reference Datasets	109
5.5.1 Meta-study of Alternative Match-pairing Methods	109
5.5.2 Hungarian Combinatorial Optimisation Algorithm	112
5.5.3 Quantification of Accuracy with which Delineations Estimate Biophysical Properties and Population Size	112
5.6 Testing the Pairwise Matching Algorithms with Synthetic Data	113
5.6.1 Synthetic Data Environment	113
5.6.2 Introduced Data Noise and Population Losses	114
5.6.3 Results of Pairwise Matching Tests	116
5.6.4 Summary Observations and Recommendation	119
5.7 The ARBOR Framework	121
5.8 Demonstration of ARBOR for Evaluating ITC Delineations	122
5.8.1 The Results of Applying ARBOR to RS-derived ITC Delineations	124
5.9 The Significance of the ARBOR Framework	126
5.10 Conclusion	129
5.11 Supplementary Information	130
5.12 Acknowledgements	130
6 STRUCTURAL: CATEGORISING THE STRUCTURAL CONDITION OF INDIVIDUAL TREES AT LANDSCAPE SCALE USING LIDAR DATA....	131
6.1 Preamble	131
6.2 Introduction	133
6.3 Aim and Objectives	136
6.4 Methodology	136
6.4.1 Fieldwork, Site Selection and Manual Operations	136
6.4.2 Data Preparation and Preliminary Observations	138
6.4.3 Visualisation of LiDAR Returns for Different Tree Structural Conditions ..	141
6.4.4 Defining Variables for Supervised Learning & Aerial LiDAR Metrics	145
6.4.5 Validation of the Trained Model Response and Tree Classification	156
6.4.6 Summary Recommendation	158
6.5 STRUCTURAL Output	160
6.6 Discussion	164

6.7 Conclusion	169
6.8 Acknowledgements.....	170
7 DISCUSSION	171
7.1 Overview.....	171
7.1.1 <i>Procedural Workflow</i>	171
7.2 Synthesis	173
7.3 Key Contributions from this Research.....	175
7.3.1 <i>The Influence of Subjectivity</i>	175
7.3.2 <i>The Development of Tree Surveying</i>	176
7.3.3 <i>The Potential for Decision Support Systems (DSSy)</i>	178
7.3.4 <i>Tree Structure Effects</i>	180
7.3.5 <i>Environmental Remote Sensing</i>	181
7.3.6 <i>Unique Remote Sensing Programming Challenges</i>	182
7.3.7 <i>Photogrammetry</i>	183
7.3.8 <i>Aerial Laser Scanning</i>	183
7.3.9 <i>The Future of Technological Approaches</i>	184
7.4 Limitations of the Research	185
7.5 Potential Research Opportunities.....	189
8 CONCLUSION.....	191
9 REFERENCES.....	195

List of Tables

Table 1	An overview of tree surveying methods currently in use in the forestry, arboriculture or tree management sectors. The word ‘objective’ refers to direct measurement or factually acquired data. The word ‘subjective’ refers to instances where a field operative uses interpretation, estimates or best guess methods to acquire ‘measurements’ for the survey method. This list is not exhaustive, but is representative of tree surveying methods frequently used in the UK, USA and worldwide.....	10
Table 2	Categories of manual tree measurements taken during field capture of ground reference data. Examples of the data recorded are also shown.	54
Table 3	Calculation of vegetation cover at 26 survey plots. Images were captured at each location and amount of sky or vegetation that occupies the image was calculated using CAN_EYE.....	57
Table 4	Summary record of ground reference field and research sites used within a remote sensing investigation, and the number of trees for the types of data recorded at each location.....	63
Table 5	LiDAR data types and description provided in ASCII format for LiDAR flightlines over Eaves Wood, UK.	65
Table 6	Descriptions of analytical metrics used in an investigation to quantify tree structural condition.	81
Table 7	Threshold limits of tree condition categories, expressed in fractal dimensions (Df).....	87
Table 8	A meta-study of several match-pairing methods showing the base matching method, and identifying whether subsequent filters or thresholds are applied. The direction of the match is also shown.....	111

Table 9	Introduction of data noise following modification of the normal distribution and standard deviation (SD) effect on the data population relative to data noise levels.	115
Table 10	Quantification of ARBOR framework scores for four individual tree crown (ITC) delineation techniques, when compared to known tree location, height and crown areas of ground reference tree data.	125
Table 11	LiDAR pulses returned for a combination of six flight line passes of Eaves Wood, Lancashire, UK. Point data 1 is unconsolidated results of all flightlines, while point data 2 is an optimised area of overlapping flightlines.	139
Table 12	Standardized and raw discriminant function coefficients as unstandardized regression weights for LiDAR return (r) variables (Murray, Blackburn et al. 2014)	142
Table 13	Correlations between the dependent (return (r)) and canonical variables (Murray, Blackburn et al. 2014).....	142
Table 14	Description of measurements calculated from LiDAR point cloud data, grouped into themed areas of inventory, intensity, area, height and other. <i>Adapted from Parkan (2018)</i>	146
Table 15	Description of a range of classifier models used in assessing the accuracy of trained models in a supervised learning analysis.	147
Table 16	Chi-square (χ^2) validation of two classification models (medium <i>k</i> NN and RUS Boost) that were trained using different training data populations (N=100 and N=235).	157
Table 17	A cross tabulation validation results of a ground reference dataset (GRD) that has been classified using a trained model, becoming model classified data (MCD). The table shows no influence of bias in any of the classification categories.....	158

Table 18	Area of woodland cover in the United Kingdom (2016), by country and tree classification (Donohue 2016).	174
Table 19	The activity fields of precision forestry (Kováčsová and Antalová 2010).	185

List of Figures

- Figure 1 A visualisation of CHM's from LiDAR data, using two different techniques.
- a. The outline of four woodland survey plots. b. typical pixelated CHM as used in many RS studies, with data pitting that causes analysis errors (Ben-Arie, Hay et al. 2009) (circular inset i, poor tree canopy resemblance with data pits as black pixels). c. a novel “splatted” CHM, closely resembling tree canopies, with data pits eliminated (Khosravipour, Skidmore et al. 2016) (circular inset ii., tree-like canopy edge with no data pits). The four conjoined square shapes are four separate field survey plots, with each plot measuring 20x20 metres (400m²) on the ground. 36
- Figure 2 The approximate location of Eaves Wood, Silverdale, Lancashire, UK. ... 52
- Figure 3 Equipment required for taking beneath crown hemispherical photographs for use in crown structure analysis 1. dSLR camera with a hemispherical lens adapter, compass and level 2. Standard camera tripod, 3. Surveyors measuring tape, 4. GPS/data logger, 5. Tree survey data sheets, 6. Sunnto clinometer, 7. DBH tape (not shown)..... 55
- Figure 4 Geolocation of ground control points (a), and undertaking a first order triangulation survey (b), to locate survey plots within woodland to aid data processing in an investigation gathering LiDAR data of Eaves Wood, Silverdale, Lancashire, UK. 59
- Figure 5 A survey plot layout for capturing data in an ALS LiDAR investigation undertaken in Eaves Wood, Lancashire, UK. The plot centre has geolocated coordinates (e.g. X=346642.5, Y=476232.5), while the plot origin at (0,0) would have coordinates -10m less than the plot centre (e.g. X=346632.5, Y=476222.5). The recording of a tree location along the X axis, would be taken from left to right, and for the Y axis would be taken from the bottom to the top. 61

Figure 6	An assessment of structural diversity of a tree population in Eaves Wood, Lancashire, UK. The data follows an ideal ‘reverse-J’ distribution, which indicates a structurally complex and diverse population (Kerr, Mason et al. 2002).....	62
Figure 7	Individual trees delineated from ALS LiDAR data of Eaves Wood. a) a tree in good crown condition, b) a tree in moderate crown condition, c) a tree in poor crown condition, d) a monolith of a dead tree (no crown) and ground points removed for visual clarity. Return (r) pulses R1-3 can be seen as yellow, red and green respectively.	64
Figure 8	Intensity image of Eaves Wood, UK, with intensity values ranging from 0 (dark) to 255 (white). The image also shows the boundary of Eaves Wood, outlined in red.	65
Figure 9	A schematic of the field method for taking a hemispherical picture from beneath a tree canopy. The camera is situated on a standard tripod, and is levelled and pointing towards the zenith viewing point (90° from the horizontal elevation). In this example, the full extent of the crown is four metres along the southern axis, and the image is taken at the two metre mid-point.	73
Figure 10	Classification descriptors for the subjective arboricultural assessment of trees. Estimated Remaining Contribution (ERC) refers to a methodology used to consider the health, condition and structure of the tree and aids in classifying the tree in to the different categories <i>adapted from</i> (Barrell 1993, Lonsdale 1999, Barrell 2001, NTSG 2011, BSI 2012). Note: The images show trees in leaf-on condition to enable ease of comparison for the condition types.	75
Figure 11	A schematic showing the optimised range for image capture (a), and the area of tree canopy structure analysed within this study (b). The area of interest is specifically the structural elements of the canopy. Too much ‘sky’ within the image reduces the amount of structure that can be analysed (a). Stem wood and other	

elements not required, are removed from the image by only analysing the structure inside a user selected bounding box area (b). The use of a bounding box allows images of both individual trees and trees within closed canopies to be analysed. . 78

Figure 12 A procedural workflow showing how tree structure images are processed for the computation of image metrics 85

Figure 13 Sample subset of predictor variables used to define the characteristics of different tree structures (*n*64). The annotations Good, Moderate, Poor and Dead refer to the field observed condition of the individual trees. Only with the measure of fractal dimension (a.), provides homogeneous clustering of field observed conditions as identified by the threshold lines. Not all predictor variables used in this study are visualised in this plot 89

Figure 14 A proportional odds model to indicate the probability (*P*) that tree structure images, quantified in fractal dimensions (Df), are indicative of an observable tree structure condition and known reference standard (*n*64). Tree images were measured for structural complexity in Df. The box plot extents identify the *P* that the structures show characteristics of the reference standard..... 90

Figure 15 Gaussian overlap used for measuring data agreement between two data sets, where the difference between the two shapes is quantified using the Jaccard similarity coefficient. 108

Figure 16 500 synthetic trees representing ground reference (GR), and RS-derived LiDAR datasets. a) models 500 GR trees, and b) represents RS-derived trees with increased noise and tree losses. This replicates typically observed effects in aerial LiDAR derived canopy height models. 114

Figure 17 An example of Gaussian curves demonstrating the change on data distribution and population density for synthetic tree data. This example represents the change in location data with the x axis equating to metres offset. This method

intentionally introduces data noise to a remote sensing dataset of synthetic trees.	115
Figure 18 A combination of three data match-pairing methods being tested for the ability to achieve predicted data pairings between synthetic GR and RS-derived data. Each pixel in plots a-c represents an assessment of normalised root mean squared error (NRMSE) at differing levels of data noise and loss. Plots d-f represent the effect of the match-pairing on the data population, expressed as a pairing ratio.....	118
Figure 19 A working example of the ARBOR framework workflow for the quantification of match-pairing agreement between remote sensing derived and ground reference data. Notes: AMPS = averaged matched-pairing similarity index, DSS = dataset size similarity index.....	122
Figure 20 ARBOR scores comparing the match-pairing success between four different ITC delineation techniques acquired from aerial LiDAR data with ground reference data over 26 survey plots.....	124
Figure 21 Outline of Eaves Wood, Lancashire, showing locations of the transect line and ground reference plots. The grey boxes indicate the overlapping LiDAR flightlines, while the black box identifies the flightline area that achieved 100% overlap, corresponding with the central transect and ground reference plots.....	139
Figure 22 Tree canopies as drawn as circular shapes in ArcGIS at 1:125 scale. The canopies are created with scaled measurements and orientated in the direction as they were found in data collection at Eaves Wood, Silverdale, Lancashire, UK. Also shown in the image is the transect line (red) and plot area (green) used in the investigation.....	141
Figure 23 Subject trees in manually observed conditions: a, b, c, and d = good, moderate, poor and dead conditions respectively. Trees marked with 1 are photographic representations of the subject trees. Trees marked with 2 are visual	

representations of trees scanned using DR ALS LiDAR, with pulse returns shown:
 r1 (Yellow), r2 (Red), r3 (Green)..... 143

Figure 24 ITC delineations of individual trees across the full study site flightline.
 These unsurveyed trees will be classified using their biophysical characteristics as
 observed in ALS LiDAR data..... 145

Figure 25 Response of model accuracy levels during model training with different
 numbers of predictor variables..... 149

Figure 26 Trained model results for the predictor variables Concave Surface Area by
 Concave Density as a tree classification metric using a medium *k*NN classifier model
 and 100 training trees from ALS LiDAR data. a) scatter plot of assigned categories,
 b) receiver operating classifier (ROC) curve for the dead category, and c) confusion
 matrix of all categories true positive classifications. Overall model accuracy is
 46.8%.....151

Figure 27 Trained model results for the predictor variables Concave Surface Area by
 Concave Density as a tree classification metric using a medium *k*NN classifier model
 and 235 training trees from ALS LiDAR data. a) scatter plot of assigned categories,
 b) receiver operating classifier (ROC) curve for the dead category, and c) confusion
 matrix of all categories true positive classifications. Overall model accuracy is 41%.
153

Figure 28 Trained model results for the predictor variables Concave Surface Area by
 Concave Density as a tree classification metric using an Ensemble RUSBoost
 classifier model and 235 training trees from ALS LiDAR data. a. scatter plot of
 assigned categories, b. receiver operating classifier (ROC) curve for the dead
 category, and c. confusion matrix of all categories true positive classifications.
 Overall model accuracy is 33.6%. 155

Figure 29	Individual tree crowns delineated from continuous data (LiDAR) and assigned into good, moderate, poor and dead categories using the STRUCTURAL method ($n=9094$).	161
Figure 30	A combined approach of using ground reference data, and using descriptive metrics on previously uncategorised remotely sensed tree data.	162
Figure 31	Empirical observations of tree condition categories and their spatial distribution throughout the study woodland. a) shows smaller, young trees to the northwest of the site. b) shows stressed trees on karst landform in the central region of the woodland, while c) shows mature, overstory trees in the east of the woodland.	164
Figure 32	The full workflow required for classifying trees at landscape scale using aerial LiDAR, field data and trained classifier models. This method uses a combination of both manual and automated techniques to produce a location map of trees that are classified from the training model.	172
Figure 33	A model defining how the operational relationship between the findings of this research can be used in a large-scale, optimised and high-resolution tree structural condition investigation.	173
Figure 34	Model testing of the impact of image post processing phases on average Df values, demonstrating 95% confidence interval (CI95%) ($n=247$). Note: Image pre-processing phases applied 1 = raw unprocessed images, 2 = applying chromatic aberration correction, 3 = applying lens distortion correction, 4 = applying image sharpening. The Df values are a logarithmic scale, demonstrated on a truncated axis.	220
Figure 35	The quantification of effect size following image post processing ($n=247$). The value of Hedge's g at 2.4504 with a confidence interval at 95%, suggests that the pre-processing phases have a significant effect on Df values.	222

Figure 36 Regression analysis of fractal dimension values following image pre-processing ($n=247$). The pre-processed Df, remains a statically relevant representation of the raw Df values with a normalised root mean squared error (NRMSE) of 0.07% ($y = 0.84*x + 0.26$, $R^2_{\text{adjusted}} = 0.7\%$). 223

Figure 37 An operational workflow for the field practitioners use of a methodology for the classification of tree crown structure in fractal dimensions (Df), using hemispherical photography. 224

Figure 38 A model of typical tree location alignment problems when comparing aerial observation data (either aerial images or LiDAR), and ground reference measurements (GR). In woodland and forest situations, trees subject to their species phototrophic habit will grow towards light, potentially causing whole canopy movement away from the original root/stem interface location (Loehle 1986, Matsuzaki, Masumori et al. 2006). Common tree form observed when collecting GR data; a) a tree with the tree crown located immediately above the stem, with a broadly equal crown distribution b) a tree with a stem lean, causing the crown’s high peak to be away from the root/stem interface location. c) as b), but with an elliptical crown distribution along a dominant directional axis e.g. north-south. d) as c) with the elliptical crown distribution along a different directional axis e.g. east-west. The directional axis angles are potentially in any direction given the immediate environmental conditions around each tree crown. 227

Figure 39 Tree density per hectare, calculated on a per plot basis from 26 survey plots. The inset table shows additional descriptive statistics for the plots. The population of this woodland follows the reverse ‘J’ population distribution, indicative of a healthy, complex woodland (Kerr, Mason et al. 2002). 228

List of Abbreviations and Acronyms

1Q	First Quartile
2D	Two Dimensional
3D	Three Dimensional
ABA	Area Based Approach (delineation)
ALS	Aerial Laser Scanning
AMPS	Average Match-pairing Similarity index
ARBOR	Assessment of Remotely-sensed Biophysical Observations and Retrieval
ASNW	Ancient Semi-natural Woodland
AUC	Area Under Curve
CA	Chromatic Aberration
CHM	Canopy Height Model
CU	Control Unit
DAG	Directed Acyclic Graph
DBH	Diameter at Breast Height
Df	Fractal Dimensions
dGPS	Differential Global Positioning System
DHP	Densities of High Points
DR	Discrete Return
dSLR	Digital Single-lens Reflex
DSS	Dataset Size Similarity index
DSSy	Decision Support Systems
FW	Full Waveform
GCP	Ground Control Points

GIS	Geographical Information System
GNSS	Global Navigation Satellite System
GPS	Global Positioning System
GR	Ground Reference
GRD	Ground Reference Dataset
GUI	Graphical User Interface.
ha	Hectares
HAG	Height Above Ground
IQR	Interquartile Range
ITC	Individual Tree Crown (delineation)
ITC _{IWD}	Inverse Watershed ITC delineation
ITC _{MAN}	Manual Individual Tree Crown Delineation
ITC _{MST}	Variable Limit Local Maxima ITC delineation incorporating Metabolic Scaling Theory
ITC _{PHO}	Photogrammetric ITC delineation
<i>k</i> NN	<i>k</i> -Nearest Neighbour
LAI	Leaf Area Index
LiDAR	Light Detection and Ranging
m	Metre
MCD	Model Classified Data
MLS	Mobile Laser Scanning
MST	Metabolic Scaling Theory
NERC	Natural Environment Research Council
NERC ARF	Airborne Research Facility
NERC ARSF	Natural Environment Research Council Airborne Research & Survey Facility

NRC	Natural Resources Canada
NRMSE	Normalised Root Mean Squared Error
OVS	Overall Visible Spread
PAWS	Plantation on Ancient Woodland Site
PCA	Principal Components Analysis
PRT	Pulse Return Time
Q3	Third Quartile
RADAR	Radio Detection and Ranging
RGB	Red, Blue and Green
RMP	Representative Match-pairing
RMSE	Root Mean Squared Error
ROC	Receiver Operating Classifier
RS	Remote Sensing
RTK	Real Time Kinematic
RUS	Random Under-sampling
SfM	Structure from Motion
SLS	Satellite Laser Scanning
STRUCTURAL	Structural Condition of Trees Using Remote Assessment by LiDAR
^{sy} Tree	Synthetic Tree
TLS	Terrestrial Laser Scanning
TS	Total Station
UAV	Unmanned Aerial Vehicle
VLM	Variable Limit Maxima
χ^2	Chi-squared

XYZ X = Eastings, Y = Northings, Z = height,
 (After the Cartesian coordinate system,
 typically height above sea level)

List of Appendices

Appendix A - Ground Reference Field Guide	209
Appendix B - Using Fractal Analysis of Crown Images to Measure the Structural Condition of Trees, Supplementary Information	219
Appendix C - ARBOR: A New Modular Framework for Assessing the Accuracy of Individual Tree Crown Delineation from Remotely-sensed Data, <i>Supplementary Information</i>	225
Appendix D - Authorship Statements	230

1 Introduction

Modern tree managers attempt to retain trees in-situ for as long as is possible, whilst trying to balance the environmental, biodiversity and amenity values of trees. At the same time, tree managers have to minimise the potential for failure and limit the amount of risk exposure in any given situation, as people, property and infrastructure are considered ‘targets’ that are worthy of protection in tree-risk management terms (Lonsdale 1999). Ultimately, the failure of trees can lead to the damage of property, personal injury, or in the most severe cases, the loss of life (Mattheck and Breloer 1994, NTSG 2011, Leong, Burcham et al. 2012). The existing academic knowledge about trees, based on how they grow and reproduce, create and store their own food resources, and generate their woody structure at a cellular level, in reality, does little to aid the decision making process of a tree manager faced with a problematic tree that requires some level of remedial intervention.

Operational tree management often begins with a tree surveyor taking observations and limited measurements of the selected trees under investigation. Surveyors rely upon their personal interpretation of individual knowledge, experiences and understanding of the observations as presented on the day of inspection (Lonsdale 1999). Following rapid assessment and consolidation of both observed and assumed ‘facts’, the surveyor then has to prescribe a tree operation that has the tree subject to destructive interventions; including the removal of physiologically valuable limb structures, or even the entire removal of a tree, decisions based on a largely speculative field assessment methodologies (Barrell 1993, Norris 2007). However,

there is often a disparity between the academic knowledge of the subject, and the application of the knowledge on an operational basis. It is a commonly accepted axiom that while tree management has its basis in science (specifically biology, plant science and silviculture), the application of scientific knowledge in tree management is for the large part, a subjective and interpretive exercise (Norris 2007).

It is understood that the identification of structural change is a proxy for localised stress symptoms, and a red flag to tree and environmental managers when considering remedial interventions or other environmental management (Barrell 1993, Mattheck and Breloer 1994, Norris 2007, NTSG 2011). However, a significant limitation of current tree surveying practices are the significant logistical and resource costs of locating, surveying and repeatedly moving between the trees that are within the survey remit. Therefore, it is recognised that solutions to these problems are required that can combine recent advancements in academic knowledge, and can fulfil the requirement to have practical, repeatable methods that can be used to advance the understanding of the structural condition of trees. It is proposed that integrated remote sensing (RS) techniques can be employed in attempting to overcome these issues, including the use of discrete return (DR) aerial laser scanning (ALS) data captured at high spatial resolution and proximal photogrammetry techniques. These RS techniques enable investigations to be conducted at significantly different scales, from the wider landscape (ALS), down to the proximal investigation of individual trees using hemispherical imagery. In addition, there is the requirement to develop a method of identifying structural features that are symptomatic of stress induced structural change.

1.1 Thesis Aim and Objectives

This project aims to develop RS methods for the objective quantification of tree structural condition, for use in the assessment and classification of trees. This aim will be met by fulfilling the following objectives:

1. To develop an objective methodology to assess the structural condition of broadleaved tree crowns from proximal hemispherical photography.
2. To develop a technique for quantifying the accuracy of individual tree crown (ITC) delineation from remotely-sensed data.
3. To develop a methodology for categorising the structural condition of individual trees across a landscape scale from ALS data.

1.2 Thesis Structure

This research proposes to build upon earlier published works where high-end technology is used as a decision support tool to aid operational tree management. Specifically focussing on developing RS methods to capture tree data at a variety of scales, then categorise the tree structure using a combination of novel field and analysis techniques. This includes both proximal data capture and distant observations of the landscape, ultimately to develop methods that can be used to characterise the condition of many trees that are observable at the wide-landscape scale.

This research is informed by the limitations of the current and traditional tree observation and assessment practices, that are used extensively throughout forest management, arboriculture and forest science, that are based on outdated, historical field techniques. These techniques are shown to be frequently dependent on user subjectivity and the

consideration of the significance of the observations by the individual field surveyor. Therefore, it is likely that the subjectivity will lead to a range of different conclusions being reached by different assessors. The requirement is therefore, to develop observation and analytical techniques that are removed, insofar as it is possible, from the subjective process.

In order to develop solutions to this research problem, additional questions and technical considerations will also be addressed. During the initial experimental research phases, the research problem is considered; does the structural condition of trees change in a way that can be independently quantified and be used to discriminate between different types of structural condition? Furthermore, can it be demonstrated that the structural condition of a tree changes in such a way that can inform an objective assessment of the tree condition? These issues relate to the first objective which is considered in Chapter 4, which demonstrates whether it is possible to quantify the complexity of tree structural condition using proximal photogrammetry.

Following the investigation of tree structure, the next research problem addressed considers the technical issue of confirming exactly where trees are located when RS data is compared to field-captured, ground reference (GR) data. Tree crown delineation alignment is a frequently overlooked issue in RS investigations, yet it is commonly used in the validation phases during analysis. GR tree measurements are taken in the field to describe the geospatial location (Euclidean space) and physical attributes of the tree, such as crown location, crown orientation and crown extent. These biophysical attributes can also be modelled from a 3D point cloud and the ITC attributes delineated from the point data using specific delineation algorithms. However, there are frequently discrepancies between the GR data and the ITC delineations of tree location and attributes, and many

previous investigations rely heavily on the acceptance of arbitrary, linear distance thresholds or similar assumptions, to confirm ITC delineation agreement between the datasets without any further validation of how well ITC delineated tree crowns match what is expected in the GR data. Correspondingly Chapter 5, which addresses the second objective, describes the development of a new framework that can quantify the extent of the similarity between tree delineations in two types of delineation data, providing the opportunity to measure the amount of agreement, and therefore, provide a way for researchers to make informed choices regarding the most suitable delineation method to provides the highest level of ITC agreement between different datasets.

The final research problem being considered is the development of a method for assessing and categorising tree structure conducted from a remote perspective, and to consider the individual biophysical characteristics of the many trees that occupy the landscape scale view. This research problem is driven by the requirement to upscale and optimise limited resources into individual tree assessment, for all the relevant trees within the field of view. These trees would be typically surveyed by individual field operatives, at exponential financial and logistical costs dependant on the extent of the survey. The solution will need to consider how to assess individual trees at the landscape scale, compare the individual to an ideal reference model dataset, and subsequently classify these trees into groups that will identify trees both in good structural condition, while also identifying other trees that are in much poorer condition. This work will provide a landscape scale assessment technique that will allow field operatives to make informed decisions about where to concentrate remedial interventions, such as an area of identified poor condition trees. This work is considered in Chapter 6, which also addresses objective 3, and describes the development of a method to use ALS LiDAR data for the optimised, remote classification of tree structure.

2 Literature Review

This literature review is to provide an in-depth evaluation of the current research landscape relating to the RS of trees. Within this context, the review will focus on operational problems faced in tree management and the complications that arise from fieldwork methodologies, including practitioner influence on tree assessments. Furthermore, there is commentary on what tree managers or researchers need to help facilitate their decision making process, and how the development of different RS technologies and techniques are being used to understand the complexities of tree assessment and tree management. These issues will be addressed through the independent review of scientific and investigative works, where there will be a critical examination of the publications, including both academic and relevant grey literature, identifying the key research themes that are relative to this project. Finally, this literature review will also enable the identification and definition of pertinent terms and technical procedures that are of relevance to or used within this project, and that are referred to throughout this thesis.

2.1 The Problem of Subjectivity

Subjectivity is the philosophical influence of one's thoughts, beliefs, personal interpretation or personal feelings that can lead to a compromise in the integrity of the operational or experimental process. Ultimately, the perspective is that for scientific or factual observations to be declared subjective, the inference is that the findings are of no more valuable to the wider scientific knowledge than a simple commentary of individual opinion. This is especially pertinent when considering the assessment of

tree crowns or canopies from the ground. Harper, McCarthy et al. (2004) undertook an investigation into tree surveyor bias when the trees were viewed from two locations; firstly, from a ground perspective using binoculars as a visual aid, and secondly from an aerial perspective, where the trees were manually climbed using standard arboricultural work positioning techniques. The time taken and for identifying tree defects (stem and branch hollows) for both surveying methods was compared against one another and against a destructive sample for overall accuracy. It was found that manual climbing was more time costly but yielded higher accuracy (82% of defects identified), while ground surveys were comparatively quick, but much less accurate at identifying defects (44% of defects identified). Furthermore, Harper, McCarthy et al. (2004) observed a correlation between the number of tree defects identified and an increase in tree diameter at breast height (DBH) size ($r^2 = 0.77$), thereby suggesting that the larger more obvious defects were more readily detected, while subtler tree defects were not readily detected using manual observation from either vantage point. It can also be considered that the method of tree crown observation may introduce an amount of surveyor bias to the observations, where not all potential defects will be identified as a result.

Notwithstanding the physical and logistical complexities of direct manual measurement of the upper parts of the tree structure, historically, tree managers, foresters, tree surveyors and scientists have frequently relied upon simple field methodologies that are entirely subjective in their method and application. Jennings, Brown et al. (1999) discuss a widely used measure of tree canopy cover, where at a predetermined measuring point the forester or tree surveyor would look vertically upward at how much tree canopy obscures the sky, and subsequently estimate a percentage of tree canopy cover at that location. Jennings, Brown et al. (1999) also

describe that even when more advanced or scientific tree crown measurement techniques are used, there is often confusion in the supporting methodological literature about what is actually being measured. For example, in the measurement of direct or indirect light levels, the area of ground under the canopy cover, or the amount of sky obscured by canopy closure. Subsequently, the field practitioners have unanswered concerns about how the generated data can be used in operational best practice or to help inform the decision process for forest or tree management interventions (Jennings, Brown et al. 1999).

For managers of trees, forests, woodland and their immediate environment around the trees, there is often a requirement to undertake tree health and safety & site assessments or tree hazard analysis surveys (Lonsdale 1999, Redmill 2002, Britt and Johnston 2008, NTSG 2011). A fundamental element of this work is the process of assessing trees, identifying which parts are likely to be problematic or have the future potential for failure, a procedure which requires a large degree of guess work on behalf of the surveyor. Redmill (2002) describes a typical risk analysis procedure, influenced by subjectivity, “risk analysis is often assumed to be objective, and its results, risk values and the decisions based on them, to be correct. Yet all stages of the process, including the techniques used, involve subjectivity. Always there is uncertainty, the need for judgement, considerable scope for human bias, and inaccuracy. The results obtained by one risk analyst are unlikely to be obtained by others starting with the same information”.

Subjectivity within tree surveys and field-based observations is an ongoing concern within the tree management industry. In a study by Norris (2007), subjectivity has been demonstrated to influence the observations of several experienced tree surveyors,

each making independent observations and coming to different conclusions when assessing the same group of trees. A potential influence for these observational differences is that it is understood that tree managers or surveyors who are aiming to introduce some form of management intervention, may be influenced by the known objectives of the management, rather than from findings based on their judgement of the situation as found at the field site (JNCC 2004). Earlier recommendations by Ghiselin (1982), states that when attempting to reach sound environmental management decisions, the logical, objective perspective can successfully be reached by field practitioners working in groups, where objective statements can be externally judged by others and ultimately, a consensus can be agreed upon.

2.1.1 Subjectivity and Tree Management

Tree managers, foresters and tree surveyors are frequently lone workers due to the operational and logistical nature of the tasks required and, due to the physical locations of the tree stock under their management. The lone worker group is one that Ghiselin (1982) argues, are predominantly subjective thinkers. Interestingly, Ghiselin (1982) further argues that in the process of reaching a final judgement, such as a tree surveyor reaching a final decision on a tree's structural condition, the decision maker commonly balances all available elements of objective, science based views, with interpretive subjective views, and ultimately arrives at a final, blended, management decision. de Groot (1992), highlights that the process of externalising subjective opinions and supporting them with descriptive, scientific statements, such as when creating tree related risk reports or forest management plans, is an attempt by the report author to rationalise the subjectivity of their findings. de Groot (1992) consequently describes the conclusions from this blending process as being "subjectivity objectified". This view is also supported by Dana, Jeschke et al. (2013) who state that in an operational environmental management situation, managers

frequently make their intervention decisions based upon the process of “subjective reasoning” rather than by using the available scientific evidence.

Within the tree management industry, there have been various attempts to minimise the impact of subjectivity in tree assessments, several of which have been published which makes their use relatively common throughout the industry as the practices are adopted by many practitioners (Table 1). While these prescriptive methodologies have an aura of objectivity, and are frequently presented as such, there remains a large degree of guesswork and subjective assessment variables that are compounded in the methodological process as attempts are made to objectively quantify the tree assessment, while at the same time, relying on largely subjective inputs. Table 1 provides an overview of several of these commonly used methodologies:

Table 1 An overview of tree surveying methods currently in use in the forestry, arboriculture or tree management sectors. The word ‘objective’ refers to direct measurement or factually acquired data. The word ‘subjective’ refers to instances where a field operative uses interpretation, estimates or best guess methods to acquire ‘measurements’ for the survey method. This list is not exhaustive, but is representative of tree surveying methods frequently used in the UK, USA and worldwide.

Survey Type	Description	Method
BS5837: 2012	British Standard 5837 tree survey method, used in relation to trees on, or near, development sites. Completed at the pre-commencement development stage, this method identifies which trees	Categorical assignment to tree retention groups, which are determined via a subjective ‘quality’ assessments and are ranked in order of value or significance to the development. Some trees are

	are worthy of retention in the long term or are best removed for the successful implementation of the development. Used on single trees and woodlands.	immediately considered not worthy of retention. Expert use.
CAVAT	Capital Asset Value for Amenity Trees (CAVAT). A street tree valuation system where trees are considered as public assets which are valued in monetary terms. Used on single trees, tree groups or woodlands in an 'urban street' context (or similar).	Accumulative financial value determined by taking a DBH measurement and assigning to a predetermined 'value band'. Adjusted by subjective estimation of life expectancy, population density in the immediate area, and judgement on public amenity performance. Expert use.
CTLA Method	Council of Tree and Landscape Appraisers (CTLA) method. A street tree valuation method where trees are considered as private assets, quantified in monetary terms. Used on single trees, tree groups or woodlands in an 'urban street' context (or similar).	Accumulative financial value determined by taking a DBH measurement, then adjusted by several variables, including the subjective observation of general condition, location, species class (via a look up table of a variety of previously interpreted characteristics). Expert use.
ISA Method	International Society of Arboriculture (ISA) Tree Hazard Evaluation method. Production of a hazard rating to identify presumed failure potential, and therefore associated risk, from potential tree failure. Used on single trees, but can include single trees in tree groups or (potentially) woodlands	Accumulative hazard rating based on combined objective i.e. is the feature present Y/N? Plus subjective field observations, including; tree part most likely to fail, the estimated size of the part, and the potential significance of the target area. Expert use.
TEMPO	Tree Evaluation Method for Preservation Orders (TEMPO). A three-part field guide to decision making that considers; amenity, expediency and the decision process. Trees are assessed for suitability in being legally protected under a tree preservation order (TPO), a	Accumulative suitability score that requires the subjective consideration of a range of variables, including; qualitative descriptors of assumed condition, and subjective prediction of life expectancy, potential future visibility after land use change, and

legal tool under UK planning legislation used for the protection of trees near building development. Used on single trees, tree groups or woodlands.

estimation of foreseeable or perceived threats. Requires expert use.

i-Tree
(ECO)

i-Tree is a series of software suites and field survey methods used to provide both urban and forest, analysis and benefits assessment. I-Tree Eco quantifies tree structure and the environmental benefits and services, that trees offer a given area. Used on single trees, tree groups, woodlands/forests and up to wider landscape application.

Accumulative, model-based street tree value system that can use minimal GR input data to estimate tree structure, function and environmental benefits by using predetermined models. Subjectivity is compounded in the model as this allows users to run analysis with very limited input data fields, potentially only; local geographic and meteorological data, with tree species and DBH measurements. The system can also run the model using estimated DBH, not direct measurements, to output customised benefits and costs data. Also recommended for expert and non-expert use.

QTRA

Quantified Tree Risk Assessment (QTRA). A tree risk assessment method to 'quantify' the level of risk attributed to trees in their location.

Accumulative 'probable risk threshold' score, based on subjective field estimations including; target, size, and probability of failure. Licenced, expert use.

Notes: **Target** – refers to people or property that are worth of protection (from tree failure or similar), **Size** – often refers to the size of the part of the tree most likely to fail. A fundamental problem with this estimated value is that a best guess must be used to predict the future failure, and then also predict the future through guessing how big the failure part will be, and not measuring the potential failure part during the observational assessment. **Probability/Likelihood of failure** – a simple estimation from the field operative, based on their individual feelings of how quickly they predict a whole tree, or tree part, may fail. Arrived at by balancing an estimation of their feelings on probability, with a temporal prediction. **DBH** – tree stem diameter taken at breast height (either 1.3m or 1.5m). **Expert use** – typically this system is recommended for use by industry specific experts. **Non-expert use** – this system can also be used by interested laymen. **Licenced** – this system requires the attendance at a training course and the completion of a formal assessment, and ongoing subscription to the service to be used commercially.

The fundamental issue with tree management subjectivity is that objectivity is the gold standard that foresters, arboriculturists or tree managers strive to achieve in their

managerial decision-making. However, there is a large reliance on a scientific base knowledge that must be vastly interpreted and applied in many unique operational situations. Even where industry best practice, guidance or recommendations are followed, there remains a strong emphasis on the need for estimation, interpretation and assumption (Stewart, O'Callaghan et al. 2013). The current situation for tree managers is that despite many attempts at maintaining professionalism and independence from subjectivity, their judgements on the best way to manage their tree stock remains idiosyncratic. The current suite of available tools, at best, only provide a set of rules that it is hoped give sufficient clarity for the tree managers to be able to (subjectively) classify an observed set of circumstances. With prior knowledge, experience, and benchmarks provided using the surveying procedures, to arrive at the management recommendation of a 'reasonable' person (Norris 2007, Stewart, O'Callaghan et al. 2013). While this approach cannot be considered an objective procedure, it is widely accepted within the tree management industries that this approach is the accepted status quo, despite being inherently famed within a large amount of subjectivity.

2.2 The Development of Tree Surveying

Historically, the main purpose behind forest management was for the production of timber; through increasing growth yields and optimising harvesting for the maximum commercial return (Wulder, Hall et al. 2005). While this commercial element remains to some degree in the majority of forest and woodland management activities, in more recent times the underlying justification for forest and woodland management has shifted to include assessment of wildlife potential, recreation (both current and potential use), aesthetics (internal and external), biological and conservation requirements (Watson 2006). This development means that the basic forest inventory

assessment of growth patterns and tree volumes no longer provides the most suitable data for the management task. Operational level monitoring now has to include sufficient information on forest structure, the success of silvicultural intervention methods, habitat, biodiversity, hydrology and soil profiling, as well as the long-term planning of the entire production cycle (Jennings, Brown et al. 1999, Wulder, Hall et al. 2005).

As a result, many variables must be measured within trees or in forest stands, for the purposes of understanding growth patterns or enabling the prediction of future yields, or for understanding the type and availability of habitat within a given area. (Strahler, Jupp et al. 2008) describe that for a great number of forest inventory and management applications, the measurement of vegetation structure is essential to aid better understanding of the tree stock attributes. Latifi, Fassnacht et al. (2015), highlight that the expansive forests of central Europe are still monitored with conventional, large-scale terrestrial inventories, where the operational management of the forests is considered challenging by the rapid environmental changes as a response to natural disturbances and many “multilayer silvicultural systems” that are in use throughout the region.

Whatever the justification is for measuring trees, for a long time, simple, easy-to-reach measurements have been taken from trees, and these are used as the input variables into a wide range of allometric equations, looking to find predictive relationships. For example, the standard measurement of tree (or top) height and DBH (Dassot, Constant et al. 2011). Several studies show however, that frequently there are significant errors in the use of allometric equations in the measurement of trees, volume estimates or for other forestry applications that require later rectification

(Dassot, Constant et al. 2011, Ahmed, Siqueira et al. 2013, Mugasha, Mwakalukwa et al. 2016). Typical GR tree measurements taken at established plots or individual trees, used for the determination of tree characteristics, include the readily accessible features of the tree; species, location, overall height, DBH, crown height, crown extent, stem density at plot or location, and a general site description (Lovell, Jupp et al. 2003). It is believed that issues with large scale environmental management are being overcome with the increased use of Light Detection and Ranging (LiDAR) RS techniques. It is believed that this will reduce issues of what are considered to be time-costly, manual, field based methodologies that when sampled can only provide rough estimates of stand attributes, and cannot account for large amounts of variability in site terrain and vegetation changes (Gorrod and Keith 2009, Dassot, Constant et al. 2011, Hamraz, Contreras et al. 2016).

Lindberg, Holmgren et al. (2012), also advise taking detailed GR observations of control trees, as this data is typically geo-referenced and frequently considered a data ‘certainty’ upon which many environmental and vegetation models are based (McNellie, Oliver et al. 2015). Valbuena (2014) and Lovell, Jupp et al. (2003) also highlight that the majority of ALS applications for forestry investigations will require a combination of additional data sources, in particular field measurement or GR data, and for complex investigations, even co-registered combinations of ALS with terrestrial laser scanning (TLS) and acquired GR data are shown to be effective (Hauglin, Lien et al. 2014).

2.2.1 Plot Establishment for Site Surveys

The connection between undertaking forest surveying and establishing specific site areas or plots is well established in practice, as in particular, ALS LiDAR becomes ever more frequently used in forest inventory applications (Hauglin, Lien et al. 2014).

To acquire accurate geolocation information about survey plot location or the biophysical properties of the vegetation within them, i.e. GR data, it is important to determine the field information with high accuracy as the GR data will serve as a cross reference to the RS data. Subsequently, this requirement leads to the use of high-gain global navigation satellite system (GNSS) or global positioning system (GPS) to provide this information for plot level or stand level data acquisition (Latifi, Fassnacht et al. 2015). In a comparative study of characterising forest structure through the combination of ALS LiDAR, RapidEye satellite imagery and auxiliary environmental GR data, Dash, Watt et al. (2016) describe an extensive set of field measurements were taken from a network of 493 field plots (0.06 ha), across a total area of 180,000 ha (surveyed area 29.58 ha/0.01% of total area). The plot centres were located with high accuracy GPS and corrected using permanent, local, differential base stations. Common forest and tree attributes were recorded at each plot, specifically attributes that are regularly used in forest management and inventory operations e.g. DBH, tree height etc. Approximately 12% of these plots (60 sites), were randomly selected and used for later model validation purposes (Dash, Watt et al. 2016).

2.3 Decision Support Systems for Tree Management

Through a review of decision support systems (DSSy) used in the European forest management sector, Segura, Ray et al. (2014) identified that the majority of operational problems causing DSSy to be employed are fundamentally related to management issues of temporal and spatial scales, and the requirement of meeting the specific objectives of decision makers or shareholders. Their investigation identified that simulation and modelling is used in 63% of instances where the DSSy is employed in a spatial context, and to optimise the application of statistical solutions with known management problems, DSSy are used in 60% of instances within the

study sample. Furthermore, Segura, Ray et al. (2014) also highlight that forest managers frequently use analytical technology to support the DSSy, with nine out of ten implementing a DSSy with other associated technologies. The DSSy would be typically augmented with a standalone database for record keeping, within an integrated geographical information system (GIS), or would use both systems concurrently.

DSSy are also used in forest and woodland management to aid the decision process for specific tree management interventions. To generate the most economically viable results concerning the harvest of trees, Accastello, Brun et al. (2017) have developed a spatial economic model to maximise the financial return of harvesting. The model identifies a range of potential options for the harvest site, and through applying a multi-criteria decision-making metric, a range of harvesting strategies are considered, and the most cost-effective approach is selected for a prescribed area. Due to the very fine financial and operational margins that tree managers and foresters work with, this study highlights the industry's need to be able to apply higher order decision models to assist in their landscape management and forest planning through using an operational optimising tool, which lead to the minimisation of expenditure or unforeseen costs to the operation. Furthermore, in the general field of wildlife conservation, research by Dana, Jeschke et al. (2013) showed that for the development of more effective environmental management, multi-criteria DSSy are considered essential in providing environmental managers with the correct agenda or framework to prioritise their most essential works in an effort to drive up efficiency. In addition, Dana, Jeschke et al. (2013) also discuss that the application of DSSy over larger geographic areas is preferential, and conclude that greater efforts are needed to develop new DSSy approaches, as only having a limited suite of management tools,

is believed to limit the potential choices for management and potentially leads to management intervention bias.

2.4 Tree Structure

Trees are complex, biological structures that are influenced by a variety of internal and external forces, which combine to produce an adaptive response in the tree as a defensive reaction to the stress. Without the ability to alter the form and shape of the structure, the biological mass of the tree would inevitably succumb to the combined extent of the forces, and eventually may suffer a catastrophic structural failure event which could prevent the tree in successfully continue its physiological processes. Ultimately, inflexibility of this type would lead to the tree's death (Mattheck 1998, Lonsdale 1999, Niklas 2001). The stresses that effect trees often persist over long periods of time and their effects are not solitary, but have a combined impact on the tree's composition and physiological structure (Niinemets 2010). As a response to these stresses, the most significant of which are considered to be gravitational force, internal growth stress and external wind forces, trees utilise adaptive strategies to minimise these effects through a process of self-optimisation (Niklas 1992, Mattheck and Breloer 1994, Mattheck 1998).

2.4.1 Dynamic Change in Tree Structure

Notwithstanding the canopy changes that occur in trees as a response to environmental stresses, some tree species also undergo seasonal changes, particularly as observed in temperate, broadleaved trees which undergo the annual leaf abscission. As Bournez, Landes et al. (2017) describe, the accurate reconstruction of tree structure from three dimensional (3D) point clouds may rely upon techniques that require the clear line of sight to the tree crown structure. When the deciduous branches begin to bear leaves, new shoots and flowering structures, careful consideration has to be made

to understand the significance of how the changes in the tree structure will affect the 3D analysis. Commonly, RS research is undertaken that investigate trees at either end of the canopy spectrum; either investigating trees in a leaf-off condition (Korpela, Orka et al. 2010, Lu, Guo et al. 2014, Ayrey, Fraver et al. 2017), or undertaking tree research that investigates trees in a leaf-on condition (Brandtberg 2007, Ørka, Næsset et al. 2009, Bouvier, Durrieu et al. 2015).

However, in a study by White, Arnett et al. (2015) which investigated the validity of investigating forest structure attributes as defined by investigative metrics and ALS data, found that the use of leaf-off data for large area investigations enabled the accurate estimation of forest attributes for both coniferous and broadleaved trees. Further, White, Arnett et al. (2015) also concluded that analysis that uses a mixed dataset of both leaf-off and leaf-on data leads to large root mean squared error (RMSE) values and bias in the investigation, and therefore the mixing of the data and model types should be avoided, a view also supported by Bouvier, Durrieu et al. (2015). Few studies have sought to understand the significance of the structural change in tree crowns as a consequence of the incremental growth of buds, new shoots or fruiting bodies as Bournez, Landes et al. (2017) describe.

2.4.2 Phenotypic Tree Structure

In a study by Korpela, Orka et al. (2010) attempts were made to improve the potential for the identification of tree species from ALS LiDAR using a bidirectional reflectance analysis. Using intensity values, Korpela, Orka et al. (2010) were able to successfully determine the most regionally important species in southern Finland; scots pine, Norway spruce and birch with an accuracy of 88-90%, however, the same study reported that in some instances, the classifiers used had difficulty determining the differences between spruce and birch. The results suggested that the overall size

of the tree structure and the tree size in comparison to neighbouring trees was a deterministic factor, which was compounded by the size of other key elements in the structure, specifically; leaf size, orientation, and overall crown density. This demonstrates that there is difficulty in classifying smaller trees, or trees with naturally fine or sparse crowns, with ALS LiDAR because of complications associated directly with the physical tree structure. In research using ALS LiDAR for the detection of individual trees from within a larger forested area, Rahman and Gorte (2008), describe that the physical characteristics of the tree structure enables the identification of tree locations due to the increased density of the tree crown around the central stem area. The increased structural complexity at the branch, stem interface is recorded as an area of increased LiDAR point density in the higher parts of the crown; densities of high points (DHP).

Rahman and Gorte (2008), further explain that the structure of the crown causes this phenomenon, as returned LiDAR pulses above a specified height threshold will be denser in the centralised area of a crown, and the density diminishes towards the crown edge. Furthermore, Rahman and Gorte (2009) identify that due to the increased surface area at the central point of the crown, even with a range of differing crown shapes including; conical, circular and flat topped, the rule holds true and provides opportunities to estimate the centralised location of a tree crown (Rahman and Gorte 2008). Therefore, it can be stated that due to measurable differences in tree crown structure complexity, it is possible to derive investigative metrics to determine geospatial observations about subject trees.

2.5 The General Principles of Remote Sensing in the Environment

Remote sensing is understood to be one of the most significant developments for environmental research and operational environmental management (Vauhkonen, Maltamo et al. 2014). Within research focussing on vegetation and the environment, RS is historically associated with studies that focus in the optical region, particularly aerial imagery captured from a satellite platform (Jones and Vaughn 2010). However, RS has a much broader range of applications and varieties of RS techniques are used across a wide range of disciplines and for vastly differing research purposes. From the quantification of entire global scale biomes, to management planning for forest ecosystems, the completion of woodland inventory to the investigation of individual tree characteristics (Vauhkonen, Maltamo et al. 2014). To provide researchers with a suite of investigative tools that can be used to successfully scrutinise the environment at a variety of possible magnitudes, it should also be recognised that RS is not simply limited to optical earth observation imagery from satellites. In its fullest sense, RS also includes techniques for data collection at a host of more proximal distances, and, with a range of unique tools other than those used for the capture of simple photographic imagery (Jones and Vaughn 2010). These modern tools include laser scanners, hand-held detectors and sensors, mobile ranging devices, all providing researchers with access to a variety of potential investigations, at ever decreasing proximities than from satellite platforms alone. This makes the use of RS more accessible and often, significantly cheaper to undertake than in the early years of RS research (Jones and Vaughn 2010, Westoby, Brasington et al. 2012, Vauhkonen, Maltamo et al. 2014).

2.5.1 Remote Sensing and Trees

Due to the strong relationship between vegetation and its reliance on its immediate environment for its ability to maintain physiological process and ensure plant survival, there has been an increasing recognition of the need to develop a range of investigative tools for the quantification of vegetation in the wider environment (Jones and Vaughn 2010). The drive for which can be seen through the many increasing needs to satisfy international or national environmental agreements and treaties (Vauhkonen, Maltamo et al. 2014), that require members states to explicitly quantify the benefits of their environmental management endeavours in a global context. For example, Mitchard, Feldpausch et al. (2014) aimed to improve estimates of forest carbon density from the Amazonian forests, where ground vegetation was surveyed on a multi-plot basis, and pantropical biomass maps were created to identify areas of greatest forest carbon capture. The focus of this study was to understand the distribution of the Amazonian forest carbon stock and its role in the global carbon cycle by comparing newly acquired RS data with previously published vegetation carbon maps developed from field sampling and the calculation of allometric projections in the region.

Mitchard, Feldpausch et al. (2014) showed through the use of RS techniques, the forest carbon density mapping was either over, or, under estimated by +/-25%, dependant on the specific region. Furthermore, that the RS techniques captured greater information about the changes in the vertical tree structure, biomass and the resulting carbon stock, than was identified in the pantropical forest biomass maps that were derived from field survey sites alone. Mitchard, Feldpausch et al. (2014) also recommend that to achieve the best insights in to the forest composition, a combined approach of acquiring RS data with a network of carefully established field plots, will

enable the calibration and validation of the RS data and lead to greater accuracy within similar studies. Research of this type highlights the suitability of using RS for large-scale vegetation investigations and the potential for accuracy improvements when acquiring environmental data. In particular, when research is dealing with the measurement and analysis of trees, and the upper parts of the tree are difficult to measure with certainty from the ground.

A review of the reconstruction of tree structure from LiDAR acquired 3D point clouds, highlighted that while tree structure is composed of varying branches, all of different length, diameter and order, that the arrangement of tree structure components is extremely complex. Mitchard, Feldpausch et al. (2014) also observe that this complexity increases when the trees are in a leaf-on condition, due to the leaves obscuring parts of the tree crown structure. Furthermore, this effect also leads to complications in understanding the tree crown geometry and may affect the ability to successfully recreate 3D tree models.

2.5.2 LiDAR

LiDAR is a RS technology that uses laser scanning to gain high resolution information about scanned surfaces or objects, and can capture data at a range of scales. LiDAR systems are principally similar to the more well-known radio detection and ranging (RADAR), however, LiDAR typically operates within the optical or near-infrared spectrum (Liang, Li et al. 2012), and is frequently used for individual tree or large area forest investigations (Vauhkonen, Maltamo et al. 2014). The basis of all active LiDAR systems is that data is captured by emitting a short duration laser light pulse towards an area or object of interest, whereas passive LiDAR systems use solar radiation to illuminate the scan scene (Killinger 2014). Lasers are classified by their operational wavelength and whether they are small footprint, DR or full waveform

(FW) systems. A key difference between the DR and FW is that all of the waveform is available for interrogation within FW, whereas as Murray, Blackburn et al. (2014) describe, DR point clouds acquire a general impression of the subjects structure, however, elements of the structure will not be represented in the dataset due to the gaps in the DR point cloud. Furthermore, Murray, Blackburn et al. (2014) state that there are opportunities to investigate the relationships between the data points to enable the investigation of additional elements of tree structures.

For most LiDAR systems, the operational waveform is in the visible, to near infra-red wavelength range, typically 1064nm to 1550nm, while some bathymetric LiDAR systems used for the penetration of water, operate at wavelengths ~532nm (Wang and Philpot 2007, Jones and Vaughn 2010, Danson, Gaulton et al. 2014, Killinger 2014). To capture data about the subject of interest, the laser scanner's sensor measures the difference in time between the emission and return detection of the pulse, known as the pulse return time (PRT). Using the speed of light and knowledge of where the scanner is in time and space with high accuracy GPS, LiDAR systems function in a similar fashion to a laser rangefinder. The time difference between the emission of a pulse, the interaction with a surface and then the receiving of the pulse back at the LiDAR sensor is measured to give information on the distance to an object. Therefore this shows the pulse position in 3D space through the computation of co-ordinates (Jones and Vaughn 2010, Vauhkonen, Maltamo et al. 2014). As described by Baltsavias (1999), this principle is summarised at equation (2.1).

$$R = c \frac{t}{2} \quad (2.1)$$

Where R is the range or distance to the object, c is the speed of light (~299,792,458 metres/second), and t is the time interval between the emission and return of the pulse (in nanoseconds) (Baltsavias 1999). Similarly, how frequently the LiDAR measures the pulse is the range resolution, which is the function of the length of the emitted pulse and the frequency of measurement intervals, expressed at Equation (2.2):

$$\Delta R = c \frac{\Delta t}{2} \quad (2.2)$$

The range resolution will influence the density of the LiDAR pulse data points that are available in the subsequent 3D point cloud (Kovalev and Eichinger 2005). When accompanying the range that the pulse is being emitted over as an experimental variable, the range resolution will have a significant influence on the data richness of the final dataset (Liang, Li et al. 2012). Valbuena (2014), describes that for operational purposes, there is a trade-off between the range resolution and the subsequent extent of the detail within the survey that can be achieved. At equation 2.3, the amplitude of the returned laser pulse is described as:

$$P_R = \frac{P_T G_T}{4\pi R^2} \times \frac{\sigma}{4\pi R^2} \times \frac{\pi D^2}{4} \times \eta_{Atm} 2\eta_{Sys} \quad (2.3)$$

Where P_R is the power of the returning pulse, P_T is the power of the transmitted pulse, G_T is the antenna transmitter gain, σ is the cross section of the object, and D is the receiving antenna aperture. η_{Atm} is the one way atmosphere attenuation coefficient, and η_{Sys} is the transmission coefficient of the LiDAR optical system (Baltsavias 1999). As the laser pulse interacts with the scanned surface and returns to

the scanner, the location, distance and frequency of the returned pulse is computed, along with other geographic and operational information, including the return number, the number of returns from each location, pulse intensity, scan angle, scan direction etc. This pulse emission and return process, or PRT phase, is repeated many times over in a single scan, potentially in the order of millions or higher, dependent on the overall scan area and resolution. Each data point can have attributes applied in post-processing and through the classification of the data, such as running algorithms identifying when a data point is returned from a ground, or above-ground, location (Jones and Vaughn 2010, Kraus 2011, Killinger 2014, Vauhkonen, Maltamo et al. 2014).

Ultimately, the data produced during a LiDAR investigation is a 3D point cloud of varying possible densities (dependent on the equipment calibration), where each data point contains XYZ coordinates and a range of accompanying data attributes that enable detailed spatial analysis to be undertaken. For these reasons, LiDAR is commonly used as an investigative tool for large geographical areas due to the opportunity to capture large amounts of attribute data, at high spatial resolution and high positional accuracy (Vauhkonen, Maltamo et al. 2014). Killinger (2014), describes the requirements for LiDAR based geographical mapping surveys of hard targets, e.g. tree structure, that the resulting data has such a high degree of accuracy it is similar to US geological surveys. Correspondingly, the US based National Institute of Standards and Technology, have created a set of calibration standards for LiDAR surveys of this type. Similarly, the Government of Canada under their office of Natural Resources Canada (NRC), has also defined a minimum specification document for the increase in consistency and measurement accuracy for ALS LiDAR

acquisition, aiming to improve collaboration and integration in cross-border ALS LiDAR data acquisition campaigns (NRC 2017).

Fundamentally, LIDAR is an elegant process by which many objects can be geospatially measured concurrently. However, the mechanism by which this is accomplished, and in particular the platform upon which the LIDAR measurements are captured, is a significant element of the LiDAR investigation. LiDAR sensors are predominantly carried via one of four platforms, either upon; an orbiting satellite, an aerial platform, a terrestrial platform (e.g. surveyors tripod), or via mobile systems (Jones and Vaughn 2010, Prost 2013). Satellite laser scanning (SLS) has the advantage of being applied to the largest-scale investigations, such as biomes or the full geographical extent of tropical forests due to the ability to capture data from a high vantage point (Hansen, Stehman et al. 2008). An operational drawback to this method however, is that due to the vast distances between the scanner and the Earth's surface, the lateral distance between the data points in the 3D point cloud are also frequently large, as Otepka, Ghuffar et al. (2013) describe, potentially up to several hundreds of metres for certain satellite RS techniques e.g. satellite laser altimetry.

ALS is predominantly undertaken from fixed or rotary-wing aircraft, upon which the LiDAR scanner is mounted, with accompanying processing computers and high-gain GPS. TLS, as the name implies, is undertaken from a ground based position, commonly fixed on a surveying tripod that can be readily moved between different locations, thereby allowing several scans of a stationary, central object to be co-registered at a later point. Mobile laser scanning (MLS) systems are either affixed to moving vehicles, e.g. all-terrain vehicles, road vehicles, trains etc., or can be mounted on backpacks while a surveyor walks across a survey site. Some MLS systems can be

held in the hands as the surveyor walks around an area of interest, while the scanning procedure is completed, such as the GeoSLAM Zeb1 3D laser scanner. All these differing scanning platforms and procedures will influence what the investigation can reveal, as the scale of the investigation also determines the ideal scanning platform to be used. Utilising a common RS approach, Lindberg, Holmgren et al. (2012) highlight that many attributes of individual trees can be readily estimated from both ALS or TLS platforms, provided that the generated point cloud has the required point density from either the correct resolution at the time of scanning or via overlapping repetitions of scan swath.

TLS is more frequently being applied to undertake the measurement of a variety of forest inventory measurements, including; tree height, dbh, stem density for a defined area, basal area assessment, and for the character assessment of tree canopies or crowns, with; gap fraction assessments, 3D modelling and virtual projections, and models of foliage distribution (Dassot, Constant et al. 2011). An advantage of using a TLS LiDAR based system is the potential for rapid deployment of the equipment, thereby enabling the opportunity for relatively easy temporal studies on a short return period, for the study of change detection within a subject, as is the approach found in the majority of current change detection studies that utilise a TLS approach (Telling, Lyda et al. 2017). Olschofsky, Mues et al. (2016) undertook research into the use of TLS for the quantification of above ground biomass (AGB), and in particular to improve the assessment of AGB over traditional methodologies, with the view that TLS can measure AGB with a higher degree of precision and accuracy. This higher measurement accuracy was exploited in the research of Raumonen, Kaasalainen et al. (2013) where TLS was used to reconstruct flexible cylinder models of above ground tree structure. This method was further developed by Åkerblom, Raumonen et al.

(2017), where quantitative structure models (QSM) were used in the automatic classification of selected tree species. The QSM method for the reconstruction of tree structure is dependent only on the distribution of the 3D points of the tree and is not influenced by other scan attributes. The potential of the QSM method to classify tree species based upon structural characteristics indicates the potential to utilise a TLS based approach in the characterisation of tree structure for condition assessment purposes.

Unfortunately, not all operational LiDAR systems are without potential difficulties. Through comparing a range of laser scanning scales and LiDAR pulse resolution, Wimmer, Schardt et al. (2000) demonstrate the advantages of achieving data rich investigations with very high resolution SLS scans. Wimmer, Schardt et al. (2000) also show that operational problems regarding missing information within forest scans can be overcome by increasing point cloud density, which further improves the performance of forest surveys and inventories. Of particular benefit to forest based investigations, is the potential to use ALS LiDAR data to georeference large forest areas in a single operation and the ability of the ALS LiDAR to penetrate the canopy and provide previously unseen information about the forest environment (Valbuena 2014). Hilker, van Leeuwen et al. (2010) highlight that the spatial resolution of the laser scan being undertaken needs to be considered appropriate to the scale or area of investigation, specifically that TLS generally has a higher point density per scan when compared to ALS.

However, the TLS range or coverage area is limited by the capacity of the sensor, potentially to only a few hundred metres. This factor would have a deterministic effect on the laser scanning method that an investigator could choose for their study, and

subsequently, would also impact on the scope of the study and the experimental question that it would be possible to investigate. Valbuena (2014) describes that although ALS LiDAR data has a vast potential application for forest based investigations, there is limited potential information that can be learnt regarding the species diversity of a forest site, and at the time of writing, only limited applications for the determination of forest health.

2.6 Photogrammetry

Photographic RS methods for capturing information about the environment, and then taking measurements from the images, has been used for many years (Evans and Coombe 1959). In recent times a comparatively cost effective RS methodology has developed with the capture of aerial imagery from high-quality, off-the-shelf digital cameras and readily accessible aerial platforms such as unmanned aerial vehicles (UAVs, also referred to as ‘drones’ particularly in nonprofessional terms). Leberl, Irschara et al. (2010) identify that from the development of the use of LiDAR based point clouds; there has been extensive sector wide discussion as to the efficacy, throughput and cost effectiveness of the use of photogrammetry, for vegetation investigations. However, Leberl, Irschara et al. (2010) also highlight that for “street-side” investigations, photogrammetric methodologies retain some advantages over LiDAR based approaches. Westoby, Brasington et al. (2012) describe modern photogrammetry techniques as providing the ability to capture high-resolution datasets from cheap, portable surveying platforms and the use of ground control points to enable 3D scene reconstruction, particularly advantageous for providing access to otherwise inaccessible or remote field sites. Furthermore, Westoby, Brasington et al. (2012) also state that there is great potential for photogrammetry methods to be used in many geoscientific or earth observation applications, in areas

with complex topography, and using image capture techniques that utilise multiple overlapping photographs. In terms of mathematical-geometric analysis, the content of an image is considered an idealised model, not a true representation of reality. This is due to unavoidable lens, camera and photographic errors that arise when using photography and photogrammetry equipment; therefore, these must be accounted for in order to enable the highest levels of accuracy to be achieved (Kraus 2011).

Liang, Jaakkola et al. (2014) identify that the use of un-calibrated hand-held digital cameras for individual tree investigations, can provide highly accurate photogrammetry derived data that is comparable to scanning individual trees with TLS. In addition, Liang, Jaakkola et al. (2014) report an 88% mapping accuracy (commission score) for image based point clouds of trees, when compared to GR tree maps. Similarly, for the comparison of leaf area index (LAI) assessment Lovell, Jupp et al. (2003) identified that there was a high commission rate between the modelled LAI from TLS acquired data, and the LAI values that were calculated directly from hemispherical imagery assessments, thereby suggesting that the use of hemispherical methods can be considered as accurate as laser quantified measurements.

2.6.1 Proximal Hemispheric Imagery

Not all photogrammetric investigations are conducted from an aerial perspective at distance. Proximal RS with digital photography is a widely accepted “indirect optical” method for assessing and quantifying tree crown characteristics (Chianucci, Chiavetta et al. 2014, Chianucci 2016), particularly due to the ease and relatively low costs of which appropriate equipment such as digital single-lens reflex (dSLR) cameras, can be obtained. In order to reduce complications of technical problems and erroneous data collection for investigations as LAI, Jonckheere, Fleck et al. (2004) describe that the use of hemispherical imagery is a preferred solution. However, Jonckheere, Fleck

et al. (2004) also recognise that there needs to be improvements in the technique in order for hemispherical imagery to be used as the preferred tool for this type of investigation. Nonetheless, Jennings, Brown et al. (1999) state that the way to achieve the most thorough measure of the extent of canopy closure is by taking a photograph at a specified measurement point beneath the crown with a 180° fisheye lens adapted camera. The resultant image is to be thresholded to distinguish between tree crown structure and the sky. Furthermore, at the time of writing, Jennings, Brown et al. (1999) state that hemispherical imagery is the “most accurate method of estimating canopy closure” when operational issues such as adverse lighting conditions are overcome.

Chianucci and Cutini (2012), describe that hemispherical images from proximal photogrammetry are maps of canopy openings or closures depending on the requirements of the study, and provide rich insights into the assessment of heterogeneity within tree crowns. Chianucci and Cutini (2012) also state that proximal photogrammetry using a zenith angle range of 0°–15°, provides ideal opportunities for the “management and monitoring” for tree canopies, particularly in applications of repeated routine canopy parameter assessment in tree inventories. Sanchez-Gonzalez, Cabrera et al. (2016) also used proximal imagery techniques to undertake data capture for forest inventories. Basal area, mean tree count and mean diameter were all assessed using hemispherical imagery, where structural parameters of the tree crowns were extracted from stereoscopic images.

2.6.2 Landscape Scale Photogrammetric Investigations

To improve the alignment of aerial imagery during photogrammetric investigations of forested landscapes is a difficult task due to the poor match of the spatial

distribution of grey-scale pixels in aerial images and the spatial distribution of the point cloud achieved with ALS LiDAR data. In the approach described by Lee, Biging et al. (2016) tree tops are extracted through image processing and an “extended-maxima transformation” with LiDAR data. This methodology was required due to the limited spatial information that is available from the aerial image, however, with the addition of the LIDAR data, enabled an improvement in accuracy and allowed the alignment of aerial images to single-tree level. Lee, Biging et al. (2016) believe that this combined approach can enable the use of aerial images to be used in fine resolution change detection investigations and enable the extraction of biophysical properties of trees due to the enhancement with LiDAR. Gobakken, Bollandsas et al. (2015) used a comparative method to investigate tree structure with both aerial imagery and small footprint LiDAR, by extracting a series of biophysical properties of forest trees, including: canopy height and density. The study showed that although forest tree structure can be assessed using an aerial photogrammetric approach, that the best overall results were actually obtained via LiDAR. Interestingly however, photogrammetric analysis performed better than the LiDAR when assessing sparse crowns and smaller or younger trees from within the wider dataset (Gobakken, Bollandsas et al. 2015).

2.7 Unique Programming Requirements of RS Data

When working with large amounts of RS data, preparatory data processing should be completed before analysis. For example, with LiDAR data, the visualised 3D point cloud will offer some recognisable impression of the scanned scene as a model representation. However, to conduct meaningful analysis of the scanned scene, Otepka, Ghuffar et al. (2013) explain that individual features will need to be located within the scene which may also require elements of the scan to be deleted.

Additionally, Otepka, Ghuffar et al. (2013) state that to draw out essential scene evidence, multiple scene features will have to be classified according to reference type and entire feature sets assigned to feature classes; for example, ground data points, above ground data points, buildings etc. It is also worth considering that the processing of LiDAR data, or indeed working with RS data in general, is computationally demanding due to the large bit size and complex file structures of the data. This suggests that working with RS data for classification or analysis requires an optimised and efficient approach (Yan, Shaker et al. 2015).

2.7.1 Canopy Height Model Data Pits

ITC delineation is the procedure wherein trees are individually segmented from RS data, and the tree locations and crown extents are described. An important element of the delineation procedure is the creation of a canopy height model (CHM). This height map is fundamental for the subsequent acquisition and analysis of forest inventory information from RS data (Jones and Vaughn 2010, Khosravipour, Skidmore et al. 2014). However, it is considered that their efficacy is often dependent of the characteristics of the forest structure being studied (Forzieri, Guarnieri et al. 2009). Traditionally, CHMs are a pixelated two dimensional (2D) image created from 3D data. The CHM is the underlying model used to identify vegetation canopy height values in forest inventories or analytical procedures. Ben-Arie, Hay et al. (2009) describe that pixelated CHM's can reveal unnatural 'pits' within the tree canopy, which are formed as a result of pixels having a much lower digital value than any of the other neighbouring pixels.

Furthermore, Ben-Arie, Hay et al. (2009) also describe that the pit formation can be as a result of several factors, such as errors in data acquisition or in post processing,

although it is difficult to precisely define where these errors arise from. The impact of the data pits is a noisy data structure in the subject canopy, which Ben-Arie, Hay et al. (2009) describes impacts on the success rate of ITC delineation. A new methodology outlined by Khosravipour, Skidmore et al. (2016) can successfully remove the CHM data pitting. This solution requires that the LiDAR points are altered to be disc shaped, or ‘splatted’ to represent a known area within the canopy, the benefits of which are twofold. Firstly and most importantly, the data pits are removed from within the tree crown shape where the LiDAR pulse has penetrated deeply within the tree crown, and secondly, the splatted CHM has an outer appearance that is visually representative of an expected tree shape when viewed from above. Figure 1 compares two CHM’s of the same field plots that were created using the two techniques.

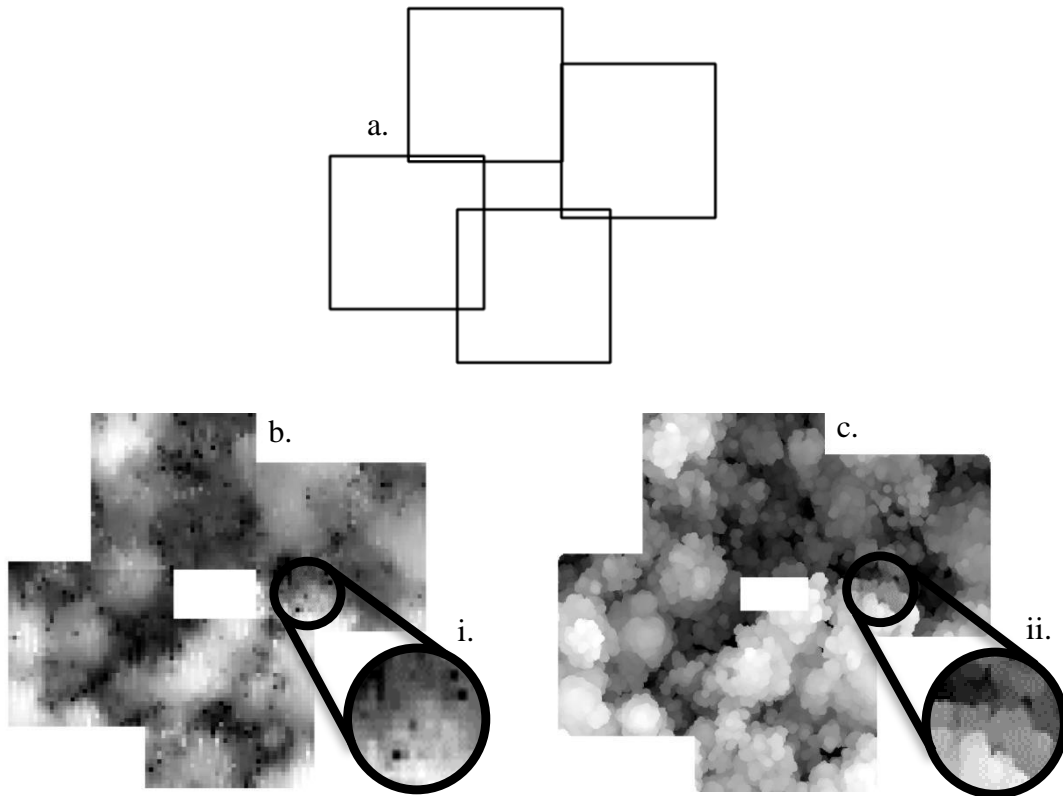


Figure 1 A visualisation of CHM's from LiDAR data, using two different techniques. a. The outline of four woodland survey plots. b. typical pixelated CHM as used in many RS studies, with data pitting that causes analysis errors (Ben-Arie, Hay et al. 2009) (circular inset i, poor tree canopy resemblance with data pits as black pixels). c. a novel “splatted” CHM, closely resembling tree canopies, with data pits eliminated (Khosravipour, Skidmore et al. 2016) (circular inset ii., tree-like canopy edge with no data pits). The four conjoined square shapes are four separate field survey plots, with each plot measuring 20x20 metres (400m²) on the ground.

2.7.2 Data Threshold Manipulation

To manage the complexity of dealing with the wide range of data in the ALS LiDAR acquired point clouds, several studies will frequently use arbitrary threshold levels as cut off points or data filters. For example, Kandare, Ørka et al. (2017) describe the removal of all data points below 1.5m for the removal of the lower strata vegetation, and to horizontally slice the remaining data at three additional threshold levels. Strîmbu and Strîmbu (2015) use a graph based approach to define the data cut-off threshold, and eliminate ground data and lower vegetation by analysing the height

histogram for the LiDAR points, however, Strîmbu and Strîmbu (2015), do not provide further explanation of how the thresholds are determined. In the study described by Ayrey, Fraver et al. (2017) overlapping segmented horizontal layers from ALS LiDAR and identifying the areas of highest point density were used to locate tree tops, along with a localised maxima algorithm. However, where there were minimally overlapping data clusters, <5 overlaps, these were considered to be frequently representative of undesirably small trees for this study. The smaller overlapping trees were described as being typically representative of trees less than 5m in height, and therefore a combined threshold of data point density and height were used as cut-off thresholds to exclude these trees from the study.

Swetnam and Falk (2014) use the application of metabolic scaling theory (MST) and applying variable limit maxima (VLM) to achieve ITC delineation. In an approach guided by observations of maximal tree crown radii of the largest trees as found in their field data Swetnam and Falk (2014), apply an exhaustive searcher routine to identify potential neighbouring trees within a specified distance threshold of a target tree. The k -nearest neighbour (kNN) search determined that potentially neighbouring trees had to be located within <21 m of the target tree. The field observed GR data showed that the largest trees within the field study area had a tree crown radii of ≤ 7 m, hence, using a justification based on field acquired GR data, and the distance search area was limited to an area within three times the biggest known tree crown radii.

2.7.3 Weighting as a Data Filter

Weighted hierarchies are used to define edge properties and in attempt to quantify levels of cohesion between corresponding properties in a directed acyclic graph (DAG) based attempts to segment trees from ALS LiDAR Strîmbu and Strîmbu (2015). This method looks for corresponding properties between a grey-level raster

height image, and a LiDAR point cloud. Through applying a weighting to data properties considered to be of greater significance, tree segmentation is achieved. The segmentation algorithm identifies the number and location of cells that span a potential tree hierarchy (location), and identifies the number of corresponding cells in the tree top area between the two datasets. Through creating a higher level DAG using the spatially rich data, a root and node patch is created. Where the corresponding elements of the patch agree on weighted elements of a predetermined cohesion score, i.e. logical, quantitative, spatial relationships between the patches, the edge weight is calculated and ITC delineation is assigned (Strîmbu and Strîmbu 2015). Strîmbu and Strîmbu (2015) conclude that the use of a weighted mean for quantified cohesion scores increased the potential to have a ITC delineation method that can be adapted to suit the complexity of different RS or LiDAR data sets.

2.8 Aerial Laser Scanning

Within the RS and environmental management communities, there is a general confidence in the potential of the use of ALS LiDAR to assist in the management of the environment, and in the scientific challenges and research opportunities that this presents (Lu, Guo et al. 2014, Zhao, Suarez et al. 2018). Particular to the characterisation of forest resources using ALS LiDAR methods, Vauhkonen, Ene et al. (2012) state that LiDAR investigations fall in to one of two main categories. Firstly, area based investigations that use ALS LiDAR for capturing data at the forest stand level, or individual tree assessments method, where single trees are scrutinised as the focus of the investigation. A review by Koenig and Höfle (2016), describes that in the majority of studies that classify trees from LiDAR isolate and extract individual trees as an initial phase, predominantly from CHMs. Data filtering commonly focusses on pulse returns and the index of returns with some biophysical tree

properties such as height. Hierarchical and non-hierarchical rules are also applied, along with measures used to exclude data noise (Koenig and Höfle 2016). The review also describes that in the majority of ALS LiDAR research, “species-specific feature behaviour” and “single feature performance” of individual trees are typically considered in general classification terms, while the ALS LiDAR studies tend to focus on geometric, radiometric or pulse waveform features to aid classification (Koenig and Höfle 2016).

2.8.1 ALS Tree Investigation

ALS LiDAR has been used to locate and classify trees in largescale environments, such as forests or woodland. Recent works conducted in in southern Finland by Yu, Hyyppä et al. (2017) tested the suitability of three spectral ranges (532nm, 1064nm and 1550nm) for the ALS in the ability to identify three different species of boreal trees. The experimental process included establishing 22 GR plots and acquiring 1903 direct measurements of trees over 5cm DBH, for validation of the RS data. Yu, Hyyppä et al. (2017) show that the best accuracy results for identifying trees (85.9%, Kappa = 0.75), were achieved using a point cloud and single tree features as a data filter. The GR trees were categorised into four categories, which showed that maidens and the healthiest dominant trees were the most accurately classified trees using the ALS LiDAR techniques with detection rates at 91.9%, and overall accuracy of 90.5%. Furthermore, the research also states that ALS used at 1064nm contain the most information for determining features between the different trees.

In the review by Koenig and Höfle (2016), it was shown that several species of broadleaved trees were successfully classified from ALS LiDAR using filtering methods on the pulse return index. Overall accuracies of 95% for leaf on and 94% for leaf off for the upper canopy layers, and at lower canopy levels, the accuracy is better

in leaf off conditions at 95%, while leaf-on investigations achieve classification accuracies of 86%. It is understood that this drop in performance in leaf-on conditions is a consequence of the upper crown shadowing out the lower sections of the crown. The significance of the pulse return order is also described in Murray, Blackburn et al. (2014) where an analysis of the standardised and unstandardized regression weighting of the four return pulses (r 1-4) used within their ALS LiDAR dataset, showed the r2 pulse (second return) has the most overall influence on the independent (canonical) variables, used to describe tree structure. Further investigation for correlations showed that data relationships between pulses r1-3 are the most reliable as a group, and again, that the “frequency and distribution of r2 exerts the greatest influence” in investigative metrics of tree structure.

2.8.2 Individual Tree Crown Delineation

The use of ALS LiDAR investigations for the mapping of individual tree locations is considered extensive, as the resulting ITC delineated location maps are a fundamental element of a “broad field of applications and users” (Eysn, Hollaus et al. 2012). However, observations within the RS community identify that there are several limiting factors with LiDAR ITC delineation due to the many technical challenges of achieving the precise co-alignment of aerially acquired data with GR measured locations (Lee, Cai et al. 2016). This situation is compounded by the reporting efforts of scientists and researchers on their ITC delineation methods and precise geometric descriptions of their criteria used in automated ITC delineation (Eysn, Hollaus et al. 2012). An operational complication with ITC delineation is the need to achieve vertical separation of overstory and understory trees from the 3D point cloud. The complex vertical arrangement of forest or woodland canopy strata frequently prevents understory trees from being accounted for (typically <60% detection rate), due to the

ITC delineation methods predominantly detecting the top of overstory trees or first return, surface points (typically >90% detection rate) (Hamraz, Contreras et al. 2017). Importantly, a study conducted over a ten year period by Zhao, Suarez et al. (2018) showed that parameters of trees calculated from LiDAR, specifically tree height, showed good correlation with field measurements, however, noticeable tree height underestimation bias increased, as the pulse density for the measurement sites decreased.

A key factor is the shadowing effect of the upper canopy that significantly decreases the penetration range of the LiDAR pulse to the lower vegetation levels (Hamraz, Contreras et al. 2017). However, Hamraz, Contreras et al. (2017) identify that by increasing the 3D cloud point density to $\sim 170 \text{ pt/m}^2$, that the point density increase enables the successful ITC delineation for understory canopy trees. This is a view that is further supported by Vauhkonen, Ene et al. (2012) who state that the successful performance of ITC algorithms was dependent on tree density and data clustering. Not all studies require such high point cloud densities for successful ITC delineation. Swetnam and Falk (2014), cite the requirement as at least one LiDAR pulse return per pixel for successful CHM creation, which for a three by three pixel tile equating to one metre on the ground, is a density of only 9 pt/m^2 , where uniform distribution is assumed. Within this study, Swetnam and Falk (2014), achieved an average density of 25 pt/m^2 and exceeded 45 pt/m^2 where LiDAR flightlines of the same area, taken on different acquisition years, were overlaid for analysis purposes.

The suitability of ITC delineation for the estimation of tree canopy biomass components was undertaken by Popescu and Hauglin (2014), where ALS LiDAR was the primary means of data capture. Popescu and Hauglin (2014), examined two of the

most frequently used tree delineation methods used. The area based approach (ABA), where the characteristics of the vertical vegetation and distribution of the biological material is identified through analysis of the LiDAR pulse returns that occupy a known area, e.g. a plot or forest area. In this method the horizontal distribution of the return pulses is not considered significant but the height distribution of the data is assessed, thereby allowing the calculation of data point density to identify tree locations (Vauhkonen, Maltamo et al. 2014). The ITC method utilises an allometric approach to identify individual tree biomass components, and subsequently the delineation of single-tree crown locations.

Popescu and Hauglin (2014) state that the ITC method has several advantages over ABA, specifically that with ITC delineation, once the trees have been located, allometric models and investigative metrics can be run to further determine individual tree characteristics. Additional improvements to the ITC methods were proposed in the work of Swetnam and Falk (2014) who identify that by using their variable limit maxima, corrected by metabolic scaling theory method (ITC_{MST}), there is an increase in precision mapping and ITC delineation of LiDAR surveyed trees. However, the authors also report that there remains discrepancies relative to tree heights and point densities. In higher canopy cover areas, i.e. >60%, the ITC_{MST} delineation method was less accurate in segmenting trees >16m tall. In areas of lower canopy cover, i.e. <50%, the ITC_{MST} was found to be the most 'generally accurate' method. Kandare, Ørka et al. (2016) investigated the effects of tree structure and LiDAR point cloud density on ITC delineation and observed that tree structure effects the level of increased omission errors, while commission rates are only slightly effected by tree structure.

Kandare, Ørka et al. (2016) also observed that ITC delineation accuracy increases in line with higher LiDAR point density and they propose a methodology for undertaking ITC delineation of LiDAR point clouds. This research aims to test the efficacy of delineation methods and gives an indication on commission error, omission error and an accuracy index for the pairwise matching between aerially delineated tree crown locations and GR observations (Kandare, Ørka et al. 2016). However, the construction of the accuracy index is based on an example of an oversimplified data matching methodology, where a match was considered successful where trees with similar crown dimensions between the ITC delineation and the GR data, and were matched on the basis of being the closest in terms for geospatial location and height. However, despite the fact that these matches were being used as a basis for the measurement of accuracy and that commission and omission values were influenced by a high accuracy score, as with other studies, Kandare, Ørka et al. (2016) neither made or reported a quantification of the suitability of the match proposed. The methodology of Kandare, Ørka et al. (2016) indicates that a match between the two datasets will still be accepted as an 'accurate' match even if the probability of the match remains unlikely. For instance, should two trees, one from each data set, be over 10 metres apart and 10 metres different in height, they would still be matched as a pair as long as the match was the best available of the other potential matches to other trees.

2.9 From the Past to the Future

It is recognised that RS has contributed greatly to the understanding of the landscape, and in particular within forest and landscape management (Takao, Priyadi et al. 2010). The use of the high-end RS technologies and methods; specific software, specialised equipment, and unique analyses, have been applied widely at the research or strategy

level. Yet there remains a significant difference between the gathering and creation of sophisticated data, and the tactical application of RS generated insights to aid the end user at the practical, operations level (Takao, Priyadi et al. 2010). In an earlier US report for the White House Office of Science and Technology Policy, Peterson, Resetar et al. (1999) recognised that although existing monitoring and surveying capabilities existed, specifically programs that relied upon a combination of ground and aerial RS observations, they failed to meet the ever more complex operational requirements that large-scale environmental management needs. This was particularly so for end-user managers who were attempting to meet environmental policy requirements in an increasingly complex policy framework.

Peterson, Resetar et al. (1999) state that although RS technologies, in particular SLS, were not the all saving panacea that could solve all operational requirements, there were some elements of RS, such as the ability to capture low-cost imagery, that were operationally beneficial. However, further drawbacks were identified as being the associated increased in costs with the subsequent requirement for RS data processing and analysis, which were perceived as being prohibitively expensive for forest management operations. Nevertheless, the Peterson, Resetar et al. (1999) report concludes that should these requirements be met, then there would be a wide desire to develop an appropriate strategic vision for the use of RS across the US forest management industries. Subsequently, Wulder, Hall et al. (2005) report that the use of RS in the forest management sector has progressively increased, principally due to the better integration of optical elements of RS (e.g. aerial imagery, aerial LiDAR), improved database repositories and the wider use of GIS technologies. Furthermore, there has also been a sector wide implementation of technology that meets the needs of forest managers (Wulder, Hall et al. 2005). While the initial vision of the Peterson,

Resetar et al. (1999) requirements appear to be slowly being met, there remains the need to keep the development of RS techniques, methodologies and applications relevant for the specific needs of the end user. An additional benefit of RS approaches, is that RS is widely seen as a valid alternative to traditional destructive investigations where in order to fully account for biomass increment trees were frequently felled, or had parts of the tree removed and modelled, and plant material was collected and measured (Jonckheere, Fleck et al. 2004)

2.9.1 Predicted Remote Sensing Trends

Accurately predicting the future with any amount of certainty is an impossible task. Nevertheless, horizon scanning forecasts generally anticipate an increase in the use of RS techniques and methodologies worldwide, and in particular an exponential growth in the use of LiDAR in its varied forms; SLS, ALS, TLS, MLS etc. (Tehrany, Kumar et al. 2017). Within recent years there has been a shift towards the development of LiDAR techniques and scanning equipment focussing on improving measurement techniques, instrument function, accuracy and precision (Telling, Lyda et al. 2017). However, there is also the desire to enable the longer-term installation of LiDAR sensors for automated or semi-automated remote monitoring of environmental change. Unfortunately, the unavoidable problem of accessing high cost equipment is largely prohibitive. However, as a result of recent and ongoing developments in the automotive and MLS sectors, the availability of hard wearing scanners with the potential for permanent or semi-permanent installation is expected to be available within the near future (Telling, Lyda et al. 2017).

Concurrently, there are indications that different methodological approaches to 3D investigations are becoming more prevalent over studies that utilise LiDAR as the main data capture method. Image processing that utilises Structure from Motion

(SfM) can create 3D models that are comparable to TLS LiDAR, and, that have the advantage of generally being more cost effective and easy to use. Therefore, for some 3D vegetation modelling investigations, it is believed that SfM would have more potential future applications (Fonstad, Dietrich et al. 2013). A significant limitation of SfM, however, is that this image-based approach cannot penetrate vegetation canopies due to shading, and can only produce a surface 3D model. It is expected that future developments in this area would likely see a fusion between TLS and SfM approaches, where high resolution models can be created using the most advantageous features from both systems (Telling, Lyda et al. 2017).

Until relatively recent technological developments, LiDAR research has most often used satellites, fixed or rotary wing aircraft, mobile or terrestrial platforms to conduct data collection. A study by Jaakkola, Hyyppä et al. (2017) suggests that there is an opportunity to further develop the use of UAVs with lightweight laser scanners, such as the Puck LITE, for the acquisition of LiDAR data in a forest environment. This is largely due to the ongoing miniaturisation of this type of scanning technology and additional payload capability of UAV platforms (Wargo, Church et al. 2014).

Once operational problems such as errors in the direct estimation of tree parameters i.e. DBH, or sensor issues such as high levels of beam divergence and range issues can be overcome, Jaakkola, Hyyppä et al. (2017) suggest that there is the opportunity for the UAV scanning of the inside of tree canopies. There will also be the potential for the calibration of UAV scans with other larger scale airborne RS data acquisition campaigns. This future vision includes operations where UAV LiDAR forest data collection is completed with the integration of UAVs and automated piloting systems (Jaakkola, Hyyppä et al. 2017). At the time of writing, Jaakkola, Hyyppä et al. (2017)

assert that this technology is currently under development with a leading robotic systems company. These ongoing developments suggest that it is accepted that there is great potential in the remote sensing of trees, and that the research community will continue to develop new methods and technologies for the investigation and classification of trees in the environment. Ultimately leading to more informed and data driven environmental management.

2.10 Summary

From this review, it can be seen that there are many opportunities for the use of RS in the management of trees, and that RS can offer solutions to resolve long-term operational issues in both tree management and research. Traditional methodologies that remain widely used, have seen limited development in the last 100 years, however, these methods remain the basis for the majority of modern tree assessments. These traditional methods are widely used to complete tree assessments for a range of purposes, from environmental studies, to protection of the public for health and safety surveys or the collection of data for forest inventory. A key limitation of these largely manual methods, are that they are both time and, financially costly techniques that only provide a limited amount of information about the subject trees.

These techniques are also limited by the physical capacity of the surveyor. Simply due to the limitations of where a surveyor can access a tree, there is a tendency to rely on the same, ground-based perspective for data capture and to measure only what the surveyor can physically touch. Either this means that large areas of the tree are not measured, or there has to be elements of data extrapolation to fill in missing information. In addition, with the continued use of the traditional methods, there is also a disproportionate reliance on the skills, knowledge and experience of the

individual surveyor for qualitative observations. This has been shown to introduce operator bias or subjectivity into the field data, upon which all subsequent measurements and calculations are based. It is recognised that there is a need to improve upon these traditional methods, and indeed, tree managers indicate the potential acceptance of new techniques and methodologies, predominantly where these new approaches can directly aid the management of the environment. However, there frequently remains some disconnection between the theoretical exploration of a problem, and the translation of the theory into practical solutions that can be employed in any real operational sense.

For successful tree management and academic research, there is often a need to record information about trees over time, in particular for capturing an evidence base for the quantification of change. This review shows that there are several RS solutions that can be employed to fill the requirements of tree managers and researchers in capturing accurate, repeatable and objective environmental data. This RS approach is valuable for investigations that will look at trees across a range of scales, from individual tree assessment, up to wider landscape applications of trees in woodland or forest settings. RS is shown to be able to provide opportunities to investigate elements of tree structure that otherwise would be unobtainable to the traditional surveyor, and furthermore, allows the capture of data that will lead to more insightful investigations and conclusions reached about the tree's condition. This review identifies more than one RS method that can be employed in this manner, specifically, the use of proximal hemispherical imagery for individual tree assessment and recommends the use of ALS LiDAR for the investigation of trees in their wider landscape setting.

This review has identified that there are particular requirements for the successful application of these RS methods. These range from ensuring that hemispherical images are captured from beneath tree crowns looking towards the zenith viewpoint, to identifying a recommended method for the reduction of data noise in LiDAR investigations and considerations for successful ITC delineation and the classification of trees using analytical metrics. Moreover, this search of the literature on the subject also indicates there are opportunities to improve on the current practice of traditional methodologies and provide a technique that is readily accessible for a field operative to be able to classify tree structure. Similarly, previous research involving ITC delineation has frequently relied upon the acceptance of arbitrary thresholds for resolving pairwise matching problems, and again, this provides the prospect for a new method for the identification of tree locations and extents, with a quantification of successful matching between two ITC datasets. Furthermore, the review also shows a need to develop a combined technological solution used for identifying and characterising tree structure, which utilises techniques that are transparent, repeatable and will indicate the amount of confidence in the application of the data for tree managers or researchers. Ultimately enabling the end-user to gain new insights on the overall condition of the trees under assessment, as a prelude to informing the decision making process for tree management or further academic research.

3 Field Sites, Methods & LiDAR Data Specification

For this research project, a substantial amount of field-based data collection was undertaken to provide a robust GR data set to be used in the validation of RS data. This necessitated the use of a series of different field methodologies, each with unique specifications and operational requirements. The fieldwork relates to a series of both direct and indirect measurements of the subject trees, using several data capture methods. These methodologies are essential for the completion of the experimental elements of this investigation, and are not covered elsewhere within this thesis. Hence, these methodologies are described to provide transparency, and, when read with the methodologies in later chapters, to enable other investigations to repeat the procedures used. These field-methodologies drawn from a variety of sources, and are either based on forestry and arboricultural industry specific best practice, or are techniques from the academic research community.

Several of these field data collection methods were used in combination in order to achieve the required objective. For example, a tree may be manually surveyed and proximally photographed. As such, each of the subsections of this chapter should not be considered isolated methods completed in sequential order, but a general record of field methodologies and data collection techniques, used concurrently where required. The trees used within the investigation were recorded across a series of different field sites each with unique combinations of tree species, age, geolocations and

topographic exposure, and in a range of differing physical conditions. Therefore, an overview of typical land use and local environmental conditions at each field site is also described.

3.1 Field Sites

The fieldwork was undertaken across three separate locations within northwest Lancashire, UK. The sites contained varied tree stocking densities, landscape character and diversely aged and structured tree communities. The remit for the subject trees located within these sites were that the trees were accessible from beneath the crown, and were considered to be within the ‘mature’ phases of tree development, which includes; early-mature, mature, late-mature, old/veteran and senescent phases (Fay and de Berker 1997).

3.1.1 Eaves Wood, Lancashire, UK

Eaves Wood is located to the north of Silverdale, Lancashire, UK ($54^{\circ}10'43.2''\text{N}$, $2^{\circ}49'13.9''\text{W}$), and has a total area coverage of 51.5 hectares. Eaves Wood can be described as secondary woodland, predominantly with closed or co-dominant canopy trees, with infrequent areas of individual maiden trees located in canopy gaps.

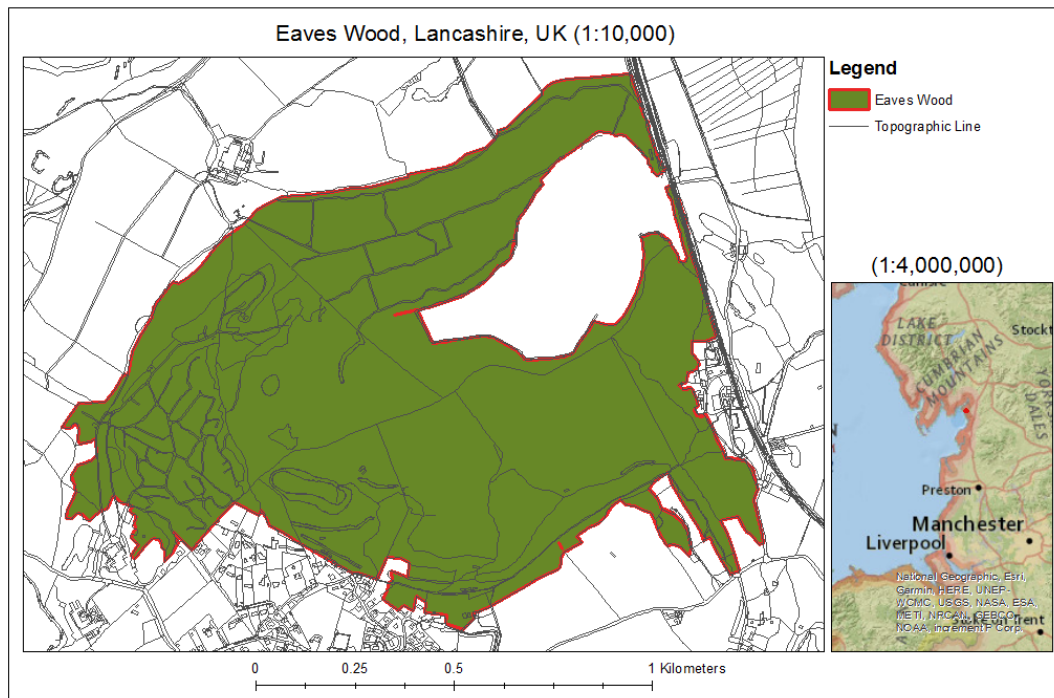


Figure 2 The approximate location of Eaves Wood, Silverdale, Lancashire, UK.

The woodland has a typical composition as is commonly found in the region. Eaves Wood is a mixed species, semi-natural forested area, with areas of ancient semi-natural woodland (ASNW) and plantation on ancient woodland sites (PAWS). The woodland composition is varied with the main tree species including; beech (*Fagus sylvatica* (L.)), small-leaved lime (*Tilia cordata*, (Mill.)), Lancaster Whitebeam (*Sorbus lancastriensis* (E.F. Warb.)), yew (*Taxus baccata* (L.)), ash (*Fraxinus excelsior* (L.)), sessile oak (*Quercus petraea* (Matt., Liebl.)), sycamore (*Acer pseudoplatanus* (L.)), spindle tree (*Euonymus europaea* (L.)) and scots pine (*Pinus sylvestris* (L.)). Notably the pine is not locally provenant and an indicator that the woodland also includes introduced tree stock. The woodland structure contains much vertical and horizontal variation, with clearly defined vegetation strata, including a mixed vegetation understory containing many large areas of hazel (*Corylus avellana* (L.)).

3.1.2 Potter Hill Fields and Park Fields, Silverdale, Lancashire, UK.

Potter Hill Fields and Park Fields are both located within the area to the north of Silverdale, Lancashire, UK ($54^{\circ}10'23.7''\text{N}$ $2^{\circ}48'54.9''\text{W}$ and $54^{\circ}10'35.5''\text{N}$ $2^{\circ}48'55.7''\text{W}$ respectively). Currently in use as informal silvopasture, the grassland is used for animal grazing under local farming management. The overstorey tree canopies, all oaks, are not currently under any active tree management. Typical of trees in lapsed management, there are several examples of trees with notably altered structure or form, due to their exposure to local environmental stresses. Such as, branch loss from storm winds or crown dieback caused by complications arising from the impact of the grazing animals.

3.2 Tree Survey Methodology

Throughout all phases of this fieldwork, each tree surveyed was either located in a survey plot and was over 5cm DBH or, was selected and individually investigated for this study. These trees had a survey conducted to record the observable condition, identify structural characteristics and biophysical properties e.g. height, crown spread etc. and other essential GR data. The tree survey required the majority of measurements to be taken using manual procedures; therefore, in order to ensure standardisation and repeatability, a technical field manual was used for reference in the field (Appendix A). A data form was used to record the data in a standardised format, using the following conventions:

Table 2 Categories of manual tree measurements taken during field capture of ground reference data. Examples of the data recorded are also shown.

Data Types	Example
• Plot ID and tree number	Plot 9, T27
• Tree species	<i>Q. petraea</i>
• XY co-ordinates	15.9, 12.3
• DBH	40
• Tree height	18.2m
• Stem lean and direction of lean	15°, NW
• Crown area (measured along two axis from the ground level)	L10.2, S8.3
• Orientation of the crown area	L-NW/SE, S-NE/SW
• Observable condition	Good ^a
• Structure type	Dominant ^b
• Other general comments about the tree, site or location	20% canopy loss, heavy epicormic growth etc.
• Ground cover assessment	1=10%, 2=35% etc. ^c

Notes: T27 - Tree ID 27, m - metres, NW – northwest, SE – southeast, SW - southwest, a). Observable condition is classified on a four point scale (good, moderate, poor, and dead), using traditional arboricultural techniques. b). Structural descriptions include dominant, co-dominant, understory, field layer, monolith, stag-headed etc. c). Ground cover assessment technique from FCIN45 (Kerr, Mason et al. 2002)

In total, 1210 trees were surveyed across three field sites (see Site and Data Summary), over 135 calendar days, totalling 1080 fieldwork hours. Importantly, this extensive GR dataset was collected during the same time frame (October 2012 – March 2014) that the natural environment research council airborne research & survey facility (NERC ARSF) undertook ALS LiDAR data collection flights over the defined research area. Therefore, this GR data is considered highly important for the calibration and validation of the ALS LiDAR data (Hladik and Alber 2012, Jakubowski, Li et al. 2013). The GR data was initially stored in a Microsoft Excel spreadsheet format (.xlsx), to facilitate the use of the data in later analysis across a range of software platforms, data storage and programming languages employed

within this study; MATLAB, Python, SQL, Ubuntu/Bash, ArcMap, ArcScene, QGIS, PostgreSQL, PDAL and GDAL.

3.3 Photogrammetry Field Methodology

Where a tree crown is to be photographed for use in the crown structure analysis (see Using Fractal Analysis of Crown Images to Measure the Structural Condition of Trees), a dSLR camera with a hemi-spherical lens adapter and standard tripod was used to capture the tree crown images (Chianucci and Cutini 2012). The equipment required for this procedure is identified in Figure 3:



Figure 3 Equipment required for taking beneath crown hemispherical photographs for use in crown structure analysis 1. dSLR camera with a hemispherical lens adapter, compass and level 2. Standard camera tripod, 3. Surveyors measuring tape, 4. GPS/data logger, 5. Tree survey data sheets, 6. Sunnto clinometer, 7. DBH tape (not shown).

To take the image, the southern axis of the crown was identified and the surveyors tape was run from the central stem to the full extent of the crown, maintaining the southerly direction of travel by reference to the compass. The crown length was measured to the nearest whole metre, and the centre point along the southern axis was identified again to the nearest whole metre, where the camera and tripod were set up. The camera is positioned with the camera lens pointing vertically upward, checked against a bubble level which is secured to the lens cover where the pitch (forwards/backwards movement) and roll (left/right movement) are levelled (Origo, Calders et al. 2017). The camera lens is situated at ~0.5m from the ground, level as at all of the sites and trees used, ensuring there was no understory vegetation to obscure the lens (Figure 3). After photographic capture, each image was proofed in the field for quality and suitability using the dSLR camera's 2.7-inch screen. Following this, other field observations and measurements were recorded on the survey sheet.

3.4 ALS Survey Plot Location and Establishment

Prior to capturing the fieldwork data for the ALS LiDAR investigation at Eaves Wood, a walk-over survey was undertaken, considering many locations for control plots where the trees within the plot would be individually surveyed. The sites were identified by assessing the canopy cover at each location through photographic imaging and calculation of gap fraction in the free software CAN_EYE as described by Weiss and Baret (2010). No detailed surveying of the tree's structural condition was undertaken during this process. The intention was to have a mixture of canopy cover conditions, ranging from ~10% to ~100% tree cover (Table 3). Two potential transect lines were identified; with many plots along each transect. The chosen transect was selected based on the potential location range across the woodland and types of tree cover available.

Table 3 Calculation of vegetation cover at 26 survey plots. Images were captured at each location and amount of sky or vegetation that occupies the image was calculated using CAN_EYE.

Plot	Sky (%)	Vegetation (%)	Plot	Sky (%)	Vegetation (%)
1	5.54	94.46	14	15.65	84.35
2	9.51	90.49	15	14.92	85.08
3	8.48	91.52	16	9.65	90.35
4	2.26	97.74	17	11.8	88.2
5	17.77	82.23	18	11.68	88.32
6	5.13	94.87	19	12.06	87.94
7	7.07	92.93	20	17.54	82.46
8	7.85	92.15	21	16.88	83.12
9	36.04	63.96	22	7.01	92.99
10	20.55	79.45	23	23.22	76.78
11	15.33	84.67	24	6.21	93.79
12	8.49	91.51	25	38.32	61.68
13	8.37	91.63	26	8.57	91.43

3.4.1 Real Time Kinematic GPS and Total Station Surveying

Twenty-six tree survey sites were identified for use as control sites, during the ALS LiDAR investigation (see STRUCTURAL: Categorising the Structural Condition of Individual Trees at Landscape Scale using LiDAR Data). To establish the 20 x 20m plots, the plot centre was geolocated and a manual tree survey of all the trees within the plot area was conducted. The exact coordinates of the plot centres had to be identified to facilitate the accurate geolocation of the trees within each plot. Achieving reliable GPS signal beneath tree canopies is problematic due to the frequent interruption of the radio signal. Therefore, a combined first-order triangulation and back sighting survey using real-time kinematic (RTK) GPS and a robotic total station (electronic theodolite), was conducted. This survey required the following equipment:

- Trimble R4 (x2) RTK GPS (GNSS)
 - GPS receivers (2 x R4 receivers)
 - GPS antenna
 - Base station radio
 - Tripod and monopod
 - Power supply
 - Ancillary cables, aerials and equipment

- Trimble S6 Total Station
 - Total station instrument
 - Trimble control unit (CU)
 - 360° prism
 - Tripod and monopod
 - Ranging pole
 - Power supply
 - Ancillary equipment

Established ground control points (GCP), such as gateposts, wall structures or other features denoted on standard topographical maps, were geolocated using the RTK GPS. The GPS is used to capture in field satellite signals, which were corrected in real-time by simultaneously receiving data from a local 'reference station'. This procedure has the potential to achieve sub 5-centimetre accuracy.



Figure 4 Geolocation of ground control points (a), and undertaking a first order triangulation survey (b), to locate survey plots within woodland to aid data processing in an investigation gathering LiDAR data of Eaves Wood, Silverdale, Lancashire, UK.

To obtain an optimised GPS signal, as all subsequent co-ordinates were collected in reference to the base station. The RTK GPS base was stationary, receiving a signal with clear line of sight to the sky for a minimum of two hours before commencing the survey. Once the co-ordinates of the GPS location were recorded, the total station (TS) was used in a line-of-sight relay procedure. This is where the ‘rover’ monopod was moved to an area beneath the surrounding tree canopy, and the location of the reflective prism was identified by the automated laser rangefinder in the TS. Where the line-of-sight could not be maintained, due to the closeness of the canopy or dense understory, the TS was moved to the last location that the rover was recorded, and the new location coordinates for the TS were entered. This required that the back sight surveying procedure was repeated from the new location; therefore permitting the capture of the location coordinates beneath the tree canopy without problems associated with the loss of GPS signal. The process of back-sighting and triangulation was repeated over many iterations moving deeper under the woodland canopy until

the desired location for a survey plot was reached, and the plot centre identified and recorded.

3.4.2 Survey Plot Establishment

Each plot centre was marked with a wooden ground stake affixed with a surveyor's benchmark in the top, which remained in-situ until the entire ALS investigation was complete. This enabled the ability to return and resurvey each site if required. The equipment required for plot establishment was:

- 8 x 30-50 metre surveyors tapes
- Surveyors benchmarks
- Field or sighting compass
- Plot co-ordinates
- Data recording equipment

From the benchmark, a 30m surveyors tape oriented along a north/south axis was placed over the plot centre. This procedure was repeated with a surveyors tape oriented along the east/west axis. Both tapes each had their 10m mark in the plot centre, with 10m of tape extending to each of the four cardinal points, thereby making the shape of a 'positive' sign. Subsequently, this was bordered with four other tapes to demark the boundary of the plot, in a 'box' shaped configuration around the initial two tapes. Again, where the north/south tape touched either of the top or bottom boundary tapes, this occurred at the 10m mark. This procedure was repeated for the east/west boundary. The effect of this arrangement was to create a boxed grid around the plot centre, with graduated measuring points on all sides, and a plot origin location (0,0) in the south western corner (Figure 5).

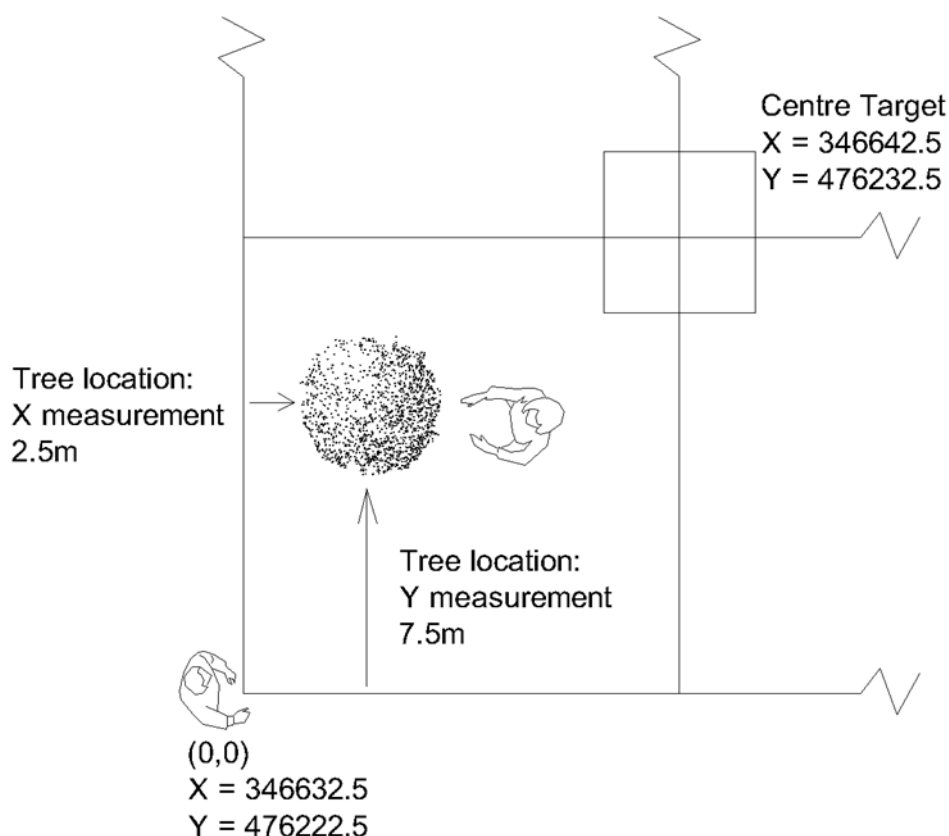


Figure 5 A survey plot layout for capturing data in an ALS LiDAR investigation undertaken in Eaves Wood, Lancashire, UK. The plot centre has geolocated coordinates (e.g. X=346642.5, Y=476232.5), while the plot origin at (0,0) would have coordinates -10m less than the plot centre (e.g. X=346632.5, Y=476222.5). The recording of a tree location along the X axis, would be taken from left to right, and for the Y axis would be taken from the bottom to the top.

Once the plot outline has been set up, it becomes clear which trees fall within or outside the survey plot. On occasions where a tree straddled the tape boundary, the location of the centre of the tree stem, i.e. where, as a seedling, the tree would have first emerged from the ground, was taken as the central reference point. If the ‘seedling centre’ was considered to be within the tape boundary, the tree was

surveyed. Correspondingly, if the seedling centre was outside of the tape boundary, the tree was not surveyed. If the seedling centre was aligned exactly on the tape boundary, the tree was considered to be within the plot and surveyed.

Following surveying of the plots, an assessment of the stocking density was calculated for each of the plots. At 20 x 20 metres, each plot represents 4% of a hectare. A density count of the tree population per plot was taken and transposed up to the hectare scale. As shown in Figure 6, the population density follows the preferred ‘reverse-J’ distribution, an ideal distribution of the tree population, and is considered indicative of a complex, structurally diverse woodland (Kerr, Mason et al. 2002).

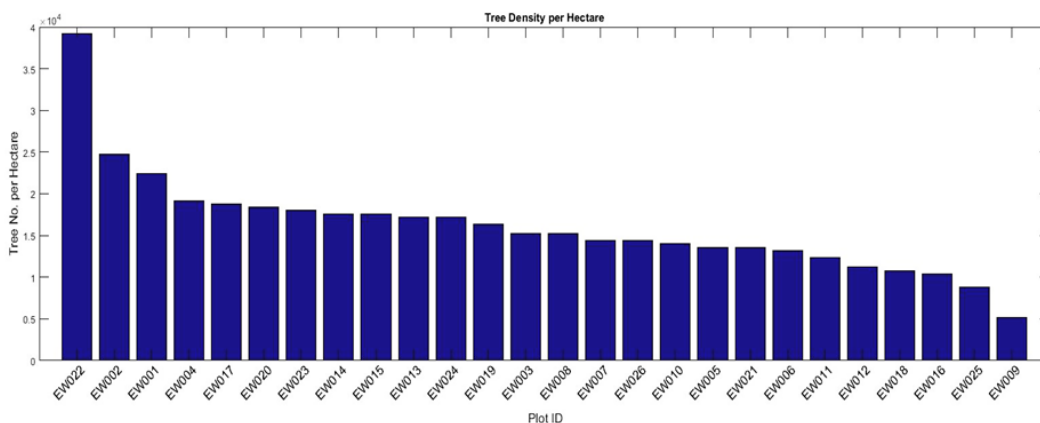


Figure 6 An assessment of structural diversity of a tree population in Eaves Wood, Lancashire, UK. The data follows an ideal ‘reverse-J’ distribution, which indicates a structurally complex and diverse population (Kerr, Mason et al. 2002).

3.5 Site and Data Summary

Following the data collection of 1210 trees across four field sites, totalling ~1080 fieldwork hours, a unique dataset has been created. The use of characteristically different field sites, each within unique local environments, provides the opportunity

to investigate a range of heterogeneous tree communities with widely differing tree structures. Similarly, changes in tree stocking densities and different environmental locations, provides a distinctive mix of tree structures, which were manually measured and recorded. The full extent of the dataset is summarised at Table 4:

Table 4 Summary record of ground reference field and research sites used within a remote sensing investigation, and the number of trees for the types of data recorded at each location.

Site	<i>N</i> Trees	ALS	Hemispherical Imagery	Tree Survey
Eaves Wood	1183	✓	29	1183
Park Fields	12	✓	3	12
Potter Hill Fields	15	✓	15	15

Notes: Numbers e.g. 1183, refer to the number of trees per method. ✓ Indicates method completed.

Through the creation of this dataset via extensive fieldwork, a unique, valuable resource has been created that is to be used for cross-reference, calibration and validation of the findings from the analytical phases of this research. Any subsequent interpretation of observations from the RS data can, therefore, be cross-referenced against known GR field observations further increasing confidence in the findings of the RS analysis.

3.6 LiDAR Data Specification

NERC ARSF collected the DR aerial LiDAR data (project code GB12.04), which was supplied in ASCII format and as LAS 1.0 point clouds, using a Leica ALS50 (phase II) LIDAR (radiation wavelength 1064nm), with a 39 megapixel [7216x5412, 12bit] digital camera (RCD) and an IPAS event controller to extract GPS data. A calibration flight was conducted in May 2012, prior to the Eaves Wood data collection in October 2012. The LiDAR sensor acquisition altitude range is between ~650 and ~2000m,

with the LiDAR data for these flightlines being acquired at ~1000m. Preliminary processing includes a calculation of georeferenced accuracy where each flightline is compared with its neighbouring flightline and assessed for elevation overlapping and horizontal planar shift. GCP's are used to correct for elevation errors. Classification of the LiDAR data is completed following the American Society of Photogrammetry and Remote Sensing (ASPRS) standard LiDAR point classification system, primarily to identify data 'noise' which enables the removal of the noisy points. The LiDAR point cloud contains returned pulse points (r) that are recorded as points 1-4 with the minimum distance between returned points being 2.7m which identifies the points as being independent (Figure 7). The intensity values of the returned points is only calculated for R1-R3, and gives an indication of the reflectivity of the returned surface ranging from 0 (dark) to 255 (white) (Figure 8). The ASCII data provides a range of descriptive statistics and measurements used within the analysis (Table 5).

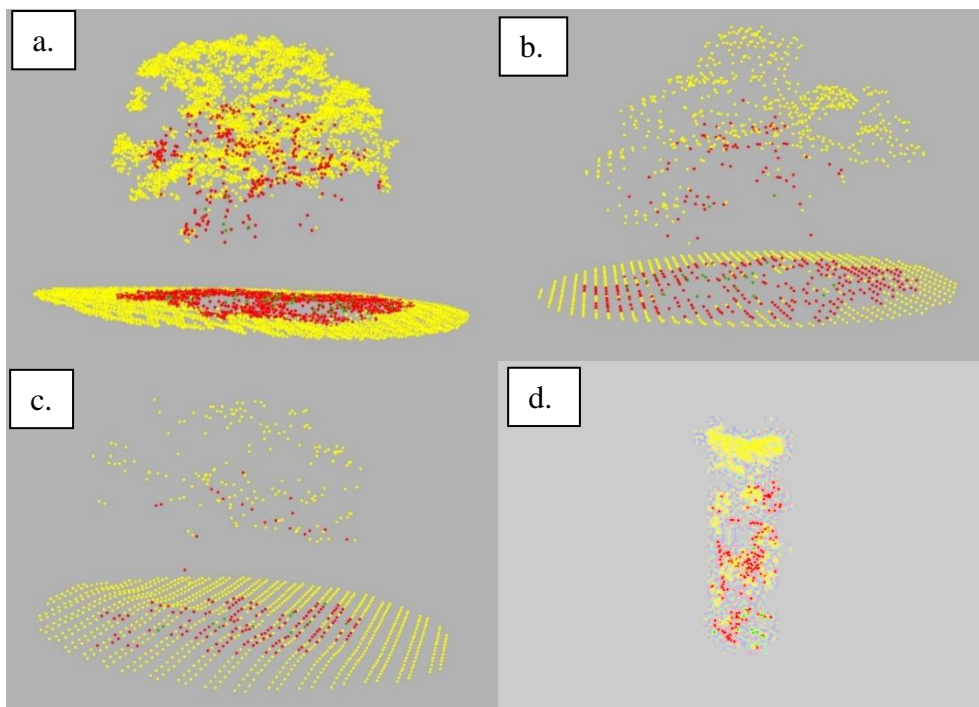


Figure 7 Individual trees delineated from ALS LiDAR data of Eaves Wood. a) a tree in good crown condition, b) a tree in moderate crown condition, c) a tree in poor crown condition, d) a monolith of a dead tree (no crown) and ground points removed for visual clarity. Return (r) pulses R1-3 can be seen as yellow, red and green respectively.

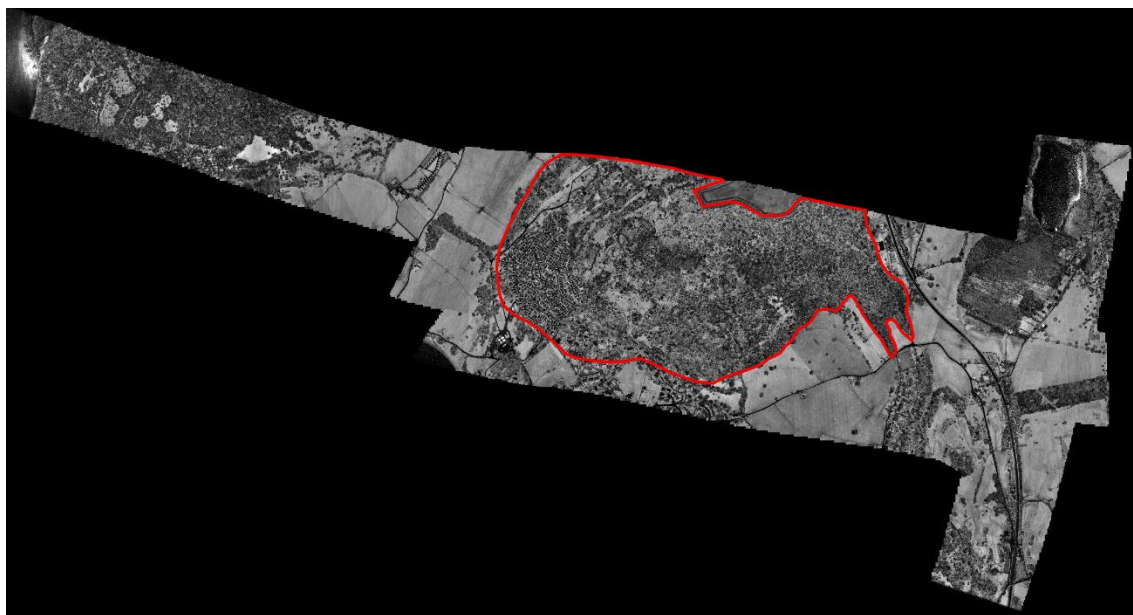


Figure 8 Intensity image of Eaves Wood, UK, with intensity values ranging from 0 (dark) to 255 (white). The image also shows the boundary of Eaves Wood, outlined in red.

Table 5 LiDAR data types and description provided in ASCII format for LiDAR flightlines over Eaves Wood, UK.

ASCII Data	Description	ASCII Data	Description
Time	GPS time (seconds)	Classification	ASPRS standard
Easting	Cartesian coordinate*	Return No.	Return echo (1-4)^
Northing	Cartesian coordinate*	No. of Returns	Times echo returned relative to return no.
Elevation	Height ASL	Scan Angle	Degree integer of laser firing
Intensity	Return pulse strength (0-255)		

* = Horizontal Datum: OSGB36 (OSTN02), Vertical Datum: Newlyn, Projection: British National

Grid. ^ = Expectation of returns (R): R1 ~100%, R2 ~10%, R3 ~1%, R4 ~0.1%.

4 Using Fractal Analysis of Crown Images to Measure the Structural Condition of Trees

4.1 Preamble

Tree crowns are used as a signpost for indicating a tree's overall physiological condition. In simple terms, when assessing tree condition, a particular emphasis is placed upon considering the visual condition and physical structure of the crown, relative to the expected condition and typical structure for the species. Resultantly, crown condition is a proxy for the overall tree condition. However, existing techniques for assessing tree crown structure frequently depend upon assigning broad qualitative categories to describe the tree crown condition. Yet, these broad categories cannot account for subtle differences between similar trees within the same category. Furthermore, the qualitative approach also doesn't answer the key question, 'are there quantifiable differences in tree structure that can be used to characterise overall tree condition?'

This chapter describes a proximal capture, photogrammetric technique that quantifies tree crown complexity and objectively measures the overall condition using tree crown complexity as a proxy for categorical methods.

Using Fractal Analysis of Crown Images to Measure the Structural Condition of Trees

Jon Murray^{1*}, George Alan Blackburn¹, James Duncan Whyatt¹
and Christopher Edwards²

¹ Lancaster Environment Centre, Lancaster University, Lancaster, LA1 4YQ

² School of Computing and Communications, Lancaster University, Lancaster,
LA1 4WA.

*Corresponding author: Tel: +44 1524 652 01; Email: j.murray3@lancaster.ac.uk

*Observations of tree canopy structure are routinely used as an indicator of tree condition for the purposes of monitoring tree health, assessing habitat characteristics or evaluating the potential risk of tree failure. Trees are assigned to broad categories of structural condition using largely subjective methods based upon ground-based, visual observations by a surveyor. Such approaches can suffer from a lack of consistency between surveyors; are qualitative in nature and have low precision. In this study, a technique is developed for acquiring, processing and analysing hemispherical images of sessile oak (*Quercus petraea* (Matt.) Liebl.) tree crowns. We demonstrate that by calculating the fractal dimensions of tree crown images it is possible to define a continuous measurement scale of structural condition and to be able to quantify intra-category variance of tree crown structure. This approach corresponds with traditional categorical methods; however, we recognise that further work is required to precisely define interspecies thresholds. Our study demonstrates that this approach has the potential to form the basis of a new, transferable and objective methodology that can support a wide range of uses in arboriculture, ecology and forest science.*

4.2 Introduction

Traditionally the assessment of tree structural condition, as used in general tree surveys, relies upon simple methodologies and ground-based observations due to the physical complexities of directly measuring tree crowns. However, these traditional techniques are time consuming, manual and largely subjective. Subjectivity has been shown to prevent the same conclusions being reached during independent tree surveys, including surveys of the same trees by different, experienced tree surveyors (Norris 2007). Predominantly these assessments rely on a tree surveyor's knowledge of ideal tree form, tree health, their ability to identify pests and disease, and the consideration of potential hazards and targets that are at risk of harm. Blennow, Persson et al. (2013) state that when managing trees or woodlands the use of subjective tree condition observations are not ideal, particularly where objective tree assessments would provide greater insights in the tree management decision process. Ultimately, traditional tree assessment procedures can result in subjective and potentially biased, field observations of tree condition, irrespective of how knowledgeable and experienced the surveyor is (Norris 2007, Britt and Johnston 2008).

Trees are self-optimising organisms that respond to a range of recurrent environmental demands and employ strategies to alter their form to minimise potential negative effects or optimise their structure for the greatest physiological benefit (Zimmerman and Brown 1971, Mattheck and Breloer 1994, Fourcaud, Dupuy et al. 2004, Pollardy 2008). In most angiosperms, the lateral branches grow almost as fast, or in some instances faster, than the terminal leader. This process results in the characteristic broad crown structure common in this tree type (Pollardy 2008, Burkhardt and Tome 2012). Tree form is typically the result of various influences

combining the genetic potential, the demands of physiological processes, spatial competition in the crown and the effects of other environmental conditions, such as thigmomorphogenic change caused by repeated wind force effects. The shedding of branches through responsive self-pruning driven by abscission, is a characteristic found in many tree species which has a direct effect on the shape of the crown (Pollardy 2008).

There are many additional reasons for trees to shed branches, or parts thereof; which are accelerated by the effects of colonising pathogens e.g. fungal infestation, or external forces such as gravity or wind force. Indeed, the tree's own physiology also increases the potential for crown dieback as trees age (King 2011). Despite many potential stimuli affecting overall tree structure, the growth habits of trees are fundamentally controlled by the genetic predisposition of individual species throughout different tree growth stages. Therefore, the characteristic structure and form of differing tree species remain visually recognisable even after the external impacts are considered (Zimmerman and Brown 1971). When trees reach late-maturity, there is a combined slowing down of both the stem diameter increment and extension growth in the crown, as a response of the influence of the tree species, genotype or its local environment (King 2011). It is the recognition of these types of biotic and abiotic structural changes that tree surveyors use to aid the classifying of trees into discrete categories, ultimately aiming to gain insights into the tree's condition.

There have been many studies of tree crown structure in recent years, many of which utilise high-end technology such as light detecting and ranging (LiDAR) as the main method of data capture (Ørka, Næsset et al. 2009, Ferraz, Saatchi et al. 2016).

Specifically with LiDAR data investigations, it is understood that the success of tree investigation algorithms for location detection or height estimation is strongly correlated to the type of tree structure under analysis (Vauhkonen, Ene et al. 2012). Through analysis of aerial LiDAR data, boreal tree species have been identified at a species level due to differences in their tree structure signatures (Lina and Hyypä 2016), or through LiDAR waveform analysis which identifies structural features within the LiDAR wave (Hovi, Korhonen et al. 2016). Aerial LiDAR investigations are often supported with aerial imagery which is captured simultaneously as image based investigations also provide opportunities for tree canopy structure analysis (Dash, Watt et al. 2016). Furthermore, photogrammetric techniques such as digital stereo imagery and radar imagery have been used in tree canopy structure investigations (Holopainen, Vastaranta et al. 2014). For many researchers or environmental managers, a restrictive element of these types of investigations is the requirement for expensive, specialised research equipment that is often mounted on an aerial platform, such as an unmanned aerial vehicle (UAV), aeroplane or satellite.

The use of hemispherical photography to undertake proximal tree crown assessments has a field history of more than 50 years, with forest ecologists, Evans and Coombe (1959) using the technique to investigate the available light climate under woodland canopies with an early prototype 'Hill' (fish eye) camera. This has remained a readily used, accessible and repeatable method for the investigation of tree canopy structure (Hale 2004, Chianucci 2016). Researchers have also previously used hemispherical imagery to assess canopy gap fraction or provide leaf area index assessments (Weiss, Baret et al. 2004, Beckschäfer, Seidel et al. 2013), as it is understood that images captured by hemispherical, or fisheye, lenses provide opportunities for photogrammetric measurement (Schwalbe, Maas et al. 2009). Conducting

photogrammetric analysis on hemispherical imagery falls within the remote, or indirect, methods of measurement which enable rapid, non-destructive determination of crown properties (Chason, Baldocchi et al. 1991, Weiss, Baret et al. 2004). Modern advancements in digital cameras, coupled with readily available hemispherical lenses or lens adapters, provide the opportunity for an off-the-shelf approach to photogrammetric research (Leblanc, Chen et al. 2005).

When tree crowns are viewed from directly beneath, looking upwards towards the zenith viewing point (90° from the horizontal elevation), holes can be observed within the crown structure. The tree crown area is a complex arrangement of tree branches, combined with observable unoccupied areas between the different parts of the tree crown. This upward looking view provides a visual separation between the tree structure and the sky, which when photographed can be converted into a binary image with the occupied and background regions of the image coded '1' and '0' respectively (Beckschäfer, Seidel et al. 2013, Sossa-Azuela, Santiago-Montero et al. 2013). Image analysis techniques for pattern recognition in tree structures have identified features of lacunarity (the size and distribution of holes), complex spatial distributions or other morphologic features (Zheng, Gong et al. 1995, Frazer, Wulder et al. 2005).

Due to the unique geometry found in nature, the dimensions of natural, physical forms cannot readily be described in simple, integral terms (Mandelbrot 1982, Dimri 2000). Mandelbrot (1982) argues that more insightful measurements are required to measure pattern complexity, such as quantifying the degree of complexity in a structure. As trees exhibit natural structural variance, Mandelbrot (1982), also notes that it is the frequently anomalous nature of tree structure whose form is sculpted by, "chance, irregularities and non-uniformity", that provides the opportunity for statistical

investigation. Rian and Sassone (2014) demonstrate that the crown structures of trees are unique in their self-affine and highly irregular branching patterns. It has been stated that fractal dimensions (Df) can be used to quantify structural complexity in a continuous measure, theoretically ranging from 0 to infinity, which can be expressed as a single value (Mandelbrot 1967, Kaye 2008). Although tree crown structures are complex shapes, there are various examples of Df being used as a predictor variable for the classification of forest canopies (Zeide and Pfeifer 1991, Zeide 1998, Jonckheere, Nackaerts et al. 2006, Zhang, Samal et al. 2007).

The aim of this study was to develop an objective methodology to assess the structural condition of broadleaved tree crowns (*Quercus sp.*) by quantifying the complexity of the tree crowns through hemispherical images taken under leaf-off conditions. This approach was designed to overcome the limitations of current subjective field methodologies. The first objective was to develop an in-field data capture technique that was suitable for a range of subject trees across a variety of structural conditions. The second objective was to develop image processing methods for the assessment of crown structural condition. The third objective was to propose a new and objective means of evaluating tree structural condition on a continuous scale.

4.3 Methodology

Throughout three study areas across northwest Lancashire, England, 64 Sessile Oak trees (*Quercus petraea* (Matt.) Liebl.) were individually photographed using hemispherical imagery obtained from beneath subject tree canopies, looking towards the zenith viewpoint (Figure 9). The trees used in the study were either individual maiden trees, or trees that were located in closed canopy, woodland conditions. The trees were photographed over a single winter season in leaf-off condition, thereby

allowing an unobscured view of the tree crown structure. To minimise potentially confounding variables, this method was applied to trees of the same species that were in the mature phases of tree development, specifically: early-mature (28%), mature (25%), late-mature (25%), veteran and senescent (22%) (Fay and de Berker 1997). To achieve a suitable sample size, a locally prolific species was used in this study.

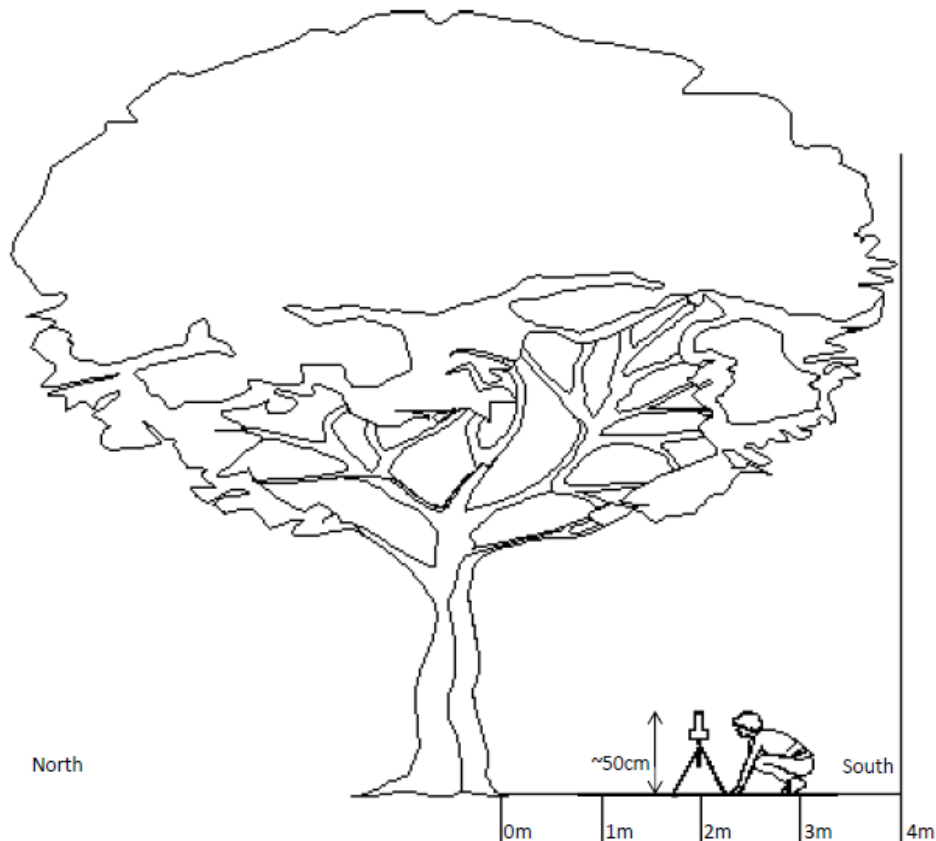


Figure 9 A schematic of the field method for taking a hemispherical picture from beneath a tree canopy. The camera is situated on a standard tripod, and is levelled and pointing towards the zenith viewing point (90° from the horizontal elevation). In this example, the full extent of the crown is four metres along the southern axis, and the image is taken at the two metre mid-point.

4.3.1 Field Methodology Development

Reference data on the trees structural condition was collected using a four-point categorical system, as is common in arboricultural assessments using traditional field techniques. The four-point method used in this research is not based upon a single specific method, but broadly upon several arboricultural tree survey methods (e.g. BS5837:2012 surveys which use a four level condition hierarchy, the ISA tree hazard evaluation, which uses four classification categories to generate an accumulative hazard score (Matheny and Clark 1994, BSI 2012), and is also comparable with a qualitative tree condition category assignment as described in Swetnam, O'Connor et al. (2016). Consequently, this approach is representative of similar tree survey methods where the assessment of trees leads to an empirical categorisation of tree condition (Figure 10).

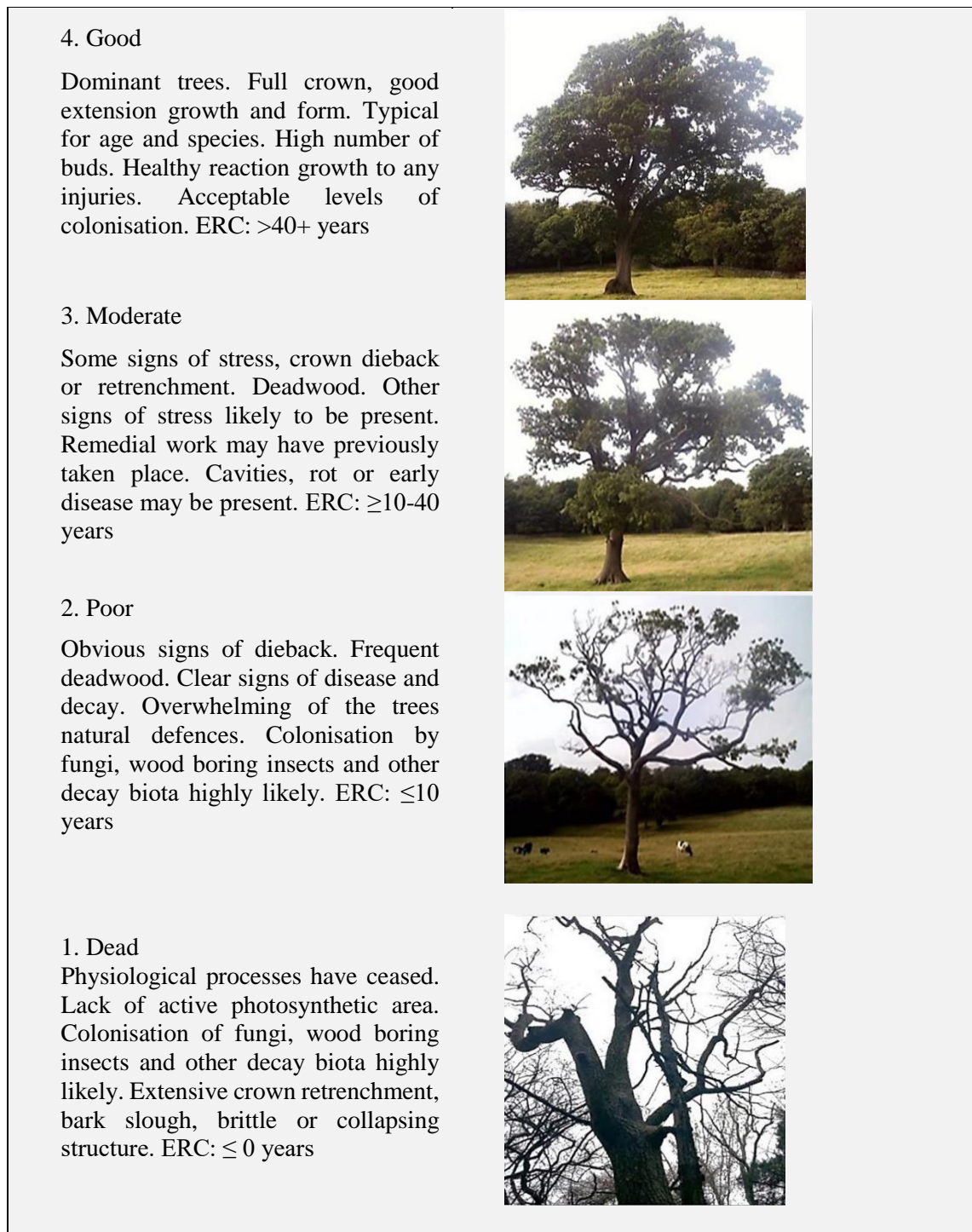


Figure 10 Classification descriptors for the subjective arboricultural assessment of trees. Estimated Remaining Contribution (ERC) refers to a methodology used to consider the health, condition and structure of the tree and aids in classifying the tree in to the different categories *adapted from* (Barrell 1993, Lonsdale 1999, Barrell 2001, NTSG 2011, BSI 2012). Note: The images show trees in leaf-on condition to enable ease of comparison for the condition types.

4.3.2 Camera Set-up

A high-resolution digital single-lens reflex (dSLR) camera (Canon EOS 550D DS126271) was used with an 18mm lens and a hemispherical lens adapter (Opteka Super Wide Fisheye Lens 0.20X). The lens adapter permits focal length conversion into a 3.6mm circular lens. The wide angle of the hemispherical lens enabled as much of each tree crown to be captured within each image as possible. The dSLR was placed on a standard photographic tripod, adjusted at each image capture location ensuring that the dSLR was positioned and levelled with the camera lens pointing vertically upward at ~0.5m from the ground level. To account for variability in solar illumination, the images were taken during uniform sky conditions. These conditions occur predominantly when the sky is overcast, although this technique can also be used just before sunrise or just after sunset, should bright daytime conditions be expected (Song, Doley et al. 2014).

4.3.3 Image Acquisition and Spatial Sampling Strategy

Initially, the number of images captured per subject tree was influenced by the overall length of the crown along the southern axis. Early trials with image capture involved taking images at 1m intervals along the southern axis, to the full extent of the crown. However, this produced a high number of replicates with large amounts of image content overlap. Inspection of these images identified two problems with this approach. Firstly, that there was ~90% replication of content between the overlapping images (Figure 11a), and secondly, that additional tree features that were not required for the analysis were also captured.

For example, additional stem wood was photographed in the images closest to the base of the tree (e.g. at 1m and 2m intervals), while large amounts of 'sky' was

captured towards the canopy edge. Neither of these image components was required in the analysis. It followed that many of the repeated images was not within the optimal range for representing the fullest area of tree crown within an image. Repeated testing indicated that the optimal location for image capture was around the mid-point of the crown axis (Figure 11). Where there was no mid-point location on an exact 1m interval of the southern axis mid-point, the distance was rounded up to the next whole metre. The southern axis was used for standardisation purposes as the subject trees are located in the Northern hemisphere and our preference was to capture images on the non-shaded, south facing side of the trees.

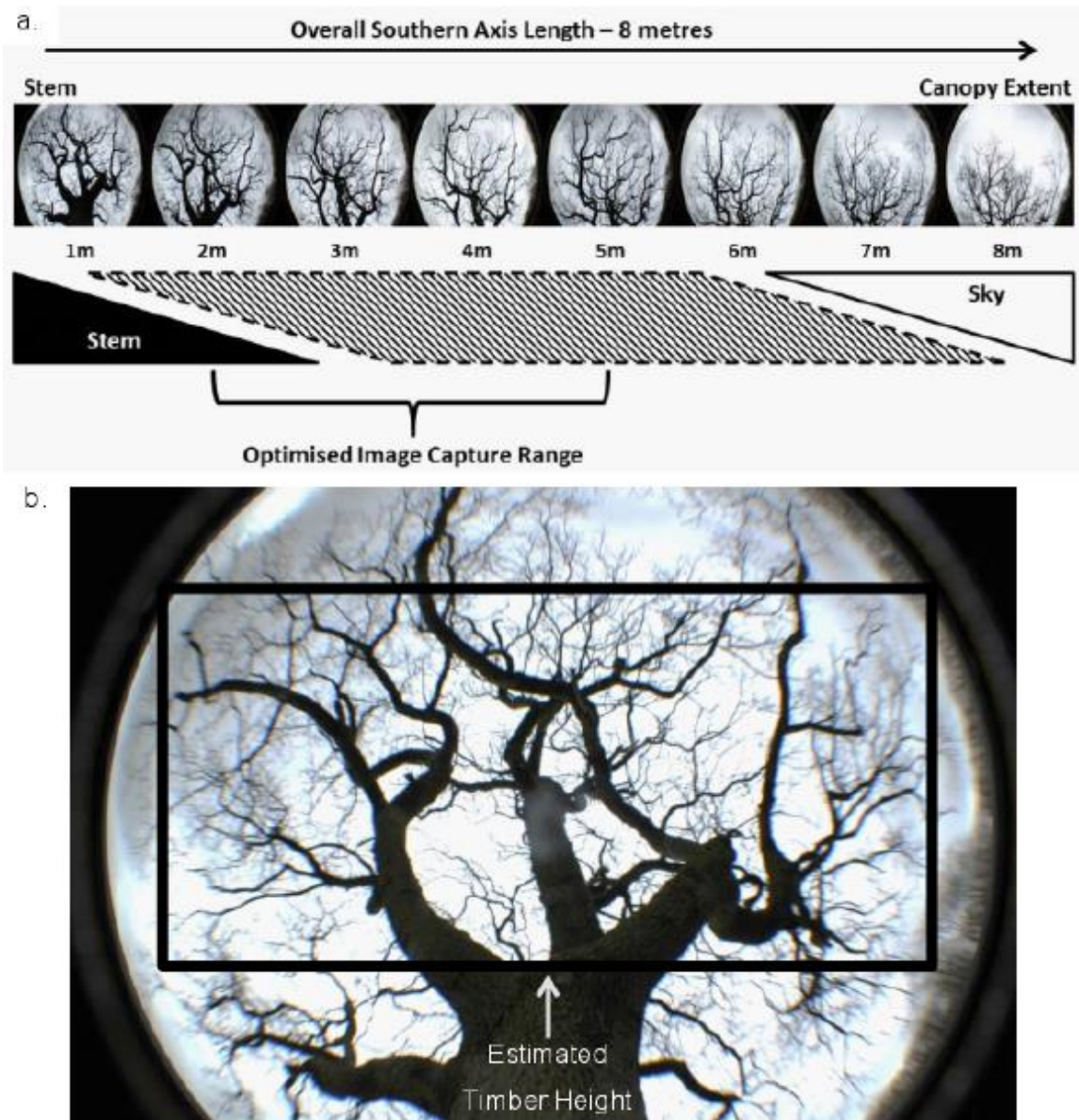


Figure 11 A schematic showing the optimised range for image capture (a), and the area of tree canopy structure analysed within this study (b). The area of interest is specifically the structural elements of the canopy. Too much ‘sky’ within the image reduces the amount of structure that can be analysed (a). Stem wood and other elements not required, are removed from the image by only analysing the structure inside a user selected bounding box area (b). The use of a bounding box allows images of both individual trees and trees within closed canopies to be analysed.

Immediately after acquisition, the quality of each image was visually assessed. This step was taken to ensure the images were suitable for later analysis and to allow additional images to be captured should the original image be unusable. The process of identifying the southern axis, setting-up the camera and completing image acquisition took between ~45 seconds to ~1.5 minutes, depending on the complexity of the local topographic environment.

4.3.4 Image Preparation

Upon return from the field, the images were re-examined on a desktop computer to check for image clarity, suitability in showing the area of interest, and for the presence of key features (Jones and Vaughn 2010). A limitation of the in-field image proofing was that this was completed on the dSLR camera's 2.7-inch screen; therefore it was conducted at a very coarse resolution. Of the original 247 images, 87 were removed for blurring or distortion errors, 96 images were removed as duplicates, leaving the sample size reduced to 64 images of individual trees, with a single image representing each tree.

Pre-processing interventions removed errors from the images that could affect the measurement of image metrics. Chromatic aberration (CA) is the misregistration of red, blue and green (RGB) channels causing interference with the dSLR Bayer-pattern sensor, leading to image deterioration and interference with pixel-based classification techniques (Schwalbe, Maas et al. 2009). In this study, CA was corrected by removing the red and blue channels, and converting the image to the green element of the RGB channels only. Quadratic or 'barrel' distortion is also associated with images captured using hemispherical lenses. A distortion correction algorithm (de Vries 2012) transformed the images from the distorted barrel extension to replicate an image captured at a normal focal length. This perspective distortion effect is influenced by

the relative distances between the lens and subject canopy at which the image is captured, therefore, it is important that the relative distance was maintained during image capture. In order to reduce the effects of blurred images caused by contrast errors between colour ranges, an image sharpening algorithm was used. This algorithm was based upon un-sharp masking, where the image is sharpened by removing a blurred negative copy of the same image. The copied mask was laid over the original, resulting in a combined image that is visually sharper. Where there were instances of unsuccessful pre-processing, the affected images were not used in the investigation.

The images were analysed in Matlab (2015a), where each image pixel was indexed and converted into binary form. This was achieved through applying uniform quantization where limited intensity resolution breaks the image colour space into individual pixels, which are indexed, and the pixel locations are mapped. A process of dithering corrects any potential quantization errors and limits the greyscale range of the image. This binarization procedure allows differentiation between the tree structure and other parts of the image, as optimum image analysis conditions are best achieved where there is high contrast between tree structure and the sky (Chen, Black et al. 1991).

4.3.5 Defining the Image Analysis Area

Chianucci and Cutini (2012), describe that it is beneficial in image processing to reduce the field of view by masking some elements of the full hemisphere, thereby achieving greater spatial representation of heterogeneous tree crowns i.e. the inclusion of both dense and sparse crown regions in the analysis. At Figure 11b, image analysis is restricted to the part of tree canopy contained within the black bounding box,

created on a per image basis. The analysis extent is influenced by standard forestry measurement conventions (West 2009), with the lower bounding box edge originating at the point of estimated timber height. In decurrent trees, this is where the main stem bifurcates to such a degree that the main stem is no longer discernible. From here, the analysis area is bordered by the upper bounding box at the edge of the tree crown and avoids the image's vignette region caused by the visible inner walls of the camera lens. The left and right boundaries of the image analysis area are demarked by adjoining lines between the upper and lower bounding box extents maximising the crown analysis area, while again, also avoiding the vignette region at the edges of the image.

4.3.6 Predictor Variable Creation

Multiple indices were generated from the tree images that were developed into image metrics which were tested, both individually and in combination, for their suitability in describing the tree structural character. A description of the metrics is shown at Table 6.

Table 6 Descriptions of analytical metrics used in an investigation to quantify tree structural condition.

Name	Description
Convex Hull Area	An area value of the smallest potential convex polygon used to envelop the indexed region in a p-by-2 matrix.
Equivalent Diameter	A scalar value for a computed circle with the same area as the indexed image.
Euler Number (32)	A scalar value that specifies the frequency of indexed objects in the image region. The Euler number subtracts porosity values (holes) representative of crown porosity using 32-bit imagery.
Euler Number (48)	A scalar value that specifies the frequency of indexed objects in the image region. The Euler number subtracts porosity values (holes) representative of crown porosity using 48-bit imagery.
Euler Number (64)	A scalar value that specifies the frequency of indexed objects in the image region. The Euler number subtracts porosity values (holes) representative of crown porosity using 64-bit imagery.

Filled Area	A scalar count identifying the number of pixels used to ‘fill-in’ the indexed image (removal of image/crown porosity), with the count extending to the full perimeter of the structure using a logical test of the region index.
Fractal Dimension	A continuous, scaled measurement of self-affinity, where repeating x and y curves are magnified by different factors and a logarithmic mean is calculated.

Euler numbers represent the amount of tree crown occupied by solid tree structure through quantifying connected pixel components, holes and vertices within the image. Initially an RGB image is indexed and an inverse colour map algorithm restricts the number of possible RGB colour values to a predetermined range, e.g. 32, 48 or 64 colours, to refine the image resolution. Each pixel is then matched to the closest colour in the colour map, and the image is subsequently binarised for analysis purposes. Euler numbers are then used to measure image topology through the frequency and area occupancy of ‘holes’ within the binarised image. These holes are subtracted from the total number of objects that occupy the image region, therefore the Euler value represents pixel occupation in the image (Chen and Yan 1988). The creation of the Euler number is defined as:

$$E = N - H \quad (4.1)$$

where N is the number of connected image components (region), and H is the number of image holes identified as separate from the region (Sossa-Azuela, Santiago-Montero et al. 2013).

Convex hulls are used to delineate a computed shape edge; therefore in this application, region convex hulls are considered representative of the tree crown edge extent and provide the opportunity to quantify the area covered by the hull shape.

Region convex hulls were created demarking a polyhedron boundary in the Euclidean plane around a known distribution of data points (X). This process defines a measurable boundary where the polygon is considered convex if all of the dataset X lie within the boundary, and any two points in X can be joined using a straight-line segment that also remains within the boundary. A limitation of convex hulls is that the outer bounds of the polygon may extend beyond the data range in order to maintain convexity, thereby potentially adding additional area to the generated polygon. Successful convex hull algorithms however, provide the smallest convex contour area within a given region (Gargano, Bellotti et al. 2007).

A similar method used in photogrammetric analysis is the calculation of equivalent diameters. The projections of equivalent diameters are frequently used in RS investigations to model the spatial distribution of tree crowns. Within this study the equivalent diameter metric represents the area occupied by the tree crown structure in each image, while also providing a potentially continuous index of equivalent circle areas. A scalar value is defined that is the equivalent area of the irregular shape within the image (Kara, Sayinci et al. 2013), and is compared to the area of a known shape, e.g. a circle, using the equation;

$$d_e = \sqrt{(4a/\pi)} \quad (4.2)$$

where a is the area of the irregular shape, and d_e is the equivalent diameter.

Finally, in order to quantify the complexity of the tree crown structure, a fractal geometric analysis approach was used to assess each image for self-affinity by calculating the logarithmic mean for the Df of each image. Df is used as a measure of

complexity as Mandelbrot (1967) recognised the merits of using Df to quantify complex change in pattern detail relative to scale. Fractal dimensions should be considered an approximation of the Kolmogorov capacity, driven by a recursive process where small elements of the image are analysed individually, before the overall Kolmogorov capacity for the image is calculated. Equation 4.3 describes the Df calculation:

$$Df = \lim_{R \rightarrow \infty} \ln N(R) / \ln(R) \quad (4.3)$$

Where N is the number of boxes needed to cover the fractal shape where it is present, R represents the unit size of the boxes, and $N(R)$ is the number of boxes required to fulfil the fractal element for the image region. *Lim* refers to the limit of R , as R approaches infinity (Bonnet, Bour et al. 2001, Moisy 2008). In order to generate an individual Df model, a box-counting function (Moisy 2008) is applied that derives a local Df at each box size, integrated with the power law:

$$N(R) = N0 * R^{-Df} \quad (4.4)$$

where $N0$ is the expected value when R equals one. As this approach is dependent on both R and Df the result is a logarithmic mean of all the Df values generated for the fractal region of the image, and is interpreted as a quantification of the structural complexity of tree crowns. The steps required to process the tree images and compute individual tree metrics are summarised at Figure 12

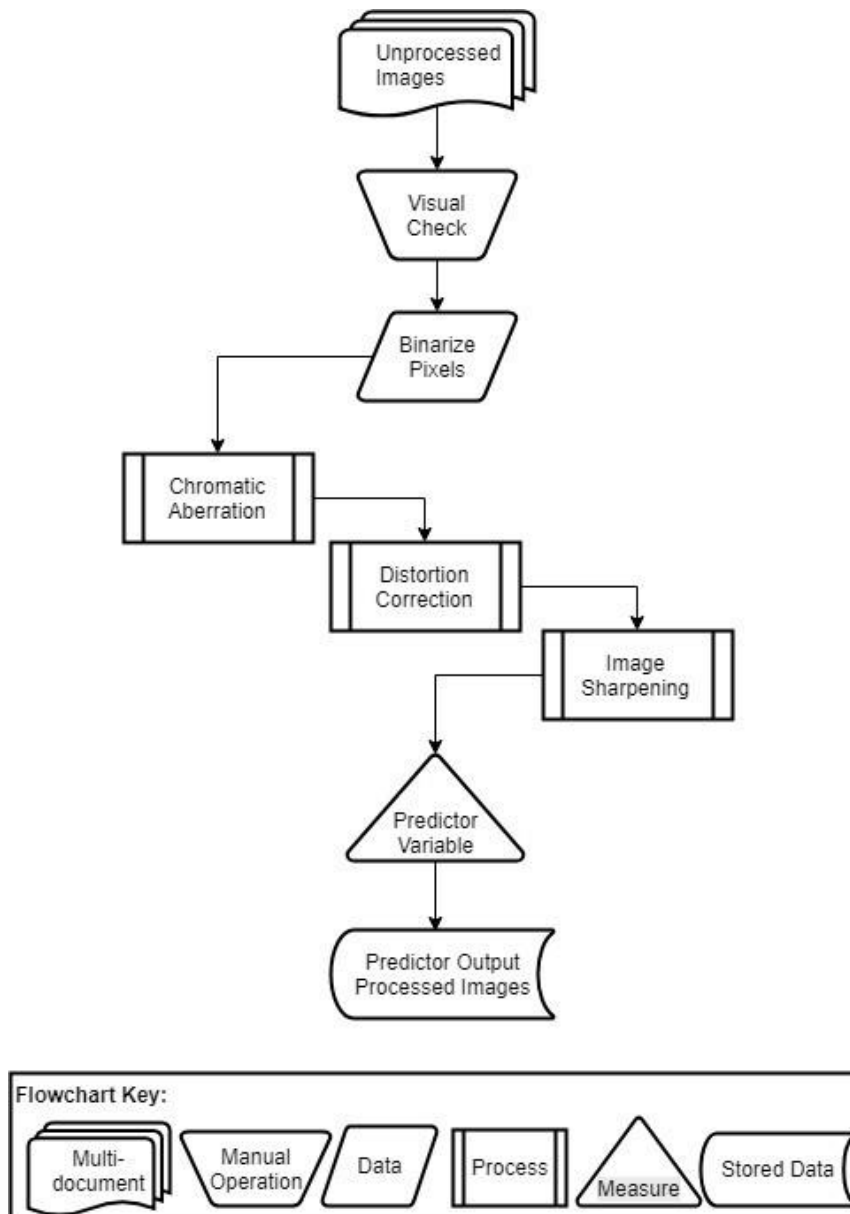


Figure 12 A procedural workflow showing how tree structure images are processed for the computation of image metrics

4.3.7 Calculating Statistical Probabilities

The suitability of the predictor variables in quantifying tree structure was tested via multinomial regression, where the observed tree conditions are categorical responses, given as:

$$\log\left(\frac{\pi_i^{(j)}}{\pi_i^{(0)}}\right) = \alpha^{(j)} + \beta_1^{(j)}X_{1i} + \dots + \beta_k^{(j)}X_{ki} \quad (4.5)$$

where X_{ki} is the k^{th} predictor variable for i , the imaginary unit. θ is the reference standard, j is the non-reference standard, and $\alpha^{(j)}$ and $\beta_1^{(j)}, \dots, \beta_k^{(j)}$ are the various unknown population parameters. The predictor variables are used to discern where a response, i.e. the tree structure, relates to the same tree characteristics that are indicative of an observed condition. Multinomial regression therefore, creates a proportional odds model where a single category of trees is specified as the reference standard and is used as a comparative measure against which all other tree categories are compared. Probability (P) estimates are calculated for all trees, to quantify the likelihood that they share the same structural characteristics as the reference standard trees. For the purposes of this study, ‘Good’ category trees, are used as the reference standard. The probability that the non-reference standard trees share the same structural characteristics of the reference standard is expressed as a P estimate percentage.

4.3.8 Outlining Classification Thresholds

To allow the comparison of continuous and categorical data, several predictor variables were used to create quantified indices to represent the structural character of the individual trees (Table 6). These variables were analysed to discriminate between the structural characteristics of individual trees and to determine how well the indices represented the field-observed classification. The predictor variable indices were grouped and analysed as individual indices, i.e. all Df values grouped as one data set, all Euler (64) values as another data set etc.

An empirical data mapping test was undertaken where homogeneity traits were observed in the predictor variable indices. Data mapping is achieved where the categorical data is plotted over the ordinal data using the two available values for each tree image e.g. categorical: Good, ordinal/predictor value: Df 1.875. The tree images were grouped by their field-observed classifications; Good, Moderate, Poor and Dead. For each of these four groups, the minimum and maximum predictor indices values showed the threshold value extent for each classification.

4.4 Results

At Figure 13a, the Df predictor variable quantifies the structural characteristics of all the assessed trees with individual Df values on a continuous scale, and displays homogenous clustering of the field-observed condition types. The group threshold extents are demarked as horizontal classification lines for the Df predictor variable in Figure 13a, where there are four separate groups of Df values consistent with their given field classifications; Good, Moderate, Poor and Dead (Table 7). In instances where heterogeneity was observed in the predictor variable indices, the data mapping could not be applied and it was not possible to define threshold extents (Figure 13b-d).

Table 7 **Threshold limits of tree condition categories, expressed in fractal dimensions (Df).**

Field Categories	Df Threshold
Good	≥ 1.6021
Moderate	≤ 1.6020 to > 1.4815
Poor	≤ 1.4814 to > 1.3423
Dead	≤ 1.3422

At Figure 13b-d, there are heterogeneous clusters of field classifications as denoted by the mixed colouring and absence of threshold lines. All sub-plots in Figure 13 show similarities with generally decreasing indices, suggesting a continuous nature to the data, and implying that the trees included in the study possessed a varying range of structural conditions. In Figure 13b, c and d, all field-observed conditions are shown in heterogeneous grouping for the different predictor variable indices, therefore demonstrating inconsistency with the field-observed classification for each predictor variable (Table 6). It follows that the remaining predictor variables (Table 6 and Figure 13b-d) do not provide a suitable mechanism to discriminate between different structural characteristics.

Euler (64) (Figure 13b.) is the only variable to output negatively skewed data, and repeatedly quantified a number of individual trees with a Euler value of '1', thereby also providing limited information on potential structural differences in these trees. Figure 13a shows the validity of Df as a continuous measure of tree structure complexity. We further demonstrate the relationship between the categorical classifications and the probability that Df values are representative of these categories in Figure 14. Within the good category, there is a ~99% probability that the trees share the same structural characteristics as the trees in the reference standard. Within the moderate category, the probability that the trees show the same structural characteristics of a good tree structure has fallen to ~89% at the median, thereby identifying a probability shift between good and moderate structural characteristics. There is a further, large median shift between the moderate and poor categories, as the median reduces to ~29% for poor category trees when compared to the reference standard. Where trees were field-observed as belonging in the dead category, there is

a decrease in probability to <1% that these trees show the same structural characteristics as the reference standard.

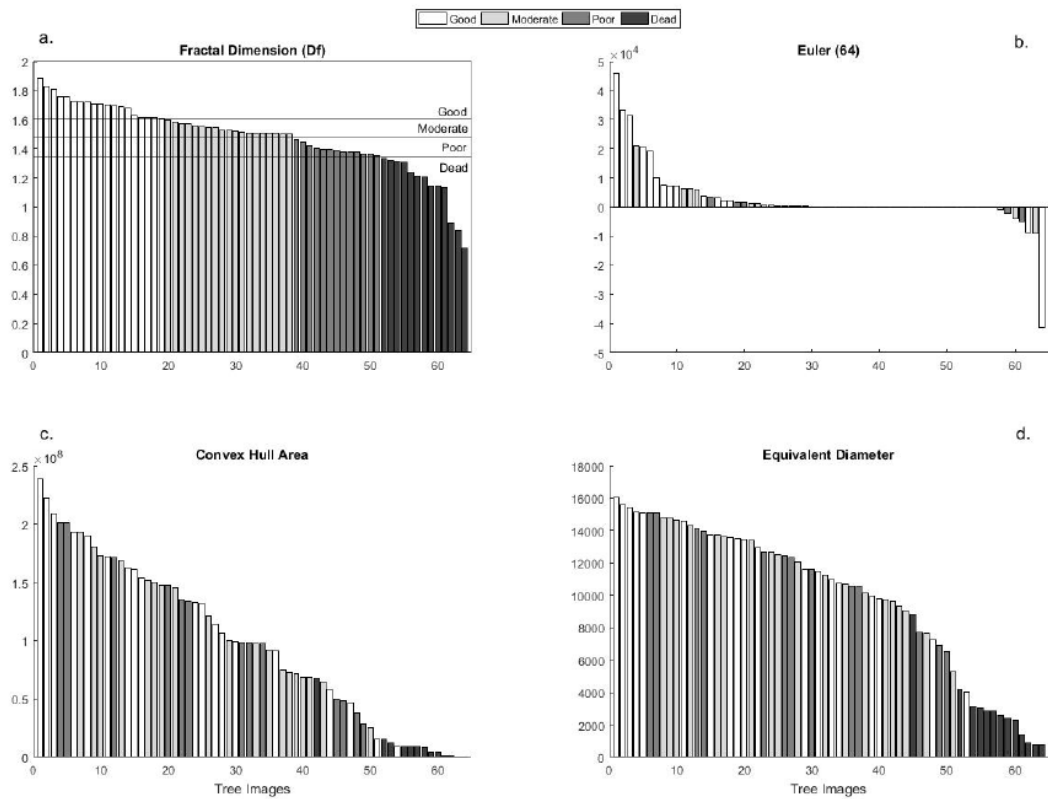


Figure 13 Sample subset of predictor variables used to define the characteristics of different tree structures ($n=64$). The annotations Good, Moderate, Poor and Dead refer to the field observed condition of the individual trees. Only with the measure of fractal dimension (a.), provides homogeneous clustering of field observed conditions as identified by the threshold lines. Not all predictor variables used in this study are visualised in this plot

Also in Figure 14, it is noticeable that there is no overlap between the overall visible spread (OVS) in the good field-observed population and any of the other potential categories, due to the OVS separation between all other field-observed categories. Similarly, this trend of OVS separation continues for each field-observed category when compared to any other category. Trees quantified as having structural

characteristics of either the moderate or poor groups have a larger interquartile range than trees observed to be in either good or dead condition. This indicates that there is a greater degree of uncertainty in characterising the moderate or poor groups of trees, particularly as the trees with the good or dead characteristics, are assigned to their relative categories with a high degree of precision. In order to identify potential subgrouping effects, where similar classification probabilities may be clustered around specific probability values, a linear regression model was calculated which identified that there was no evidence of subgrouping and that the probability data range is randomly spread ($r^2 = 0.86$, P -value 0.01).

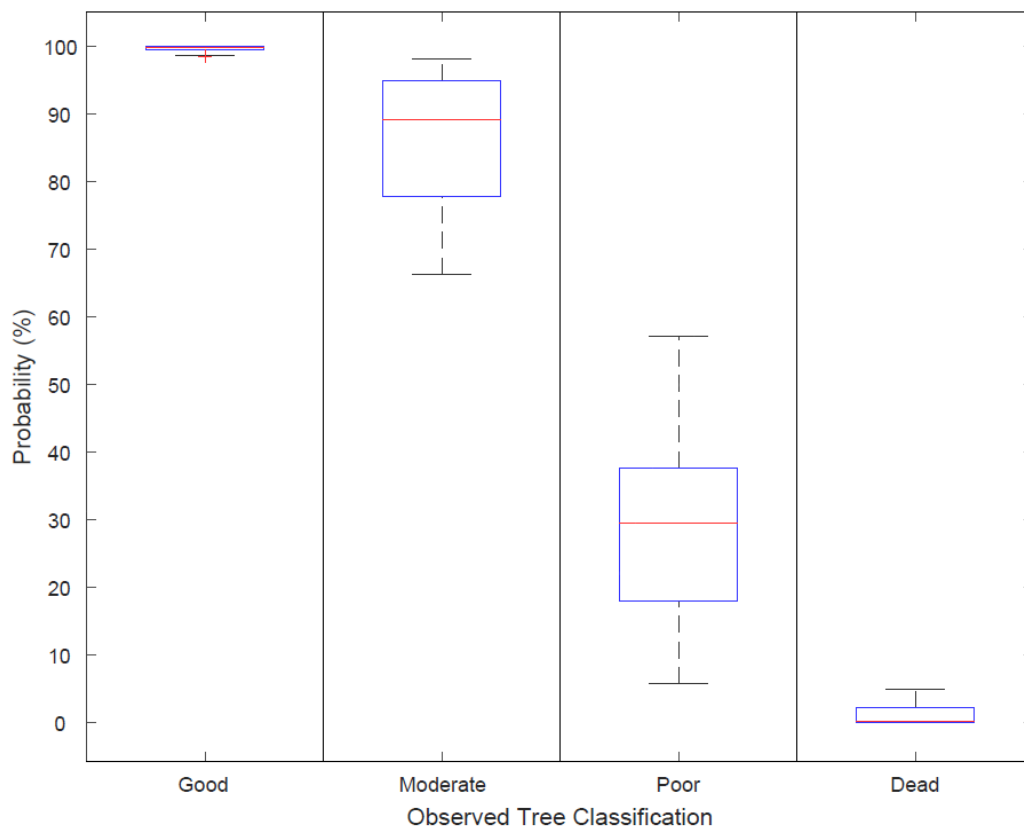


Figure 14 A proportional odds model to indicate the probability (P) that tree structure images, quantified in fractal dimensions (Df), are indicative of an observable tree structure condition and known reference standard ($n64$). Tree images were measured for structural complexity in Df . The box plot extents identify the P that the structures show characteristics of the reference standard.

4.5 Discussion

This study presents a methodology for the objective assessment of tree crown structure, through analysing tree crown structure in hemispherical images. The underlying aim of this study is to reduce the degree of subjectivity currently accepted within tree surveying and assessment, and to provide opportunities for high resolution intra-category assessment of tree structure. Mandelbrot (1967) states that the question of how to accurately measure tree crowns, with the inherent complexity of objectively assessing various shapes, forms, structural porosity, all of varying sizes, is not a simple task that can be solved with classical geometry. Following the findings of this study, it is possible to quantify tree structural complexity using D_f as an objective predictor variable using a relatively proximal photogrammetric method and computational analysis (Figure 13), thereby increasing the objectivity and repeatability of structural assessment, whilst also reducing the potential for bias from field measurements.

Through quantifying tree structure in D_f and creating a proportional odds model, the probabilities that field-observed, 'good' classified trees displayed the structural characteristics of structurally sound trees, was found to be statistically very high at $P \sim 99\%$. Due to the way the proportional odds model functions, achieving this high level of probability is essential for the reliable characterisation of the remaining structural condition types. It is suggested that this method of analysis could be transferred to many other investigations of tree structure where the model is trained on a species-specific basis across differing structural architectures.

Following the creation of the model, the probabilities of trees with moderate, poor or dead observed classes reduce at the median to $P \sim 89\%$, $P \sim 29\%$ and $P < 1\%$

respectively when compared to the reference standard images (Figure 14). These changes in median levels reflect a measured reduction of the tree crown structure complexity. The continuous nature of the Df scale provides a unique measurement of individual tree structure characteristics, as opposed to individual trees being arbitrarily grouped into coarse-resolution, homogenous categories where intra-category differences cannot be easily identified. This insight provides the researcher or practitioner with the opportunity to further sub-divide each classification group, and to monitor intra-category variance over time. This methodology has the potential for the long-term monitoring of pest, disease or pathogen progression, or for the quantification of structural decline, particularly with trees of high conservation, landscape or heritage value. This could include the monitoring of naturally occurring veteran trees, to quantify their rate of structural decline, particularly in areas where there is potential conflict with the public. Furthermore, this method could also be used to guide and inform the process of tree veteranisation, where pre-veteran, mature trees are intentionally injured and receive structural alterations to mimic the structure of naturally occurring veterans with the aim of providing valuable habitats that would otherwise only be found on the most mature trees (Bengtsson, Hedin et al. 2012).

As shown in Figure 13a there is a wide range of Df values, homogenous grouping of field-observations, and no clustering of the *P* ranges for each potential category. Therefore, it can be stated that tree structure is more accurately quantified in a structural condition continuum than with traditional categorical classification methods. Tree structure measurably degenerates the more trees senesce; tree crown structures change as branch death and limb shedding occur, which ultimately leads to a general decrease in the fractal nature of tree crowns (Mäkelä and Valentine 2006). Through understanding phenotypic tree structures and the biological response of trees

to environmental stress, there is the potential to relate tree structure complexity to an overall indication of tree health or general condition. Tree crown structures are indicative of the amount of photosynthetically active area in the tree required for homeostatic equilibrium, and therefore is considered to act as a reliable indicator of tree health (Burkhart and Tome 2012).

An advantage of this method is the potential to measure intra-category differences in tree structure complexity and with the computerised storage and easy retrieval of this data, the same analysis can be repeated over time, allowing the accurate tracking of tree structure change. Sudden catastrophic damage to a tree crown is readily recognisable, such as when following a strong wind event. However, more subtle or prolonged tree crown degeneration as a result of biotic or abiotic stress; such as pathogen ingress, or sudden death as a result of heavy, late frosts, could be measured and identified over repeat iterations of surveying. It is recognised that in the immediate period after the sudden death of a tree via these more subtle means, that the structure will likely not have changed significantly, and although potentially dead, a tree could still be classified as good due to the immediate retention of its ‘good’ structure, further reinforcing the requirement for temporal studies to monitor the subtle changes of the tree crown. Further developments of this method should include a refinement of the methodology to accurately measure more subtle structural change in the finer structures of the crown edge.

The traditional coarse categorical classification methods do not provide a clear mechanism for measuring subtle structural degeneration as the thresholds for the each potential category are poorly defined and only provide generalised categories for the tree classification. For tree-risk managers such as local government tree officers or

utility company infrastructure managers, a structural condition continuum can be used to objectively quantify the probabilities that their tree stock is in a suitable condition. Through quantifying tree structure in a continuous Df scale, specific, measurable thresholds for remedial intervention may be defined. With a categorical approach, tree-risk managers have the limitation of allocating broad categories such as ‘poor’ or ‘dead’ as the triggers for remedial intervention. This limitation greatly increases the number of trees that will be designated as requiring remedial work, compounded by the additional costs and labour requirements. As a higher resolution method, our new approach has the potential to limit unnecessary remedial works, lowering tree management expenditure, and would facilitate limited resources being used in more focussed interventions. We acknowledge that additional work is required to quantify the extent of these improvements, particularly in respect to health and safety related tree management.

This investigation used a single broadleaved tree species, and we recognise that further work is required to determine where categorical thresholds exist for other tree species. This would follow the work of Morse, Lawton et al. (1985), who observed that there are differences in the structural complexity of varying vegetation species when they are measured in Df. During a pilot study phase, we identified that there are different thresholds for condition categories in different tree species. The other broadleaved species photographed in various quantities prior to this investigation, were; *Acer pseudoplatanus* (L.), (*Fraxinus excelsior* (L.), *Quercus rubra* (L.), *Fagus sylvatica* (L.), *Betula pubescens* (Ehrh.), *Crataegus monogyna* (Jacq.), and *Pinus sylvestris* (L.). Initial observations suggest that there are likely to be interspecies differences from the small sample numbers used, therefore, this research could also be extended to consider other tree species.

In training the reference category for the proportional odds model, trees that are observed as being in a sound structural condition and are representative of trees in good condition for that species, are identified as the reference category trees. These become the standard against which the remaining trees of the same species are compared. In the process of developing the model, a small degree of user intervention is required to define the parameters of the model and to interpret the model efficacy. Similarly, a user defined bounding box is created to identify the area of interest for the image analysis. This method ensures the procedure can be applied across the full range of tree crown images. The creation of the bounding box is governed by the user following a set of standards that are influenced by standard forestry conventions (West 2009), and the simple requirement to only identify the tree crown of interest and no other elements, such as the image vignette region. An important distinction to highlight is that the procedure remains a dependable and independent methodology, despite the user intervention as the image analysis, statistical querying and computation of the Df value are all autonomous and therefore, remain objective. This methodology does not purport to entirely remove the requirement for practitioner intervention. We also recognise a potential limitation of this methodology is the reliance on the southern axis for capturing crown images. During methodology development, the southern axis was used to standardise fieldwork when capturing tree crown images. It is recommended that additional field trials should be undertaken to determine the sensitivity of capturing images from differing cardinal points or multiple locations per tree.

4.6 Conclusion

The methodology described in this study for assessing the structural condition of trees is commensurate with traditional techniques. The development of a proximal, hemispherical image field methodology enabled the data capture of many trees in a range of different physical conditions and locations, and satisfies the first objective of this study. The second objective was met with the analysis and objective measurement of hemispherical tree structure images. Finally the ranking of individual trees by the automated calculation of the continuous Df values, satisfies the third objective. It can be stated that the traditional techniques which identify broad categories of structural condition are very coarse, as they do not account for intra-category structural variability and are highly subjective. Our approach enables the assessment of tree condition to be completed with a greater level of precision than was previously possible due to the continuous nature of the Df measurement. Fundamentally, this concept provides a repeatable and objective way to characterise tree crown structure, which can be used to improve the objectivity of tree surveying and inform the specific management of trees with high amenity value. We recognise that further work is required to define the sensitivity of the image acquisition protocol, and to gain further understanding of the full extent of intra-species differences. Nonetheless, it is envisaged that this methodology could form the basis for a new range of analytical measures that will enable tree, environmental or ecological managers to gain greater insights and make more informed decisions about the tree stock under their management.

4.7 Funding

This research is supported by an Engineering and Physical Sciences Research Council (EPSRC) studentship for the lead author [EP/L504804/1].

4.8 Supplementary Information

The following supplementary material is available at *Forestry* online: Statistical analysis of the image pre-processing effect on the predictor variable, D_f , and a recommended workflow for field operations, data collection and processing.

4.9 Acknowledgements

The lead author would like to thank Dr. V. Karloukovski, Lancaster Environment Centre, Lancaster University, for discussions on fractal dimensions, and, Dr. E. Eastoe, Department of Mathematics and Statistics, Lancaster University, for providing statistical advice. The authors would also like to thank the anonymous reviewers for their valuable comments and suggestions to improve the quality of this paper.

4.10 Conflict of interest statement

None declared.

5 ARBOR: A New Framework for Assessing the Accuracy of Individual Tree Crown Delineation from Remotely- sensed Data

5.1 Preamble

A frequent problem within RS studies that assess trees in the environment, is quantifying the amount of agreement when identifying the same tree that is represented in two datasets e.g. a tree in aerially acquired RS data and the same tree in GR data. This agreement problem also occurs when comparing two RS datasets. In whichever dataset is used, the spatial location of a tree will be identified and the extent of the crown defined through a process of crown delineation. The delineation process can be completed via various methods, including manual or computational delineations, which describe the spatial and biophysical properties of the tree crown when viewed from a (2D) plan perspective. For validation purposes, it is important to achieve a high level of agreement between the two datasets. However, as the individual trees are described in two unique datasets, each tree could potentially have differences between the two locations, two crown extents and two tree heights, leading dataset disagreement and uncertainty in the identification of each tree when compared to the reference dataset.

Currently, the published literature describes a range of techniques that use arbitrary thresholds to suggest a level of agreement between the RS and GR data. Frequently, these methods do not provide adequate quantification when accounting for biophysical differences between the crowns, or the assessment of spatial differences in (3D) Euclidean space. The literature identifies the regular use of simple linear-distance agreement, which fails to fully consider various data alignment issues present in the tree crown delineations.

Following from quantifying the observable structural change within tree crowns, this chapter answers the fundamental questions of, ‘exactly where are the trees within the data?’, and ‘what level of agreement is there between two datasets that is used to describe the same trees?’

ARBOR: A New Framework for Assessing the Accuracy of Individual Tree Crown Delineation from Remotely-sensed Data

Jon Murray^{1*}, David Gullick¹, George Alan Blackburn¹, James Duncan Whyatt¹,
and Christopher Edwards²

¹Lancaster Environment Centre, Lancaster University, Lancashire, LA1 4YQ

²School of Computing and Communications, Lancaster University, Lancaster, LA1 4WA.

*Corresponding author: Tel: +44 1524 652 01

Email: j.murray3@lancaster.ac.uk

To assess the accuracy of individual tree crown (ITC) delineation techniques the same tree needs to be identified in two different datasets, for example, ground reference (GR) data and crowns delineated from LiDAR. Many studies use arbitrary metrics or simple linear-distance thresholds to match trees in different datasets without quantifying the level of agreement. For example, successful match-pairing is often claimed where two data points, representing the same tree in different datasets, are located within 5m of one another. Such simple measures are inadequate for representing the multi-variate nature of ITC delineations and generate misleading measures of delineation accuracy. In this study, we develop a new framework for objectively quantifying the agreement between GR and remotely-sensed tree datasets: the Accuracy of Remotely-sensed Biophysical Observation and Retrieval (ARBOR) framework. Using common biophysical properties of ITC delineated trees (location, height and crown area), trees represented in different data sets were modelled as overlapping Gaussian curves to facilitate a more comprehensive assessment of the level of agreement. Extensive testing quantified the limitations of some frequently used match-pairing methods, in particular, the Hausdorff distance algorithm. We demonstrate that within the ARBOR framework, the Hungarian combinatorial optimisation algorithm improves the match between datasets, while the Jaccard similarity coefficient is effective for measuring the correspondence between the matched data populations. The ARBOR framework was applied to GR and remotely-sensed tree data from a woodland study site to demonstrate how ARBOR can identify the optimum ITC delineation technique, out of four different methods tested, based on two measures of statistical accuracy. Using ARBOR will limit further reliance on arbitrary thresholds as it provides an objective approach for quantifying accuracy in the development and application of ITC delineation algorithms.

Keywords

LiDAR, Individual Tree Crown (ITC), Delineation, Error Detection, Data Matching, Accuracy.

Highlights

1. ARBOR answers the need for a standardised ITC delineation accuracy assessment
2. Similarity of RS-derived and reference trees assessed using biophysical properties
3. Optimised algorithm applied to matching RS-derived and reference tree populations
4. ARBOR quantifies accuracy using biophysical data and data population size
5. ARBOR is a modular framework for the objective assessment of ITC delineations

5.2 Introduction

Individual tree crown (ITC) delineation is an important technique for many environmental remote sensing (RS) studies. These types of investigations include data driven activities such as forest inventories and management, carbon and biomass accounting, tree growth modelling and many other geo-spatial data applications. The ability to accurately delineate individual trees from remotely sensed data is essential for many forest monitoring applications (Eysn, Hollaus et al. 2012, Jakubowski, Guo et al. 2013, Duncanson, Dubayah et al. 2015, Wu, Yu et al. 2016, Zhen, Quackenbush et al. 2016). ITC delineation, sometimes referred to as tree segmentation, is typically associated with the analysis of high resolution optical imagery or 3D point clouds captured from light detection and ranging (LiDAR). ITC delineation is a process where different methods, often computational and automated, identify high peaks in canopy data as the first step in locating individual trees. This phase is followed by a segmentation procedure, such as watershedding, valley formation or other similar methods, to determine the locations and crown perimeters of individual trees. Typically, to assess the validity of ITC delineation a comparison is made with ground reference (GR) tree data. The comparison requires that individual trees are matched between the two datasets and this pairing is used to assess accuracy of the ITC

delineation. In many studies, Euclidean distance is used to pair trees from the different datasets. This has the effect of considering the tree-to-tree matching problem only from a plan perspective, and does not account for tree height or crown area (Yu, Hyyppä et al. 2006, Kwak, Lee et al. 2007, Hladik and Alber 2012, Lu, Guo et al. 2014, Zhen, Quackenbush et al. 2016, Yu, Hyyppä et al. 2017).

Additional insights can be obtained through the combination of ITC delineated trees and other spatial data. For example, canopy height models (CHM) characterise the upper surfaces of the delineated tree crown area and provide opportunities to calculate biophysical properties such as tree height or crown area (Rahman and Gorte 2009). Zhen et al., (2016), note that validation is a key issue in ITC delineation studies. Typically, validation involves assessment of the outputs of ITC delineation procedures in terms of the precision and accuracy of tree locations and biophysical properties (Leckie, Walsworth et al. 2016). However, there are other issues that complicate the match-pairing ITC delineation, such as the self-optimising growth habits of trees in woodlands (see *supplementary information* – Appendix C). Any resulting ITC delineation anomalies can subsequently lead to the spurious identification of tree crowns (Kwak, Lee et al. 2007), causing the pairing of trees that should not be present in the dataset, or otherwise, through the generation of false-positive matches.

Problems that occur in the match-pairing process are further compounded when analysing data population sizes. A significant consideration when matching pairs of trees is the directionality of the match that is made. Essentially this is the matching of data A to data B in the matching sequence, or, matching data B to data A. Errors that arise from directionality differences can result in the same matches not being achieved

in both directions, influenced by the data that is used first as the primary dataset. A solution is bidirectional matching, i.e. matching A-B then B-A, and selecting the best agreement (Singh, Evans et al. 2015). However, this approach reduces the data population as the unmatched trees are unassigned, leading to losses from the dataset. An additional problem is that sorting the order of the data effects match-pairings, as does the order sequence that the algorithm attempts the pairings (Holmgren and Lindberg 2013), for example, matching the tallest trees first. Some data preparation methods sort data by size as part of the processing steps (Kandare, Ørka et al. 2016), however, within tree-to-tree matched-pairing, this may block later trees in the dataset that would have been a more suitable pairing, as the primary tree is already allocated to a corresponding tree. GR data frequently contains many smaller and lower canopy trees that are readily assigned to pairings that are not a suitable match (Holmgren and Lindberg 2013). Trees that are observed in the GR data and not seen in the ITC delineation are data omissions as a product of the data population A, not being the same size as the population B or *vice-versa*. Similarly, commission errors occur where trees are incorrectly assigned to a match-pairing, or assigned to the wrong tree (Holmgren and Lindberg 2013). Typically these errors are related to the ITC delineation method used.

Despite the recognised importance of data validation, in a meta-analysis of 210 studies, only 14.3% validated ITC delineation at a forest stand level, 30% validated ITC delineation on individual trees, and 23.3% at both levels Zhen, Quackenbush et al. (2016). Significantly, in 32.4% of the studies, no ITC validation was attempted at all. This suggests that there is a pressing need for a standardised method for evaluating the accuracy of ITC delineation techniques, which can be applied widely and consistently Zhen, Quackenbush et al. (2016). It is also apparent from the literature

that no standardised accuracy assessment procedure currently exists, and where ITC delineation techniques have been evaluated this has been on the basis of arbitrary metrics or simple linear distance thresholds. Therefore, there is the need for analytical metrics to quantify the accuracy with which ITC delineations estimate data population size and tree biophysical properties. The research outlined in this paper describes a repeatable and transparent solution for validating ITC delineation techniques that can be applied to individual trees, plots or stands. This paper describes the development of the Assessment of Remotely-sensed Biophysical Observations and Retrieval (ARBOR) framework.

5.3 Aim and Objectives

The aim of this research is to develop a technique for quantifying the accuracy of ITC delineation methods. This requires improving tree-to-tree match-pairing with metrics that include additional analytical parameters beyond simple location or linear distance measurement. Furthermore, metrics are required to find an optimal way in applying the match-pairing to, and achieving the best match for, the overall data population. This approach needs to be robust to the influence of directionality, data order and data omissions. If fulfilled, these requirements allow ITC delineation accuracy in RS data to be assessed in an objective manner. This will be achieved by addressing the following objectives:

1. Identifying a suitable technique for quantifying the similarity of a tree as represented in RS-derived and ground reference datasets, using the biophysical properties: tree location, height and crown area.

2. Determining an optimal algorithm for matching an entire population of trees represented in both RS-derived and ground reference datasets, avoiding introduced bias from directionality, data omissions and other similar factors.
3. Developing metrics for quantifying the accuracy of population size and tree biophysical properties
4. Applying the optimal algorithm and metrics to quantify the accuracy of a variety of ITC delineation methods applied to RS data of a woodland study site.

5.4 Methodology

The methodology for developing the ARBOR framework directly addresses each of the objectives outlined above. Objectives 1-3 will be met by development and testing within a synthetic data environment, to establish the validity of the different analytical elements that will be used within the ARBOR framework. Following the development of the framework and validation of the components that will be used in ARBOR, Objective 4 will be met by applying the ARBOR framework to quantify the match-pairing of real-world data, therefore, providing proof of concept.

5.4.1 Quantifying the Similarity of a Tree as Represented in RS-derived and Ground Reference Datasets

5.4.1.1 Defining the Biophysical Properties of a tree.

Jing, Hu et al. (2012) state that differentiation between natural tree crowns is influenced by both the width and depth of the inter-canopy space, in addition to the computationally delineated, circular crown shape. Correspondingly, each tree crown in this study can be considered to have at least a location, height and crown area. To quantify correspondence between two trees, or more specifically, a tree represented in RS-derived data and the same tree in the GR data, the metric criteria has to consider spatial proximity, tree height and overall crown area. Also, for the accuracy

comparison to be made on a like-for-like basis, metrics should report successful similarity indices with values of between 0 (impossible) and 1 (certain or identical).

5.4.1.2 Limitations of Commonly Used Tree-to-tree Match-pairing Methods

Some tree-to-tree match-pairing agreements are based upon the Euclidean distance between trees (Yu, Hyypä et al. 2006), however, this approach has problems that may not be adequately resolved. For example, the 2D measurement of the planar distance between the tops of trees assumes that each tree only has a singular apical point. Kaartinen, Hyypä et al. (2012) note that additional trees in the lower canopy can lead to omission errors between GR and ITC delineated trees. Alternatives consider tree-to-tree pairwise-matching from a 3D model perspective, with linear distance statistics such as the Hausdorff distance algorithm, used to assess the linear correspondence between two points from different datasets (Yu, Hyypä et al. 2006, Yu, Hyypä et al. 2017, Zhao, Suarez et al. 2018). The Hausdorff algorithm meets the metric criteria following rescaling the index between 0 and 1, however, due to the distance between the delineated edges of a tree crown, omission errors can occur. Hausdorff can be used in data point comparison, but can be influenced by directionality. To counter this effect, a geometric shape for the crown, such as a circle, has to be used when calculating Hausdorff.

5.4.2 Gaussian Overlapping and the Jaccard Similarity Coefficient

The analysis of the overlaps between two Gaussian curves (also known as a Gaussian overlap model), measures the comparative distance between the two distributions (Nowakowska, Koronacki et al. 2014). This approach uses the curve centre as the tree location, with the apex indicating the overall tree height and the area under the curve representing the circular crown area. A component overlap analysis of the mixed, normal data distributions identifies changes in the curve location, height and crown

area between the overlapping parabolas (Nowakowska, Koronacki et al. 2015). A Gaussian overlap models where a single tree, identified and described in both datasets, can be aligned to a potential match in the opposing dataset and any similarities in the biophysical properties compared and quantified. Issues regarding complexities in the biophysical properties of trees are discussed further in *supplementary information* (Appendix C).

To satisfy the analysis criteria, the area of overlap between each Gaussian representation of the tree's biophysical properties is assessed. Similar trees achieve greater Gaussian overlap than non-similar trees. To quantify the overlap as a normalised value, the Jaccard similarity coefficient is calculated. Jaccard is the quotient produced by the division of the intersection by the union and measures the observable similarities between two finite data sets. Functionally, Jaccard is a simple measure of the binary distance between data and describes the presence or absence of data, as defined at equation (5.1).

$$J(A, B) = \frac{|A \cap B|}{|A \cup B|} = \frac{|A \cap B|}{|A| + |B| - |A \cap B|} \quad (5.1)$$

A perfect match is a Jaccard value of one, while inferior matches decrease Jaccard towards zero. Due to the infinite nature of the tails on a Gaussian curve, an absolute score of zero cannot be achieved as an inferior score representing a more heavily degenerated match always remains mathematically possible.

Figure 15 uses some examples to demonstrate the Gaussian overlap method and Jaccard coefficient. Figure 15a shows two synthetic trees with a poor match with differing locations, heights and overall crown size (Jaccard 0.01). Figure 15b shows an improved commission for location and crown size; however, some commissioning differences remain (Jaccard 0.25). Figure 15c shows a close alignment in size and location, with small commission losses in height, resulting in a close match (Jaccard 0.9), whilst Figure 15d shows a low commission between height, crown size and location (Jaccard 0.15). Figure 15e shows a close match in location, but a low match in crown height and size (Jaccard 0.40) and Figure 15f shows an offset in the location, similar crown size and minor differences in height (Jaccard 0.74).

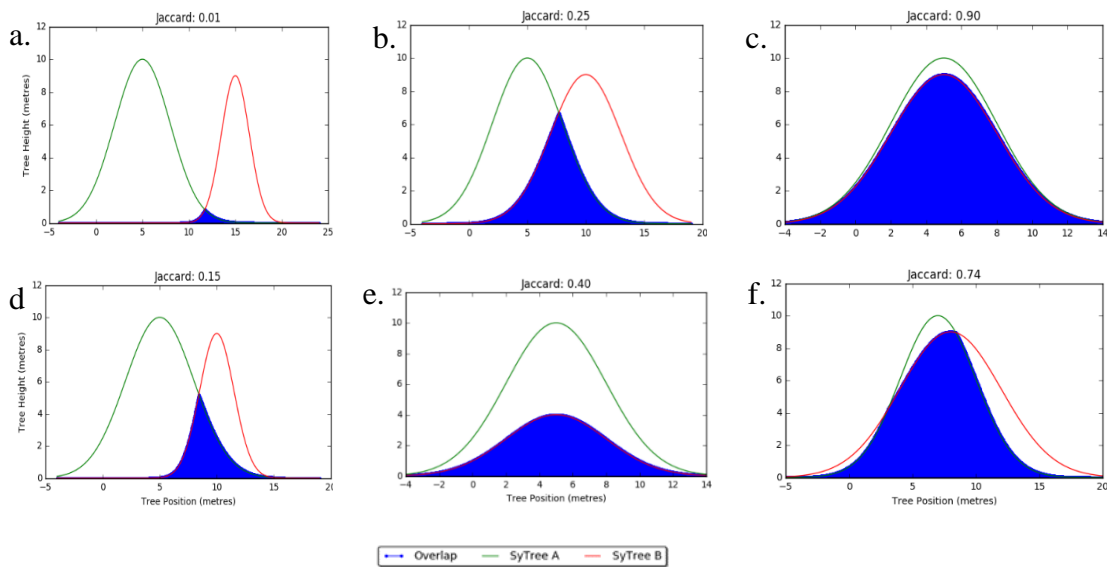


Figure 15 Gaussian overlap used for measuring data agreement between two data sets, where the difference between the two shapes is quantified using the Jaccard similarity coefficient.

5.5 Optimal Algorithm for Matching Populations of Trees Represented in both RS-derived and Ground Reference Datasets

5.5.1 Meta-study of Alternative Match-pairing Methods

Following a review of highly-cited papers from peer-reviewed journals, published 2003-2017, it is apparent that many different match-pairing methods are used when evaluating agreement between GR and RS-derived data. These match-pairing methods have been consolidated into Table 8, where similar methods are grouped together (base matching method, filtered or thresholded, and sorting priority). These groups are further subdivided into methodological categories including, for example; data filtering by height, area, distance and angle. Table 8 also shows where a threshold has been applied either to the base or secondary matching filters. The direction of the match for each method is indicated as; 1) matching the GR to the RS-derived data, 2) matching RS-derived to the GR data, or 3) attempting a match in one direction, then in the other (bidirectionality) and selecting the match with the highest agreement. All of these different matching directions can potentially lead to different pairs of trees being matched, across the varying permutations. Following the review (Table 8), two representative match-pairing (RMP) methods are defined, that replicate common match-pairing methods used in the literature:

- **RMP 1: Hausdorff Distance Algorithm**

(Trees paired by distance to one another, the closest achieving a pair)

- **RMP 2: Within Neighbourhood, Sorted by Area and within a Height Threshold**

(Sort A by area. Define neighbourhood of 21m. Find trees within 5m of one another, and closest sized crown areas are matched)

These two RMP methods were subsequently compared to a new approach (see Hungarian Combinatorial Optimisation Algorithm) in a test using synthetic tree data (Testing the Pairwise Matching Algorithms with Synthetic Data).

Table 8 A meta-study of several match-pairing methods showing the base matching method, and identifying whether subsequent filters or thresholds are applied. The direction of the match is also shown.

Papers	Base Matching Variables				Thresholds or Filters				Sorting Priority		Match Direction				
	Location	Neighbour-hood	Height	Area	With Threshold	Height	Area	Angle	Acceptance Level	Distance		Crown Length	With Threshold	Tallest/Biggest	Shortest/Smallest
(Hamraz, Contreras et al. 2016)	*					*		*	*			*			A<->B@
(Kandare, Ørka et al. 2017)	*									*		*			B->A
(Maltamo, Mustonen et al. 2004)	*					*						*			A<->B@
(Koch, Heyder et al. 2006)	*					*									A<->B@
(Kaartinen, Hyypä et al. 2012)	*				*										A<->B@
(Kaartinen, Hyypä et al. 2012)	*				*	*									A<->B@
(Kaartinen, Hyypä et al. 2012)	*				*	*						*			A<->B@
(Kaartinen, Hyypä et al. 2012)		*	*		*				*			*	*		A<->B@
(Kaartinen, Hyypä et al. 2012)		*	*		*								*		A<->B@
(Kaartinen, Hyypä et al. 2012)		*	*		*								*		A<->B@
(Jing, Hu et al. 2012)				*	*										A->B
(Jing, Hu et al. 2012)				*	*										B->A
(Lee, Slatton et al. 2010)				*		*					*				B->A
(Singh, Evans et al. 2015)	*									*					A<->B@
(Holmgren and Lindberg 2013)	*					*	*						*		A->B
(Rahman and Gorte 2009)	*						*						*		A->B
(Kandare, Ørka et al. 2016)	*					*				*				*	A->B
(Maltamo, Packalen et al. 2005)	*					*							*	*	B->A
(Swetnam and Falk 2014)	*				*	*	*							*	AXB
(Brandtberg, Warner et al. 2003)			*		*					*				*	B->A
(Reitberger, Schnörr et al. 2009)	*				*	*						*		*	B->A

Notes: **A** = Ground reference (GR) data. **B** = RS-derived (RS) data. **A->B** = GR matched on to RS. **B->A** = RS matched on to GR. **A<->B@** = match attempted in both directions and the best match chosen. **AXB** = match directionality not described.

5.5.2 Hungarian Combinatorial Optimisation Algorithm

The Hungarian algorithm (also called the Kuhn–Munkres algorithm or Munkres assignment algorithm) is described in detail by Kuhn (1955). The Hungarian algorithm was originally defined to resolve the “assignment problem” in operations mathematics (Kuhn 1955), and has been used widely in data science, but rarely in RS or environmental studies. In this approach, the description of the data size and suitability of a match available is used in the algorithm, meaning the biophysical properties of trees from each dataset; location, height and crown area are also analysed, thereby meeting the metric criteria. The Hungarian algorithm attempts all possible pairing combinations for each point in data A against each point in data B and then *vice-versa* and outputs the optimal overall match-pairing.

5.5.3 Quantification of Accuracy with which Delineations Estimate Biophysical Properties and Population Size

Following the completion of match-pairing and Gaussian overlap assessment two accuracy metrics were calculated. The match-pairing success is quantified by the average match-pairing similarity index (AMPS). This function is the average match-pairing agreement as measured using the Gaussian overlap method (Gaussian Overlapping and the Jaccard Similarity Coefficient) calculated across all tree pairings. Higher AMPS values indicate a better overall quality of match for the paired trees. In addition to AMPS, the relative dataset sizes are also quantified to identify disparities in tree population size in GR and RS-derived datasets, for example, to show the effects of pairing directionality. The dataset size similarity index (DSS) is defined as the comparison between the total number of trees in the two datasets A and B, against the number of match-pairings achieved, expressed as a normalised value. As with AMPS,

high DSS scores are preferred as this indicates similar tree population sizes in the two datasets.

5.6 Testing the Pairwise Matching Algorithms with Synthetic Data

5.6.1 Synthetic Data Environment

A synthetic environment was created to compare the biophysical attributes of RS trees, using common tree structure values typically output from ITC delineation. For simplicity, the synthetic tree (^{sy}Tree) attributes used were a known location, a predefined crown shape (circle), and a known crown area. During initial testing a single tree was modelled, ^{sy}Tree A, where the biophysical attributes of a real-world tree was randomly selected from within the 5th to 95th percentile of a broadleaved GR tree sample. By taking the biophysical attributes of ^{sy}Tree A, and using randomised offsetting of ^{sy}Tree A's location, changing the height and crown area values, a second tree was created, ^{sy}Tree B. The biophysical attribute alterations were recorded as 'known changes' between the two ^{sy}Tree populations. In subsequent testing phases, similar to the work of Romanczyk, van Aardt et al. (2013) a synthetic environment was used to simulate a complex woodland area containing 500 new ^{sy}Trees (^{sy}Tree A₅₀₀).

As before, the ^{sy}Tree A₅₀₀ population was subject to randomised location, height and crown area changes, further creating a secondary population, ^{sy}Tree B₅₀₀. This produced trees ranging from 3 to 14m tall, with crown diameters between 0.75 and 1.4 times the size of the sampled GR tree average. This procedure ensured that all 500 ^{sy}Trees had intra- and inter-population biophysical attribute differences. The recorded alterations were used as a known changes index for measuring predicted differences

between ^{sy}Tree A₅₀₀ and ^{sy}Tree B₅₀₀, against the observed differences. Variation from the known changes index identified commission error. Figure 16 depicts 500 ^{sy}Trees, showing a) tree canopies in the predicted reference phase, and b) following data noise and population losses. The ^{sy}Tree crowns are organised by height, replicating the presentation of the data as though observed in a CHM.

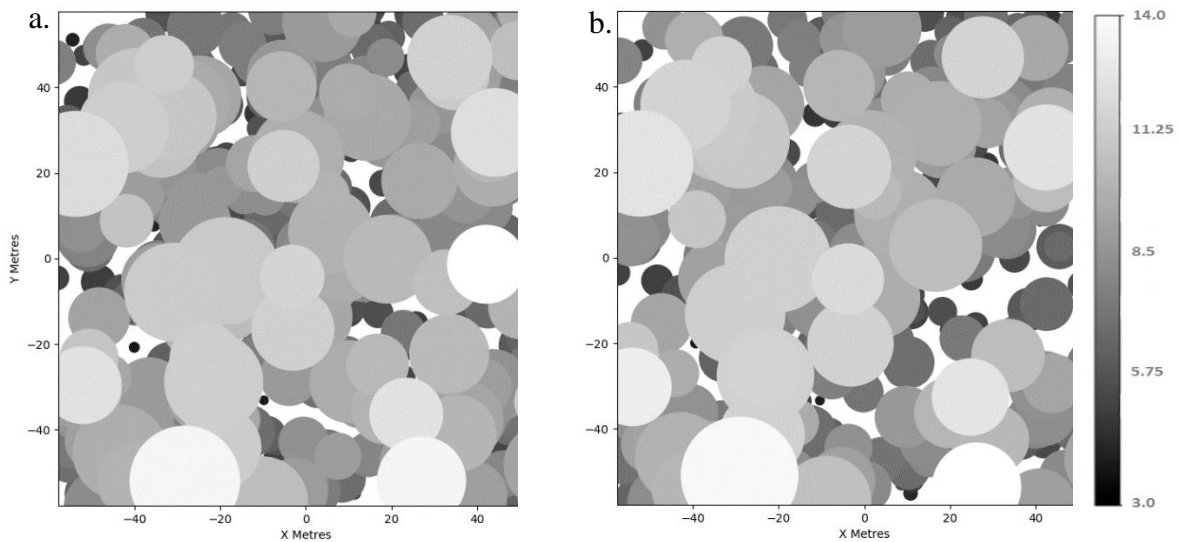


Figure 16 500 synthetic trees representing ground reference (GR), and RS-derived LiDAR datasets. a) models 500 GR trees, and b) represents RS-derived trees with increased noise and tree losses. This replicates typically observed effects in aerial LiDAR derived canopy height models.

5.6.2 Introduced Data Noise and Population Losses

Sensitivity testing between the ^{sy}Tree populations was undertaken by increasing data noise levels and population losses, to intentionally imbalance the datasets. The ^{sy}Tree A population remained unchanged while the ^{sy}Tree B population received randomised changes in location, height and crown area on an incremental scale (1-5). Each randomised variable used an individual set of Gaussian curves replicating the common commission problems that occur between RS-derived and GR datasets.

Figure 17 illustrates changes in the location variable as each biophysical parameter had a unique set of curves. The biophysical properties of the ^{5y}Tree B population were modified by +/- of a random sample, within the appropriate distribution, relative to the prescribed noise level (Table 9). Data population losses were simulated by removing a randomised amount in incremental steps of 10% of the dataset up to a maximum of 50% removal. The introduction of data noise and loss from the tree populations, was applied across all iterations of match-pairing algorithms, to test the robustness of the different pairing methods.

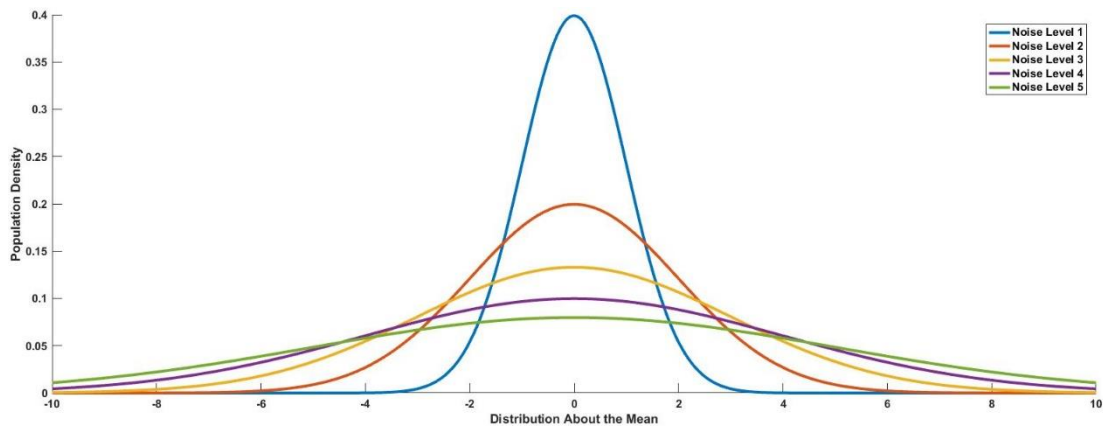


Figure 17 An example of Gaussian curves demonstrating the change on data distribution and population density for synthetic tree data. This example represents the change in location data with the x axis equating to metres offset. This method intentionally introduces data noise to a remote sensing dataset of synthetic trees.

Table 9 Introduction of data noise following modification of the normal distribution and standard deviation (SD) effect on the data population relative to data noise levels.

Data Noise Level	Population (%) by Standard Deviation (SD)
1	SD1 = 68% +/-1, 95% +/-2, 99% +/-3
2	SD2 = 68% +/-2, 95% +/-4, 99% +/-6
3	SD3 = 68% +/-3, 95% +/-6, 99% +/-9
4	SD4 = 68% +/-4, 95% +/-8, 99% +/-12
5	SD5 = 68% +/-5, 95% +/-10, 99% +/-15

5.6.3 Results of Pairwise Matching Tests

To measure the tolerance between the predicted reference (dataset A) and observed values (dataset B), normalised root mean squared error (NRMSE) was calculated for each match-pairing method; RMP1 (Hausdorff distance), RMP2 (neighbourhood and area), and a new method, Hungarian with Gaussian overlap (Figure 18a-f). NRMSE describes the distance of the residuals from the predicted 1:1 line on a normalised scale (Figure 18a-c). This quantifies the match-pairing performance against the expected known changes index. Low NRMSE scores are preferable to high scores, hence within Figure 18a-c the scale bar is inverted. Each match-pairing method was tested with incremental data noise (level 0-5), and data population losses (0-50%). A ratio of matched-pairs was calculated for each data population (Figure 18d-f). For example, if 50 trees from 500 is paired, this achieves a paired ratio of 0.1, while pairing 450 trees achieves a paired ratio of 0.9.

Figure 18a establishes that RMP1, the Hausdorff distance match-pairing method, at noise level 0.25, achieves ~0.6 NRMSE. Furthermore, a small increase in the noise level to 0.5, significantly reduces the efficacy of the RMP1 method in achieving match-pairing to ~1.0 NRMSE. This is a uniform response across all additional levels of noise and all combinations of data population losses. In Figure 18d, the paired achieved measure for RMP1, shows a paired ratio score of 1.0 across all combinations of noise and loss. This unidirectional method demonstrates a complete data population pairing between the A and B datasets, where the matching is completed in the direction of B-A.

Figure 18b & e shows the RMP2 match-pairing method (neighbourhood and area). In comparison to Figure 18a & d, there is an uplift in results, with ~0.0 NRMSE achieved

at 0 noise and 0% loss. Within Figure 18b the NRMSE score is maintained across the same level of data noise. However, a gradual increase in data noise up to level 1 rapidly diminished the NRMSE to ~ 0.6 , at the 0% loss level. The trend follows throughout that as noise and loss increases, the NRMSE results indicate a worsening match-pairing performance. This continues to noise level 1.5, where the NRMSE values across all amounts of data loss are between ~ 0.9 to ~ 1.0 NRMSE. Figure 18e indicates that very low levels of noise is tolerated throughout all permutations of data losses (1.0 NRMSE at noise level 0). Only marginal increases in data noise, to 0.25, rapidly reduce the pairing ratio to ~ 0.6 . At the point of noise level 1 the pairing ratio has decreased to ~ 0.1 across all permutations. At noise level 2, the pairing ratio is reduced to 0.0. Figure 18e demonstrates this bidirectional method achieves a full pairing ratio of 1.0 across all data losses to 50% at noise level 0. A marginal increase in noise to 0.25 reduces the paired matching ratio to ~ 0.6 across all losses. This rapid decrease continues to noise level 1, where only a ~ 0.2 paired ratio is achieved, and by noise level 1.5, the paired ratio further reduces to ~ 0.0 . Therefore, this bidirectional routine is demonstrably affected by the data losses applied.

Figure 18c and f shows the new approach of using the Hungarian and Gaussian overlap match-pairing method. Within Figure 18c this method maintains 0.0 NRMSE across all data loss levels, up to the 0.5 noise level. At noise level 1, the analysis shows a low reduction to ~ 0.1 NRMSE across all data loss levels to 50%, which is a significant improvement over the previous two match-pairing methods at the same noise level. There is a further increase to ~ 0.2 NRMSE at noise level 2, again, this is broadly spread across all loss levels. Figure 18c shows that from this noise level, the metric achieves low incremental rises in NRMSE scores, with the method achieving ~ 0.6 NRMSE at noise level 3. This continues up to the highest noise level of all of

the match-pairing methods, where at noise level 3.75 a ~ 1.0 NRMSE is reached. Figure 18f identifies that throughout all combinations of increasing data noise, the Hungarian and Gaussian overlap match-pairing method maintains the ideal paired ratio 1.0, withstanding all effects of data loss up to 50%. This bidirectional, optimised method outperforms the RMP2 method in paired ratio results and equals the paired ratio output for RMP1.

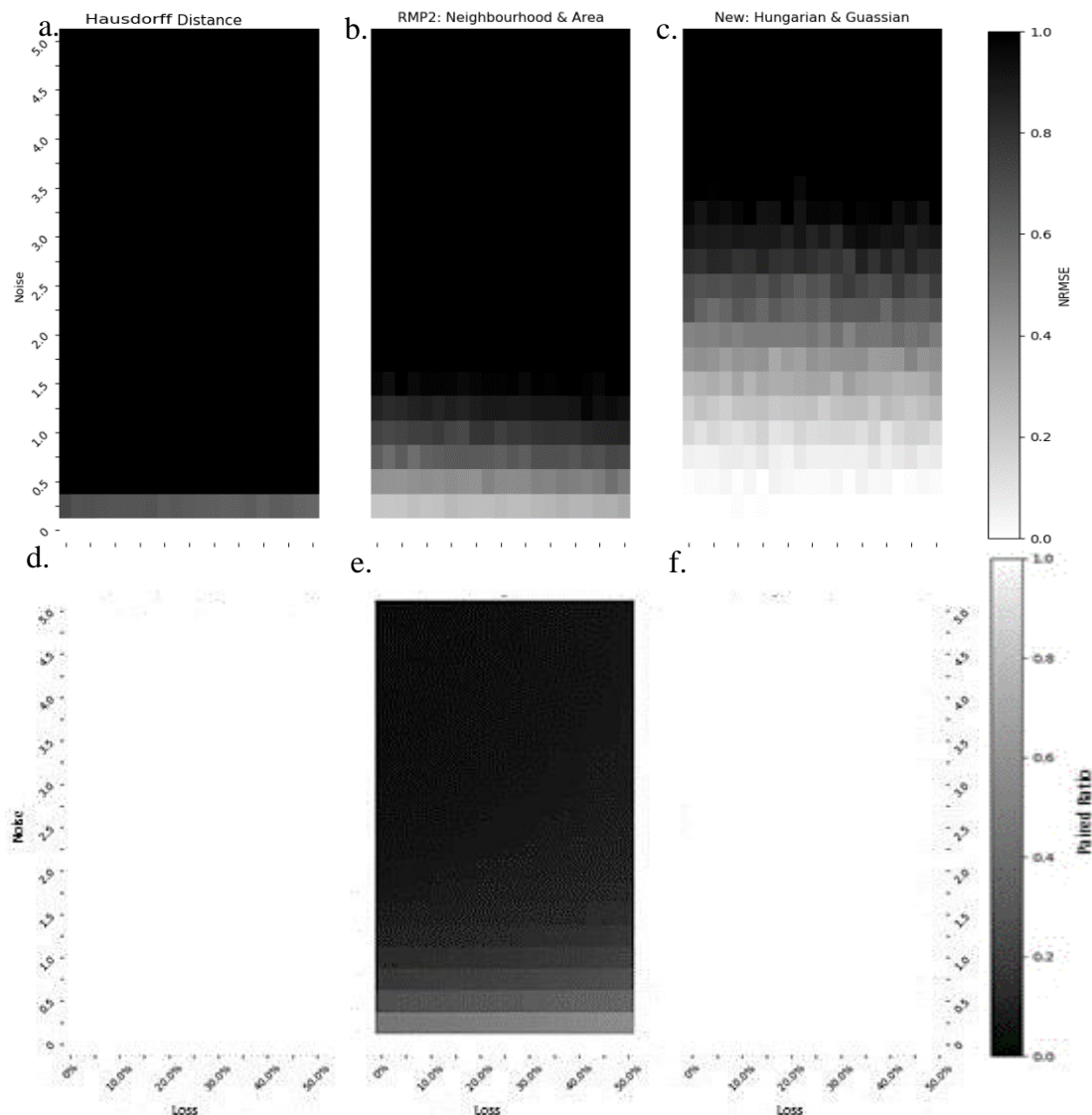


Figure 18 A combination of three data match-pairing methods being tested for the ability to achieve predicted data pairings between synthetic GR and RS-derived data. Each pixel in plots a-c represents an assessment of normalised root mean squared error (NRMSE) at differing levels of data noise and loss. Plots d-f represent the effect of the match-pairing on the data population, expressed as a pairing ratio.

5.6.4 Summary Observations and Recommendation

RMP1 (the Hausdorff distance method), for almost all of the possible data noise and loss combinations, fails to provide reliable match-pairings against the known changes. The method computes ~ 1.0 NRMSE from very low levels of data noise (Figure 18a). The inability to accommodate this noise is due to the way the Hausdorff algorithm uses a linear distance measure between the edges of two shapes. In this application, this is the outer edges of two ITC tree crowns. Correspondingly, the Hausdorff distance score reduces the closer the crowns are to one another, before the crown edges touch when reaching a ‘union’.

The situation changes, however, at the point that the crown edges begin to intersect (Marošević 2018). Where a smaller crown passes inside a larger crown, as is typical when aligning GR and RS-derived trees, the Hausdorff distance increases as the crown edges begin to move away from each other and the crowns wholly overlap, despite the crown centroids not yet being aligned (Marošević 2018). This makes the Hausdorff distance algorithm unreliable in match-pairing using circular crowns. In considering the data population, Figure 18d demonstrates a paired ratio of 1.0 for the unidirectional method. As the match-pairing runs, the algorithm seeks matches for all trees within the response dataset B. When all the matches in B are filled against A, the algorithm is completed and returns the ratio 1.0 (100% matched). Achieving the paired ratio of 1.0 is maintained up to the 50% data loss, despite there being up to 50% remaining unmatched trees in the A dataset. This highlights that as the method matches in a single direction, false-positive results can be reached when data size is not reported.

RMP2, the neighbourhood and area match pairing method, demonstrates an improved performance when compared to RMP1 (Figure 18b & e). However, there is a rapid reduction in the ability of this method to accurately achieve the predicted levels of match-pairing after the introduction of very low levels of data noise (Figure 18b). This is a consequence of the neighbourhood and area thresholds that limit the amount of available matches. As shown in Figure 18b, the threshold effect is compounded rapidly with increasing data noise and population loss. Notably, Figure 18e demonstrates that despite the bidirectional matching routine, the pairing ratio rapidly decreases to ~ 0.1 , (~ 50 trees) at noise level 1.5. During bidirectional matching, A is matched to B, then B to A, and the best match retained ($A=B$). However, the implication is that the match-pairing may not necessarily occur with the same trees, for example, A matches to B, but B matches to a third tree ($B=C$), therefore $A \neq B$, so A is discarded without a match. This effect, and the influence of up to 50% data losses, means that the bidirectional, RMP2 method, artificially reports acceptable levels of matches only with the reduced numbers of trees that remain. Significantly, the number of true matches achieved, as demonstrated by the paired ratio is very low (Figure 18e).

The new Hungarian and Gaussian overlap match-pairing method provides the highest levels of agreement with the predicted measures, including into the highest levels of data noise (Figure 18c). The final NRMSE values are measured at more than twice the noise level achieved than RMP2. RMP1 reduced to ~ 1.0 NRMSE at noise level 0.5, while RMP2 achieved ~ 1.0 NRMSE at noise level 1.5. However, the Hungarian and Gaussian match-pairing method continues to achieve ~ 0.6 NRMSE at noise level 3, and finally reaching ~ 1.0 NRMSE at noise level 3.75. This indicates that at more than double the noise level of the next best performing method, the Hungarian and Gaussian method is considerably more robust to the influence of improper matches.

The stability of this method is further demonstrated in Figure 18f, where the match-pairing method returns a paired ratio of 1.0 across all levels of data noise, and data losses. This is due to the optimised, bidirectional nature of the Hungarian algorithm. The algorithm attempts to pair all possible combinations of each data point in A, with all possible combinations of points in B, then similar to the bidirectional approach, the process is repeated *visa-versa*. However, in the Hungarian algorithm, the routine searches for a match-pair from the opposing dataset for every individual data point within the primary data, considering every possible data point in the opposing dataset, and attempting all possible parameter combinations before the best match is achieved. Therefore, this method achieves a true-positive match from all available options, and a 1.0 paired ratio score for the entire data population.

In summary, within the analysis framework conducted in a synthetic environment, the Hungarian and Gaussian curve match-pairing is demonstrated as being the most effective in accurately resolving the match-pairing problem between GR and RS-derived data. Therefore, following the metrics development and analysis phase, the Hungarian and Gaussian curve match-pairing method is the recommended approach for use in quantifying match-pairing agreement with real-world data.

5.7 The ARBOR Framework

Following the findings of the analysis and results above, the final implementation of the ARBOR framework is illustrated at Figure 19. This structure defines the developmental phase output with a simple, worked example of how the ARBOR framework would interact with two datasets representing a sample of GR trees ($n=100$), and RS-derived trees for the same area ($n=60$).

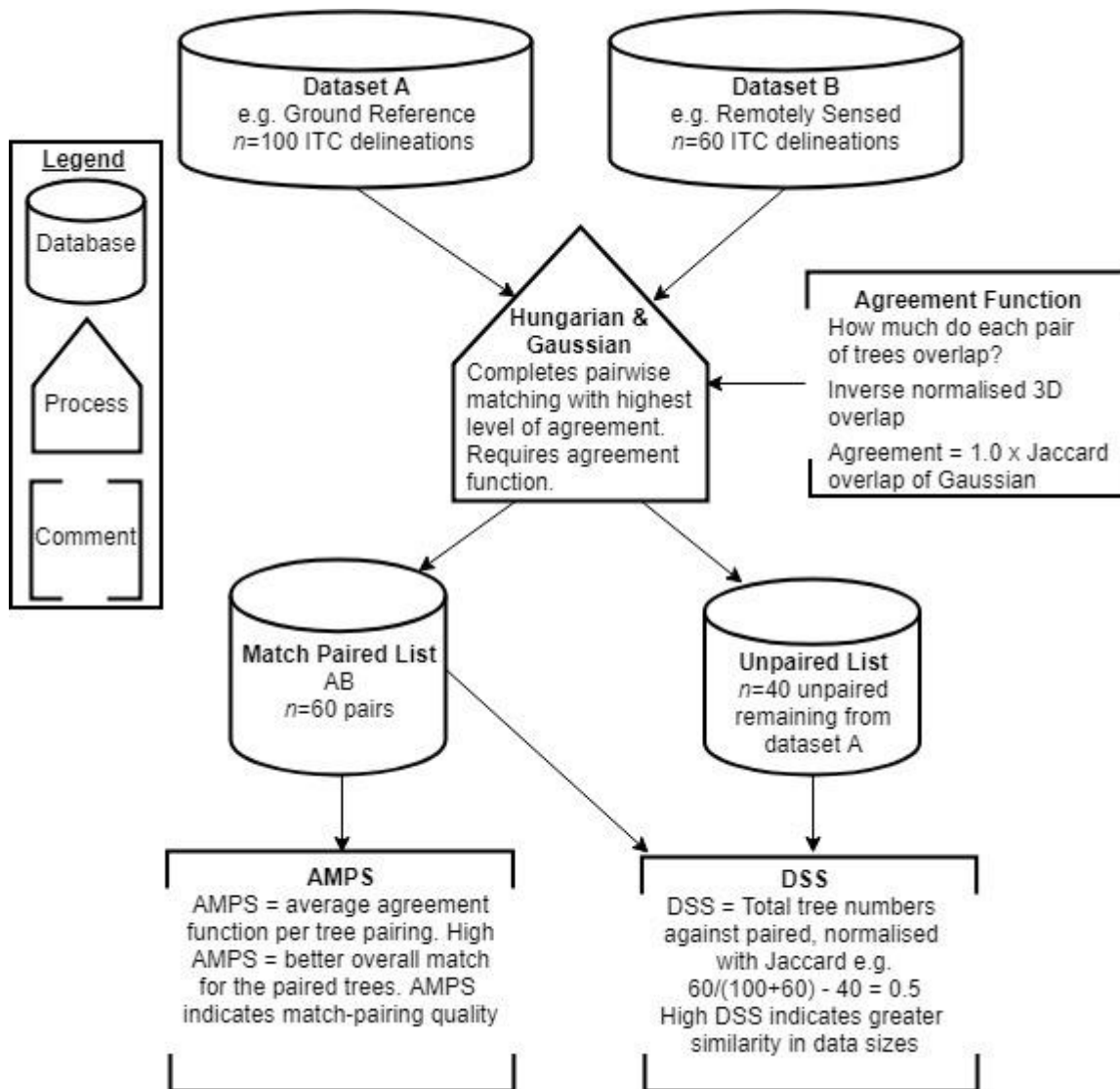


Figure 19 A working example of the ARBOR framework workflow for the quantification of match-pairing agreement between remote sensing derived and ground reference data. Notes: AMPS = averaged matched-pairing similarity index, DSS = dataset size similarity index

5.8 Demonstration of ARBOR for Evaluating ITC Delineations

To demonstrate the principal of the ARBOR framework for quantifying agreement between GR and RS-derived data, the model described in Figure 19, was applied to a large, broadleaved woodland study site that had been scanned by a fixed-wing aircraft, generating ALS LiDAR and digital photography data, and contained twenty-six,

20x20m GR plots, that were manually surveyed with biophysical tree attributes measured and recorded (see *supplementary information* – Appendix C).

The GR plots were identified in the LiDAR data and CHMs for each GR plot was created. Each GR plot was delineated using four different methods. A technician experienced in both manual tree surveying and remote sensing undertook manual ITC delineation (ITC_{MAN}) by digitising vector polygons in ESRI ArcGIS, using a similar approach as described in Brandtberg and Walter (1998). The polygon followed tree crown edges on the CHM, defining crown outlines, crown areas and location centroids. Inverse watershed ITC delineation (ITC_{IWD}) is a frequently used technique (Kwak, Lee et al. 2007, Jing, Hu et al. 2014). ITC_{IWD} identifies valleys (gulleys), and in a top-down approach, locates tree crown edges where adjacent tree crowns meet. This delineation procedure produces a network of connected valleys with the ITC_{IWD} delineated crowns as ‘islands’ between the valleys, and outputs a vector-defined crown edge, location and crown area (Kwak, Lee et al. 2007, Jing, Hu et al. 2014).

A variable limit local maxima ITC delineation algorithm, incorporating metabolic scaling theory (MST) predictions to remove data noise (ITC_{MST}), was also used Swetnam and Falk (2014). The ITC_{MST} method initially uses inverse watershed delineation, but refines tree locations and assignment with MST, outputting individual tree locations, crown areas, and tree heights. Finally, a photogrammetric ITC delineation technique (ITC_{PHO}) was applied to high resolution optical imagery to define tree crown boundaries and locations. For all ITC delineation methods the resulting vector polygons provide tree crown location, centralised height points, and circular shaped tree crowns.

5.8.1 The Results of Applying ARBOR to RS-derived ITC Delineations

The delineation techniques ITC_{MAN} , ITC_{IWD} , ITC_{MST} and ITC_{PHO} were individually analysed against the GR data using the ARBOR framework, where Gaussian overlap replicates the biophysical characteristics of trees and defines the AMPS (averaged match-pairing similarity index) and DSS (dataset size similarity index) to optimise pairwise matching and to measure data population correspondence. Figure 20 demonstrates that the four ITC delineation techniques achieved varying levels of match-pairing agreement.

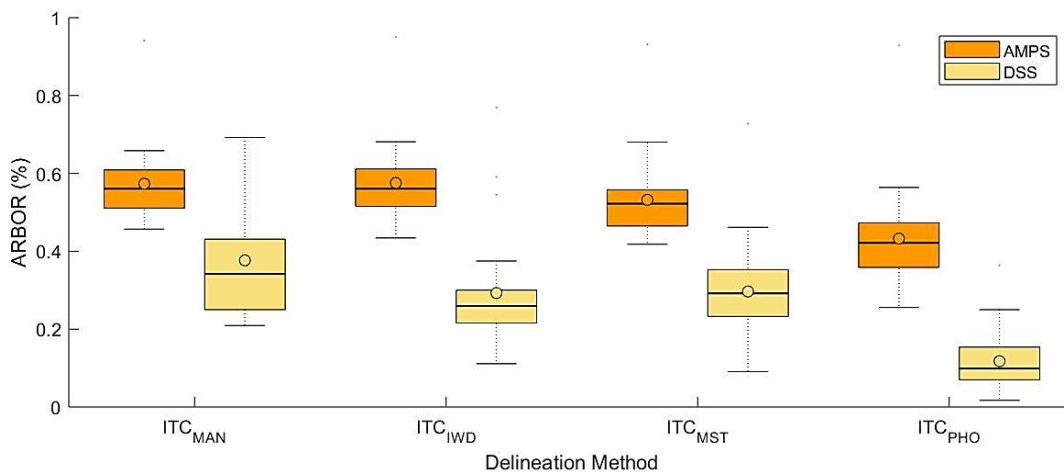


Figure 20 ARBOR scores comparing the match-pairing success between four different ITC delineation techniques acquired from aerial LiDAR data with ground reference data over 26 survey plots.

ITC_{MAN} and ITC_{IWD} have the highest AMPS values, indicating that these delineation techniques have a similar level of accuracy (Table 10). The ITC_{MST} delineation also achieved a level of accuracy commensurate with the ITC_{MAN} and ITC_{IWD} methods, although this was marginally lower. The interquartile range (IQR) of the AMPS is similar for all four ITC methods. All four methods show marginal positive skewing in the AMPS values indicating a majority of results are to the upper end of the IQR, and that the median result is closely aligned to the first quartile (1Q) results.

The ITC_{MAN} achieved the highest DSS values indicating the highest overall level of accuracy in measuring biophysical tree attributes. For the automated delineation techniques, ITC_{IWD} , ITC_{MST} and ITC_{PHO} achieved lower DSS values of 0.26, 0.29 and 0.1 at the median respectively. The ITC_{MAN} indicates a large third quartile (Q3) range to the maximum (~10%). Overall, ITC_{IWD} , ITC_{MST} and ITC_{PHO} show largely balanced distributions in their respective DSS IQR. The ITC_{PHO} achieved the lowest overall ARBOR scores in both AMPS and DSS, when compared against the other delineation techniques.

In all of the results for both AMPS and DSS values across all four delineation techniques show the mean, visualised as a circle, is greater than the median line (Figure 20). This indicates there is a longer upper tail, showing a positive skew to these results. This also shows that the median result is closely aligned to the 1Q. The only exception is the DSS mean for the ITC_{MST} where both the mean and median are closely aligned (Figure 20).

Table 10 Quantification of ARBOR framework scores for four individual tree crown (ITC) delineation techniques, when compared to known tree location, height and crown areas of ground reference tree data.

Delineation	ARBOR Framework (%)											
	AMPS						DSS					
	Q1	Med	Mean	Q3	Min	Max	Q1	Med	Mean	Q3	Min	Max
ITC_{MAN}	0.51	0.56	0.57	0.61	0.46	0.66	0.25	0.34	0.38	0.43	0.21	0.69
ITC_{IWD}	0.52	0.56	0.58	0.61	0.43	0.68	0.22	0.26	0.29	0.30	0.11	0.38
ITC_{MST}	0.46	0.52	0.53	0.56	0.42	0.68	0.23	0.29	0.30	0.35	0.09	0.46
ITC_{PHO}	0.36	0.42	0.43	0.47	0.26	0.56	0.07	0.10	0.12	0.15	0.02	0.25

Notes: AMPS = averaged matched-pairing similarity index, DSS = dataset size similarity index, MAN = manual, IWD = inverse watershedding, MST = variable limit maxima with metabolic scaling theory, PHO = photogrammetric method.

The application of ARBOR to RS-derived ITC delineation and GR data, demonstrates how the framework can quantify differences in ITC delineation techniques, and allows a discriminatory assessment for identifying the ITC delineation technique which would achieve the highest levels of accuracy for the data user.

5.9 The Significance of the ARBOR Framework

Culvenor (2002) states that achieving the successful delineation of trees is problematic. Outlining trees from homogenous groups, without explicitly quantified GR data can lead to repeated errors. The aim of this study was to develop a framework for objectively quantifying the agreement between two datasets, focussing on common commission errors in RS data, with increased data noise and data population differences. The ARBOR framework was developed and then applied to real-world data to quantify the commission agreement between four different ITC delineation techniques and GR datasets (Figure 20). This type of analysis is frequently absent from RS studies that utilise ITC delineation techniques, which instead, rely upon arbitrary height or other cut-off thresholds to infer the level of agreement (Næsset 2002, Listopad, Drake et al. 2011, Hyypä, Yu et al. 2012). However, the findings from this research indicates that simple measures, thresholding and not accounting for the biophysical parameters of trees leads to low levels of true-positive match-pairing between GR and RS-derived data (Figure 18).

Throughout Figure 18a-f, there is a general tendency of higher match-pairing performance at lower noise levels, with a diminishing of NRMSE as noise levels increase. Concurrently, increasing data loss, from 0 to 50%, further impacts on the efficacy of the match-pairing. In all cases, noise affecting the data has the greatest effect, while data loss, less so. What is clear is that introducing data noise alters the

biophysical parameters that the trees are being matched on, and therefore, assessment of these parameters should always be included as variables when seeking ITC delineation agreement with GR data. Figure 18a-c shows that match-pairing methods are sensitive to shifts in the biophysical tree structure under analysis. The data losses, or differences in tree population numbers between the two datasets, has a different effect.

Where data in the observed dataset B (e.g. LiDAR) has fewer trees, poorer matches are achieved as the limited tree population will have greater tree numbers available for matching in the opposing dataset A (e.g. GR). Using some methods, such as Hausdorff distance, unmatched tree data is discarded from the analysis when all trees in dataset B are matched. Without measuring the dataset size, the match-pairing analysis declares a successful match even where there are fewer trees in one set than the other. This creates a false positive result, where changes in the data population and quantification of the unmatched pairings is not reported (Figure 18d-e). Furthermore, this analysis has shown that the frequently used match-pairing method, Hausdorff distance, significantly underperforms in reaching agreement between GR and RS datasets, particularly when exposed to increasing data noise and losses, as readily occurs in real-world RS data (Figure 18a & d). However, through the creation of the ARBOR framework, a demonstrably robust framework has been established to quantify agreement between GR and RS-derived data.

The approach used to develop the ARBOR framework was similar to Ole Ørka, Næsset et al. (2009) where a synthetic testing environment was used to replicate complex RS tree datasets, with naturally occurring variations in tree size, shape and location. During early iterations of metric testing, it was recognised that each tree in

the two datasets must achieve a bilateral matching agreement. However, this was problematic as it was observed that this lead to ‘hugging pairs’ within the data assignment. Specifically, where once assigned a matched pair, e.g. ^{SY}Tree A1 to ^{SY}Tree B1, the assignment excluded any other potential match even where a subsequent potential match was better suited. Further analysis showed that the order of the match-agreement process is a relevant factor in achieving high agreement match-pairing. To overcome this problem, the Hungarian combinatorial optimisation algorithm was used to search through all the potential combinations in the parallel dataset. An advantage of the Hungarian algorithm is the optimising nature of the routine where the algorithm cannot reach completion with an unsuitable data assignment. Therefore, the algorithm attempts all possible data combinations between the two datasets and completes only when the fullest level of agreement is reached.

The AMPS index quantifies the similarity between the datasets as a measure of the biophysical tree properties agreement, represented as Gaussian overlap (Figure 15), while the DSS index provides a measure of population size estimates from ITC delineations. Contrary to the views of Kaartinen, Hyypä et al. (2012) who state that the comparison of delineation results between different datasets cannot be achieved due to the variability in crown structures of different species, this research demonstrates that by using GR representations of trees as simple objects (with location, height and area), and matching these objects to ITC delineations using a Gaussian curve model and the Hungarian algorithm, accuracy assessment becomes possible (Figure 20). Therefore, the ARBOR framework provides a new opportunity for quantifying the confidence of ITC delineation techniques in RS investigations. Figure 20 and Table 10 demonstrate that recommendations can be given about the efficacy and suitability of different ITC delineation techniques applied to remotely-

sensed data. We can define optimal ITC delineation methods, as shown by the AMPS and DSS values calculated within the ARBOR framework.

The principal emphasis of this work was to enable the quantification of pairwise match agreement between GR and RS-derived datasets. However, we also recognise there are opportunities for the ARBOR framework to quantify other types of data agreement, for example, tree delineations derived from aerial photography matched with those from aerial or terrestrial LiDAR. Due to the modular nature of the ARBOR framework, it can be adapted, as is required in future studies, to include a range of different match-pairing metrics not incorporated into this study and to generate alternative statistical measures of ITC delineation accuracy. Furthermore, in this study the ARBOR framework was used for quantifying the accuracy of ITC delineation in a complex semi-natural temperate broadleaved woodland. Given the demonstrable robustness of the tree matching technique and sensitivity of the accuracy metrics, the ARBOR framework holds potential as an objective and transferable tool that can be applied across the full range of forest types.

To enable the distribution and further application of the ARBOR framework, a portal has been developed to allow the uploading and analysis of match-pairing data, to provide objective quantification of the accuracy of ITC delineations.

5.10 Conclusion

It is recognised that achieving accurate ITC delineation is a difficult task, particularly in broadleaved tree crowns. Currently there are no standardised techniques or measures of the amount of agreement between RS-derived and GR datasets. Many potential errors arise in the alignments of these data, however, a common approach to addressing these errors is to apply arbitrary cut-off thresholds. These thresholds are

intended to determine whether the same individual tree is identified within the two different datasets, but there are limitations in these approaches, particularly as some match-pairing methods can lead to false-positive results. Furthermore, the reporting of ITC delineation accuracy is limited in general. Through the use of a synthetic test environment, an optimised algorithm was identified for matching RS-derived and GR tree populations and statistical metrics were developed for quantifying ITC delineation accuracy based on biophysical attributes and data population size. These methods were incorporated into the ARBOR framework which provides a practical approach for achieving and quantifying match-pairing agreement between RS-derived and GR datasets. Therefore, the ARBOR framework is proposed as a standardised solution for future ITC delineation accuracy assessment.

5.11 Supplementary Information

Supplementary information is included with this submission.

5.12 Acknowledgements

The authors thank NERC ARF for their contribution to this research through the provision of facilities and resources for the capture of the remotely-sensed data of the study site. This research was supported by an EPSRC studentship for the lead author: EP/L504804/1.

6 STRUCTURAL: Categorising the Structural Condition of Individual Trees at Landscape Scale using LiDAR Data

6.1 Preamble

Within tree management, forest science and environmental management, there is frequently the need to identify specific features in trees, or to identify trees that are representative of a particular condition. Although technologies already exist for the rapid acquisition of environmental data, current tree surveying practices still relies upon historic surveying techniques. Functionally, this often means that many trees would have to be manually surveyed by operatives in the field. A key element of these traditional surveying methods, is the unguided or reactive nature of the survey. Essentially, the tree surveyors go into the field only with limited knowledge of the area needed to be surveyed, aided by following a transect line on a map or similar. The surveyors have no prior understanding of the expected tree condition within a specific area, and cannot optimise their survey efforts by focussing on a specific area of interest.

The earlier research chapters have identified that there are quantifiable changes in tree structure that can be used to give an indication of tree condition (Chapter 4). Also that

the extent of data agreement between two datasets used to describe the spatial and biophysical and structural properties of the same tree, can be quantified using a novel methodology that aids in defining surveyor confidence in the available data (Chapter 5). Following on from these findings, this chapter answers the question; ‘is it possible to use technology to assess individual tree structure remotely?’, and, ‘can this assessment be used to aid the decision process in tree management?’

STRUCTURAL: Categorising the Structural Condition of Individual Trees at Landscape Scale using LiDAR Data

Jon Murray^{1*}, George Alan Blackburn¹, James Duncan Whyatt¹
and Christopher Edwards²

¹ Lancaster Environment Centre, Lancaster University, Lancaster, LA1 4YQ

² School of Computing and Communications, Lancaster University, Lancaster, LA1 4WA.

*Corresponding author: Tel: +44 1524 652 01; Email: j.murray3@lancaster.ac.uk

Trees are an environmental resource that offer a range of benefits in both rural and urban contexts. Trees are however, subject to a wide range of environmental stressors that interfere with their structure, which can lead to catastrophic structural failure in the worst cases. The tree management, or arboricultural, industries often manage trees from the perspective of risk reduction where trees are in close proximity to members of the public or property, such as critical infrastructure, that are considered worthy of protection. However, there are operational difficulties for tree managers, in that no current assessments of risk are truly objective, and remedial management works is typically reactive in nature. Using a combined approach of ground reference (GR) data with light detection and ranging (LiDAR) data captured from an aerial laser scanning (ALS) platform, this paper introduces an objective means of quantifying tree structure. A population of 9094 individual tree crowns that are automatically delineated were assigned into four condition categories using analytical metrics derived from LiDAR data, using a medium K-nearest neighbour (kNN) classifier with principal components analysis (PCA) activation. This data-driven tree condition categorisation is validated against the GR data to a high level of confidence. This paper demonstrates that the Structural Condition of Trees Using Remote Assessment by LiDAR (STRUCTURAL), is a valid development in digital forestry, and provides a definitive proof of concept that enables tree managers to remotely quantify and categorise the structural condition of tree stock under their care, leading to more informed decision making and proactive management interventions.

Keywords - LiDAR, Metrics, Data Classification, Tree Assessment, Airborne Laser Scanning.

6.2 Introduction

Trees are complex, dynamic structures, subject to a variety of external forces which elicit biophysical responses in tree structures through adaptive morphology, a strategy that minimises the negative impacts of the external forces (Mattheck 1998, Lonsdale

1999, Niklas 2001). Healthy trees use adaptive morphology to accommodate exposure to repeated structural stresses, such as; gravitational force, wind drag in storm or high wind events, fungal pathogens effects, frost, drought, internal growth stress and intentional damage by humans. All of these can affect the tree structure, which initiates a range of unique biophysical responses through structural self-optimisation (Niklas 1992, Mattheck and Breloer 1994, Mattheck 1998). Many of the stressors that trees are exposed to are prolonged, interact with one another, and lead to accumulated impacts on the tree morphology (Niinemets 2010). As a consequence, trees can structurally fail for a variety of reasons.

Amongst tree-risk managers it has long been acknowledged that analysing risk is a highly subjective process which can on occasion, expose tree risk managers to litigation (Lonsdale 1999, Redmill 2002). Traditional tree surveying commonly relies upon a fieldwork operative using visual tree assessment methods from the ground level (Mattheck and Breloer 1994). These operatives rely upon individual judgements for key variables, for instance, the tree part most likely to fail, the mass of the tree part and the impact potential, while also speculating on the effects on potential targets that may or may not be present (e.g. International Society for Arboriculture Tree Risk Assessment method, Visual Tree Assessment method, Quantified Tree Risk Assessment method, Bartlett Tree Survey method etc.). The quality and consistency of these assessments depend on the observation skills, individual interpretation, and prior experience of the observer who provides a holistic assessment on the day of the survey. The tree-risk industry has attempted to standardise manual tree assessment methodologies, aiming to *quantify* tree failure potential. However, the findings of Norris (2007) suggest great variation in the responses throughout the industry. In this study, 12 experienced tree surveyors each assessed eight ‘hazardous’ trees using eight

common tree assessment methodologies. Norris (2007) identified there was low correlation between the expert's findings, using each assessment method, with the observations of the hazardous subject trees. Furthermore, Sankarana, Mishraa et al. (2010) state that traditional tree-risk assessment methodologies are frequently inadequate for their intended purpose, and both labour intensive and prohibitively costly.

Remote Sensing (RS) methods are used in tree management to record individual tree characteristics which are analysed using relatively simple methods (Holmström 2002). Many previous RS investigations focus on tree assessment at the stand or landscape level, particularly from aerial laser scanning (ALS) platforms using light detection and ranging (LiDAR), but assess tree cover as a single unit area, rather than as a series of individual tree crowns, for example, the general assessment of forest cover, the identification of forest parameters or the derivation of vegetative properties (Andersen, McGaughey et al. 2005, Maltamo, Packalen et al. 2005, Suarez, Ontiveros et al. 2005, Henning and Radtke 2006, Ustin and Gamon 2010, Swatantran, Dubayah et al. 2011). Bortolot and Wynne (2005), recognised the potential of using LiDAR for "individual tree-based management". Suarez, Ontiveros et al. (2005) have also noted that ALS LiDAR can provide additional layers of information about canopy structure, beyond the reach of manual tree assessment methods. ALS LiDAR can also be utilised in-situations wherein easy access is not possible or in instances where large amounts of data need to be captured in a single attempt. Whilst it is unlikely that RS techniques will ever entirely replace visual tree inspections, it is expected that they will provide opportunities to enhance larger scale surveys by directing practitioners towards the areas of the highest management interest, enabling proactive interventions to be applied, an ideal that is notably absent from many of the

current, reactive tree assessment practices. As described in Murray, Blackburn et al. (2018) due to the unique differences in individual trees, there is the need for objectively classifying tree structural condition, therefore, this paper describes the development of the Structural Condition of Trees Using Remote Assessment by LiDAR (STRUCTURAL) method.

6.3 Aim and Objectives

The aim of this research is to develop a methodology for categorising the structural condition of individual trees from discrete return (DR) LiDAR data captured via an ALS platform. This will be fulfilled by meeting the following objectives:

1. To visualise LiDAR returns for different tree structural conditions as the basis for developing metrics
2. To define predictor variables used for the development of LiDAR metrics and for conducting supervised learning and classification
3. To complete a validation of the classification model response and classified tree data
4. To demonstrate a procedural workflow, from data processing, through to data analysis and procedural output

6.4 Methodology

6.4.1 Fieldwork, Site Selection and Manual Operations

6.4.1.1 Woodland Character

The woodland used as a study site is of a typical nature found in north-west England.

Described as a mixed species, semi-natural woodland, containing distinct areas of

Ancient Semi Natural Woodland (ASNW) and Plantation on Ancient Woodland Site (PAWS). The woodland includes areas under a variety of different woodland management practices and canopy cover types, ranging from individual, open grown trees (maidens) through to areas of total canopy closure. The woodland is described in further detail in Field Sites, Methods. During the fieldwork phase, it was noted that the horizontal and vertical strata of the woodland varied on an east to west basis, with trees in the west being predominantly smaller, understory trees with a sporadic overstory and large areas of canopy gaps, and trees to the east being predominantly mature overstory trees, creating a complex upper canopy with fewer understory trees (see Eaves Wood, Lancashire, UK).

6.4.1.2 Plot Selection

A transect line (and buffer zone) was established to help identify areas of homogenous tree cover. During the site identification process, no formal assessment of individual tree condition was taken, but to measure differences between potential survey sites, hemispherical photographs were taken of the underside of the canopy over the proposed plot centres. These images were subsequently processed to quantify the canopy cover found at each site using CAN-EYE software, e.g. canopy closure at 40% cover (see ALS Survey Plot Location and Establishment). 26 survey plots were identified that were situated along or within 30 meters of the transect line as the local conditions and canopy cover directed. At the centre of each survey plot a geolocated ground marker was placed.

Lu, Guo et al. (2014) state that achieving accurate GPS signals beneath tree canopies is problematic, and when considering the effects of dense woodland canopies, acquiring location by GPS alone cannot be assured. Consequently, an extensive back-

sighting procedure using a combined (differential) dGPS and total station robotic survey was used to improve accuracy in geolocating the survey plots beneath the tree canopies. Each tree ≥ 5 DBH within the survey plot was manually geolocated and several variables were recorded e.g. species, DBH, height, crown spread etc. using readily available arboricultural equipment, for example, clinometer, surveyors tape, DBH tape, laser hypsometer. In addition to this base field data, the condition of each tree was assessed at the time of the survey. This manual assessment conforms to the current best industry practices used in the arboricultural industry in the UK, and is based upon the principles as described by Lonsdale (1999) and BS5837:2012 (BSI 2012). These field methods were also informed by the Forest Inventory and Analysis program (Schomaker, Zarnoch et al. 2007).

6.4.2 Data Preparation and Preliminary Observations

6.4.2.1 Data Merging, Point Classification and Study Area Definition

To ensure the greatest LiDAR data distribution throughout the survey area, the woodland site was flown with ~85% swath overlap between six flight lines. This returned 29,435,261 LiDAR pulses, creating the point cloud for the woodland (Table 11). The flightlines were centred above the transect line and GR plots where a smaller flightline area achieved 100% overlap. Through a process of data merging and clipping to the flightline overlap area coordinates, the periphery of the point cloud (<100% overlap) was excluded from the study area (Figure 21). This process reduced the point cloud to 8,829,963 data points, covering 38.4ha of the site. All LiDAR returns within this zone achieved an average ground point density of 23.02m² (Table 11 & Figure 21).

Table 11 LiDAR pulses returned for a combination of six flight line passes of Eaves Wood, Lancashire, UK. Point data 1 is unconsolidated results of all flightlines, while point data 2 is an optimised area of overlapping flightlines.

Return (r)	Point Data 1		Point Data 2	
	Number	Percentage	Number	Percentage
1	24,386,772	82.85%	6,864,595	77.74%
2	4,538,672	15.42%	1,703,915	19.29%
3	496,169	1.69%	248,474	2.81%
4	13,648	0.05%	12,979	0.1%

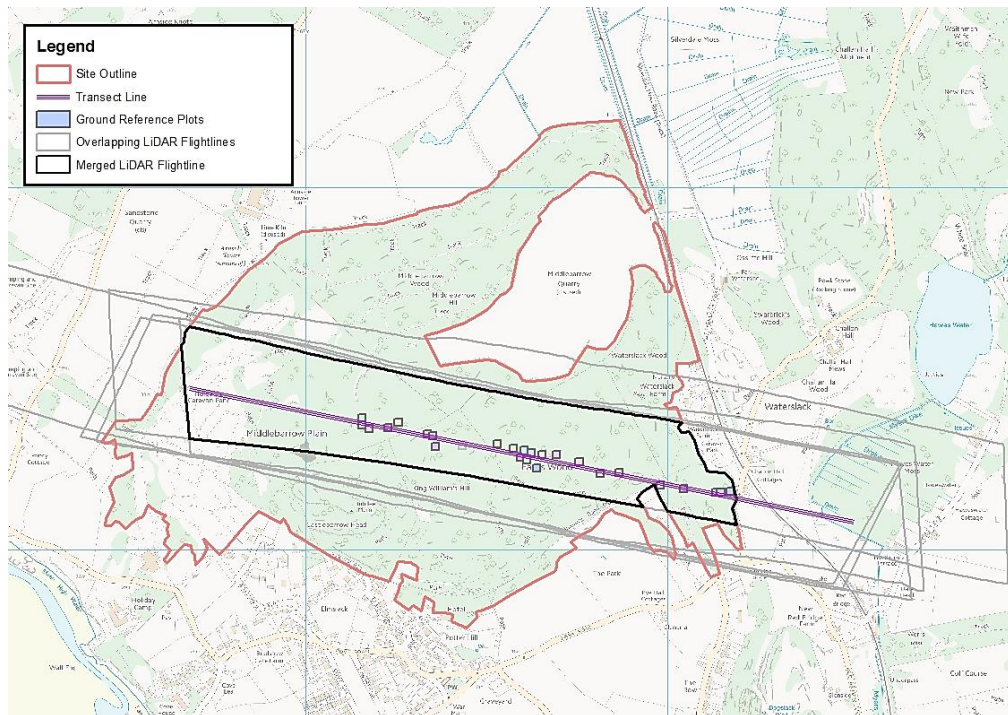


Figure 21 Outline of Eaves Wood, Lancashire, showing locations of the transect line and ground reference plots. The grey boxes indicate the overlapping LiDAR flightlines, while the black box identifies the flightline area that achieved 100% overlap, corresponding with the central transect and ground reference plots.

Following the clipping and merging of the flightlines, a point classification algorithm was used to discriminate preferred data points from non-essential data. This followed the standard specifications of ASPRS (2013), with LiDAR point classes assigned as; 2 – ground, 3 – low vegetation, 4 – medium vegetation, 5 – high vegetation, and, 7 – low point (noise). Other point classes for buildings, water, rail etc. were not assigned as the woodland does not contain these features, and are not of interest in this study.

6.4.2.2 Data Processing for Training Data

When processing GR individual tree locations it was considered important to adopt a consistent method when extracting LiDAR data for selected plots for a training dataset. Although several ITC delineation techniques exist for the identification of individual trees from within larger datasets (Chen, Baldocchi et al. 2006, Bian, Zou et al. 2014, Swetnam and Falk 2014, Ayrey, Fraver et al. 2017), these frequently underestimate the overall tree population (Hamraz, Contreras et al. 2017). Therefore, these approaches were not used to define the training dataset. Following the guidance of Lu, Guo et al. (2014) individual tree locations were manually digitised using XY coordinate (centroid) and crown areas of the GR data (Figure 22).

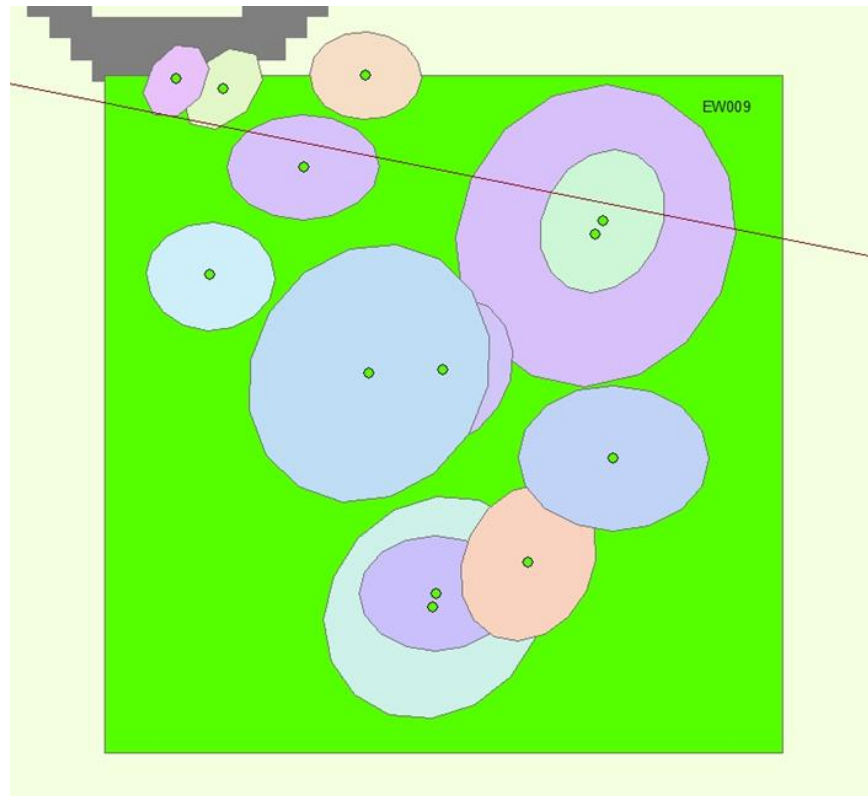


Figure 22 Tree canopies as drawn as circular shapes in ArcGIS at 1:125 scale. The canopies are created with scaled measurements and orientated in the direction as they were found in data collection at Eaves Wood, Silverdale, Lancashire, UK. Also shown in the image is the transect line (red) and plot area (green) used in the investigation.

6.4.3 Visualisation of LiDAR Returns for Different Tree Structural Conditions

A pilot investigation was undertaken using maiden control trees (see Potter Hill Fields and Park Fields, Silverdale, Lancashire, UK.). Easy access to these trees facilitated taking precise GR measurements, and the trees were readily identified in the LiDAR data. The control trees were categorized as; good, moderate, poor and dead (Figure 23). Point cloud observations indicated apparent differences in the LiDAR and tree structure interaction, particularly the pulse return frequencies within different areas of the tree structure (Figure 23).

The tree structure and LiDAR return pulses were further investigated in a modest trail of 238 randomly selected trees, reported as Murray, Blackburn et al. (2014). This analysis shows that structural character can be inferred through the occurrences of return pulses, where both standardized and unstandardized regression weightings were defined as discriminant function coefficients for the return pulses 1-4 (Table 12)

Table 12 Standardized and raw discriminant function coefficients as unstandardized regression weights for LiDAR return (r) variables (Murray, Blackburn et al. 2014)

Variable	Raw	Standardized
r1	-0.00429	-1.71796
r2	0.00780	1.64426
r3	-0.03895	-1.46073
r4	0.42858	0.81466

Table 12 shows that r2 influences the canonical variable as a discriminate function to the largest amount (r2 - 1.64426), suggesting the r2 pulses have the greatest descriptive value (Murray, Blackburn et al. 2014). Furthermore, the positive correlation shows that r1-3 exerts the greatest influence in describing tree structure (Table 13). This observation can be used to aid the development of tree structure metrics (Murray, Blackburn et al. 2014), and is supported by the observations of Hamraz, Contreras et al. (2017), who also support the view that LiDAR points are denser from first to third r points respectively.

Table 13 Correlations between the dependent (return (r)) and canonical variables (Murray, Blackburn et al. 2014).

Variable	Correlation
r1	0.87948
r2	0.74750
r3	0.68438
r4	0.34560

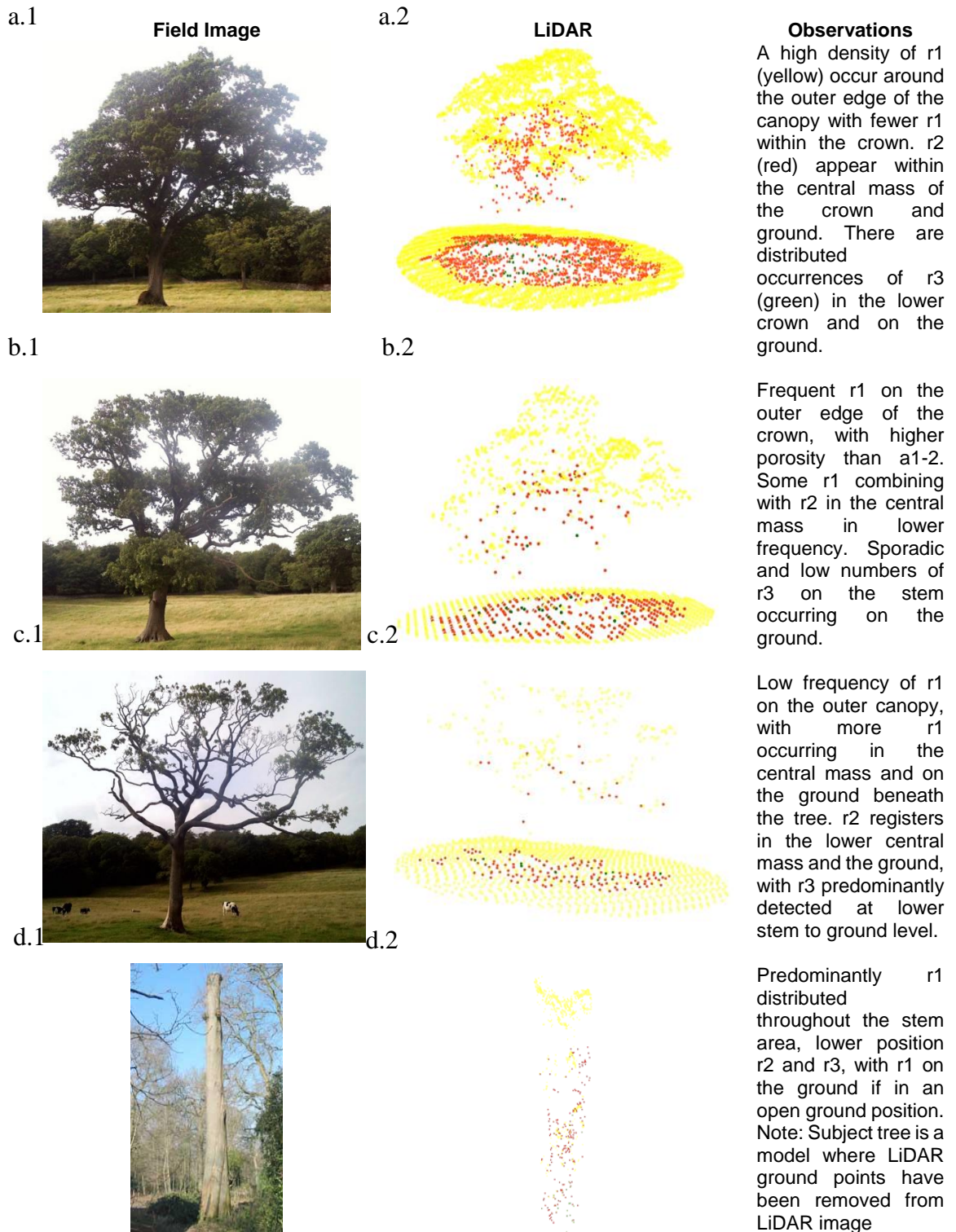


Figure 23

Subject trees in manually observed conditions: a, b, c, and d = good, moderate, poor and dead conditions respectively. Trees marked with 1 are photographic representations of the subject trees. Trees marked with 2 are visual representations of trees scanned using DR ALS LiDAR, with pulse returns shown: r1 (Yellow), r2 (Red), r3 (Green).

6.4.3.1 Quantification of Tree Delineations with the ARBOR Method

The merged LiDAR flightline (Figure 21) was used to delineate all trees that were modelled during the ALS LiDAR data acquisition. This process defines the location and biophysical parameters of all trees including those that are within the flightline, and both inside and outside of the 26 GR survey plots. It follows that these unsurveyed, ITC delineated trees (Figure 24) are the subject of supervised classification. The quality of the ITC delineation method was quantified within the ARBOR framework to assess the accuracy of matching the ITC delineated trees with the surveyed GR data. The ITC_{MST} delineation method uses inverse watershedding delineation and incorporates metabolic scaling theory (MST) predictions to remove data noise Swetnam and Falk (2014), and in an analysis comparing the efficacy of four ITC delineation methods using the ARBOR framework, the ITC_{MST} delineation method was shown to have a comparatively high match-pairing agreement (0.52 AMPS) and, achieved the highest dataset similarity size following the matching (0.29 DSS) of the automated ITC delineation methods tested (see ARBOR: A New Framework for Assessing the Accuracy of Individual Tree Crown Delineation from Remotely-sensed Data).

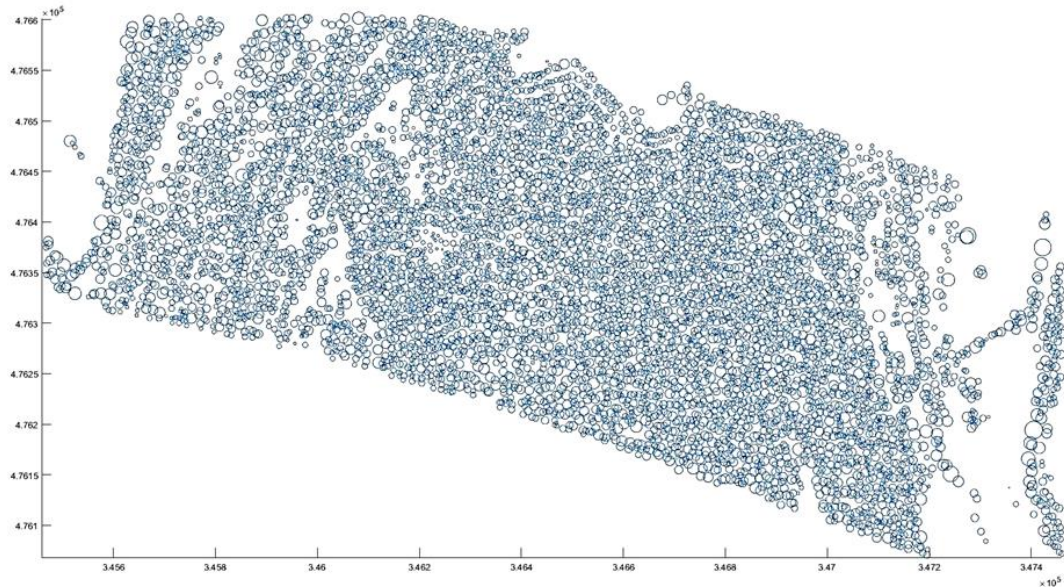


Figure 24 ITC delineations of individual trees across the full study site flightline. These unsurveyed trees will be classified using their biophysical characteristics as observed in ALS LiDAR data.

6.4.4 Defining Variables for Supervised Learning & Aerial LiDAR Metrics

6.4.4.1 LiDAR Measurement Variables

A series of measurements were computed from the LiDAR point cloud to describe the subject area. These relate to common investigative themes, for example; inventory (e.g. number of trees), areas and surfaces (e.g. fitted surface area), heights (e.g. 90th quantile of point heights), intensity (e.g. maximum intensity) and other measures (e.g. principle component elements). Table 14 describes 51 measurements calculated from the ALS LiDAR data to be used as predictive variable measurements.

Table 14 Description of measurements calculated from LiDAR point cloud data, grouped into themed areas of inventory, intensity, area, height and other. *Adapted from Parkan (2018)*

	Measure	Description	Measure	Description	
Inventory	X	Longitude	HeightQ90	90th Quantile of Point Heights	Heights
	Y	Latitude	HeightQ75	75th Quantile of Point Heights	
	Z	Height	HeightQ50	50th Quantile of Point Heights	
	NPoints	Point number	HeightQ25	25th Quantile of Point Heights	
	LRFrac	Last Return Fraction	HeightSkew	Height Skewness	
	FRFrac	First Return Fraction	HeightKurt	Height Kurtosis	
	SRFrac	Single Return Fraction	HeightCV	Coefficient of Variation of Point Heights	
	OpacityQ50	Opacity Value 50th Quantile	HeightSD	Standard Deviation of Point Heights	
	TotHeight	Total Height	HeightMed	Median of Point Heights	
	AspRatio	Aspect Ratio	HeightMean	Mean of Point Heights	
Intensity	IntSRQ50	Single return 50th quantile	ConvArea	Convex Area	Area & Surfaces
	IntLRQ50	Last return 50th quantile	ConvVol	Convex Volume	
	IntFRQ50	First return 50th quantile	ConvSuArea	Convex Surface Area	
	IntSkew	Skewness	ConvSpSurf	Convex Specific Surface	
	IntKurt	Kurtosis	ConcVol	Concave Vol	
	IntCV	Coefficient of variation	ConvLacuna	Convex Hull Lacunarity	
	IntSD	Standard deviation	ConcSuArea	Concave Surface Area	
	IntMax	Maximum	Convexity	Convexity	
	IntMean	Mean average	CrownDiam	Crown Diameter	
	IntQ90	Values to 90th quantile	ConcSpSurf	Concave Specific Surface	
	IntQ75	Values to 75th quantile	ConcArea	Concave Area	
	IntQ50	Values to 50th quantile	ConvDens	Convex Point Density	
	IntQ25	Values to 25th quantile	ConcDens	Concave Point Density	
	Other	PCVar3	Principle Component Variance 1	ConvFrac	
PCVar2		Principle Component Variance 2	ConcFrac	Concave Boundary Fraction	
PCVar1		Principle Component Variance 3			

6.4.4.2 Supervised Learning Routines

To undertake supervised learning, individual tree samples were chosen at random from 21 of the 26 GR survey plots. These trees were assigned to train the initial predictor models, while 5 survey plots were retained for later model validation. The training trees were grouped by their arboricultural survey categorisation (good, moderate, poor or dead categories, Figure 23), and then randomly selected from the groups. These four categories were used as the ‘response’ variable for a supervised learning analysis conducted in MATLAB (*vers.* 2017a), where several different training and classifier models were used in order to define the highest predictive model accuracy (Table 15). To reduce the impacts of dimensionality and the potential

influence of random variables, principle components analysis (PCA) was applied where the reduction criterion explained variance to 95%. In considering the number of predictor variables and model combinations, the learning routine repeated over 2500 training iterations, fivefold cross-validation supports the predictive strength of the model.

Table 15 Description of a range of classifier models used in assessing the accuracy of trained models in a supervised learning analysis.

Classifier Models													
Decision Trees		Discriminant Analysis		Regression		Support Vector Machine (SVM)		Nearest Neighbour (kNN)		Ensembles			
Type	Info.	Type	Info.	Type	Info.	Type	Info.	Type	Info.	Type	Info.		
Coarse	Few leaves (max 4)	Linear	Linear inter-class boundaries	Logistic	Simple function of predictor combination	Linear	Simple linear separation	Fine	Fine distinction (1 N)	Boosted	Max. learners & splits		
	Medium		Quadratic			Non-linear inter-class boundaries	Quadratic		Non-linear separation		Medium	Moderate distinction (10 N)	Bagged
		Fine				Many leaves (max 100)	Cubic		Non-linear separation		Coarse	Coarse distinction (100 N)	Subspace Discriminant
						Fine Gaussian	Fine class distinction (sqrt(p)/4)	Cosign	Cosign distance metric (10 N)	Subspace kNN	Subspace with nearest neighbour learners		
						Medium Gaussian	Moderate class distinction sqrt(p)	Cubic	Cubic distance metric (10 N)	RUSBoost Trees	Skew data boost with decision tree learners		
						Coarse Gaussian	Coarse prediction sqrt(p)*4	Weighted	Medium distinction, weighted distance (10 N)				

Notes: SQRT = square root, P = predictor variables, N = neighbour.

6.4.4.3 LiDAR Metric Development

To define LiDAR metrics that will inform the description of the tree structure and condition for analysis, several predictor variables were generated using the *Digital Forestry Toolbox* (Parkan 2018) (Table 14). These measurements were combined in many ways, attempting to demonstrate tree features and achieve high model accuracy in the output model. For example:

- **Inventory** (NPoint, FRFrac, TotHeight, CrownDiam)

Number of pulse points, by first return fraction, total tree height and crown diameter

- **Height** (HeightQ90, TotHeight, HeightCV, HeightSD)
Height of points in the 90th quantile, by total tree height, height standard deviation and height coefficient of variation
- **Intensity** (IntFRQ50, IntSD, IntCV,)
Intensity values of the first returns in 50th quantile, by intensity standard deviation and intensity coefficient of variation
- **Area and Surface** (ConvVol, ConvSuArea, ConvSpSurf, ConvLacuna, ConvFrac, Convexity, CrownDiam)
Convex volume, by convex surface area, convex specific surface, convex lacunarity, convex fraction, convexity measure and crown diameter.
- **Other** (PCVar1, PCVar2, NPoint)
Principle component variance 1, by principle component variance 2 and number of pulse points

(List not exhaustive)

While many combinations of predictor measurements were used, it was observed that many combinations of these variables had a negative impact on the model accuracy. In the worst combinations, six or more combined predictor variables achieved a maximum of only 17% model accuracy per training iteration. Reducing the number of predictor variables had the corresponding effect of increasing model accuracy (Figure 25).

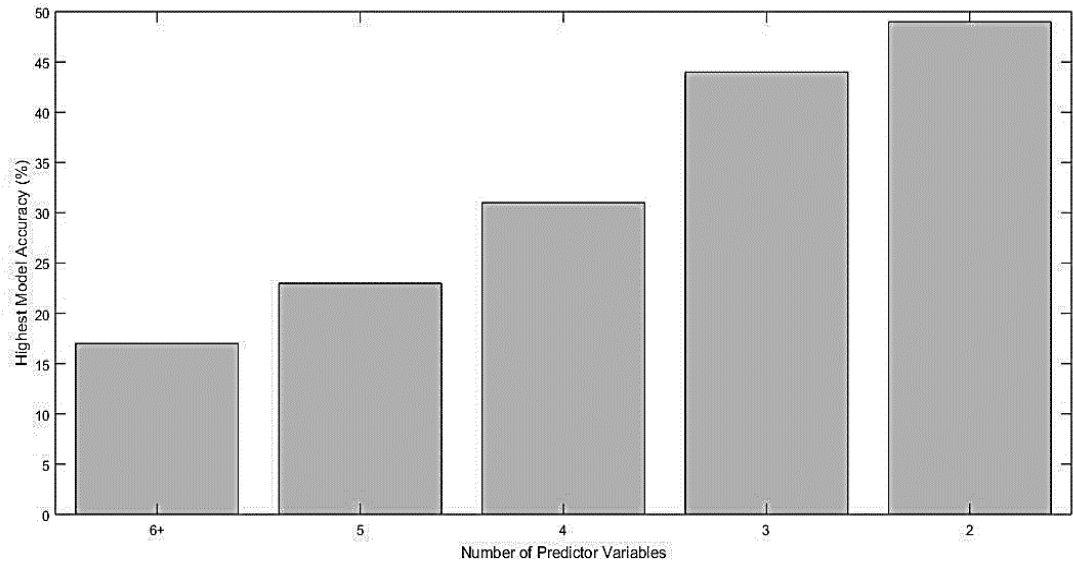


Figure 25 Response of model accuracy levels during model training with different numbers of predictor variables

6.4.4.4 Testing Metrics and Classification Model Accuracy

During the training phase 25 training trees in each of the four response categories were used to train the model ($n=100$). The training data population was governed by the number of trees in the response categories with the lowest population numbers, e.g. 25 dead trees observed within 21 training plots, therefore the remaining 3 response categories also had 25 in their training populations. The measures *concave surface area*, which is the area of a concave hull or alpha shape (Edelsbrunner and Ernst 1994), and *concave density*, the number of LiDAR points divided by the total volume of the concave hull (Shi, Wang et al. 2018), were used as a classification prediction metric achieved 46.8% accuracy scores over the model training iterations, using the medium *kNN* classifier with principal components analysis (PCA) activation.

Figure 26a-c, shows the results of the classification process. Figure 26a shows the distribution of correctly classified points, grouped by categories, verified by the

trained model. Figure 26b shows the receiver operating classifier (ROC) curve which indicates both true and false positive values. A perfect ROC curve is represented as a right angle to the upper left corner, poor ROC results plot closer to a 45° line. The area under the curve (AUC) quantifies the classifier quality, with the classifier model achieving 0.7 AUC (Figure 26b). The confusion matrix (Figure 26c) identifies the model efficacy in achieving true-positive classifications for each category. In this model, dead and moderate classifications achieve 60% and 56% respectively, while the good and poor categories achieve 32% and 36% true-positive classifications.

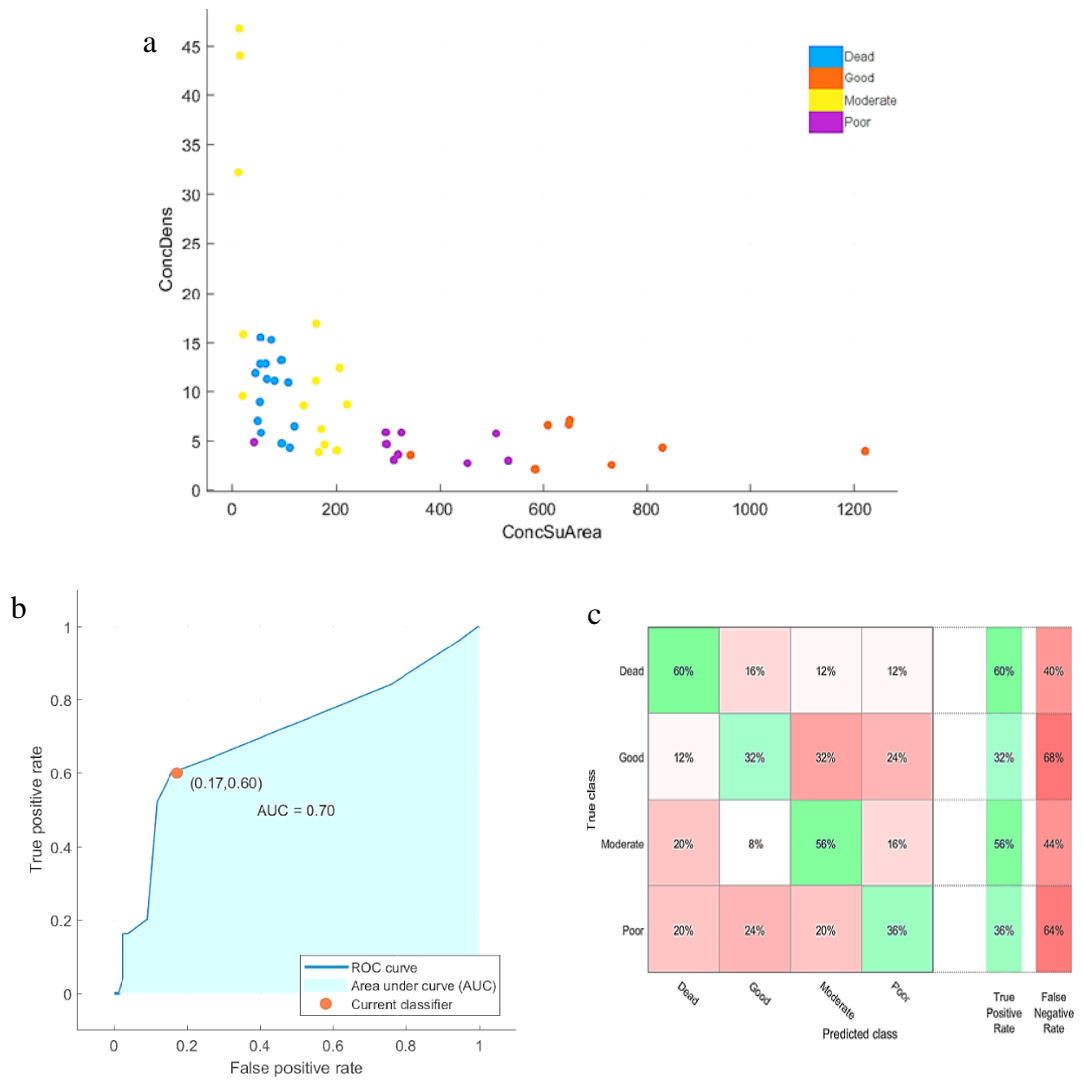


Figure 26 Trained model results for the predictor variables Concave Surface Area by Concave Density as a tree classification metric using a medium *k*NN classifier model and 100 training trees from ALS LiDAR data. a) scatter plot of assigned categories, b) receiver operating classifier (ROC) curve for the dead category, and c) confusion matrix of all categories true positive classifications. Overall model accuracy is 46.8%.

6.4.4.4.1 Model Retraining

Within the original training data, the categorical data distributions were observed as; good 70%, moderate 20%, poor 5%, and dead 5%. Therefore, in the initial training

phase, all the categories were under-represented in the training data, at 25% for each category. Additional trees from the plot survey areas were added to the training data, aiming to replicate the original category distributions, thereby increasing the training dataset to 235 trees. The redistributed data population became; good 48%, moderate 30%, poor 11%, and dead 11%. The classification models were retrained using the previous routines and measures (Table 14 and Table 15).

6.4.4.4.2 Medium *kNN* Classifier Model

The retrained data was used with the prediction metric, concave surface area by concave density, and achieved 41% model accuracy with the medium *kNN* classifier and PCA activation. Figure 27a shows the point distribution, grouped by classification and verified by the trained model. The new data showed a minor ROC curve change in the dead category 0.69 AUC (Figure 27b). The confusion matrix changed across all categories when compared to Figure 26c, with true positives as; good 65%, moderate 43%, poor 4% and dead 20%. This is a true positive increase in the largest data categories, i.e. good and moderate, however, the change also shows a reduction in true positives for dead and poor, which are now weak model learners due to the training model population data imbalance (Model Retraining).

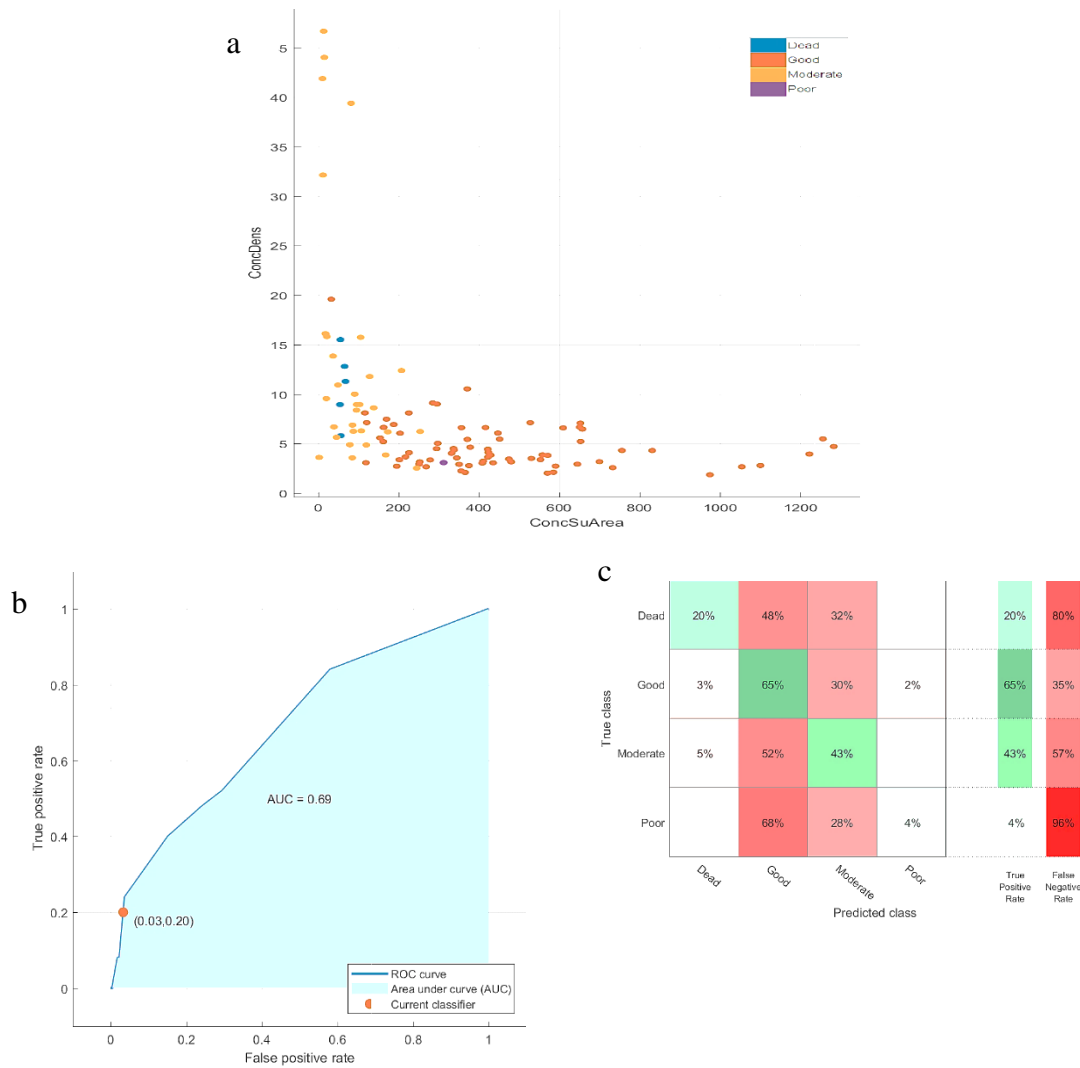


Figure 27 Trained model results for the predictor variables Concave Surface Area by Concave Density as a tree classification metric using a medium *kNN* classifier model and 235 training trees from ALS LiDAR data. a) scatter plot of assigned categories, b) receiver operating classifier (ROC) curve for the dead category, and c) confusion matrix of all categories true positive classifications. Overall model accuracy is 41%.

6.4.4.4.3 *RUSBoost Classifier Model*

Seiffert, Khoshgoftaar et al. (2010) recognise the impact of training class imbalance can lead to the formation of “suboptimal classification models”. The *RUSBoost*

algorithm is a model classifier that can overcome the problems of skewed data modelling (Seiffert, Khoshgoftaar et al. 2010). RUSBoost conducts random undersampling (RUS) of the dominant classes until achieving a balance in the classifier data. Simultaneously, the minor dataset is boosted further improving model learning with the weaker predictor variables. The technique, advantages and disadvantages are explained further in Seiffert, Khoshgoftaar et al. (2010). Figure 27a shows the point distribution, grouped by categories, and verified by the model. The ROC curve is identical to the medium *k*NN model, at 0.69 AUC (Figure 28b). The confusion matrix has the true positive classifications as; good 26%, moderate 40%, poor 36% and dead 44% (Figure 28c). The RUSBoost accuracy is 33.6%.

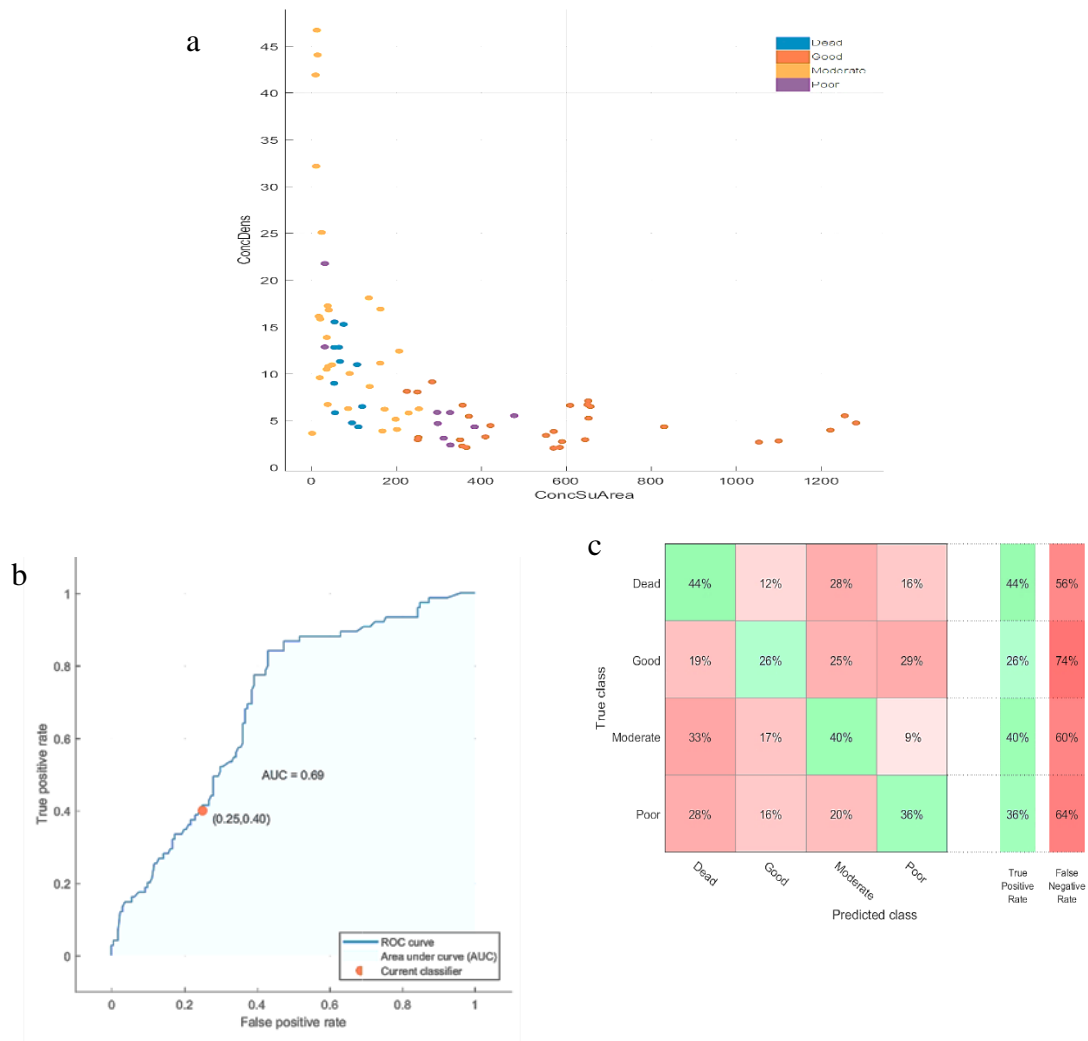


Figure 28 Trained model results for the predictor variables Concave Surface Area by Concave Density as a tree classification metric using an Ensemble RUSBoost classifier model and 235 training trees from ALS LiDAR data. a. scatter plot of assigned categories, b. receiver operating classifier (ROC) curve for the dead category, and c. confusion matrix of all categories true positive classifications. Overall model accuracy is 33.6%.

6.4.5 Validation of the Trained Model Response and Tree Classification

6.4.5.1 Validation by Chi-square (χ^2)

The model validation was undertaken by running each classification model, in turn, on an unclassified dataset. The unclassified dataset is a mirrored duplicate of the GR dataset (GRD) used during the training of the classification model, however, the dataset intentionally contains no tree classification values. The models classify each tree within the data, either $N=100$ or $N=235$, as required by the test parameters. Hereafter, this data set is referred to as model classified data (MCD). To establish the If there is independence between the MCD and GRD datasets, the Chi-square statistic (X^2) and p -values are calculated for each model classifier (medium k NN(a), medium k NN (b), or, RUS Boost). As described by Ringuest (1986), this is an optimal method for validating predictive models using categorical data. The classification models have been trained under two different training regimes ($N=100$ and $N=235$), therefore, require separate validation to reflect the two levels of training data (Table 16). Expressed as hypotheses for this test:

- H_0 : Ground referenced data (GRD) and model classified data (MCD) are independent
- H_1 : Ground referenced data (GRD) and model classified data (MCD) are dependent

Table 16 Chi-square (χ^2) validation of two classification models (medium *k*NN and RUS Boost) that were trained using different training data populations (N=100 and N=235).

MCD	Medium <i>k</i> NN (a) $\chi^2(p)$	Medium <i>k</i> NN (b) $\chi^2(p)$	RUSBoost $\chi^2(p)$
N=100	60.5 ($p=1.0756e-09$)	-	96.5 ($p=7.8828e-17$)
N=235	-	70.5 ($p=1.1868e-11$)	136.0 ($p=6.7713e-25$)

Note: **MCD** = Model Classified Data. **Medium *k*NN** = *k*-nearest neighbour, with 10 neighbour distinctions. **RUSBoost** = Alleviates class imbalance with random undersampling and boosted learning.

Table 16 identifies the trained model medium *k*NN(a) are the least independent, therefore, the H_0 can be rejected under the medium *k*NN (N=100) classification model at a very highly significant level ($p=1.0756e-09$). The very small *p* value suggests that the model output result is very unlikely to have arisen by chance under the context of the null hypothesis (H_0), that the two classifications are independent. Further investigation to determine if there is repeated misclassifications favouring particular categories is shown at Table 17. Here an even spread of misclassifications is shown and no particular category dominates the table, therefore, the classification model is not introducing a consistent bias.

Table 17 A cross tabulation validation results of a ground reference dataset (GRD) that has been classified using a trained model, becoming model classified data (MCD). The table shows no influence of bias in any of the classification categories.



6.4.5.2 Validation by Plot Level Assessment

In addition to the model validation, 5 GR survey plots were withheld from the model training for validation of how well the ITC delineated tree crowns represented the physical characteristics of the GR trees. The Jaccard similarity coefficient was calculated for the five sites, resulting in a 0.30 Jaccard similarity for the sites (1.0 indicates 100% similarity). The low Jaccard score reflects the dissimilarity in crown area size between the two datasets. Within this validation step, the GR tree crowns are the dominant area within the union across all sites, and all crowns.

6.4.6 Summary Recommendation

Despite a large number of LiDAR derived measured being analysed for suitability as predictor variables (Table 14), the metrics concave surface area by concave density, consistently achieved higher overall model accuracies when used with several classification models. Following several iterations of analysing different measures and various training models, many analyses returned very low model accuracy results

which precluded them from further consideration as classifier models (Figure 25). However, the medium *k*NN classifier model consistently achieved high model accuracy results within the developmental phases. When training the classifier model using the initial concave surface area and concave density, with PCA activation ($n=100$), model accuracy 46.8% was achieved. It was believed that the model training would be influenced by not having the same data distribution as observed in the GR data, therefore the training dataset was increased to $n=235$, attempting to rebalance the data distribution (Model Retraining). However, this resulted in a negative impact on the model accuracy, reducing to 41% as a response to the additional, imbalanced training data distribution (Medium *k*NN Classifier Model). To counter the imbalanced data, the classifier model RUSBoost was used with the same increased population dataset ($n=235$), as this classifier is the preferred option for imbalanced datasets containing one or more weak training categories. However, the analysis also returned a low model accuracy; 33.6% (RUSBoost Classifier Model).

Statistical validation of the strength of these metrics were tested for both χ^2 test of independence and plot level dataset equivalence using the Jaccard similarity coefficient (Validation of the Trained Model Response and Tree Classification). In both validation phases for independence (Table 16 & Table 17), it can be seen that the medium *k*NN classifier model is the least independent from the training data ($p=1.0756e-09$), and further, that the classifier does not introduce a consistent bias. Therefore, resulting from achieving the highest levels of model accuracy and statistical validation, the measures concave surface area and concave density ($n=100$), with the medium *k*NN classifier and PCA activation are recommended as the classification metric to be used in STRUCTURAL, for classifying a large, previously unclassified, ITC delineated data set ($n=9094$).

6.5 STRUCTURAL Output

The geo-spatial output from STRUCTURAL identifies trees that are categorised using the selected trained classifier (medium *k*NN with PCA, concave surface area by concave density), and applied to the unclassified data, that have not been previously subject to manual GR classification. Trees are subsequently assigned into one of four categories: good, moderate, poor and dead, akin to the same process as the GR classification (Figure 29). This output dataset can then be integrated into either a desktop or mobile GIS (Figure 30).

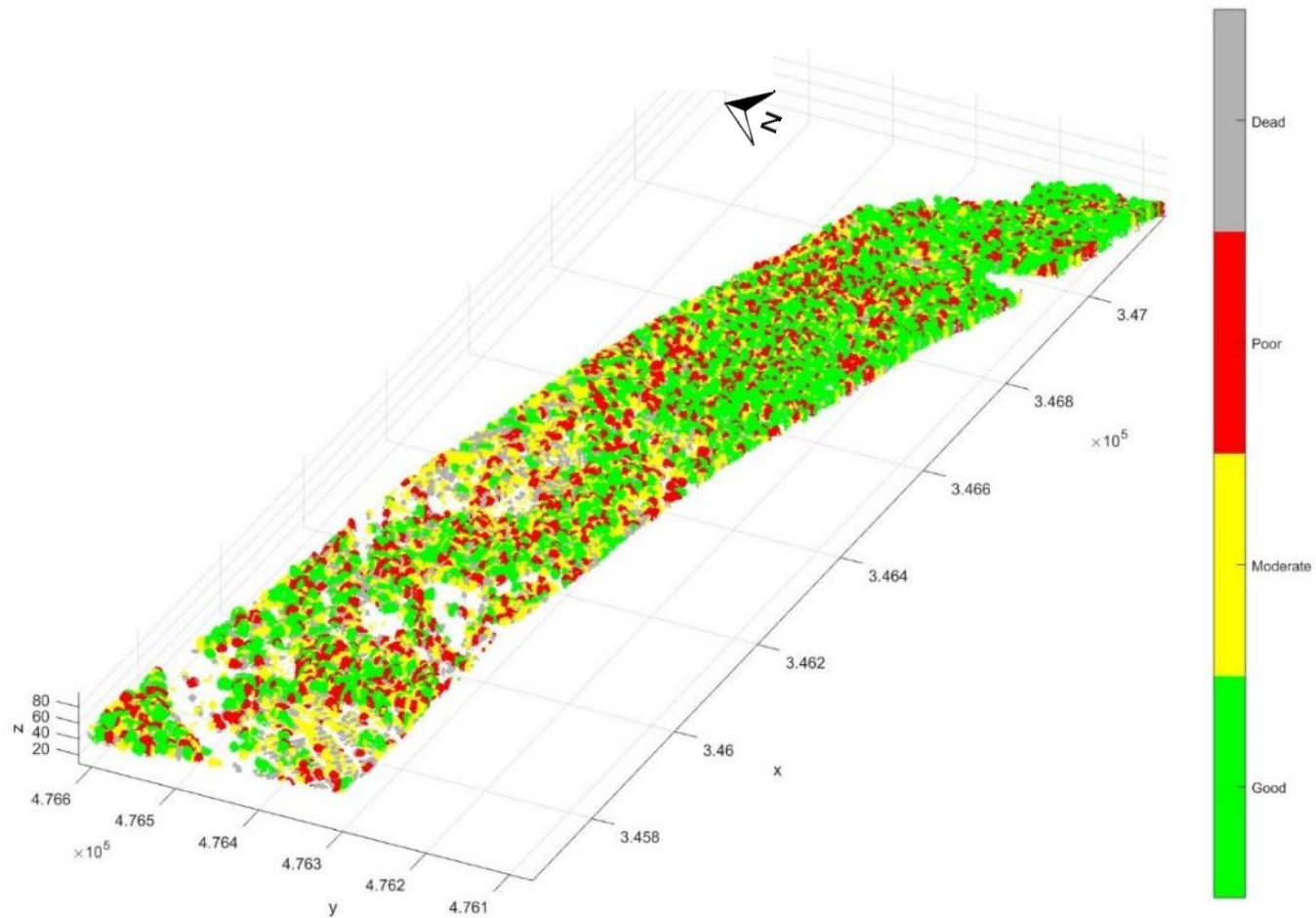


Figure 29 Individual tree crowns delineated from continuous data (LiDAR) and assigned into good, moderate, poor and dead categories using the STRUCTURAL method ($n=9094$).

Remote Sensing Tools for the Objective Quantification of Tree Structural Condition
from Individual Trees to Landscape Scale Assessment

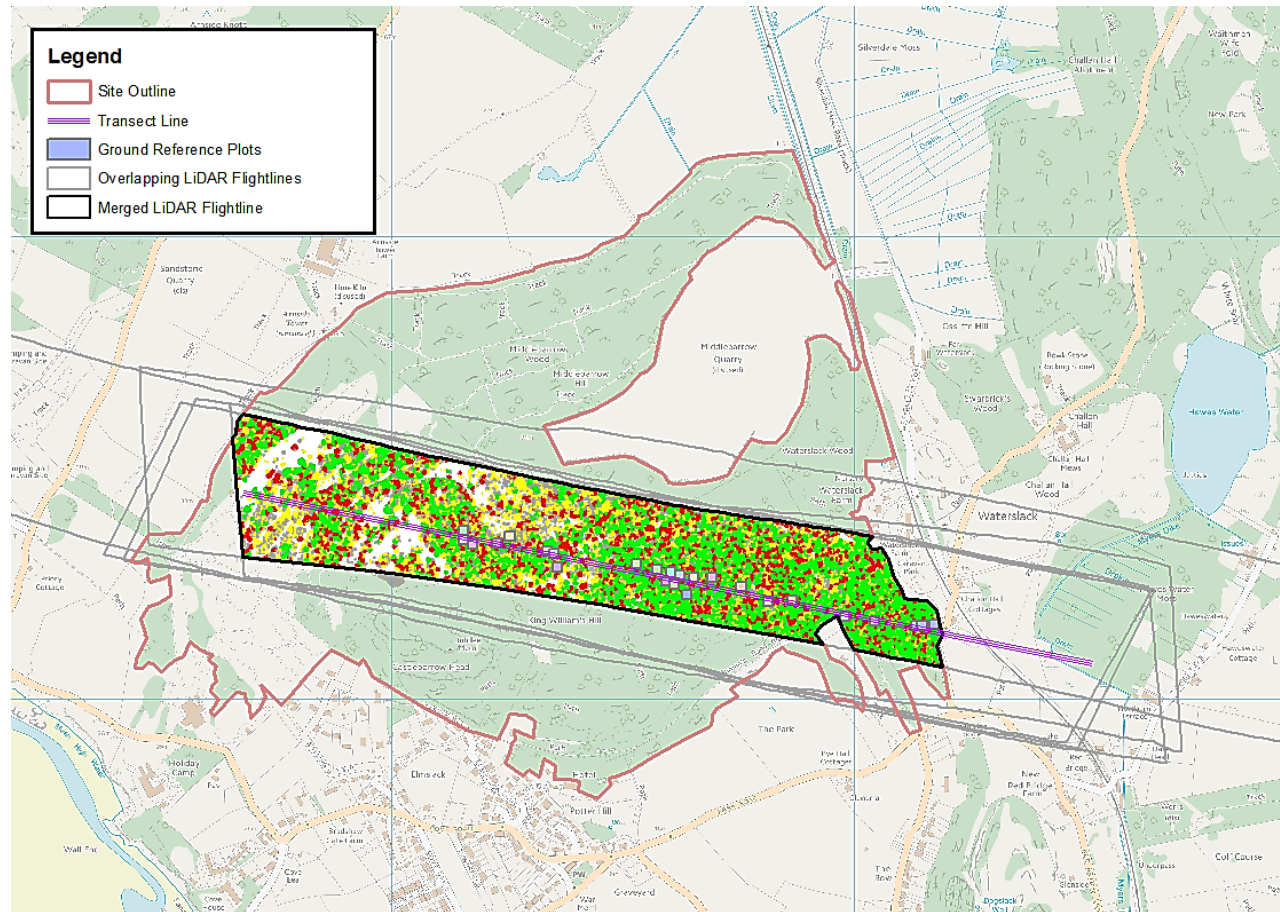


Figure 30 A combined approach of using ground reference data, and using descriptive metrics on previously uncategorised remotely sensed tree data.

From an empirical assessment of the STRUCTURAL output (Figure 30), it can be seen that the dispersal of the predicted tree conditions throughout the woodland follows the expected distribution, and reflects the condition of the woodland (see Field Sites). Within the GIS map at Figure 30, it can be seen that in the areas of smaller sporadically spaced trees to the west of the woodland there is a larger proportion of moderate and poor condition trees (yellow and red), particularly in areas that relate to the underlying karst landform (Figure 31a & b). Similarly, in the areas of ANSW and more structurally complex overstory trees to the east of the woodland (Figure 31c), there is a higher proportion of trees that have classified as belonging to the good category. Intermixed within the eastern end of the woodland are a number of poor trees, which suggests the identification of trees in the lower-overstory are suppressed by the dominant overstory.

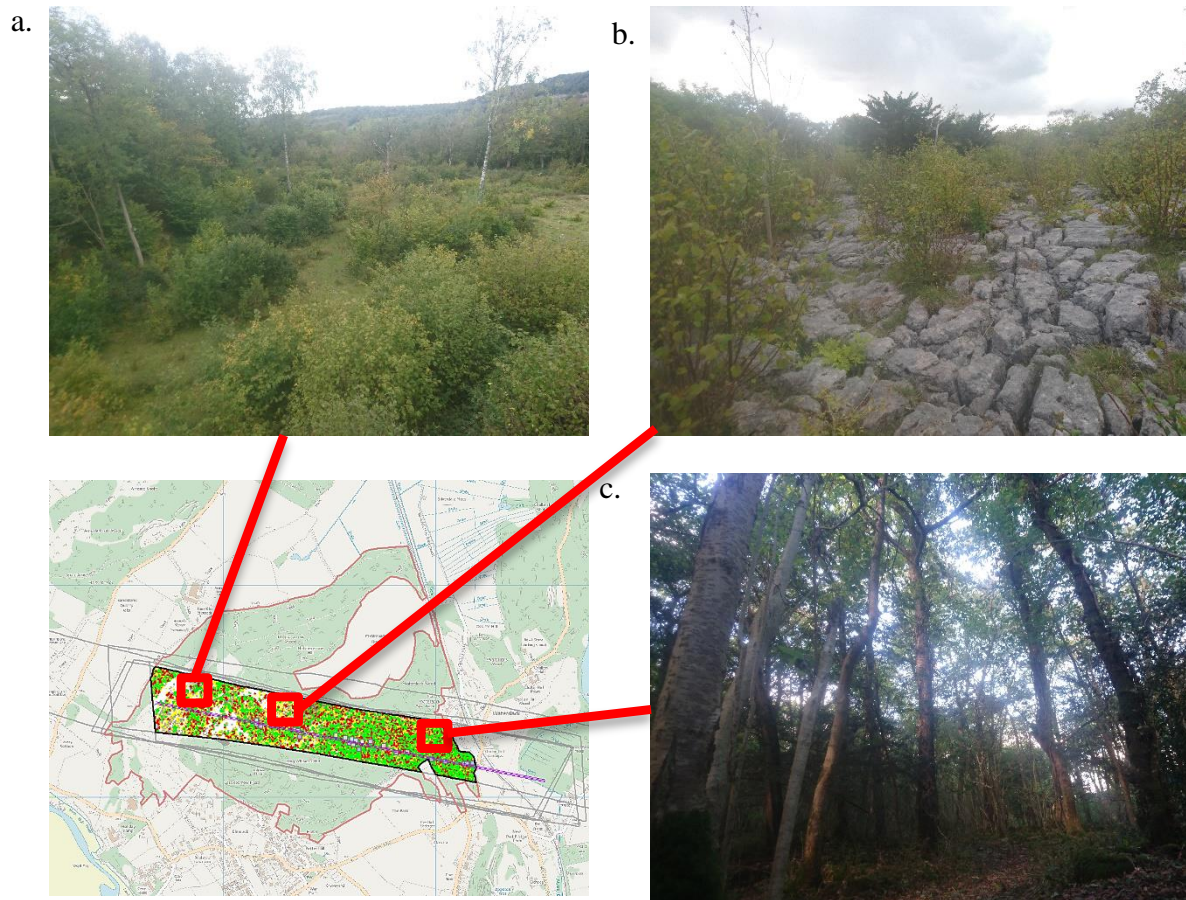


Figure 31 Empirical observations of tree condition categories and their spatial distribution throughout the study woodland. a) shows smaller, young trees to the northwest of the site. b) shows stressed trees on karst landform in the central region of the woodland, while c) shows mature, overstory trees in the east of the woodland.

6.6 Discussion

The aim of this study was to develop a method that could be used to conduct woodland or landscape scale tree surveying and classification of structural condition, by employing RS techniques. The accuracy levels of all STRUCTURAL classification models can be attributed to overall accuracy of the input data. Following the delineation assessment methods described in ARBOR: A New Framework for

Assessing the Accuracy of Individual Tree Crown Delineation from Remotely-sensed Data, the GR and RS-derived ITC delineations have ARBOR scores of 0.52 AMPS and 0.29 DSS. AMPS is the quantification of the match-pairing success between the two datasets, and DSS is the measure of similarity in the two dataset sizes, therefore, the success of the classifier models are limited by the low agreement levels of the input data. Nonetheless, STRUCTURAL classifications were statistically validated as a proxy for determining a level of confidence in the classifications made in the wider dataset ($n=9094$). Due to the ordinal nature of the tree condition category data, only a limited range of statistical tests may be applied. Nonetheless, the statistical validity of the categorisation of unclassified data was defined at Validation by Chi-square (χ^2), where the test of independence identified that the chosen model metric for STRUCTURAL; medium k NN with PCA activation and concave surface area by concave density ($n=100$), expressed the lowest levels of independence to a highly significant level ($p=1.0756e-09$). Avoiding a false-positive statement, it cannot be said that there is dependence between the two datasets, GR and RS-derived data, but the tests indicate that the H_0 was rejected, and further, Table 17 indicates that there is no dominance of any particular category or introduced bias from the classifier model. It is recognised that a further phase of validation is also possible, where the mapped output (Figure 34) is used to direct surveyors to unsurveyed woodland areas and are subjected to the same GR surveying routines as used in the initial field work, and the correlation between the two procedures is calculated. However, it is not possible to conduct this additional phase of fieldwork within the timeframe of this project.

As described in the results (Testing Metrics and Classification Model Accuracy), the training models are not predominantly influenced by higher data population numbers in the training model. The greatest influence is the quality of the reference trees used

in the model training and the impact of skewness in this data. It was expected that as the GR data was dominated by trees in the good category (70%), this should also be reflected in the training data (Model Retraining). However, having modified the data distribution to include more good category trees, model accuracy reduced to 41%. To counter the impact of the underrepresented categories of poor and dead skewing the training data, the RUSBoost classification model was applied. The reduction of dominant training data populations by random undersampling, and boosting the subordinate data, achieved a more even distribution of true-positives, going from; good 65%, moderate 43%, poor 4% and dead 20% (Figure 26c), to; good 26%, moderate 40%, poor 36% and dead 44% (Figure 28c). The use of RUSBoost as a classifier model provides a solution to the problem of training a model with weakened, or underrepresented, training data. A drawback to applying the RUSBoost method, as highlighted by Seiffert, Khoshgoftaar et al. (2010) is that as the method manipulates the loss of data in an intelligent randomized process, some information will be lost from the training process.

The impact of this on classifying trees with ALS LiDAR, despite achieving model classification across all tree categories, and relatively high ROC assessment (0.69 AUC), is a reduction in model accuracy to 33.6%. In this application the negative effect precluded the continuance of this classification method for this application. However, it is envisaged that sensitivity testing of RUSBoost with smaller data population differences, e.g. 5% 10%, could demonstrate that RUSBoost is a valuable tool for refining marginal tree classification data issues in STRUCTURAL. Other models may have achieved higher model accuracies, in one case, a model accuracy of 57.4% was achieved with the medium Gaussian SVM classification model, however, these higher accuracies come at the cost of not classifying any of the weak learners

i.e. poor and dead, due to their lower numbers. The medium Gaussian SVM was able to achieve true positive rates of 82% and 60% respectively for the good and moderate categories. Many iterations of the different potential models generated high classifications using the SVM Medium Gaussian model classifier, which achieved 100% categorisation of the good category, although, this classifier scored 0% for all other condition categories. This suggests that further investigation could identify positive relationships with specific metrics, training models and classifiers for favouring the identification of specific tree condition categories.

A limitation of the technique is the influence of RS-derived data in reflecting the observed GR measurements. As identified in the validation phase, Validation by Plot Level Assessment, the LiDAR delineations are geometrically smaller than the GR delineated crowns. This is an effect of the relative height above ground (HAG) level that the delineations are made. The GR crown delineation is made at ~1.3m from the ground i.e. the approximate chest height of the field surveyors, sighted upwards towards with the crown measured at the widest point that the surveyor can discern from this location. Conversely, the RS-derived ITC delineations are created from a top down perspective, starting at the highest pixel in a LiDAR generated CHM. The crown edges are developed where the CHM indicates a similarity between two adjacent heights in the model, or simply, where two crowns abut at a similar height location in the upper canopy. This means that tree crowns are delineated at two heights above the ground, making the GR delineations larger than the ITC delineations in most circumstances, with the exception of ITC delineation errors where several smaller crowns are conjoined into an artificially larger group. The impact of this is that with two datasets of differing crown area sizes, one of the key variables in training the model classifier, that sub-optimal model training can occur thereby further

reducing model accuracy. Future improvements could be made through the development of a 'height acquired' metric, where the height level of the ITC delineated crowns is extrapolated to the computed live crown height or the same HAG as the GR crown measurements.

Conversely, an additional benefit from STRUCTURAL is the identification of trees that are in the poor to dead categories. Many woodland conservation efforts require the creation of woodland habitat that benefits decomposers, or mammals that require specific woodland habitat e.g. woodpeckers and standing dead trees. Some management interventions used in conservation deliberately veteranise or even intentionally kill healthy trees in order to provide this required habitat (Bengtsson, Hedin et al. 2012). Veteranisation of trees is also included within the Higher Tier Countryside Stewardship scheme in the UK, where landowners are required to include specific management practices when in receipt of government grants (NE 2018). STRUCTURAL has the potential to be used in countrywide conservation and grant work monitoring, a time and resource costly practice that is currently undertaken by approved grant-aid monitors physically travelling between sites to conduct assessments. For the large scale adoption of STRUCTURAL, it is acknowledged that full, or semi-, automation of the classification process would be required for additional end-user benefits. Significant investment in the development of new programming would be required to integrate these approaches with auto-detection methodologies, although this was beyond the means and scope of this modest study. Furthermore, it is recognised that the development of a dataset containing a range of trees of different species, ages, sizes and conditions would generate additional improvements in classification. Currently, STRUCTURAL does not discriminate between tree species due to the nature of LiDAR only assessing the upper canopy,

however, if the method was scaled up to include large scale surveys of prominently maiden trees, such as are typically found in a cityscape, then an improvement to the method would be the integration with a computational species identification phase, that would also draw upon the subsequent condition dataset.

It is important to state that this method is not intended as a tool to predict tree failure, nor will it remove risk-exposure for tree managers or landowners. What STRUCTURAL does achieve, through the provision of classified spatial data (Figure 34), is to identify key areas where resources should be directed to, allowing the commencement of proactive remedial interventions, thereby reducing the overall liability exposure as a result. This would be of specific value to managers of critical infrastructure, such as the highways and rail networks, or by boosting the resilience of power distribution networks to outages caused by the failure of trees. Furthermore, the STRUCTURAL method provides a significant developmental step in moving away from simple models of ‘lollipop’ trees based on photogrammetry, to the assessment of LiDAR derived objects, with the potential for the assessment of multiple attributes, in particular, the assessment of tree structural condition.

6.7 Conclusion

Classifying trees from analysing aerial LiDAR, as demonstrated in this work, is another phase in the move towards the wider application of digital forestry, where advanced technologies provide tree resource managers with increasingly detailed information about the tree stock under their management, and allowing the adoption of an informed, proactive management style. Whilst the different training models used in this study had a reduced validation accuracy, this work provides the proof of concept that these methods are tangible for achieving higher levels of accuracy. This

will require improvements in the data preparation phases to increase the classification accuracy of the output maps, used to guide resources towards individual trees that require prioritised management intervention.

6.8 Acknowledgements

The authors thank NERC ARF for their contribution to this research through the provision of facilities and resources for the capture of the remotely-sensed data of the study site. The lead author would also like to thank Dr. M. Parkan, École Polytechnique Fédérale de Lausanne, Lausanne (EPFL), for insightful comments relating to some technical elements of this work. This research was supported by an EPSRC studentship for the lead author: EP/L504804/1.

7 Discussion

7.1 Overview

The experimental phases of this study have been addressed throughout chapters 4, 5 and 6, where new methods and experimental results have been presented. The Synthesis describes the link between the research in this thesis, and describes its potential for future applications. This discussion will also draw together the key themes of the literature review and reflect on how the experimental phases of this thesis contribute to the wider knowledge within the framework of the Thesis Aim and Objectives. In particular, the Key Contributions from this Research section reflects on how this research relates to the issues raised in the individual sections of the literature review. Also considered in this summary, are the Limitations of the Research and recommendations for Potential Research Opportunities within this subject area.

7.1.1 Procedural Workflow

The final procedural workflow of the required steps to categorise trees at the woodland scale using STRUCTURAL is shown in Figure 32. The model has a manual phase for fieldwork data collection, which is used to train the classifiers, which is then combined with the computational phases which include data processing, model training in parallel mode and classification of data. STRUCTURAL ends with the production of geospatial outputs that represent the classification of trees at landscape scale.

Remote Sensing Tools for the Objective Quantification of Tree Structural Condition
from Individual Trees to Landscape Scale Assessment

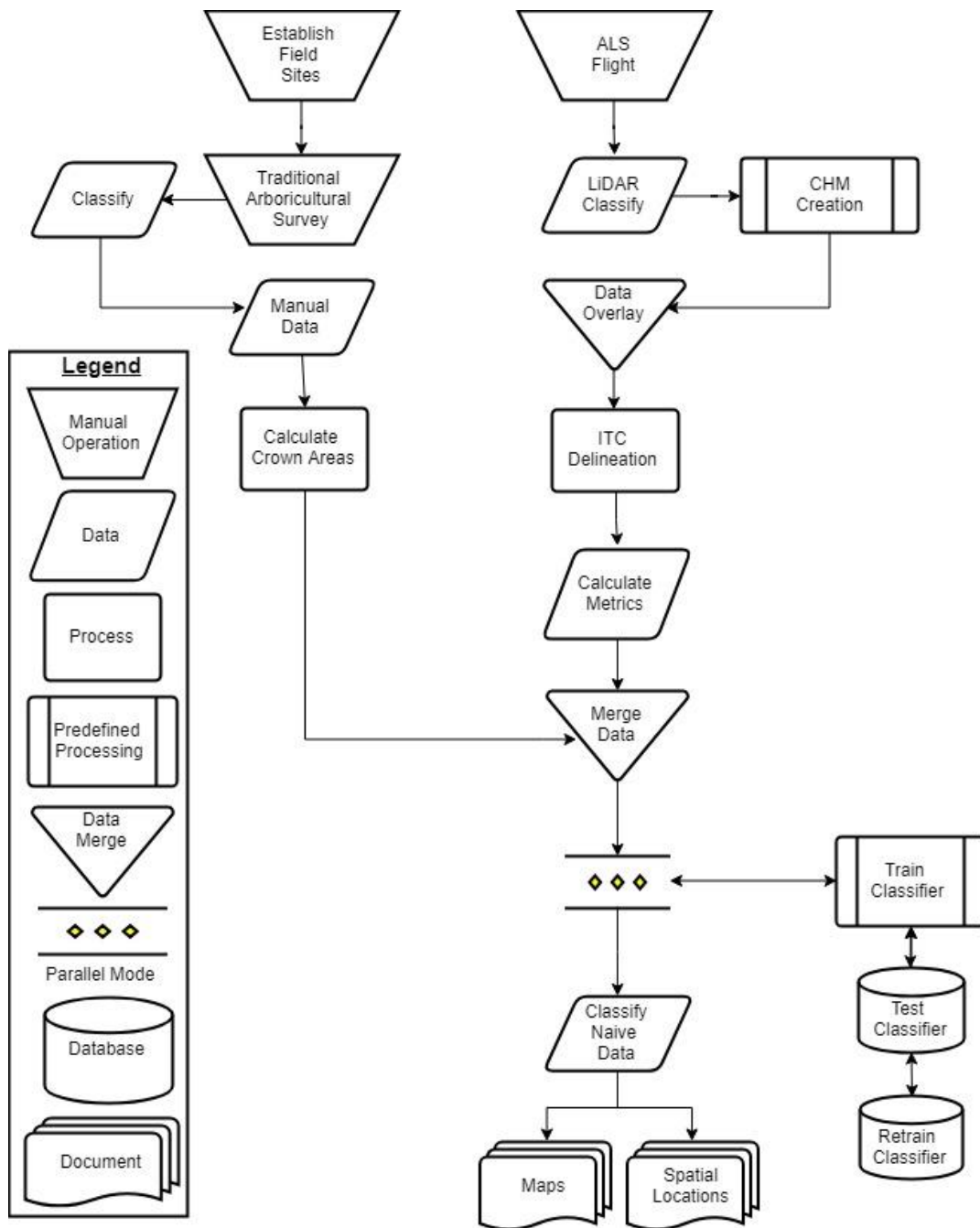


Figure 32 The full workflow required for classifying trees at landscape scale using aerial LiDAR, field data and trained classifier models. This method uses a combination of both manual and automated techniques to produce a location map of trees that are classified from the training model.

7.2 Synthesis

The methods defined within this research have been developed based upon sound empirical observations, independent analysis and statistical justification, and function as individual, stand-alone tools for quantifying tree crown complexity (chapter 4), optimising match-pairing (chapter 5), and remotely categorising the structural condition of trees (chapter 6). However, the greatest impact from the development of these methods is the potential to use these tools in a multi-scale, investigative method for assessing tree structural condition using combined, high-resolution investigation methods that foresters, arboriculturists, environmental managers and researchers would not have previously achieved using traditional investigative methods. Figure 33 demonstrates the potential application of this combined approach:

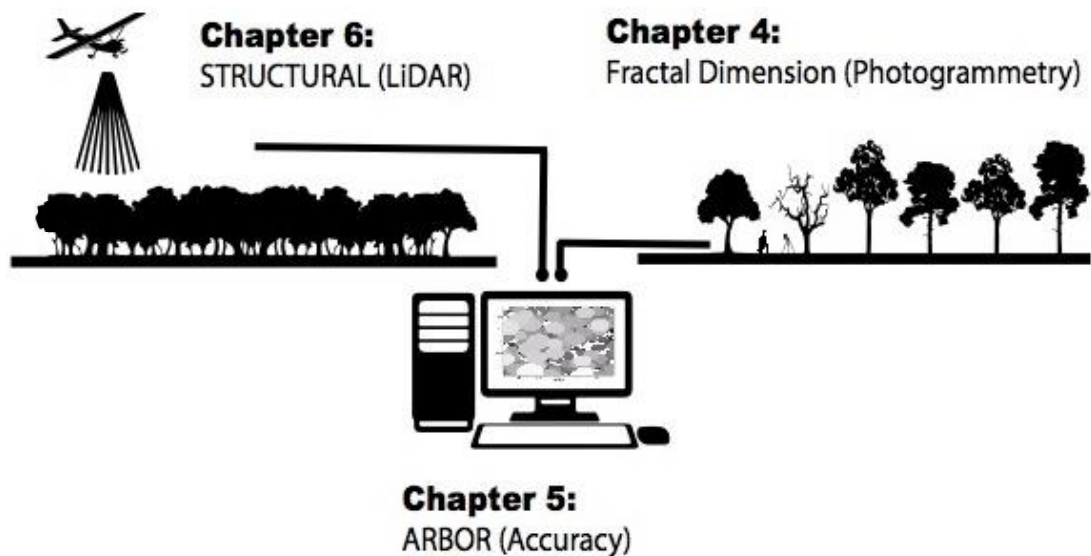


Figure 33 A model defining how the operational relationship between the findings of this research can be used in a large-scale, optimised and high-resolution tree structural condition investigation.

The tree investigation could begin with an ALS survey of the landscape and, following the LiDAR data-collection, STRUCTURAL and ARBOR are used to identify and define to reportable levels of accuracy, where trees are located and

calculate a series of tree measurements used to define the tree structural condition. The next phase is the assignment of personnel and resources to the predetermined locations, as indicated by the STRUCTURAL mapping, where a proposed work schedule would be refined by analysing trees using the proximal photogrammetric method. This would further improve field information about which trees are in the highest need of remedial intervention using the analysis of intra-category variance, expressed in Df on the structural condition continuum. The potential for achieving this level of optimised working, and the data driven prioritisation of resources, was not realised before the development of the techniques described in this thesis.

It is known that the alignment between GR and LiDAR data is difficult to quantify particularly in complex, semi-natural temperate broadleaved woodland, which within the United Kingdom there is an estimated 3.16M hectares of woodland (Table 18). Approximately half of this area is under broadleaf cover (Donohue 2016). Therefore, the potential for quantifying the structural condition of trees using the methods developed in this study is significant in the UK alone.

Table 18 Area of woodland cover in the United Kingdom (2016), by country and tree classification (Donohue 2016).

	Share of Land Mass	Conifer*	Broadleaf*
England	10%	340	966
Wales	15%	150	156
Scotland	18%	1,059	377
Northern Ireland	8%	66	46
* Area in thousands of hectares	Totals	1,615	1,545

7.3 Key Contributions from this Research

7.3.1 The Influence of Subjectivity

Ghiselin 1982), suggests that foresters, tree managers and surveyors are typically lone workers and subjective thinkers when considering tree management interventions. By conducting typical operational duties where scientific-based observations are applied to investigate trees with the intention of reaching an evidence-based decision, a large degree of subjectivity is included in the decision-making process. In attempting to move towards impartiality and minimising subjectivity from the decision-making process, the development of methods that a lone-worker could undertake without assistance, is preferred. The Methodology in chapter 4 only requires the field operative to manually set up the camera equipment, take the image and proof this image in the field. Crucially with this method, any individual physically able to access the location of the base of the tree and take a picture will be able to capture data, consequently, removing the need for expert intervention. Subsequent analysis is automated, therefore, this approach removes individual interpretation and subjectivity from quantifying the tree crown structure and removes “subjective reasoning” effects (Dana, Jeschke et al. 2013). In addition, the Methodology in chapter 4 demonstrates that it is possible to achieve fine resolution assessment when determining intracategory variance, by utilising the analysis of self-affinity in Df using a structural condition continuum; a tree characterisation metric that did not exist prior to the completion of this research.

As shown in chapter 5, there are quantifiable differences within tree populations when GR data is compared to ITC delineation data. It is understood these differences can be a product of data shadowing, where ALS LiDAR does not achieve the full penetration of the canopy depth, thereby, not all of the understory trees will be fully

delineated in all circumstances (Wallace, Lucieer et al. 2014). To quantify this effect, the ARBOR framework utilises the Jaccard similarity coefficient as the basis of the DSS index (Quantification of Accuracy with which Delineations Estimate Biophysical Properties and Population Size), takes the union of two datasets and quantifies the intersectional area. Where there is an element of directionality in an analysis, there will always be an inferior dataset that reduces the overall accuracy of the match-pairing. Assessing this problem and providing a mechanism for quantifying this effect is a significant development for RS research in this area, as to the best of current knowledge, this level of information has not been reported in any similar ITC delineation research.

7.3.2 The Development of Tree Surveying

Throughout tree management operations, particularly at landscape scale, there is the requirement to capture tree data to inform timely, and appropriate, interventions (Jennings, Brown et al. 1999, Wulder, Hall et al. 2005). In particular, Strahler, Jupp et al. (2008), highlight the importance of measuring tree structure. These requirements are the fundamental basis for the paradox of the successful, data-driven management of trees. The paradox is that tree management typically has to be conducted over a wide variety of scales influenced by the unit area of management (e.g. individual tree, copse, orchard, shelterbelt, woodland or forest and with many unit size combinations in-between). However, in traditional tree management, trees are surveyed on an individual basis and observations are scaled up using allometric equations. Unfortunately, allometric equations have been shown to be unreliable for this purpose (Dassot, Constant et al. 2011, Ahmed, Siqueira et al. 2013, Mugasha, Mwakalukwa et al. 2016). As shown in chapter 6, applying the classifying metrics to ITC crowns delineated from LiDAR, provides the opportunity for remotely classifying the tree

population (Figure 30), allowing management operations to be directed straight to the areas where remedial interventions are most required. The main benefit of STRUCTURAL is the potential for removing retrospective analysis and classification as is the current practice, to a predictive analysis and categorisation phase, before tree surveyors undertake surveying in predefined areas (see STRUCTURAL Output). The application of STRUCTURAL enables prior understanding of the tree stock structural condition to be determined, which will in turn optimise in-field surveying efforts. This approach will enable predictive management strategies to be enacted, as is expected in tree management, despite current methods predominantly being reactive or based on best-guess allometry.

Many studies indicate that despite the long reliance on the traditional methods for data capture, there are inconsistencies and inaccuracies in the measurement and calculation of tree and forest parameters (Dassot, Constant et al. 2011, Ahmed, Siqueira et al. 2013, Mugasha, Mwakalukwa et al. 2016). This suggests that in the face of few known alternatives, the combined approaches of manual surveying and allometric scaling will continue to be the accepted status-quo for the majority of the tree management industries. It follows therefore, that there is a pressing need for novel solutions to overcome the issues associated with the tree management paradox. How can individual tree assessment be accurately and successfully conducted over large scales, with only limited operational resources? Hauglin, Lien et al. (2014) state that ALS LiDAR is becoming an invaluable tool for forest inventory data collection. With the high level of data achievable through RS data acquisition, particularly when conducted across a range of scales relative to the scale of the unit area of management, the question arises what RS methods will offer the potential to overcome the tree management paradox? Through the development of the techniques described in

chapters 4, 5 and 6, it is clear that all methods have a role in forming a cohesive approach to address the tree management paradox, where resources can be focussed on the required areas (see STRUCTURAL Output), confidence in the ITC delineation methods can be quantified (chapter 5), and individual trees can be rapidly and objectively assessed (chapter 4).

7.3.3 The Potential for Decision Support Systems (DSSy)

Dana, Jeschke et al. (2013) describe the pressing need for improving the limited suite of management tools with additional DSSy, highlighting that the development RS techniques are directly aligned to the needs of industry. Providing enhanced information about tree stock for inventories, across forests or other similar unit areas of management, are a direct improvement to the available tools for tree managers, and would enable the focussed deployment of limited forest management resources, specifically to where the interventions are most needed (see STRUCTURAL Output). Segura, Ray et al. (2014) identify that the main problems of using DSSy to aid large scale tree management relate to temporal and spatial scales. Additionally, forest managers frequently use statistically supported analysis, and 90% of forest managers within their investigation were prepared to integrate analytical methods and other associated technologies. This finding shows a willingness to integrate technological developments enabling more informed environmental management decisions to be reached. A fundamental element of this thesis study justification was provide solutions to industry related resource constraints in an environmentally sympathetic and viable way. Although specific cost-benefit analyses was beyond the scope of this study, the development of new methods for understanding tree structure (chapter 4), reducing ITC delineation problems (chapter 5) and remotely classifying tree structural

condition (chapter 6), provides new mechanisms that tree managers can exploit to aid operational decision making.

While the ARBOR framework is proposed as the solution to the delineation problem, it is recognised that this is not a static problem that can be fully resolved with only one approach. This is why the ARBOR framework is a flexible, modular system that can be manipulated to suit different circumstances (Figure 32). This addresses a significant issue in RS research that has been under-reported in many peer-reviewed publications. The development of the ARBOR framework is in response to this gap in scientific knowledge where flawed procedures lead to the acceptance of conclusions based on the use of arbitrary thresholds or poorly matched data. Furthermore, analysis of the published methods shows that reported successful match-pairings of ITC delineated trees were subject to the influence of directionality, leading to false-positive results. Taken as a completed solution, the ARBOR framework can immediately be used by other researchers to quantify, and importantly, report the success of their ITC delineation efforts, therefore, increasing transparency in the method. It is understood that different researchers will use a variety of ITC delineation techniques to achieve specific goals (Table 8). Such as, in forest inventory or tree classification studies, however, accuracy issues in the inventory or classification phase may have resulted from improper match-pairing that previously had not been accounted for. By not accurately quantifying the match-pairing process, valid inventory or classification procedures may be discounted from use due to low accuracies that are not directly attributable to the classification method. The ARBOR framework provides a quantified solution to this problem, and will facilitate the future optimisation of ITC delineation studies. The STRUCTURAL method categorises trees using RS at a woodland scale, with LiDAR remotely measuring many trees at

the same time (Figure 21). To aid transparency and increase the potential for adoption of STRUCTURAL, the method has been modelled as an operational workflow (Figure 32). Furthermore, the process outputs a categorised, geospatial dataset that can be used operationally and integrated into predicted management planning to direct resources to lower categorised trees (Figure 30).

7.3.4 Tree Structure Effects

It is well documented that trees have dynamic structures that are subject to internal, external, biotic and abiotic forces, leading to alterations in form and structure (Niklas 1992, Mattheck and Breloer 1994, Mattheck 1998, Lonsdale 1999, Niklas 2001, Niinemets 2010). What is less well documented, is how those many structurally altering effects are used by tree managers attempting to understand the tree stock structural condition and drawing meaningful conclusions about the significance of the observations. The method from chapter 4 provides a clear mapping of changes in observable structural condition with traditional arboricultural observations, and it is believed, provides for the first time data that has been quantified to the level of intra-category variation, a resolution level that has previously been absent from coarse categorical methods (Figure 14).

Modelling of tree structures, particularly 3D investigations or reconstruction, is said by Bournez, Landes et al. (2017) to require clear line of sight with the structure. This reasoning provides justification for the use of leaf-off investigative methodology, as is used in chapter 4 and a separate strategy is used in chapter 5 where the trees were in leaf-on conditions. Furthermore, as supported by the views of Further, White, Arnett et al. (2015) using the discreet approach of applying different investigation types relative to the seasonal tree growth stage in broadleaves, i.e. leaf-off or leaf-on,

reduces bias. This emphasis has been an underlying consideration throughout this study, where proposed methods lead towards impartiality, and away from the introduction of subjectivity.

7.3.5 Environmental Remote Sensing

As supported by many environmental studies, RS is considered a developmental tool that aides greater understanding of the environment for a range of applications, notably, in the management of trees, woodland or forests (Vauhkonen, Maltamo et al. 2014). RS provides many opportunities for investigation, using a range of tools and at a variety of scales (Jones and Vaughn 2010, Westoby, Brasington et al. 2012, Vauhkonen, Maltamo et al. 2014). In order to support the capture of RS data, it is necessary to establish GR plots to enable validation of observations made on RS data (Mitchard, Feldpausch et al. 2014). Bournez, Landes et al. (2017) state that the complexity of tree structure, with many varying sized branches in all possibilities of convoluted arrangements, increases in leaf-on conditions. This increasing complexity was important to the establishment of chapter 4, where it was a requirement to show that tree structure changed relative to observable structural condition, as was always assumed but not proven or quantified by tree managers. Similarly, knowing that the complexity of tree crowns changes when in leaf-on condition also influenced where the individual trees are in the LiDAR data chapter 5, and the creation of area and density point distribution focussed metrics in the chapter 6 that were validated against directly measured GR plots. Therefore, within the framework of this study, it was considered important to consider what part of the tree structure, crown or canopy is being investigated, the time of year the investigation would take place (due to seasonal changes, particularly in deciduous tree populations), and to have viable GR data available to cross-validate against

An unintended advantage of STRUCTURAL is the determination of broader environment characteristics around the trees, coinciding with the tree structural condition categories (Figure 30 and Figure 23). As described in Field Sites, there is an approximate west to east division of the woodland character, which is reflected in the soil and bedrock distribution. Informal soil profiling was conducted during plot establishment fieldwork across the woodland where, in the west, trees were predominantly on top of limestone pavement and thin soils to ~5cm depth (Figure 30 and Figure 31). Similarly, within the western and central woodland there are a notable number of moderate to poor trees, which correspond to these macro-environmental conditions. Although the soil profile to the east of the woodland is only marginally deeper, to depths of ~20cm, it here that higher numbers of good category trees are observed. Additional good trees are observed to the east, it is believed that the influence of dominant trees are obscuring the understory of suppressed, poorer structural condition and that the distribution of the poor tree (red) in this spatial zone, is indicative of upper canopy gaps which show lower to middle canopy trees that are in poorer conditions (Figure 30 and Figure 31).

7.3.6 Unique Remote Sensing Programming Challenges

Several phases of data processing have been used in preparation for the analyses used in this study, which is typical with many forms of RS data. Due to the data volumes involved, data preparation prior to analysis requires an optimised approach (Yan, Shaker et al. 2015). In preparation for chapter 5 and 6, following Otepka, Ghuffar et al. (2013) all LiDAR data was classified allowing the identification of ground and non-ground points, vegetation and other scene features (ASPRS 2013). This LiDAR processing also included the removal of non-essential data outside of the area of investigation (Figure 21) and data noise removal.

7.3.7 Photogrammetry

Photogrammetric methods have been long available to practitioners as a research tool (Evans and Coombe 1959). When considering a suitable solution for the rapid characterisation and quantification of tree structure, the potential for transferability to operational use was also considered. This led to the use of easily accessible equipment (dSLR camera and tripod), avoiding cost prohibitive or specialist RS equipment such as terrestrial LiDAR (Leberl, Irschara et al. 2010). Liang, Jaakkola et al. (2014) also state that hand-held dSLR cameras can be used in individual tree investigations and can capture data comparable to terrestrial LiDAR. This photogrammetric approach is also supported by Westoby, Brasington et al. (2012) who consider that modern photogrammetry facilitates high-resolution portable data acquisition, enabling the field practitioner ready access to difficult field sites, unencumbered by heavy RS equipment. Boosting accessibility is required to encourage tree and forest managers to adopt a new photogrammetric technique which improves upon traditional categorical methods, as it is understood tree managers embrace the use of supportive technologies when given the opportunity (Segura, Ray et al. 2014). It is within this ethos that the field method described in chapter 4 was devised, to provide a practical and portable solution to assessing the complexity of tree structural condition.

7.3.8 Aerial Laser Scanning

In a review by Koenig and Höfle (2016), it was stated that most ALS LiDAR investigations isolate individual trees and extract data via delineation from CHMs, and apply data filtering to create an index of biophysical properties. These are the methods used in both chapter 5 and chapter 6, which focus on individual tree assessment at differing landscape scales. Within chapter 5, developing a new methodology for locating trees within LiDAR data was not a research objective, moreover, the focus was on working within the framework of what methods the

research community currently use during ITC delineation and quantifying the effectiveness of these methods. Furthermore, the use of ALS is shown to provide opportunities for the creation of investigative metrics to understand tree structural condition as is conducted in chapter 6. Murray, Blackburn et al. (2014) discuss the significance of different pulse return values, and the potential influence on canonical variables that are used to describe tree structure. This approach was used in chapter 6 where a metric was defined that reflects the interrelationship of point densities and crown surface structure (Table 14), as a proxy for enabling the classification of tree crowns from an ALS LiDAR perspective. Kandare, Ørka et al. (2016) describe an increase in accuracy within ITC delineation methods in line with increasing point cloud density (Figure 21).

7.3.9 The Future of Technological Approaches

The research chapters of this thesis, chapters 4, 5 and 6, have all focussed on improving the objective quantification of tree structural condition. As is commonly the case with technology, there is a general movement towards the miniaturisation of equipment meaning that more RS equipment will be available for regular operational use, leading to more data driven environmental investigations (Jaakkola, Hyypä et al. 2017). This move suggests that there will be ongoing opportunities for the integration of new techniques and methodologies in the environmental sector, and in particular, increasing the use of RS in tree and forest management through the adaptation of “precision forestry”, where novel tools and technologies are used to improve forest management, as shown at Table 19 (Kováčsová and Antalová 2010).

Table 19 The activity fields of precision forestry (Kováčsová and Antalová 2010).

Precision Forestry	
Activity	Description
1. Surveying	Terrestrial laser scanner, GPS, INS and digital surveying equipment
2. Remote Sensing	CIR, Airborne laser scanner
3. Contact-free measuring	Materials testing, measuring, computer tomography, ultrasound, video
4. Monitoring	Radio frequency identification (RFID), electronic nose (aroma)
5. Decision Support	Decision-making and harvest planning
6. Information Systems	GIS, DSS and visualisation software
7. Hardware	Computer hardware

The new methods for assessing tree structure using proximal hemispherical imagery described in chapter 4 meets 1, 3, 5, 6 and 7, while chapter 5 fulfils the activity fields 2, 3, 5, 6 and 7. The landscape scale classification of trees with ALS LiDAR in chapter 6, aligns with 1, 2, 3, 5, 6 and 7 of the precision forestry activity fields (Table 19). Therefore, it can be stated that all of the developmental methods described in this thesis are closely aligned with expected trends in future tree and forest management.

7.4 Limitations of the Research

Throughout this research project the focus has remained on developing techniques that will improve the remote sensing of trees for different applications, but predominately, to develop methods or processes that can be used in further studies or in an operational capacity for the management of trees. Several additional lines of research were identified during the research and development phases, but were discounted from further consideration on the basis of not being within the immediate scope of this research.

Within the method described in chapter 4, it was perceived that the use of the southern axis only for capturing the tree crown images was both beneficial in demonstrating that the method worked using a standardised approach, but also potentially limiting as not all cardinal points of the tree crown were imaged (Figure 11). While this method was chosen for proving the concept based on replication and the growth habits of trees, it is expected that there will be inter-crown differences relative to the cardinal point that the tree has been photographed from (for example, where the subject tree may be next to a wall or building, or unsuitable access to the area). It was recognised that additional time should have been taken in capturing images from all the cardinal points i.e. north, west and east, considering these as individual Df measures, and subsequently calculating the probabilities in the proportional odds model and ranking the trees by the average of the combined Df measurements.

However, following the completion of chapter 4, the image capture methods were applied to a new, externally funded project which compared Df values from photogrammetry with TLS data to quantify the structural complexity of orchard trees as a proxy for defining top-fruit yield. The significance of this application, is that these were dwarf orchard trees and subsequently, at the limits of what could be achieved from the photogrammetry method. Furthermore, the field method was altered by changing the axis location, placing the camera (body) height at ground level and capturing images from different cardinal points. Similar to a pilot study, this demonstrated that the chapter 4 method adapted to new operational parameters, and further, supports the proposal to assess the potential extent of the chapter 4 method in a range of different uses or field applications (Appendix B).

A limitation of chapter 5 was that it was not directly tested across a range of different tree mosaics and populations, such as ITC delineated trees in a regularly-spaced, coniferous plantation, or extensive parkland with individual maiden trees. While it is expected that there will be differences in how these datasets perform within the ARBOR framework, it was considered important to establish that the methodology behind the function of the ARBOR framework was sound. Therefore, by developing ARBOR to quantify the ITC delineated tree populations in the most complex tree canopy data, specifically temperate broadleaved deciduous woodland, it was believed that this would enable later testing of the framework across a range of less complex tree populations. Furthermore, that this approach would increase the prospects for transferability of the framework, as it was developed to accommodate the nuances of the most challenging data available.

Within chapter 6, the training dataset was initially limited by the number of dead category trees in the model. All other categories had significant numbers in the data population, as expected in the order of good, moderate, poor (see Model Retraining). However, while there were more dead trees within the woodland, these trees were often not within the survey plots and therefore were not surveyed. This arose from the survey plots being initially established for a parallel study where dead category trees were not within the study remit, therefore, they were discounted where they occurred (in the parallel study). To achieve a larger representative sample of dead trees, additional dead trees should be singled out from other locations within the woodland. This course of action was not followed during GR data capture due to the extensive, additional fieldwork required in locating, and completing the RTK GPS back-sighting survey. Furthermore, dead trees could also be measured where they are located in easily accessible areas, such as in maiden tree locations. In addition, trees categorised

as 'poor' were also typically smaller and less developed than the overstory trees. This made it difficult to assign the correct LiDAR dataset to the GR data, as poor trees were frequently overtopped and were not immediately noticeable in the peaks of the CHM on visual inspection. On several occasions within the training data, manual cross-checking ensured match-pairing between the GR and RS-derived data was appropriate, and that the auto-generated pair was not to an overstory tree from within the data. These developmental problems also highlight the need for further exploratory work in matching the GR and RS-derived data, in particular reference to Z-values or heights when extracting data for analysis.

As discussed by Hamraz, Contreras et al. (2017) there is a significant underestimation of understory trees (typically 90% overstory detection and only 60% understory detection) due to the shadowing effect of the overstory. Hamraz, Contreras et al. (2017) propose a solution where a higher density of points/m² enables increased understory tree detection, which was enacted within the data preparation phase in chapter 6,. However, after following this advice the ground point density was on average, 23 points/m², while other studies report higher levels of ground point density to 40-60 points/m². Therefore, it was accepted that there will be some understory trees that are shadowed out of the dataset by the dominant overstory, and tree structural condition categorisations are likely only being stated for the overstory in the east of the study site (Figure 30). The solution to this study limitation would be to develop a data training procedure, leading to the categorisation of individual tree structure that does not require the generation of CHMs as part of the analysis, and that computes data relationships directly from the delineated point clouds of individual trees

7.5 Potential Research Opportunities

Further to the findings of this thesis, it is believed that additional research should focus on the relationship between tree structure and the potential for tree failure in high wind or storm events (Gullick, Blackburn et al. 2017). There is the well-known phenomenon of increased tree sail area having a larger surface area for wind to exert force upon. This suggests that trees in fuller crown vigour are at higher risk of branch or limb failure, or potentially whole tree failure where other factors such as insufficient ground anchorage is a factor (Mattheck and Breloer 1994). However, it should also be recognised that strong wind events can lead to a reduction of the crown sail area through the loss of leaves, therefore, the wind force will exert directly upon the (smaller surface area) structure of the tree. RS techniques using LiDAR can be used to classify tree species and therefore define the relationship between the general strength of the species, the complexity of the tree structure and the amount of wind force being applied that will be able to be modelled (following combined meteorological experimentation) and used to improve tree failure measurement and prediction models, based on the assessment of biophysical tree properties (Henry, Palmer et al. 2017).

An inevitable consequence of surveying is that the data represents a single moment in time when the subject was observed, therefore, the data generated will only reflect the subject structural condition as observed on that specific day. Therefore, it follows that there is an opportunity to gain greater insight into the development of tree structural conditions with the use of temporal studies of the same woodland site area. With historic ALS LiDAR data of the study site, there is the opportunity to quantify tree structural condition change over time, and in a validation step, identify the potential of the metrics and classification model to map the progressive change of the

tree structural conditions (Figure 32), potentially identifying change from a good structural condition, with a tree degenerating through the structural condition continuum and ending in full decline and the dead category. The wider implications of temporal LiDAR studies is that this approach could also be used to monitor the outbreak and progression of tree disease, such as the recent *Chalara fraxinea* outbreak across Europe (Goberville, Hautekèete et al. 2016), following the prior collection of base data and initial categorisation of ITC delineated trees in the landscape.

An ambition for this work has been to develop methodologies and practices that can be used operationally, however, there also remains the opportunity to undertake development of this research to bring it up to full distribution potential. Within this project, there has been the reliance on bespoke computer programming languages and platforms e.g. Matlab, that would in its current form, prevent the majority of lay people from being able to implement these methods operationally, without specific programming experience or training. Further work therefore, could concentrate on creating a web-based, front-end graphical user interface (GUI) for the uploading and automatic analysis of hemispherical images for Df analysis, the creation of the ARBOR portal and a web GUI for the STRUCTURAL method. At the time of writing, the development of the ARBOR portal is underway, however, the remaining GUI's are not within the timeframe or resources of this study and therefore, will remain an opportunity for follow-up work on GUI development to increase the potential for operational take-up.

8 Conclusion

The aim of this research was to develop novel RS methods for the quantification of tree structural condition, which can be used for the observation and classification of trees in complex, semi-natural temperate broadleaved woodland. This endeavour was undertaken with the emphasis on the development of objective, technology-rich solutions that would offer an improvement over traditional tree surveying methods. The traditional methods have been shown to be influenced by subjectivity either as a result of the survey methodology, as a result of data processing or by the unintentional influence of the surveyor. To achieve this aim, the research objectives were to 1) develop an objective methodology for assessing tree structure using proximal hemispherical photography, 2) develop a technique for quantifying the accuracy of ITC delineations of RS data, and 3) to develop a methodology for categorising the structural condition of individual trees at landscape scale from ALS data. As such, these research objectives have been met through the completion of the work described in chapters 4, 5, and 6.

This research produced several key findings that will contribute to the wider knowledge of this subject area. Chapter 4 described a new method to classify tree structural complexity using proximal photogrammetry, in a way that minimises introduced subjectivity or bias. By utilising a simple, repeatable field method and through conducting independent, computational analysis of the tree crown images, a very-high statistical probability classification of the tree structure can be achieved. As a field surveyor is only required to identify the tree on the ground, set up a camera

and take a photograph, while the analysis and classification is conducted independently by the program, therefore, the objectivity and repeatability of the classification method is significantly increased. Furthermore, the assessment of tree crown structure using Df as a continuous measure provides the opportunity for much greater insights into the unique features within individual tree crowns. This is a significant improvement over arbitrary grouping and provides a new approach for the measurement of intra-category variance, and at a level of precision that was not previously available.

Further to the classification of tree structure, a novel approach for objectively quantifying the amount of agreement between two RS datasets, is described in chapter 5 as the ARBOR framework. This is a significant contribution to the RS community as it is shown that recurring alignment errors in RS data has been widely under-reported throughout the available literature. Further, it is acknowledged that prior to the development of ARBOR, no other standardised accuracy assessment procedure for quantifying commission errors in RS delineation data existed. ARBOR was rigorously tested on both synthetic (with varying levels of data complexity and noise) and real-world data, therefore, can be considered a robust method that can be adopted as the RS specific method to be used in quantifying the commission agreement in RS delineations. This development is a substantial improvement over the reliance on arbitrary height or other variable thresholds that were previously used to infer levels of data agreement.

Furthermore, chapter 6 describes a new RS method for the remote analysis and classification of individual trees at the landscape scale, using aerial LiDAR. The STRUCTURAL method utilises analytical metrics that quantify the tree structure (as

it is represented in the LiDAR point cloud data), to provide a novel approach to classifying trees from a remote perspective. The STRUCTURAL method also utilises the RS data agreement method ARBOR, which is the first real application of this method in an operational survey of this type. The STRUCTURAL method is shown to be statistically robust as a consequence of the extended training data analysis that provided machine learning inputs, which also increased the method's validation accuracies. This makes the STRUCTURAL method a viable, technology-rich solution to a real-world tree management problem that was both time and logistically costly for field operatives.

The main contribution of this research to the advancement of digital forestry, is that this work provides the opportunity to utilise the suite of methods described in this thesis, to undertake informed, predictive management of tree stock (Figure 33), with additional potential insights for researchers or practitioners gained by monitoring tree structural change over time, allowing detailed, long-term monitoring of trees that are of prominent standing or are considered high value for amenity, conservation or ecological purposes. In addition, the contribution of ARBOR to experimental RS research is that other RS practitioners can now quantify the level of agreement in their data, and publish these values, thereby increasing the transparency and confidence in the wider experimental RS research.

It is recognised that there remain future research priorities from this body of work. Particularly, the Df analysis of tree structure could be used to define intra-species differences, and the development of a structural Df index for the classification of individual tree species. In addition, further work is required in the STRUCTURAL method for individual species identification, and to operationalise the method, which

would enable the implementation of the method within regular tree management surveying protocols.

By developing novel procedures and tools within this thesis, a new suite of methods have been produced that can be used to provide greater levels of tree structural condition information than was achievable previously. Therefore, this development represents a significant contribution to RS science and the emerging discipline of digital forestry.

9 References

- Accastello, C., F. Brun and E. Borgogno-Mondino (2017). "A Spatial-Based Decision Support System for wood harvesting management in mountain areas." Land Use Policy **67**: 277-287.
- Ahmed, R., P. Siqueira, S. Hensley and K. Bergen (2013). "Uncertainty of Forest Biomass Estimates in North Temperate Forests Due to Allometry: Implications for Remote Sensing." Remote Sensing **5**(6): 3007.
- Åkerblom, M., P. Raunonen, R. Mäkipää and M. Kaasalainen (2017). "Automatic tree species recognition with quantitative structure models." Remote Sensing of Environment **191**: 1-12.
- Andersen, H.-E., R. J. McGaughey and S. E. Reutebuch (2005). "Estimating Forest Canopy Fuel Parameters Using LiDAR Data." Remote Sensing of Environment **94**: 441-449.
- ASPRS (2013). LAS Specification. Version 1.4 - R13. Bethesda, Maryland., The American Society for Photogrammetry & Remote Sensing: 1-28.
- Ayrey, E., S. Fraver, J. A. Kershaw, L. S. Kenefic, D. Hayes, A. R. Weiskittel and B. E. Roth (2017). "Layer Stacking: A Novel Algorithm for Individual Forest Tree Segmentation from LiDAR Point Clouds." Canadian Journal of Remote Sensing **43**(1): 16-27.
- Baltsavias, E. P. (1999). "Airborne laser scanning: basic relations and formulas." ISPRS Journal of Photogrammetry and Remote Sensing **54**(2-3): 199-214.
- Barrell, J. (1993). "Pre-planning Tree Surveys: Safe Useful Life Expectancy (SULE) is the Natural Progression." Arboricultural Journal **17**(1): 33-46.
- Barrell, J. (2001). SULE: Its Use and Status into the New Millennium. NAAA Arboricultural Conference. Sydney, Australia, NAAA
- Beckschäfer, P., D. Seidel, C. Kleinn and J. Xu (2013). "On the Exposure of Hemispherical Photographs in Forests." iForest – Biogeosciences and Forestry **6**: 228-237.
- Ben-Arie, J. R., G. J. Hay, R. P. Powers, G. Castilla and B. St-Onge (2009). "Development of a pit filling algorithm for LiDAR canopy height models." Computers & Geosciences **35**(9): 1940-1949.
- Bengtsson, V., J. Hedin and M. Niklasson (2012). Veteranisation of Oak – Managing Trees to Speed Up Habitat Production. Trees Beyond the Wood. Sheffield, International Union of Forest Research Organisations (IUFRO): 1-11.
- Bian, Y., P. Zou, Y. Shu and R. Yu (2014). "Individual Tree Delineation in Deciduous Forest Areas with LiDAR Point Clouds." Canadian Journal of Remote Sensing **40**(2): 152-163.
- Blennow, K., J. Persson, A. Wallin, N. Vareman and E. Persson (2013). "Understanding Risk in Forest Ecosystem Services: Implications for Effective Risk Management, Communication and Planning." Forestry **87**(2): 219-228.

- Bonnet, E., O. Bour, N. E. Odling, P. Davy, I. Main, P. Cowie and B. Berkowitz (2001). "Scaling of Fracture Systems in Geological Media." Reviews of Geophysics **39**(3): 347–383.
- Bortolot, Z. J. and R. H. Wynne (2005). "Estimating Forest Biomass Using Small Footprint LiDAR Data: An Individual Tree-based Approach that Incorporates Training Data." ISPRS Journal of Photogrammetry & Remote Sensing **59**: 342–360.
- Bournez, E., T. Landes, M. Saudreau, P. Kastendeuch and G. Najjar (2017). "FROM TLS POINT CLOUDS TO 3D MODELS OF TREES: A COMPARISON OF EXISTING ALGORITHMS FOR 3D TREE RECONSTRUCTION." Int. Arch. Photogramm. Remote Sens. Spatial Inf. Sci. **XLII-2/W3**: 113-120.
- Bouvier, M., S. Durrieu, R. A. Fournier and J.-P. Renaud (2015). "Generalizing predictive models of forest inventory attributes using an area-based approach with airborne LiDAR data." Remote Sensing of Environment **156**(Supplement C): 322-334.
- Brandtberg, T. (2007). "Classifying individual tree species under leaf-off and leaf-on conditions using airborne lidar." ISPRS Journal of Photogrammetry and Remote Sensing **61**(5): 325-340.
- Brandtberg, T. and F. Walter (1998). "Automated delineation of individual tree crowns in high spatial resolution aerial images by multiple-scale analysis." Machine Vision and Applications **11**(2): 64-73.
- Britt, C. and M. Johnston (2008). Trees in Towns II. London, Department for Communities and Local Government.
- BSI (2012). Trees in Relation to Design, Demolition and Construction - Recommendations. B. S. Institute, BSI Standards Limited.
- Burkhardt, H. E. and M. Tome (2012). Modelling Forest Trees and Stands. New York, Springer.
- Chason, J. W., D. D. Baldocchi and M. A. Huston (1991). "A Comparison of Direct and Indirect Methods for Estimating Forest Canopy Leaf Area " Agricultural and Forest Meteorology **57**: 107-128.
- Chen, J. M., T. A. Black and R. S. Adams (1991). "Evaluation of Hemispherical Photography for Determining Plant Area Index and Geometry of a Forest Stand." Agricultural and Forest Meteorology **56**(1-2): 129-143.
- Chen, M.-H. and P.-F. Yan (1988). "A Fast Algorithm to Calculate the Euler Number for Binary Images." Pattern Recognition Letters **8**(5): 295-297.
- Chen, Q., D. Baldocchi, P. Gong and M. Kelly (2006). "Isolating individual trees in a savanna woodland using small footprint lidar data." Photogrammetric Engineering and Remote Sensing **72**(8): 923-932.
- Chianucci, F. (2016). "A Note on Estimating Canopy Cover from Digital Cover and Hemispherical Photography." Silva Fennica **50**(1): 1-10.
- Chianucci, F., U. Chiavetta and A. Cutini (2014). "The estimation of canopy attributes from digital cover photography by two different image analysis methods." Iforest-Biogeosciences and Forestry **7**: 255-259.
- Chianucci, F. and A. Cutini (2012). "Digital Hemispherical Photography for Estimating Forest Canopy Properties: Current Controversies and Opportunities." iForest **5**: 290-295.

- Culvenor, D. S. (2002). "TIDA: an algorithm for the delineation of tree crowns in high spatial resolution remotely sensed imagery." Computers & Geosciences **28**(1): 33-44.
- Dana, E. D., J. M. Jeschke and J. García-de-Lomas (2013). "Decision tools for managing biological invasions: existing biases and future needs." Oryx **48**(1): 56-63.
- Danson, F. M., R. Gaulton, R. P. Armitage, M. Disney, O. Gunawan, P. Lewis, G. Pearson and A. F. Ramirez (2014). "Developing a dual-wavelength full-waveform terrestrial laser scanner to characterize forest canopy structure." Agricultural and Forest Meteorology **198**: 7-14.
- Dash, J. P., M. S. Watt, S. Bhandari and P. Watt (2016). "Characterising Forest Structure Using Combinations of Airborne Laser Scanning Data, RapidEye Satellite Imagery and Environmental Variables." Forestry **89**: 159 –169.
- Dassot, M., T. Constant and M. Fournier (2011). "The use of terrestrial LiDAR technology in forest science: application fields, benefits and challenges." Annals of Forest Science **68**(5): 959-974.
- de Groot, W. T. (1992). Environmental Science Theory Concepts and Methods in a One-World, Problem-Oriented Paradigm. Amsterdam, Elsevier.
- de Vries, J. (2012). Barrel and Pincushion Lens Distortion Correction, Mathworks.
- Dimri, V. P. (2000). Application of Fractals in Earth Sciences. Rotterdam, Netherlands., A.A. Balkema.
- Donohue, P. (2016). Woodland Area, Planting and Restocking. IFOS-Statistics. Edinburgh, Forest Research: 1-22.
- Duncanson, L. I., R. O. Dubayah, B. D. Cook, J. Rosette and G. Parker (2015). "The importance of spatial detail: Assessing the utility of individual crown information and scaling approaches for lidar-based biomass density estimation." Remote Sensing of Environment **168**: 102-112.
- Edelsbrunner, H. and P. M. Ernst (1994). "Three-dimensional Alpha Shapes." ACM Trans. Graph. **13**(1): 43-72.
- Evans, G. C. and D. E. Coombe (1959). "Hemispherical and Woodland Canopy Photography and the Light Climate." Journal of Ecology **47**(1): 103-113.
- Eysn, L., M. Hollaus, K. Schadauer and N. Pfeifer (2012). "Forest Delineation Based on Airborne LIDAR Data." Remote Sensing **4**(3).
- Falkowski, M. J., A. M. S. Smith, P. E. Gessler, A. T. Hudak, L. A. Vierling and J. S. Evans (2008). "The influence of conifer forest canopy cover on the accuracy of two individual tree measurement algorithms using lidar data." Canadian Journal of Remote Sensing **34**: S338-S350.
- Fay, N. and N. de Berker (1997). Veteran Trees Initiative Specialist Survey Method. Peterborough, UK. , English Nature.
- Ferraz, A., S. Saatchi, C. Mallet and V. Meyer (2016). "Lidar detection of individual tree size in tropical forests." Remote Sensing of Environment **183**: 318-333.
- Folk, R. L. (1951). "A Comparison Chart for Visual Percentage Estimation." SEPM Journal of Sedimentary Research **21**(1): 32-33.

- Fonstad, M. A., J. T. Dietrich, B. C. Courville, J. L. Jensen and P. E. Carbonneau (2013). "Topographic structure from motion: a new development in photogrammetric measurement." Earth Surface Processes and Landforms **38**(4): 421-430.
- Forzieri, G., L. Guarnieri, E. R. Vivoni, F. Castelli and F. Preti (2009). "Multiple attribute decision making for individual tree detection using high-resolution laser scanning." Forest Ecology and Management **258**(11): 2501-2510.
- Fourcaud, T., L. Dupuy, D. Sellier, P. Ancelin and P. Lac (2004). Analysis of the Relationship Between Tree Structure and Biomechanical Functions. 4th International Workshop on Functional-Structural Plant Models (FSPM04), Montpellier, France.
- Frazer, G. W., M. A. Wulder and K. O. Niemann (2005). "Simulation and Quantification of the Fine-scale Spatial Pattern and Heterogeneity of Forest Canopy Structure: A Lacunarity-based Method Designed for Analysis of Continuous Canopy Heights." Forest Ecology and Management **214**: 65-90.
- Gargano, G., R. Bellotti, F. de Carlo, S. Tangaro, E. Tommasi, M. Castellano, P. Cerello, S. C. Cheran and C. Fulcheri (2007). A novel Active Contour Model algorithm for contour detection in complex objects. 2007 IEEE International Conference on Computational Intelligence for Measurement Systems and Applications.
- Ghiselin, J. (1982). "Reaching environmental decisions: Making subjective and objective judgments." Environmental Management **6**(2): 103-108.
- Gobakken, T., O. M. Bollandsas and E. Naesset (2015). "Comparing biophysical forest characteristics estimated from photogrammetric matching of aerial images and airborne laser scanning data." Scandinavian Journal of Forest Research **30**(1): 73-86.
- Goberville, E., N.-C. Hautekèete, R. R. Kirby, Y. Piquot, C. Luczak and G. Beaugrand (2016). "Climate change and the ash dieback crisis." Scientific Reports **6**: 35303.
- Gorrod, E. J. and D. A. Keith (2009). "Observer variation in field assessments of vegetation condition: Implications for biodiversity conservation." Ecological Management & Restoration **10**(1): 31-40.
- Gullick, D., A. Blackburn, D. Whyatt, P. Vopenka and J. Abbatt (2017). "Tree Risk Evaluation Environment for Failure and Limb Loss (TREEFALL): Predicting Tree Failure within Proximity of Infrastructure on an Individual Tree Scale."
- Hale, S. (2004). Managing Light to Enable Natural Regeneration in British Conifer Forests. F. Commission. Edinburgh, Forestry Commission: 1-6.
- Hamraz, H., M. A. Contreras and J. Zhang (2016). "A robust approach for tree segmentation in deciduous forests using small-footprint airborne LiDAR data." International Journal of Applied Earth Observation and Geoinformation **52**: 532-541.
- Hamraz, H., M. A. Contreras and J. Zhang (2017). "Forest understory trees can be segmented accurately within sufficiently dense airborne laser scanning point clouds." Scientific Reports **7**(1): 6770.
- Hansen, M. C., S. V. Stehman, P. V. Potapov, T. R. Loveland, J. R. G. Townshend, R. S. DeFries, K. W. Pittman, B. Arunarwati, F. Stolle, M. K. Steininger, M. Carroll and C. DiMiceli (2008). "Humid tropical forest clearing from 2000 to 2005 quantified by using multitemporal and multiresolution remotely sensed data." Proceedings of the National Academy of Sciences **105**(27): 9439-9444.

- Harper, M. J., M. A. McCarthy, R. van der Ree and J. C. Fox (2004). "Overcoming bias in ground-based surveys of hollow-bearing trees using double-sampling." Forest Ecology and Management **190**(2): 291-300.
- Hauglin, M., V. Lien, E. Næsset and T. Gobakken (2014). "Geo-referencing forest field plots by co-registration of terrestrial and airborne laser scanning data." International Journal of Remote Sensing **35**(9): 3135-3149.
- Henning, J. G. and P. J. Radtke (2006). "Ground-based Laser Imaging for Assessing Three-dimensional Forest Canopy Structure " Photogrammetric Engineering & Remote Sensing **72**(12): 1349 - 1358.
- Henry, R. C., S. C. F. Palmer, K. Watts, R. J. Mitchell, N. Atkinson and J. M. J. Travis (2017). "Tree loss impacts on ecological connectivity: Developing models for assessment." Ecological Informatics **42**: 90-99.
- Hilker, T., M. van Leeuwen, N. C. Coops, M. A. Wulder, G. J. Newnham, D. L. B. Jupp and D. S. Culvenor (2010). "Comparing canopy metrics derived from terrestrial and airborne laser scanning in a Douglas-fir dominated forest stand." Trees-Structure and Function **24**(5): 819-832.
- Hladik, C. and M. Alber (2012). "Accuracy assessment and correction of a LIDAR-derived salt marsh digital elevation model." Remote Sensing of Environment **121**: 224-235.
- Holmgren, J. and E. Lindberg (2013). "Tree Crown Segmentation Based on a Geometric Tree Crown Model for Prediction of Forest Variables." Canadian Journal of Remote Sensing **39**(S1): S86-S98.
- Holmström, H. (2002). "Estimation of Single-tree Characteristics using the *k*NN Method and Plotwise Aerial Photograph Interpretations." Forest Ecology and Management **167**: 303-314.
- Holopainen, M., M. Vastaranta and J. Hyyppä (2014). "Outlook for the Next Generation's Precision Forestry in Finland." Forests **5**(7): 1682-1694.
- Hovi, A., L. Korhonen, J. Vauhkonen and I. Korpela (2016). "LiDAR waveform features for tree species classification and their sensitivity to tree- and acquisition related parameters." Remote Sensing of Environment **173**: 224-237.
- Hyyppä, J., X. W. Yu, H. Hyyppä, M. Vastaranta, M. Holopainen, A. Kukko, H. Kaartinen, A. Jaakkola, M. Vaaja, J. Koskinen and P. Alho (2012). "Advances in Forest Inventory Using Airborne Laser Scanning." Remote Sensing **4**(5): 1190-1207.
- Jaakkola, A., J. Hyyppä, X. Yu, A. Kukko, H. Kaartinen, X. Liang, H. Hyyppä and Y. Wang (2017). "Autonomous Collection of Forest Field Reference—The Outlook and a First Step with UAV Laser Scanning." Remote Sensing **9**(8): 785.
- Jakubowski, M. K., Q. Guo, B. Collins, S. Stephens and M. Kelly (2013). "Predicting Surface Fuel Models and Fuel Metrics Using Lidar and CIR Imagery in a Dense, Mountainous Forest." Photogrammetric Engineering & Remote Sensing **79**(1): 37-49.
- Jakubowski, M. K., W. K. Li, Q. H. Guo and M. Kelly (2013). "Delineating Individual Trees from Lidar Data: A Comparison of Vector- and Raster-based Segmentation Approaches." Remote Sensing **5**(9): 4163-4186.
- Jennings, S. B., N. D. Brown and D. Sheil (1999). "Assessing forest canopies and understorey illumination: canopy closure, canopy cover and other measures." Forestry: An International Journal of Forest Research **72**(1): 59-74.

Jing, L., B. Hu, H. Li, J. Li and T. Noland (2014). Automated individual tree crown delineation from LIDAR data using morphological techniques. 35th International Symposium on Remote Sensing of Environment. H. Guo. Bristol, Iop Publishing Ltd. 17.

Jing, L., B. Hu, T. Noland and J. Li (2012). "An individual tree crown delineation method based on multi-scale segmentation of imagery." ISPRS Journal of Photogrammetry and Remote Sensing **70**: 88-98.

JNCC (2004) "Common Standards Monitoring Guidance for Woodland Habitats." 1-26.

Jonckheere, I., S. Fleck, K. Nackaerts, B. Muys, P. Coppin, M. Weiss and F. Baret (2004). "Review of methods for in situ leaf area index determination." Agricultural and Forest Meteorology **121**(1): 19-35.

Jonckheere, I., K. Nackaerts, B. Muys, J. V. Aardt and P. Coppin (2006). "A Fractal Dimension-based Modelling Approach for Studying the Effect of Leaf Distribution on LAI Retrieval in Forest Canopies " Ecological Modelling **197**: 179-195.

Jones, H. G. and R. A. Vaughn (2010). Remote Sensing of Vegetation: Principles, Techniques and Applications. Oxford, Oxford University Press.

Kaartinen, H., J. Hyypä, X. Yu, M. Vastaranta, H. Hyypä, A. Kukko, M. Holopainen, C. Heipke, M. Hirschmugl, F. Morsdorf, E. Næsset, J. Pitkänen, S. Popescu, S. Solberg, B. M. Wolf and J.-C. Wu (2012). "An International Comparison of Individual Tree Detection and Extraction Using Airborne Laser Scanning." Remote Sensing **4**(4): 950.

Kandare, K., H. O. Ørka, J. C.-W. Chan and M. Dalponte (2016). "Effects of forest structure and airborne laser scanning point cloud density on 3D delineation of individual tree crowns." European Journal of Remote Sensing **49**(1): 337-359.

Kandare, K., H. O. Ørka, M. Dalponte, E. Næsset and T. Gobakken (2017). "Individual tree crown approach for predicting site index in boreal forests using airborne laser scanning and hyperspectral data." International Journal of Applied Earth Observation and Geoinformation **60**: 72-82.

Kara, M., B. Sayinci, E. Elkoca, I. Öztürk and T. B. Özmen (2013). "Seed Size and Shape Analysis of Registered Common Bean (*Phaseolus vulgaris* L.) Cultivars in Turkey Using Digital Photography." Journal of Agricultural Sciences **19**: 219-234.

Kaye, B. H. (2008). A Random Walk Through Fractal Dimensions. West Sussex, England., John Wiley and Sons.

Kerr, G., B. Mason, R. Boswell and A. Pommerening (2002). Monitoring the Transformation of Even-aged Stands to Continuous Cover Management. F. Commission. Edinburgh, Forestry Commission: 1-12.

Khosravipour, A., A. K. Skidmore and M. Isenburg (2016). "Generating spike-free digital surface models using LiDAR raw point clouds: A new approach for forestry applications." International Journal of Applied Earth Observation and Geoinformation **52**: 104-114.

Khosravipour, A., A. K. Skidmore, M. Isenburg, T. Wang and Y. A. Hus (2014). "Generating Pit-free Canopy Height Models from Airborne Lidar." Photogrammetric Engineering & Remote Sensing **80**(9): 863-872.

Killinger, D. K. (2014). 10 - Lidar (light detection and ranging) A2 - Baudelet, Matthieu. Laser Spectroscopy for Sensing, Woodhead Publishing: 292-312.

- King, D. A. (2011). Size Related Changes in Tree Proportions and Their Potential Influence on the Course of Height Growth. Size and Age Related Changes in Tree Structure and Function. F. C. Meinzer, B. Lachenbruch and T. E. Dawson. New York, Springer Science. **4**.
- Koenig, K. and B. Höfle (2016). "Full-Waveform Airborne Laser Scanning in Vegetation Studies—A Review of Point Cloud and Waveform Features for Tree Species Classification." Forests **7**(9): 198.
- Korpela, I., H. O. Orka, M. Maltamo, T. Tokola and J. Hyypä (2010). "Tree Species Classification Using Airborne LiDAR - Effects of Stand and Tree Parameters, Downsizing of Training Set, Intensity Normalization, and Sensor Type." Silva Fennica **44**(2): 319-339.
- Kováčsová, P. and M. Antalová (2010). "Precision forestry - definition and technologies." Šumarski List **134**(11/12): 603-611.
- Kovalev, V. A. and W. E. Eichinger (2005). Elastic Lidar: Theory, Practice, and Analysis Methods, John Wiley & Sons, Inc.
- Kraus, K. (2011). Photogrammetry - Geometry from Images and Laser Scans, De Gruyter.
- Kuhn, H. W. (1955). "The Hungariain Method for the Assignment Problem." Naval Research Logistics Quarterly **2**: 83-97.
- Kwak, D.-A., W.-K. Lee, J.-H. Lee, G. S. Biging and P. Gong (2007). "Detection of individual trees and estimation of tree height using LiDAR data." Journal of Forest Research **12**(6): 425-434.
- Latifi, H., F. E. Fassnacht, J. Müller, A. Tharani, S. Dech and M. Heurich (2015). "Forest inventories by LiDAR data: A comparison of single tree segmentation and metric-based methods for inventories of a heterogeneous temperate forest." International Journal of Applied Earth Observation and Geoinformation **42**(Supplement C): 162-174.
- Leberl, F., A. Irschara, T. Pock, P. Meixner, M. Gruber, S. Scholz and A. Wiechert (2010). "Point Clouds: Lidar versus 3D Vision." Photogrammetric Engineering and Remote Sensing **76**(10): 1123-1134.
- Leblanc, S. G., J. M. Chen, R. Fernandes, D. W. Deering and A. Conley (2005). "Methodology Comparison for Canopy Structure Parameters Extraction from Digital Hemispherical Photography in Boreal Forests." Agricultural and Forest Meteorology **129**: 187-207.
- Leckie, D. G., N. Walsworth and F. A. Gougeon (2016). "Identifying tree crown delineation shapes and need for remediation on high resolution imagery using an evidence based approach." ISPRS Journal of Photogrammetry and Remote Sensing **114**: 206-227.
- Lee, J.-H., G. S. Biging and J. B. Fisher (2016). "An Individual Tree-Based Automated Registration of Aerial Images to Lidar Data in a Forested Area." Photogrammetric Engineering & Remote Sensing **82**(9): 699-710.
- Lee, J., X. Cai, J. Lellmann, M. Dalponte, Y. Malhi, N. Butt, M. Morecroft, C. B. Schönlieb and D. A. Coomes (2016). "Individual Tree Species Classification From Airborne Multisensor Imagery Using Robust PCA." IEEE Journal of Selected Topics in Applied Earth Observations and Remote Sensing **9**(6): 2554-2567.
- Leong, E. C., D. C. Burcham and Y.-K. Fong (2012). "A Purposeful Classification of Tree Decay Detection Methods." Arboricultural Journal: The International Journal of Urban Forestry **34**(2): 91-115.

- Liang, S., X. Li and J. Wang (2012). Advanced Remote Sensing: Terrestrial Information Extraction and Applications. Oxford, Elsevier.
- Liang, X., A. Jaakkola, Y. Wang, J. Hyypä, E. Honkavaara, J. Liu and H. Kaartinen (2014). "The Use of a Hand-Held Camera for Individual Tree 3D Mapping in Forest Sample Plots." Remote Sensing **6**(7): 6587.
- Lina, Y. and J. Hyypä (2016). "A Comprehensive but Efficient Framework of Proposing and Validating Feature Parameters from Airborne LiDAR Data for Tree Species Classification." International Journal of Applied Earth Observation and Geoinformation **46**: 45-55.
- Lindberg, E., J. Holmgren, K. Olofsson and H. Olsson (2012). "Estimation of stem attributes using a combination of terrestrial and airborne laser scanning." European Journal of Forest Research **131**(6): 1917-1931.
- Listopad, C., J. B. Drake, R. E. Masters and J. F. Weishampel (2011). "Portable and Airborne Small Footprint LiDAR: Forest Canopy Structure Estimation of Fire Managed Plots." Remote Sensing **3**(7): 1284-1307.
- Loehle, C. (1986). "Phototropism of Whole Trees: Effects of Habitat and Growth Form." The American Midland Naturalist **116**(1): 190-196.
- Lonsdale, D. (1999). The Principles of Tree Hazard Assessment and Management. London, HMSO.
- Lovell, J. L., D. L. B. Jupp, D. S. Culvenor and N. C. Coops (2003). "Using airborne and ground-based ranging lidar to measure canopy structure in Australian forests." Canadian Journal of Remote Sensing **29**(5): 607-622.
- Lu, X. C., Q. H. Guo, W. K. Li and J. Flanagan (2014). "A bottom-up approach to segment individual deciduous trees using leaf-off lidar point cloud data." Isprs Journal of Photogrammetry and Remote Sensing **94**: 1-12.
- Mäkelä, A. and H. T. Valentine (2006). "Crown Ratio Influences Allometric Scaling in Trees." Ecology **87**(12): 2967-2972.
- Maltamo, M., P. Packalen, X. Yu, K. Eerikainen, J. Hyypä and J. Pitkanen (2005). "Identifying and Quantifying Structural Characteristics of Heterogeneous Boreal Forests Using Laser Scanner Data." Forest Ecology and Management **216**: 41-50.
- Mandelbrot, B. (1967). "How Long Is the Coast of Britain? Statistical Self-Similarity and Fractional Dimension." Science **156**(3775): 636-638.
- Mandelbrot, B. (1982). The Fractal Geometry of Nature. San Francisco, CA, USA., W. H. Freeman and Company.
- Marošević, T. (2018). "The Hausdorff Distance Between Some Sets of Points." Mathematical Communications **23**(2): 247-257.
- Matheny, N. P. and J. R. Clark (1994). A Photographic Guide to the Evaluation of Hazard Trees in Urban Areas, International Society of Arboriculture.
- Matsuzaki, J. U. N., M. Masumori and T. Tange (2006). "Stem Phototropism of Trees: A Possible Significant Factor in Determining Stem Inclination on Forest Slopes." Annals of Botany **98**(3): 573-581.

Mattheck, C. (1998). Design in Nature: Learning From Trees. Verlag Berlin Heidelberg, Springer.

Mattheck, C. and H. Breloer (1994). The Body Language of Trees: A Handbook for Failure Analysis. London, UK., The Stationary Office.

McNellie, M. J., I. Oliver and P. Gibbons (2015). "Pitfalls and possible solutions for using geo-referenced site data to inform vegetation models." Ecological Informatics **30**: 230-234.

Mills, S. J., M. P. G. Castro, Z. R. Li, J. H. Cai, R. Hayward, L. Mejias and R. A. Walker (2010). "Evaluation of Aerial Remote Sensing Techniques for Vegetation Management in Power-Line Corridors." Ieee Transactions on Geoscience and Remote Sensing **48**(9): 3379-3390.

Mitchard, E. T. A., T. R. Feldpausch, R. J. W. Brienen, G. Lopez-Gonzalez, A. Monteagudo, T. R. Baker, S. L. Lewis, J. Lloyd, C. A. Quesada, M. Gloor, H. ter Steege, P. Meir, E. Alvarez, A. Araujo-Murakami, L. Aragao, L. Arroyo, G. Aymard, O. Banki, D. Bonal, S. Brown, F. I. Brown, C. E. Ceron, V. C. Moscoso, J. Chave, J. A. Comiskey, F. Cornejo, M. C. Medina, L. Da Costa, F. R. C. Costa, A. Di Fiore, T. F. Domingues, T. L. Erwin, T. Frederickson, N. Higuchi, E. N. H. Coronado, T. J. Killeen, W. F. Laurance, C. Levis, W. E. Magnusson, B. S. Marimon, B. H. Marimon, I. M. Polo, P. Mishra, M. T. Nascimento, D. Neill, M. P. N. Vargas, W. A. Palacios, A. Parada, G. P. Molina, M. Pena-Claros, N. Pitman, C. A. Peres, L. Poorter, A. Prieto, H. Ramirez-Angulo, Z. R. Correa, A. Roopsind, K. H. Roucoux, A. Rudas, R. P. Salomao, J. Schiatti, M. Silveira, P. F. de Souza, M. K. Steininger, J. Stropp, J. Terborgh, R. Thomas, M. Toledo, A. Torres-Lezama, T. R. van Andel, G. M. F. van der Heijden, I. C. G. Vieira, S. Vieira, E. Vilanova-Torre, V. A. Vos, O. Wang, C. E. Zartman, Y. Malhi and O. L. Phillips (2014). "Markedly divergent estimates of Amazon forest carbon density from ground plots and satellites." Global Ecology and Biogeography **23**(8): 935-946.

Moisy, F. (2008). boxcount. Paris, France, Université Paris Sud.

Morse, D. R., J. H. Lawton, M. M. Dodson and M. H. Williamson (1985). "Fractal Dimension of Vegetation and the Distribution of Arthropod Body Lengths." Nature **314**: 731-733.

Mugasha, W. A., E. E. Mwakalukwa, E. Luoga, R. E. Malimbwi, E. Zahabu, D. S. Silayo, G. Sola, P. Crete, M. Henry and A. Kashindy (2016). "Allometric Models for Estimating Tree Volume and Aboveground Biomass in Lowland Forests of Tanzania." International Journal of Forestry Research **2016**: 13.

Murray, J., G. A. Blackburn, D. Whyatt and C. Edwards (2014). Investigating the Structural Condition of Individual Trees using LiDAR Metrics. Geographical Information Systems Research UK (GISRUK), Glasgow, The University of Glasgow.

Murray, J., G. A. Blackburn, J. D. Whyatt and C. Edwards (2018). "Using Fractal Analysis of Crown Images to Measure the Structural Condition of Trees." Forestry: An International Journal of Forest Research **91**(4): 480-491.

Næsset, E. (2002). "Predicting forest stand characteristics with airborne scanning laser using a practical two-stage procedure and field data." Remote Sensing of Environment **80**(1): 88-99.

NE (2018). Countryside Stewardship: Higher Tier Manual: 1-160.

Niinemets, Ü. (2010). "Responses of Forest Trees to Single and Multiple Environmental Stresses from Seedlings to Mature Plants: Past Stress History, Stress Interactions, Tolerance and Acclimation " Forest Ecology and Management **260**: 1623–1639.

- Niklas, K. J. (1992). Plant Biomechanics: An Engineering Approach to Plant Form and Function. London, The University of Chicago Press Ltd.
- Niklas, K. J. (2001). Wind, Size and Tree Safety. Tree Structure and Mechanics: How Trees Stand Up and Fall Down, City of Savannah, Georgia, U.S., International Society of Arboriculture.
- Norris, M. (2007). Tree Risk Assessments – What Works – What Does Not –Can We Tell? International Society of Arboriculture; Australia Chapter (ISAAC) Conference, Perth, Australia., International Society of Arboriculture; Australia Chapter.
- Nowakowska, E., J. Koronacki and S. Lipovetsky (2014). "Tractable Measure of Component Overlap for Gaussian Mixture Models." arXiv **1407**(7172.1): 1-24.
- Nowakowska, E., J. Koronacki and S. Lipovetsky (2015). "Clusterability assessment for Gaussian mixture models." Applied Mathematics and Computation **256**: 591-601.
- NRC (2017). Federal Airborne LiDAR Acquisition Guideline. N. R. C. P. S. Canada. Canada, Government of Canada: 1-63.
- NTSG (2011). Common Sense Risk Management of Trees. Guidance on Trees and Public Safety in the UK for Owners, Managers and Advisers. N. T. S. Group. Edinburgh, Forestry Commission.
- NTSG (2011). Common Sense Risk Management of Trees. Guidance on Trees and Public Safety in the UK for Owners, Managers and Advisers. Edinburgh, Forestry Commission.
- Ole Ørka, H., E. Næsset and O. M. Bollandsås (2009). "Classifying Species of Individual Trees by Intensity and Structure Features Derived from Airborne Laser Scanner Data " Remote Sensing of Environment **113**: 1163–1174.
- Olschofsky, K., V. Mues and M. Köhl (2016). "Operational assessment of aboveground tree volume and biomass by terrestrial laser scanning." Computers and Electronics in Agriculture **127**: 699-707.
- Origo, N., K. Calders, J. Nightingale and M. Disney (2017). "Influence of levelling technique on the retrieval of canopy structural parameters from digital hemispherical photography." Agricultural and Forest Meteorology **237–238**: 143-149.
- Ørka, H. O., E. Næsset and O. M. Bollandsås (2009). "Classifying species of individual trees by intensity and structure features derived from airborne laser scanner data." Remote Sensing of Environment **113**(6): 1163-1174.
- Ørka, H. O., E. Næsset and O. M. Bollandsås (2009). "Classifying Species of Individual Trees by Intensity and Structure Features Derived from Airborne Laser Scanner Data " Remote Sensing of Environment **113**: 1163–1174.
- Otepka, J., S. Ghuffar, C. Waldhauser, R. Hochreiter and N. Pfeifer (2013). "Georeferenced Point Clouds: A Survey of Features and Point Cloud Management." ISPRS International Journal of Geo-Information **2**(4): 1038-1065.
- Parkan, M. (2018). Digital Forestry Toolbox for Matlab/Octave, GIS Research Laboratory, EPFL.

- Peterson, D. J., S. Resetar, J. Brower and R. Diver (1999). *Forest Monitoring and Remote Sensing: A Survey of Accomplishments and Opportunities for the Future*. Washington, White House Office of Science and Technology Policy: 1-99.
- Pollardy, S. G. (2008). *Physiology of Woody Plants*. USA, Elsevier.
- Popescu, S. C. and M. Hauglin (2014). Estimation of Biomass Components by Airborne Laser Scanning. *Forestry Applications of Airborne Laser Scanning: Concepts and Case Studies*. M. Maltamo, E. Næsset and J. Vauhkonen. Dordrecht, Springer Netherlands: 157-175.
- Prost, G. L. (2013). *Remote Sensing for Geoscientists* CRC Press.
- Rahman, M. Z. A. and B. Gorte (2008). *Individual tree detection based on densities of high points from high resolution airborne LiDAR*. GEOBIA - Pixels Objects Intelligence: GEOgraphic Object Based Image Analysis for the 21st Century, Alberta, Canada, ISPRS.
- Rahman, M. Z. A. and B. G. H. Gorte (2009). *Tree Crown Delineation from High Resolution Airborne LiDAR Based on Densities of High Points*. Laser Scanning, Paris, ISPRS.
- Raunonen, P., M. Kaasalainen, M. Åkerblom, S. Kaasalainen, H. Kaartinen, M. Vastaranta, M. Holopainen, M. Disney and P. Lewis (2013). "Fast Automatic Precision Tree Models from Terrestrial Laser Scanner Data." *Remote Sensing* **5**(2): 491-520.
- Redmill, F. (2002). "Risk Analysis - A Subjective Process." *Engineering Management Journal* **12**(2): 91-96.
- Rian, I. M. and M. Sassone (2014). "Tree-inspired dendriforms and fractal-like branching structures in architecture: A brief historical overview." *Frontiers of Architectural Research* **3**(3): 298-323.
- Ringuest, J. L. (1986). "A chi-square statistic for validating simulation-generated responses." *Computers & Operations Research* **13**(4): 379-385.
- Romanczyk, P., J. van Aardt, K. Cawse-Nicholson, D. Kelbe, J. McGlinchy and K. Krause (2013). "Assessing the impact of broadleaf tree structure on airborne full-waveform small-footprint LiDAR signals through simulation." *Canadian Journal of Remote Sensing* **39**(sup1): S60-S72.
- Rybansky, M., M. Brenova, J. Cermak, J. v. Genderen and S. Å (2016). "Vegetation structure determination using LIDAR data and the forest growth parameters." *IOP Conference Series: Earth and Environmental Science* **37**(1): 012031.
- Sanchez-Gonzalez, M., M. Cabrera, P. J. Herrera, R. Vallejo, I. Canellas and F. Montes (2016). "Basal Area and Diameter Distribution Estimation Using Stereoscopic Hemispherical Images." *Photogrammetric Engineering and Remote Sensing* **82**(8): 605-616.
- Sankarana, S., A. Mishraa, R. Ehsania and C. Davis (2010). "A Review of Advanced Techniques for Detecting Plant Diseases." *Computers and Electronics in Agriculture* **72**: 1-13.
- Schomaker, M. E., S. J. Zarnoch, W. A. Bechtold, D. J. Latelle, W. G. Burkman and S. M. Cox (2007). *Crown-Condition Classification: A Guide to Data Collection and Analysis*. Southern Research Station, Asheville, NC., U.S. Department of Agriculture Forest Service: 78.
- Schwalbe, E., H.-G. Maas, M. Kenter and S. Wagner (2009). "Hemispheric Image Modelling and Analysis Techniques for Solar Radiation Determination in Forest Ecosystems." *Photogrammetric Engineering & Remote Sensing* **75**(4): 375-384.

Segura, M., D. Ray and C. Maroto (2014). "Decision support systems for forest management: A comparative analysis and assessment." Computers and Electronics in Agriculture **101**: 55-67.

Seiffert, C., T. M. Khoshgoftaar, J. Van Hulse and A. Napolitano (2010). "RUSBoost: A Hybrid Approach to Alleviating Class Imbalance." IEEE Transactions on Systems, Man, and Cybernetics - Part A: Systems and Humans **40**(1): 185-197.

Shi, Y., T. Wang, A. K. Skidmore and M. Heurich (2018). "Important LiDAR Metrics for Discriminating Forest Tree Species in Central Europe." ISPRS Journal of Photogrammetry and Remote Sensing **137**: 163-174.

Song, G.-Z., D. Doley, D. Yates, K.-J. Chao and C.-F. Hsieh (2014). "Improving Accuracy of Canopy Hemispherical Photography by a Constant Threshold Value Derived from an Unobscured Overcast Sky. ." **44**: 17-27.

Sossa-Azuela, J. H., R. Santiago-Montero, M. Pérez-Cisneros and E. Rubio-Espino (2013). "Computing the Euler Number of a Binary Image Based on a Vertex Codification." Journal of Applied Research and Technology **11**(3): 360-370.

Stewart, M. G., D. O'Callaghan and M. Hartley (2013). "Review of QTRA and Risk-based Cost-benefit Assessment of Tree Management." Arboriculture & Urban Forestry **34**(4): 165-172.

Strahler, A. H., D. L. B. Jupp, C. E. Woodcock, C. B. Schaaf, T. Yao, F. Zhao, X. Yang, J. Lovell, D. Culvenor, G. Newnham, W. Ni-Miester and W. Boykin-Morris (2008). "Retrieval of forest structural parameters using a ground-based lidar instrument (Echidna®)." Canadian Journal of Remote Sensing **34**(S2): S426-S440.

Strîmbu, V. F. and B. M. Strîmbu (2015). "A graph-based segmentation algorithm for tree crown extraction using airborne LiDAR data." ISPRS Journal of Photogrammetry and Remote Sensing **104**: 30-43.

Suarez, J. C., C. Ontiveros, S. Smith and S. Snape (2005). "Use of Airborne LiDAR and Aerial Photography in the Estimation of Individual Tree Heights in Forestry." Computers and Geosciences **31**: 253-262.

Swatantran, A., R. Dubayah, D. Roberts, M. Hofton and J. Bryan Blair (2011). "Mapping Biomass and Stress in the Sierra Nevada Using LiDAR and Hyperspectral Data Fusion." Remote Sensing of Environment **115**: 2917-2930.

Swetnam, T. L. and D. A. Falk (2014). "Application of Metabolic Scaling Theory to reduce error in local maxima tree segmentation from aerial LiDAR." Forest Ecology and Management **323**: 158-167.

Swetnam, T. L., C. D. O'Connor and A. M. Lynch (2016). "Tree Morphologic Plasticity Explains Deviation from Metabolic Scaling Theory in Semi-Arid Conifer Forests, Southwestern USA." PLoS ONE **11**(7): e0157582.

Takao, G., H. Priyadi, W. Ikbal Nursal and eds. (2010). The operational role of remote sensing in forest and landscape management: Focus group discussion proceedings. Bogor, Indonesia, Center for International Forestry Research (CIFOR).

Tehrany, M. S., L. Kumar and M. J. Drielsma (2017). "Review of native vegetation condition assessment concepts, methods and future trends." Journal for Nature Conservation **40**: 12-23.

- Telling, J., A. Lyda, P. Hartzell and C. Glennie (2017). "Review of Earth science research using terrestrial laser scanning." Earth-Science Reviews **169**: 35-68.
- Ustin, S. L. and J. A. Gamon (2010). "Remote Sensing of Plant Functional Types." New Phytologist **186**: 795–816.
- Valbuena, R. (2014). Integrating Airborne Laser Scanning with Data from Global Navigation Satellite Systems and Optical Sensors. Forestry Applications of Airborne Laser Scanning: Concepts and Case Studies. M. Maltamo, E. Næsset and J. Vauhkonen. Dordrecht, Springer Netherlands: 63-88.
- Vauhkonen, J., L. Ene, S. Gupta, J. Heinzl, J. Holmgren, J. Pitkänen, S. Solberg, Y. Wang, H. Weinacker, K. M. Hauglin, V. Lien, P. Packalén, T. Gobakken, B. Koch, E. Næsset, T. Tokola and M. Maltamo (2012). "Comparative testing of single-tree detection algorithms under different types of forest." Forestry: An International Journal of Forest Research **85**(1): 27-40.
- Vauhkonen, J., M. Maltamo, R. E. McRoberts and E. Næsset (2014). Introduction to Forestry Applications of Airborne Laser Scanning. Forestry Applications of Airborne Laser Scanning: Concepts and Case Studies. M. Maltamo, E. Næsset and J. Vauhkonen. Dordrecht, Springer Netherlands: 1-16.
- Wallace, L., A. Lucieer and C. S. Watson (2014). "Evaluating Tree Detection and Segmentation Routines on Very High Resolution UAV LiDAR Data." IEEE Transactions on Geoscience and Remote Sensing **52**(12): 7619-7628.
- Wang, C.-K. and W. D. Philpot (2007). "Using airborne bathymetric lidar to detect bottom type variation in shallow waters." Remote Sensing of Environment **106**(1): 123-135.
- Wargo, C. A., G. C. Church, J. Glaneueski and M. Strout (2014). Unmanned Aircraft Systems (UAS) Research and Future Analysis. Aerospace Conference, Big Sky, MT, USA, Institute of Electrical and Electronics Engineers (IEEE).
- Watson, B. (2006). Trees - Their Use, Management, Cultivation and Biology. Wiltshire, The Crowood Press Ltd.
- Weiss, M. and F. Baret (2010). "CAN_EYE V6.3.3 USER MANUAL." 1-56.
- Weiss, M., F. Baret, G. J. Smith, I. Jonckheere and P. Coppin (2004). "Review of Methods for In-situ Leaf Area Index (LAI) Determination Part II. Estimation of LAI, Errors and Sampling." Agricultural and Forest Meteorology **121**: 37–53.
- Weiss, M., F. Baret, G. J. Smith, I. Jonckheere and P. Coppin (2004). "Review of methods for in situ leaf area index (LAI) determination: Part II. Estimation of LAI, errors and sampling." Agricultural and Forest Meteorology **121**(1–2): 37-53.
- West, P. W. (2009). Tree and Forest Measurement. London, Springer Science & Business Media.
- Westoby, M. J., J. Brasington, N. F. Glasser, M. J. Hambrey and J. M. Reynolds (2012). "'Structure-from-Motion' photogrammetry: A low-cost, effective tool for geoscience applications." Geomorphology **179**: 300-314.
- White, J. C., J. T. T. R. Arnett, M. A. Wulder, P. Tompalski and N. C. Coops (2015). "Evaluating the impact of leaf-on and leaf-off airborne laser scanning data on the estimation of forest inventory attributes with the area-based approach." Canadian Journal of Forest Research **45**(11): 1498-1513.

- Wimmer, A., M. Schardt, M. Ziegler, G. Ruppert, K. Granica, U. Schmitt, H. Gallaun and J. Hyypä (2000). "Forest Inventory by means of Satellite Remote Sensing and Laser Scanning." International Archives of Photogrammetry and Remote Sensing **XXXIII**(B7): 1316-1324.
- Wu, B., B. Yu, Q. Wu, Y. Huang, Z. Chen and J. Wu (2016). "Individual tree crown delineation using localized contour tree method and airborne LiDAR data in coniferous forests." International Journal of Applied Earth Observation and Geoinformation **52**: 82-94.
- Wulder, M. A., R. J. Hall and S. E. Franklin (2005). "Remote sensing and GIS in forestry." Remote sensing for GIS managers. ESRI Press, Redlands: 351-362.
- Yan, W. Y., A. Shaker and N. El-Ashmawy (2015). "Urban land cover classification using airborne LiDAR data: A review." Remote Sensing of Environment **158**(Supplement C): 295-310.
- Yu, X., J. Hyypä, A. Kukko, M. Maltamo and H. Kaartinen (2006). "Change Detection Techniques for Canopy Height Growth Measurements Using Airborne Laser Scanner Data." Photogrammetric Engineering & Remote Sensing **72**(12): 1339–1348.
- Yu, X., J. Hyypä, P. Litkey, H. Kaartinen, M. Vastaranta and M. Holopainen (2017). "Single-Sensor Solution to Tree Species Classification Using Multispectral Airborne Laser Scanning." Remote Sensing **9**(2)(108): 1-16.
- Yu, X. W., J. Hyypä, M. Vastaranta, M. Holopainen and R. Viitala (2011). "Predicting individual tree attributes from airborne laser point clouds based on the random forests technique." Isprs Journal of Photogrammetry and Remote Sensing **66**(1): 28-37.
- Zeide, B. (1998). "Fractal analysis of foliage distribution in loblolly pine crowns." Canadian Journal of Forest Research **28**(1): 106-114.
- Zeide, B. and P. Pfeifer (1991). "A Method for Estimation of Fractal Dimension of Tree Crowns." Forest Science **37**(5): 1253-1265.
- Zhang, D., A. Samal and J. R. Brandle (2007). "A Method for Estimating Fractal Dimension of Tree Crowns from Digital Images." International Journal of Pattern Recognition and Artificial Intelligence **21**(3): 561-572.
- Zhao, K., J. C. Suarez, M. Garcia, T. Hu, C. Wang and A. Londo (2018). "Utility of multitemporal lidar for forest and carbon monitoring: Tree growth, biomass dynamics, and carbon flux." Remote Sensing of Environment **204**: 883-897.
- Zhen, Z., L. J. Quackenbush and L. J. Zhang (2016). "Trends in Automatic Individual Tree Crown Detection and Delineation-Evolution of LiDAR Data." Remote Sensing **8**(4): 26.
- Zheng, X., P. Gong and M. Strome (1995). "Characterizing Spatial Structure of Tree Canopy Using Colour Photographs and Mathematical Morphology." **21**(4).
- Zimmerman, M. H. and C. L. Brown (1971). Trees: Structure and Function. New York, Springer-Verlag.

Appendix A - Ground Reference Field Guide

Tree Surveying Conventions

For this investigation you will need to record various information about the woodland survey plots. In order to facilitate this several pieces of equipment are required, this will include:

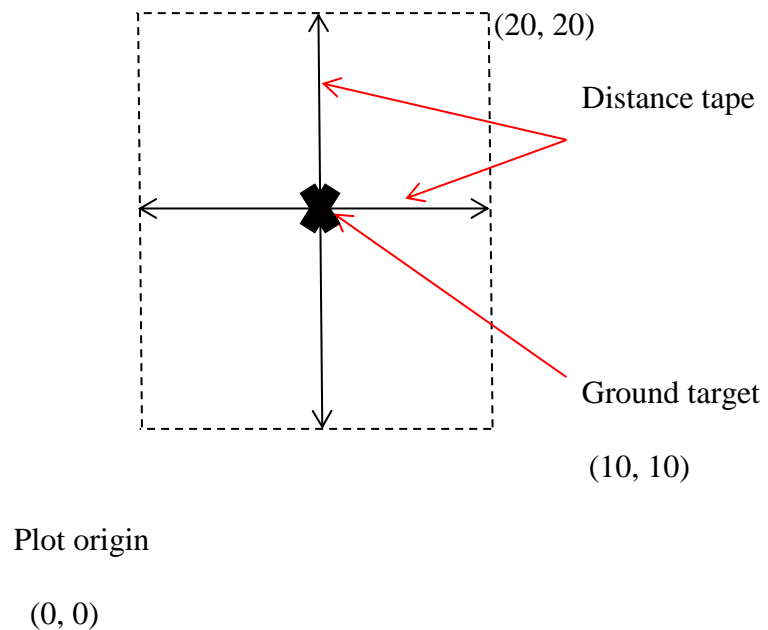
- Data Sheets/Data logger
- DBH tape
- Survey Tape
- Clinometer
- Binoculars
- Identification books

Along with other vital equipment like wet weather gear/boots, mobile phone etc.

Forest inventory description

1. Plot description

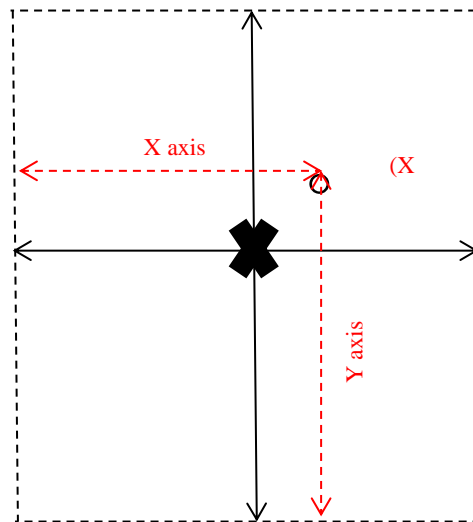
1. A 20m X 20m square plot will be set-up at each sampling point.



2. Sampling plot is set-up by laying distance tapes across the ground target point, extending from East to West and from North to South. So the ground target point is at (10, 10) coordinates of the sampling plot.
3. The origin of the sampling plot is at the lower left corner with coordinates (0, 0).

2. Tree location (X & Y)

1. Tree location (X & Y) is measure from the lower left corner (0, 0) of the sampling plot (NOT FROM THE CENTRE POINT OF THE PLOT).



Example data entry: X = 12.1, Y = 13.3

3. DBH (diameter at breast height)

1. DBH is measure using the DBH tapes at 1.3 m above ground.
2. All trees with height more than 1.3m above ground and DBH equal or greater than **5cm** will be surveyed.
3. See **Addendum – Measuring Trees** for further information.

Example data entry: DBH = 56

4. Tree height

1. Tree height is measured using a Sunnto clinometer to the tree's highest point.

2. Use normal Suunto surveying conventions - See Addendum - **Take an Optical Reading with a Suunto** for further information
3. To save time, don't calculate in the field, but record the ranges e.g. +80, -10 and the distance e.g. 10.2m, so calculations can be completed off site

Example data entry: +80, -10, 10.2m

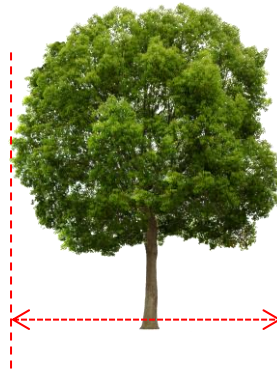
5. Tree lean

1. Visually assess whether or not the tree stem has a lean
2. Standing at the stem/root interface (buttress) use a compass to decide the direction of lean
3. Record the direction if appropriate e.g. NW
4. Leave column blank if no lean

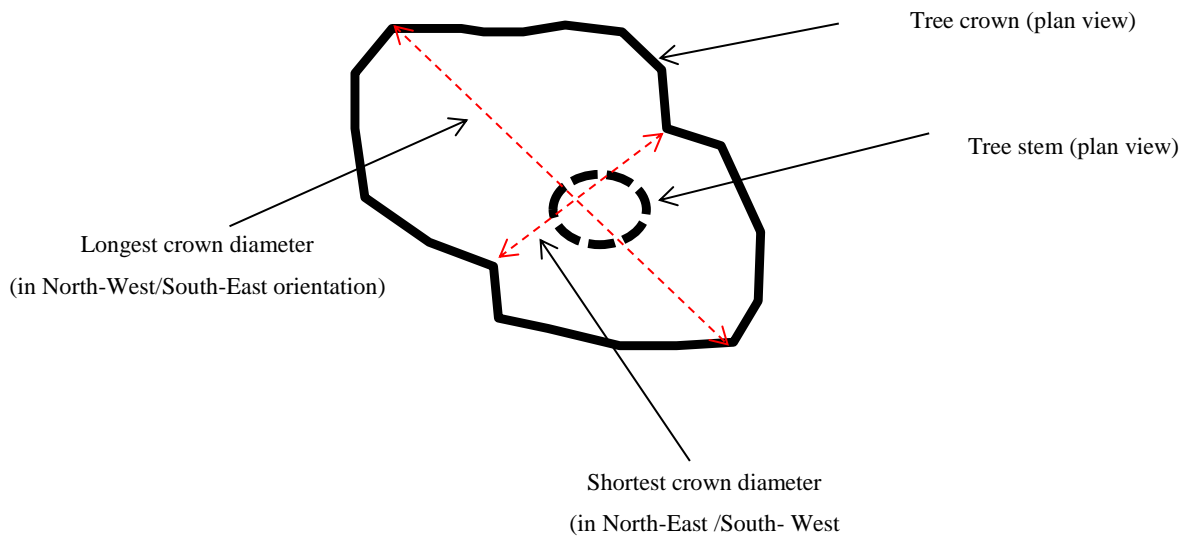
Example data entry: NW

6. Tree crown

1. Tree crown is measured at the longest and shortest distance of crown outer edges. Distance tapes will be applied from underneath the canopy and sighted upwards.



Remote Sensing Tools for the Objective Quantification of Tree Structural Condition
from Individual Trees to Landscape Scale Assessment



Example data entry: Crown long – 3, NW/SE, Crown short – 1 NE/SW

7. Tree species

1. Identify the trees within the plot that are over 5cm DBH
2. Use the tree species table (**Addendum – Tree Species Codes**) to add the identifying code for each tree.
3. Tree ID books should be used to confirm
4. If unsure, photograph the tree form, bark, leaves, fruits and record the file name of the photographs next to the data entry on the form

Example data entry: SY, OK, HAZ

8. Health

1. Make an informed estimation on the general health and condition of each tree
2. Look for signs of disease or decay and make a general note
3. Record your findings in the data sheet using codes P, M, G for Poor, Moderate, Good, and Dz, D, Dx, for diseased, decayed, and dead.
4. It is not important to know the exact disease or decay type

Example data entry: P, Dz

9. Ground Cover Assessment

1. Assess ground cover within the whole of the plot using FCIN45 conventions
2. Using the codes at the bottom of the survey sheet, record the percentage of each type of ground coverage

3. Assist your estimation by using the percentage cover guide found at **Addendum - Chart for Estimating Percentage Cover Composition of Ground Conditions** by comparing the coverage that you can see with the coverage indicated with the blocked images
4. Totals can run over 100% as cover types may overlap

Example data entry: 1 = 90%, 5 = 30% etc.

Note: It will be best to record this as the last data entry for the plot

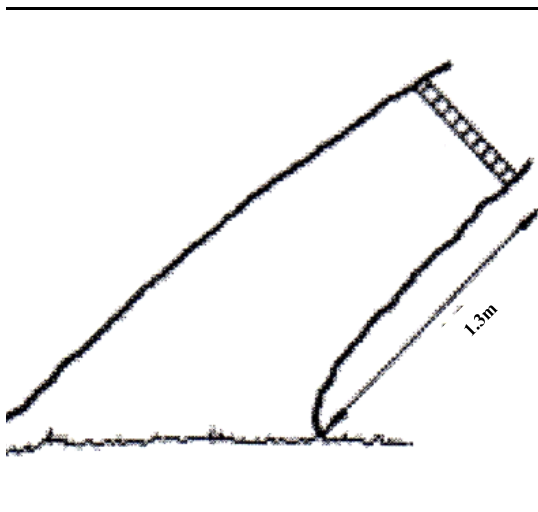
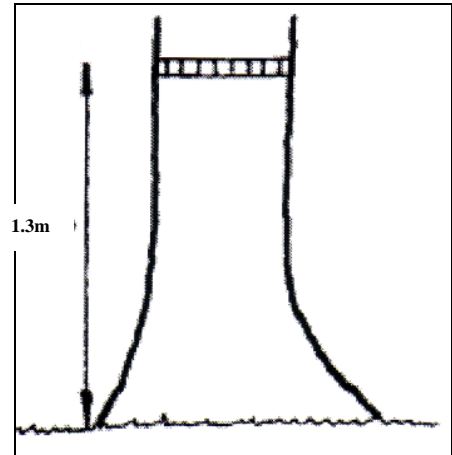
Addendum - Measuring Trees

DBH – Diameter at Breast Height

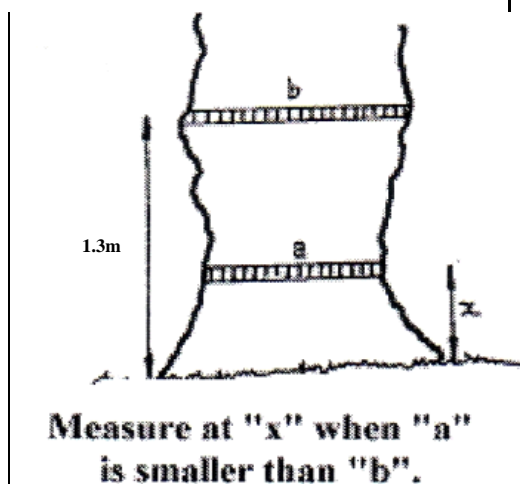
The height at which trees have their diameter measured is fixed at **1.3m** above ground level when undertaking work related to forestry or woodland management.

It is important to ensure that the tape is taut, level and perpendicular to the tree and is not twisted or caught on burrs or other branches.

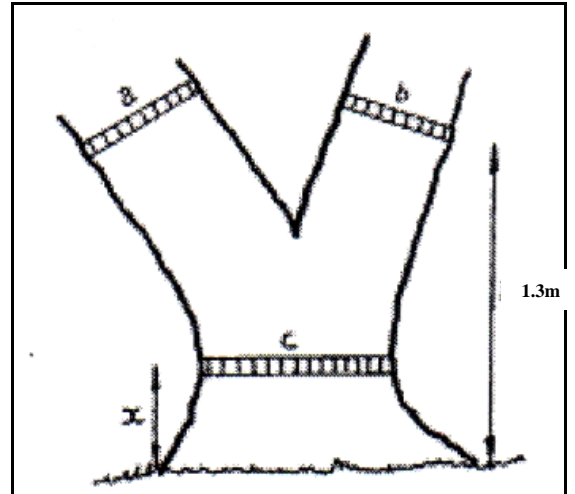
Unfortunately not all trees are nice and straight and equally the ground they're on isn't nice and flat, so in these instances the way DBH is measured differs.



When a tree is leaning over the DBH should be measured on the underside of the tree.



Where there is an anomaly at 1.3m e.g. a swelling or branch, then the DBH should be measured at the thinnest point of the tree below the anomaly.



Finally, when it comes to trees with more than one stem you have a choice. The options open are measure the DBH at the thinnest point below the stems or measure each individual stem and record them separately. This decision would often be made by the instructing party or determined by the aim of the survey.

Addendum - Take an Optical Reading with a Suunto

Measure the horizontal distance from the base of a vertical tree (or the position directly beneath the tree tip of a leaning tree) to a location where the required point on the tree (e.g. tree tip) can be seen.

1. Sight at the required point on the tree:
 - Using one eye: Close one eye and simultaneously look through the Suunto at the scale and 'beside' the Suunto at the tree. Judge where the horizontal line on the Suunto scale would cross the tree.
 - Both eyes: With one eye looking at the Suunto scale and the other looking at the tree, allow the images to appear to be superimposed on each other and read where the horizontal line on the Suunto scale crosses the tree. Note: If you suffer from astigmatism (a common situation where the eyes are not exactly parallel), use the one eye approach.
2. Read from the percent scale and multiply this percentage by the horizontal distance measured in step 1.
3. Site to the base of the tree and repeat steps 2 - 3.
4. Combine the heights from steps 3 and 4 to determine total tree height:
 - Add the 2 heights together if you looked up to the required point in step 2 and down to the base of the tree in step 6.
 - Subtract the height to the base of the tree from the height to the required point if you are on sloping ground and had to look up to **both** the required point and the base of the tree.
5. Check all readings and calculations.

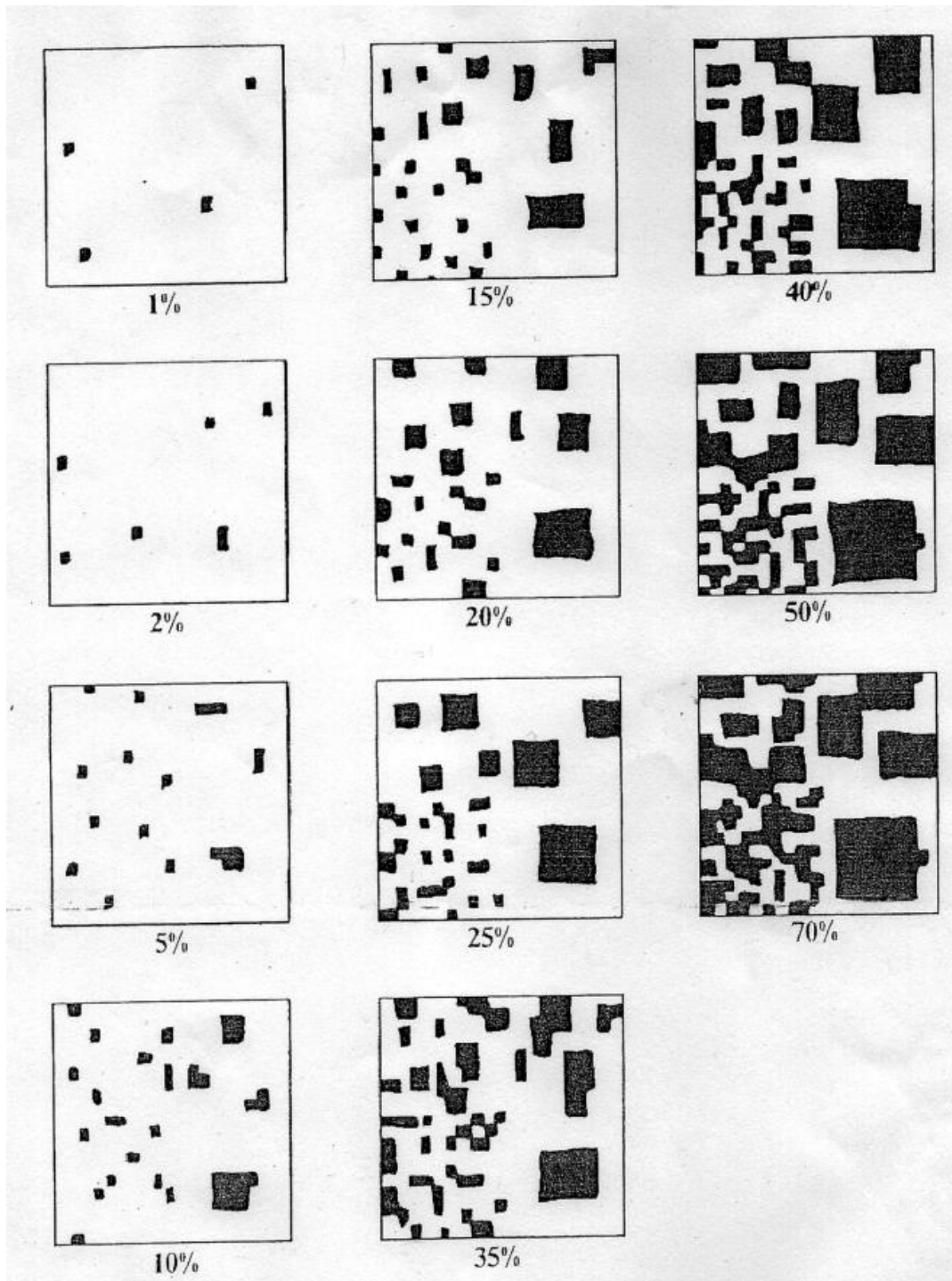
Suunto - Problems

All these methods have one big problem. When measuring the height of a “normal” tree it is usually easy to see the very top of the tree due to its form. However with a lot of broadleaved trees their form hinders your ability to see the top unless you are stood a very long way from it. Therefore, you have to use your judgment to be able to estimate where the top of the tree is and get an accurate angle measurement.

Addendum - Tree Species Codes

	Tree Species		Other
OK	Oak	MB	Mixed Broadleaves
TOK	Turkey Oak	MC	Mixed Conifer
AH	Ash	XC	Other Conifer
PO	Poplar	ha	Hectares
SY	Sycamore	c.ha	Approximate hectares
CSY	Copper Sycamore	P1963	Planting year
SC	Sweet chestnut	Pc.1900	Approx. planting year
HC	Horse chestnut	nr	Natural regeneration
BE	Beech	AWS	Ancient Woodland Site
CBE	Copper Beech	PAWS	Plantation on Ancient Woodland Site
BI	Birch	Cpt	Compartment
FM	Field maple	m	Metre
CAP	Crab apple	cm	Centimetre
HAZ	Hazel	OG	Open Ground
WL	Willow	PROW	Public Right of Way
PWL	Pussy Willow	JKN	Japanese Knotweed
CAR	Alder	HB	Himalayan Balsam
EM	Elm		
WRC	Western Red Cedar		
HAW	Hawthorn		
RW	Rowan		
CH	Cherry		
WCH	Wild Cherry		
HB	Horn Beam		
FA	False Acacia (Robinia)		
LC	Lawson's Cypress		
HOL	Holly		
BOX	Box		
LI	Lime		
ELD	Elder		
BTh	Black Thorn		
PYR	Pear (Pyrus)		
HL	Hybrid Larch		
BuP	Bhutan Pine		
CP	Corsican pine		
SP	Scots pine		

Addendum - Chart for Estimating Percentage Cover Composition of Ground Conditions



Appendix B - Using Fractal Analysis of Crown Images to Measure the Structural Condition of Trees, Supplementary Information

Image Pre-processing

The pre-processing interventions were applied to the raw images and at each phase of processing were statistically checked for suitability. This procedure focussed on the interventions that were observed to have an effect on the further usability of images in this study. Concurrently, the interventions were also statistically tested for suitability of use in the study.

Quantitative Strength of Pre-processing Phases

In order to establish that the three different pre-processing interventions were having a measurable effect on the data, when applying each pre-processing phase, confidence intervals were calculated using the following formula where n is the sample size and s is the standard deviation:

$$\bar{X} \pm Z \frac{s}{\sqrt{n}} \quad (1)$$

At Figure 34, the pre-processing interventions are represented as one; for the baseline or uncorrected image Df values; two, after applying a chromatic aberration correction; three, after lens distortion correction; and four, after image sharpening. As shown in Figure 34, there is a general positive effect caused by each of the post processing interventions on the image Df values. The dataset confidence level at CI95%, suggests that each post processing intervention has a reliable and repeatable influence on the Df values at each successional stage.

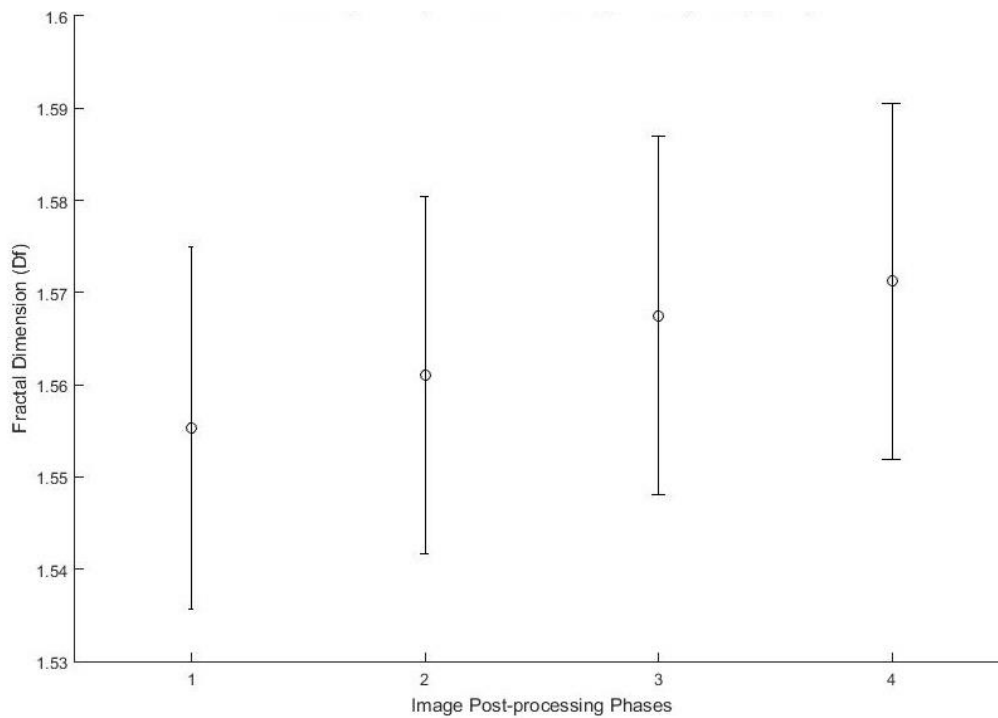


Figure 34 Model testing of the impact of image post processing phases on average Df values, demonstrating 95% confidence interval (CI95%) ($n=247$). Note: Image pre-processing phases applied 1 = raw unprocessed images, 2 = applying chromatic aberration correction, 3 = applying lens distortion correction, 4 = applying image sharpening. The Df values are a logarithmic scale, demonstrated on a truncated axis.

Although the CI bars overlap, potentially suggesting there is no statistical conclusion to be drawn; it should be noted that CI are not a test of statistical significance. A paired, two sample t-test was used assessing the significance between the uncorrected Df data (phase one), and the Df data following the final post processing stage (phase four). The result is a p -value of $p=0.005$, therefore that the differences in the effects of the post processing interventions on the Df values are considered very highly significant.

Validity Testing of Pre-processing

In order to quantify the effect of the before and after the phases of post processing, the corrected effect size was calculated using Hedge's g . This test quantifies the effectiveness of the post processing interventions. Hedge's g , follows as:

$$\left(d_s = \frac{\bar{X}_1 - \bar{X}_2}{\sqrt{\frac{(n_1 - 1)SD_1^2 + (n_2 - 1)SD_2^2}{n_1 + n_2 - 2}}} \right) \quad (2)$$

$$\times \left(1 - \frac{3}{4(n_1 + n_2) - 9} \right)$$

Where SD is standard deviation and n is frequency of values for the two variables; Df values before and after the pre-processing interventions. As can be seen in Figure 35, this results in a large impact on the Df values with the Hedge's g effect size at 2.4504.

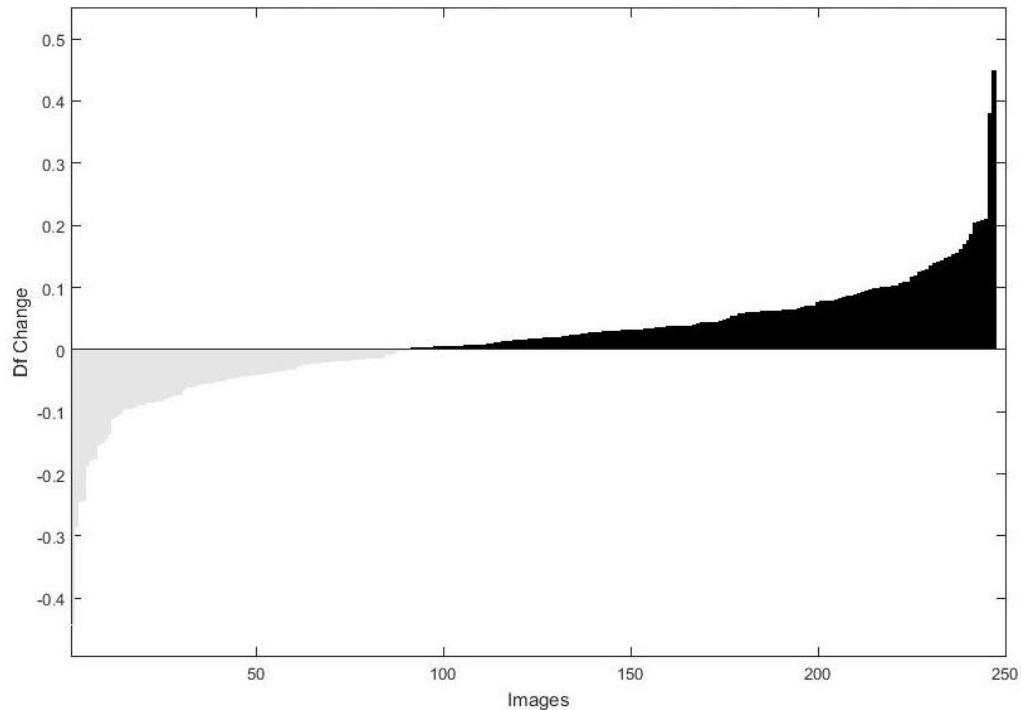


Figure 35 The quantification of effect size following image post processing ($n=247$). The value of Hedge's g at 2.4504 with a confidence interval at 95%, suggests that the pre-processing phases have a significant effect on Df values.

Due to the combination of the assessment of the effect size (Hedge's g 2.4504), supported with a confidence interval of CI95% and a statistical significance of $p < 0.005$, the image post processing phases have had a significant effect on the quality and usability of the images, thereby enabling the images to be used in subsequent analysis within this study.

Model Fitting

Following the pre-processing interventions, the corrected images were reanalysed through generating a second Df score. These are compared with the original, raw Df to identify the extent of residuals between the two data sets in order to estimate the extent of potential statistical error. This phase of the investigation also indicates whether unwanted data noise has been added in to the Df values, and identifies the correlation of remapping the pre-processed Df back to the raw Df values. As can be

observed from Figure 36 the sampled standard deviation of the modelled Df very closely agrees with the original, unprocessed Df values at 0.07% utilising normalised root mean squared error (NRMSE).

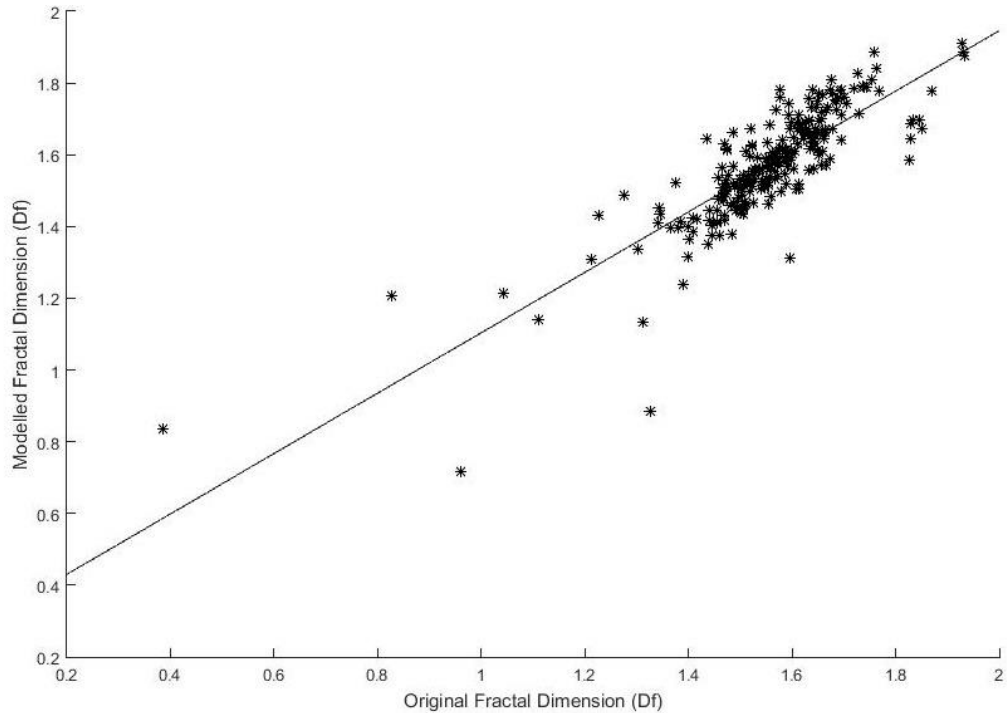


Figure 36 Regression analysis of fractal dimension values following image pre-processing ($n=247$). The pre-processed Df, remains a statically relevant representation of the raw Df values with a normalised root mean squared error (NRMSE) of 0.07% ($y = 0.84*x + 0.26$, $R^2_{\text{adjusted}} = 0.7\%$).

Recommended Field and Data Processing Workflow

The development of the techniques used during this research provides an operational methodology for the objective classification of tree structure. This procedure has two phases split between field and office based work (Figure 37). In phase one, using predefined rules for the selection of trees in accordance with the survey requirements, a tree would be selected, photographed at the mid-point of the crown and the image checked in the field using the same field methodology as described earlier in this paper. This process would be repeated for several iterations in order to create a reference data set for each tree species within the survey. The second phase also

follows the earlier described process of uploading the tree images (to a desktop computer with the required code), defining a bounding box for the crown area to be analysed and the Df value to be calculated. Finally, to achieve objective classification for the individual trees, the Df values of each tree image would be cross-checked against the reference data threshold levels of the individual tree species (e.g. Table 2 of main article).

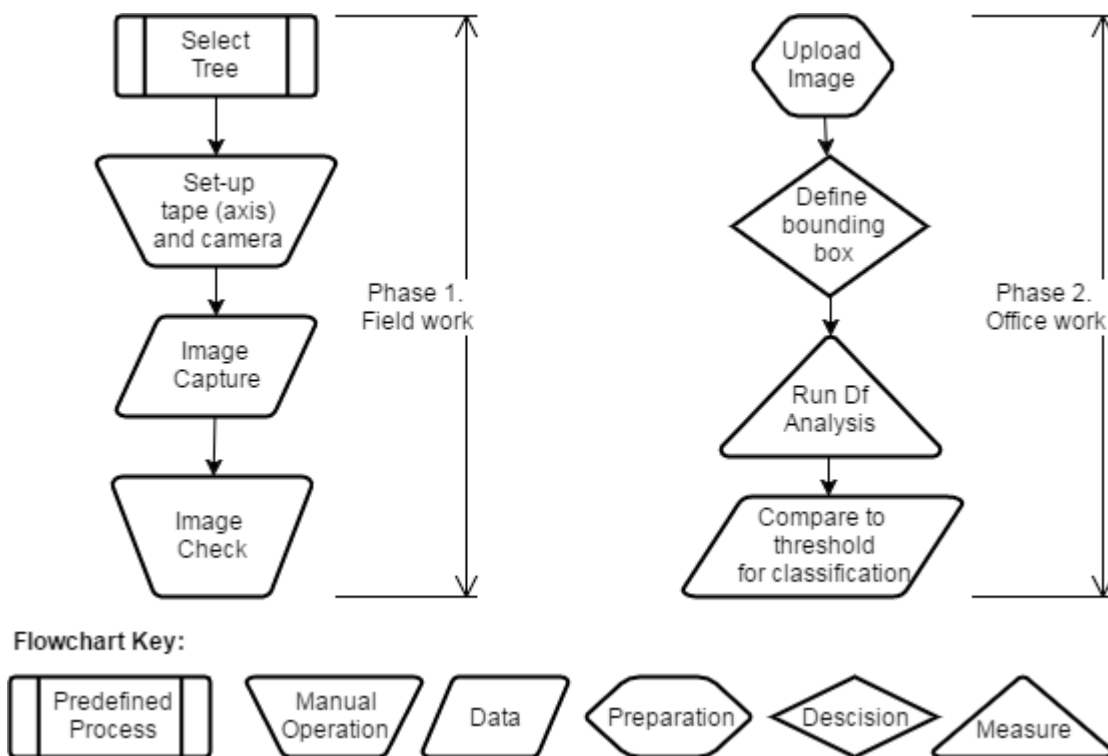


Figure 37 An operational workflow for the field practitioners use of a methodology for the classification of tree crown structure in fractal dimensions (Df), using hemi-spherical photography.

Appendix C - ARBOR: A New Modular Framework for Assessing the Accuracy of Individual Tree Crown Delineation from Remotely-sensed Data, *Supplementary Information*

Crown Delineation and Tree Growth

In some circumstances, such as coniferous plantations with well-spaced trees, delineating tree crowns can achieve a high degree of delineation success (Falkowski, Smith et al. 2008). However, not all trees grow in such ideal circumstances. Individual tree crown (ITC) delineation methods intended for coniferous trees can be problematic when applied to the ITC delineation of deciduous trees, due to the wide range of tree crown sizes and interconnecting crowns, and with larger tree canopies frequently split in to several smaller crowns during the ITC delineation process (Lu, Guo et al. 2014). As tree canopies become more complex, indicative of the intricate crown mixes in broadleaved canopies, achieving successful ITC delineation is more difficult. Repeated problems to overcome include crown inter-connectivity, increased stem density per area, infrequent open spaces or canopy gaps, and high numbers of individual tree species each with their own unique crown structure characteristics. These issues cause the potential to satisfactorily delineate tree crowns from the heterogeneous canopy mix to reduce rapidly (Falkowski, Smith et al. 2008, Yu, Hyyppa et al. 2011, Jing, Hu et al. 2014, Lu, Guo et al. 2014, Rybansky, Brenova et al. 2016).

The perspective from which the tree crowns are viewed during data capture also has an impact. Valbuena 2014) describes that tree positions differ significantly when they are determined from the ground using field techniques, or when the location is determined aerially via RS methods. Often field measurements need correcting, and a deterministic, systematic method applied to identify which stem locations represent

the same tree in both the ground reference (GR) and aerial remote sensing (RS) data. Chen, Baldocchi et al. (2006) also note that there are some individual species anomalies. The delineation of mature oak crowns is further complicated by the tendency of oak trees to produce crown sections, where large branches and sub-crowns are viewed as individual trees in light detection and ranging (LiDAR) data, thereby leading to incorrect crown delineation through overestimating the tree population (Bian, Zou et al. 2014).

Measuring Tree Crowns

Tree crowns typically grow with a positively phototropic habit, subject to the individual phototropism response for the tree species (Matsuzaki, Masumori et al. 2006). Trees are therefore, predisposed to grow towards canopy gaps or spaces where there is available light (Loehle 1986). As a result of this phenomena, in forested or woodland situations, whole canopy movement towards available light occurs leading to changes in the tree's structural form (Loehle 1986). This tree crown movement towards available light becomes a notable issue when comparing aerially laser scanned (ALS) LiDAR with GR data during tree investigations (Yu et al., 2017). In the course of GR data capture, the absolute position of the tree location is typically at the tree base, or root/stem interface, by field operatives intending to avoid any ambiguous estimation of the central point of the tree crown from the ground (Mills, Castro et al. 2010). However, when completing computerised ITC delineation the central point of the crown is frequently not immediately above the GR measured tree location due to environmental conditions causing 'sweep' in the stem, thus offsetting the crown, particularly in woodland or forested areas (Eysn, Hollaus et al. 2012) (Figure 38). It could be proposed that a simple solution to this problem is to locate the stem on the ground and record its geo-coordinates, record the direction of crown

offset, the total area of the crown and attempt to locate the central mass of the crown. However, this procedure is limited by the biophysical complications of measuring the aerial parts of the tree crown from the ground. There is the potential for measuring errors; including a subjective assessment when considering where the crown edge is located, should the crown be beyond the physical reach of the field operative. This field method will also not account for any offset anomalies caused by upper-crown branches producing unexpected high-point peaks.

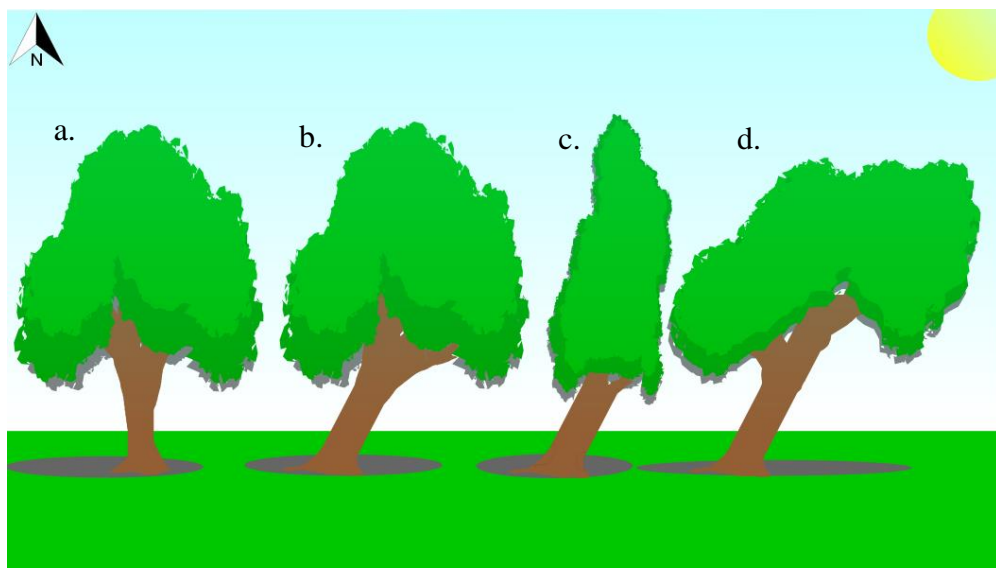


Figure 38 A model of typical tree location alignment problems when comparing aerial observation data (either aerial images or LiDAR), and ground reference measurements (GR). In woodland and forest situations, trees subject to their species phototropic habit will grow towards light, potentially causing whole canopy movement away from the original root/stem interface location (Loehle 1986, Matsuzaki, Masumori et al. 2006). Common tree form observed when collecting GR data; a) a tree with the tree crown located immediately above the stem, with a broadly equal crown distribution b) a tree with a stem lean, causing the crown's high peak to be away from the root/stem interface location. c) as b), but with an elliptical crown distribution along a dominant directional axis e.g. north-south. d) as c) with the elliptical crown distribution along a different directional axis e.g. east-west. The directional axis angles are potentially in any direction given the immediate environmental conditions around each tree crown.

Ground Reference Site Description

A 51.5 hectare woodland in the northwest of England, UK, was used as a study site (Eaves Wood, Silverdale, Lancashire, UK. 54°10'43.2"N, 2°49'13.9"W). The site is predominantly mixed-broadleaf tree species, with individual coniferous species infrequently distributed amongst the broadleaf. Typical for woodland of this provenance, there are also mixed-conifer coups where the conifer trees dominate, however, these areas are spatially limited and closely relate to the underlying karst landform. The woodland has a diverse vertical and horizontal canopy structure (Figure 39), ranging from young, small scrubland to areas of well-developed, multi-strata ancient semi-natural woodland (ASNW). The woodland has heterogeneous mixing of species and a varied horizontal spatial arrangement across the site, including areas of canopy gaps, woodland rides, and bare earth.

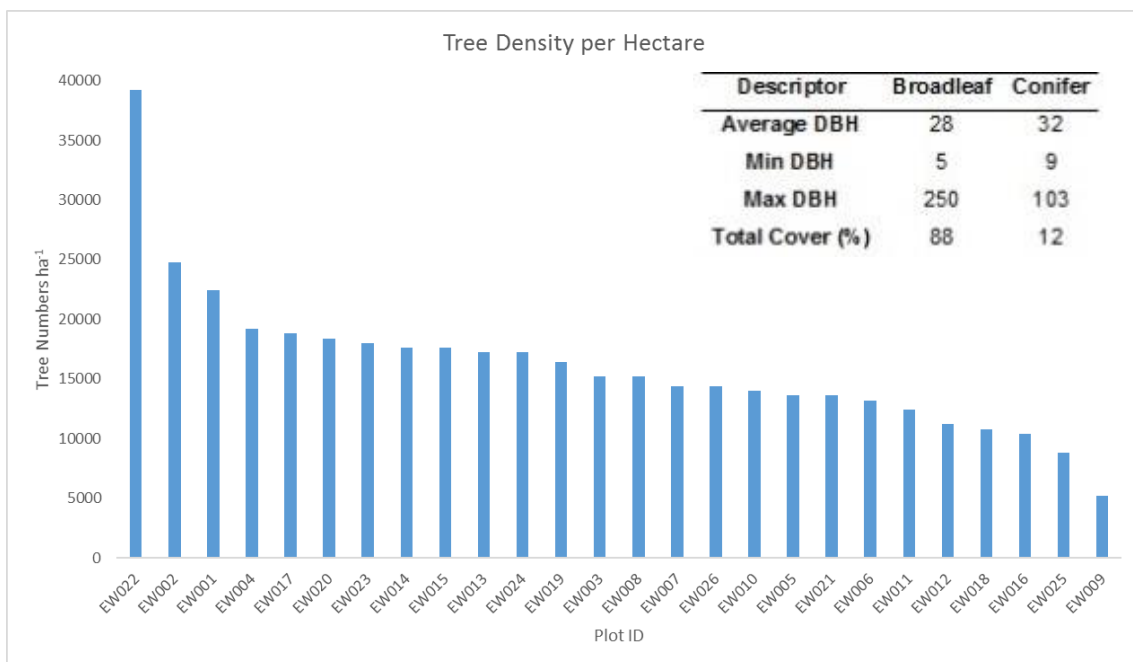


Figure 39 Tree density per hectare, calculated on a per plot basis from 26 survey plots. The inset table shows additional descriptive statistics for the plots. The population of this woodland follows the reverse ‘J’ population distribution, indicative of a healthy, complex woodland (Kerr, Mason et al. 2002).

Twenty-six plots were established within a thirty metre buffer zone of a single transect line running west to east across the woodland. Each plot was 20 x 20m (total GR survey area of 10,400m²), and orientated north south. The canopy cover at each of the plots ranged from 10% up to 90%, checked via a process of in-field visual assessment (Folk 1951), cross-referenced with photographic imaging analysis. The plot centres were geolocated using real-time kinematic global positioning (RTK GPS), with a theoretical sub-centimetre location accuracy following post-processing. Biophysical tree attributes were recorded where the centre of a tree was located within the plot boundary, specifically; tree location (XY), total height (Z), crown extent and area, and other ancillary information; species, diameter at breast height (DBH) and general observations about tree condition or local environment. This GR data followed standard forest measurement conventions (West 2009), and was collected using manual tree measurement equipment: clinometer, field compass, surveyors and DBH tapes.

Appendix D - Authorship Statements

Title of Paper Using Fractal Analysis of Crown Images to Measure the Structural Condition of Trees

Publication Status Published ✓ Accepted for Publication

Submitted for Publication Unpublished, written in manuscript style

Publication Details Murray, J., G. A. Blackburn, J. D. Whyatt and C. Edwards (2018). "Using Fractal Analysis of Crown Images to Measure the Structural Condition of Trees." *Forestry: An International Journal of Forest Research* 91(4): 480-491.

Name of Principal Author Jon Murray

Contribution to the Paper Lead authorship, concept, development, experimentation and analysis, content creation.

Overall percentage (%) 90

Signature  **Date: 28.09.2018**

Co-Author Contributions

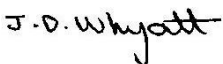
By signing the authorship statement, each co-author certifies that:

1. The principal author's stated contribution to the publication is accurate (as detailed above);
2. Permission is granted for the candidate to include the publication in the thesis; and
3. The sum of all co-author contributions is equal to 100% less the candidate's stated contribution.

Name of Co-Author **George Alan Blackburn**
Contribution to the Paper Supervisory role, manuscript guidance and proofing.

Signature  **Date: 01.10.2018**

Name of Co-Author **James Duncan Whyatt**
Contribution to the Paper Supervisory role, manuscript guidance and proofing.

Signature  **Date: 28.09.2018**

Name of Co-Author **Christopher Edwards**
Contribution to the Paper Supervisory role, manuscript guidance and proofing.

Signature  **Date: 09.10.2018**

Appendices

Title of Paper ARBOR: A New Framework for Assessing the Accuracy of Individual Tree Crown Delineation from Remotely-sensed Data

Publication Status Published Accepted for Publication

Submitted for Publication ✓ Unpublished, written in manuscript style

Publication Details Submitted to Remote Sensing of Environment

Name of Principal Author Jon Murray

Contribution to the Paper Lead authorship, concept, development, experimentation and analysis, content creation.

Overall percentage (%) 80

Signature  **Date: 28.09.2018**

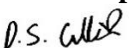
Co-Author Contributions

By signing the authorship statement, each co-author certifies that:

1. The principal author's stated contribution to the publication is accurate (as detailed above);
2. Permission is granted for the candidate to include the publication in the thesis; and
3. The sum of all co-author contributions is equal to 100% less the candidate's stated contribution.

Name of Co-Author **David S. Gullick**

Contribution to the Paper Technical development and analysis.

Signature  **Date: 28.09.2018**

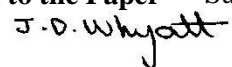
Name of Co-Author **George Alan Blackburn**

Contribution to the Paper Supervisory role, manuscript guidance and proofing.

Signature  **Date: 01.10.2018**

Name of Co-Author **James Duncan Whyatt**

Contribution to the Paper Supervisory role, manuscript guidance and proofing.

Signature  **Date: 28.09.2018**

Name of Co-Author **Christopher Edwards**

Contribution to the Paper Supervisory role, manuscript guidance and proofing.

Signature  **Date: 09.10.2018**

Title of Paper STRUCTURAL: Categorising Individual Trees at Woodland Scale from LiDAR Data

Publication Status Published Accepted for Publication
Submitted for Publication Unpublished and written in a manuscript style ✓

Publication Details No details at present, considering journal options

Name of Principal Author Jon Murray

Contribution to the Paper Lead authorship, concept, development, experimentation and analysis, content creation.

Overall percentage (%) 90

Signature  **Date: 28.09.2018**

Co-Author Contributions

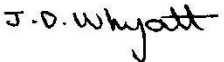
By signing the authorship statement, each co-author certifies that:

1. The principal author's stated contribution to the publication is accurate (as detailed above);
2. Permission is granted for the candidate to include the publication in the thesis; and
3. The sum of all co-author contributions is equal to 100% less the candidate's stated contribution.

Name of Co-Author **George Alan Blackburn**
Contribution to the Paper Supervisory role, manuscript guidance and proofing.

Signature  **Date: 01.10.2018**

Name of Co-Author **James Duncan Whyatt**
Contribution to the Paper Supervisory role, manuscript guidance and proofing.

Signature  **Date: 28.09.2018**

Name of Co-Author **Christopher Edwards**
Contribution to the Paper Supervisory role, manuscript guidance and proofing.

Signature  **Date: 09.10.2018**